Measurement System Assessment Studies for Multivariate and Functional Data

by

Banafsheh Lashkari

A thesis
presented to the University of Waterloo
in fulfillment of the
thesis requirement for the degree of
Doctor of Philosophy
in
Statistics

Waterloo, Ontario, Canada, 2024

Examining Committee Membership

The following served on the Examining Committee for this thesis. The decision of the Examining Committee is by majority vote.

External Examiner:	Jiguo Cao Professor, Department of Statistics and Actuarial Science, Simon Fraser University
Supervisor:	Shoja'eddin Chenouri Professor, Department of Statistics and Actuarial Science, University of Waterloo
Internal Member:	Stefan H. Steiner Professor, Department of Statistics and Actuarial Science, University of Waterloo
	Pengfei Li Professor, Department of Statistics and Actuarial Science, University of Waterloo
Internal-External Member:	Ehsan Toyserkani Professor, Department of Mechanical and Mechatronics Engineering, University of Waterloo

Author's Declaration

I hereby declare that I am the sole author of this thesis. This is a true copy of the thesis, including any required final revisions, as accepted by my examiners.

I understand that my thesis may be made electronically available to the public.

Abstract

A measurement system analysis involves understanding and quantifying the variability in measurement data attributed to the measurement system. A primary goal of such analyses is to assess the measurement system's impact on the overall variability of the data, determining its suitability for the intended purpose. While there are established methods for evaluating measurement systems for a single variable, their applicability is limited when dealing with other data types, such as multivariate and functional data. This thesis addresses a critical gap in the literature concerning the assessment of measurement systems when dealing with multivariate and functional observations. The primary objective is to enhance the understanding of measurement system assessment studies, particularly focusing on multivariate measurements and extending to functional data measurements.

Chapter 1 serves as an introduction. We review several statistical properties and parameters for assessing the measurement systems. This chapter includes some real-world examples of measurement system assessment problems for multivariate and functional data and elaborates on the challenges involved. We also outline the contents that will be explored in the subsequent chapters.

While the literature on measurement system analysis in multivariate and functional data domains is limited, there is also a notable absence of a systematic theoretical investigation for univariate methods. In Chapter 2, we address this gap by conducting a thorough theoretical examination of measurement system assessment estimators for univariate data. The chapter explores various estimation methods for estimating variance components and other essential parameters crucial for measurement system analysis. We provide a comprehensive scrutiny of the statistical properties of these estimators. This foundational understanding serves as the basis for subsequent exploration into the more intricate domains of multivariate and functional data.

In Chapter 3, we extend the scope of measurement system assessment to include multivariate data. This chapter involves adapting the definitions of measurement system assessment parameters to multivariate settings. We employ transformations that yield summary scalar measures for variance-covariance matrices, with a specific focus on the determinant, trace, and Frobenius norm of the variance-covariance matrix components. Building upon the statistical concepts and properties discussed in Chapter 2, we conduct a targeted review of existing theories related to variance-covariance component estimation. A key emphasis is placed on the statistical properties of estimators introduced for one of the parameters in measurement system assessment—the signal-to-noise ratio. Our investigation includes an exploration of its convergence properties and the construction of approximate confidence

intervals. Additionally, we conduct a comparative analysis of the application of three transformations, namely, the determinant, the trace, and the Frobenius norm, based upon their asymptotic properties.

In Chapter 4, our exploration takes a significant step forward as we establish a framework for assessing measurement systems tailored to functional data types. This involves extending the definition of parameters used in the evaluation of measurement systems for univariate data by applying bounded operators on covariance kernels. To estimate the measurement system assessment parameters, we first provide methods to estimate the covariance kernel components. Initially, we explore a classical estimation approach without smoothing. Subsequently, we leverage specialized tools in functional data analysis, within the framework of reproducing kernel Hilbert space (RKHS), to obtain smooth estimates of the covariance kernel components.

The fifth chapter is devoted to a case study application, where we apply the developed framework to a real-world functional dataset. Specifically, we analyze the surface roughness of printed products in the context of additive manufacturing. The comprehensive analysis in Chapter 5 employs statistical methods for univariate and multivariate data types and techniques from functional data analysis.

We are in the process of converting the materials in Chapters 2, 3, and 4 to three separate articles for submission.

Acknowledgements

I want to thank everyone who has supported me along the way.

I am deeply grateful to my supervisor, Professor Shoja Chenouri, for introducing me to statistical thinking and guiding me through my academic journey. His patience, constant support, encouragement, and the countless hours he dedicated to consultations have boosted my confidence and helped me grow. I am truly thankful for the enriching experience under his mentorship.

I would like to express my gratitude to my thesis committee members, Professors Jiguo Cao, Stefan Steiner, Pengfei Li, and Ehsam Toyserkani, for reviewing my thesis and providing insightful comments. I am also thankful to Professor Jock MacKay for reviewing the earlier draft of my thesis and offering valuable feedback and suggestions, particularly on the industrial aspects of my research.

My appreciation also extends to the Multi-Scale Additive Manufacturing Lab for providing the dataset that inspired the research presented in this thesis. Additionally, I thank Dr. Farzad Liravi for his assistance in accessing and understanding the dataset.

It was a privilege to earn my Ph.D. in Statistics at the University of Waterloo, collaborating with esteemed faculty, staff, and students from various departments. I am especially grateful to everyone in the Department of Statistics and Actuarial Science and the Faculty of Mathematics. I also want to express my heartfelt appreciation to all my fantastic friends in the Faculty of Mathematics, with whom I have shared countless memorable moments.

I sincerely thank my parents for a lifetime of love, unwavering support, and encouragement to follow my academic aspirations. Special thanks to my brother, Amir, whose warmth has comforted me during difficult and joyful moments.

Dedication

I dedicate this work in loving memory of my father, whose wisdom, kindness, and boundless love inspire me daily. This thesis is a tribute to his influence and profound impact on my life.

Table of Contents

List of Figures

List of Tables

Chapter 1

Introduction

1.1 Introduction

Maintaining and continuously enhancing quality is of paramount importance for all organizations; from the manufacturing industry to public services such as transportation healthcare, and education. In the manufacturing industry, quality is inextricably linked to meeting pre-determined specifications. To meet and exceed users' expectations, suppliers have to continually strive to enhance their processes and products. In this environment, key decisions about the process and products are greatly influenced by the quality and reliability of the measurement data (Montgomery, 2020).

In the early 1990s, the Automotive Industry Action Group (AIAG) (1995) described the quality of the measurement data in the automotive industry as "the statistical properties of repeated measurements obtained from a measurement system under stable conditions". The measurement system, according to AIAG (1995) and Montgomery (2020), encompasses all the components involved in collecting data, including the instruments or gauges, the operator(s), the software, the method, or the protocols used, the conditions under which the data is collected, and the environment in which measurement takes place.

The measurement data often deviate from the reference or the true value of the characteristic being measured. Two critical aspects to consider for the quality of measurement data are accuracy and precision (Vardeman and Jobe, 2016). Both these factors indicate the closeness of the measured values to the true value. Accuracy pertains to the closeness of the average of measurements to the true value and can be affected by various factors such as the calibration of the measuring instrument, environmental conditions, and the

operator's skills. Precision, on the other hand, refers to the closeness of repeated measurements to each other and can be influenced by factors such as the sensitivity of the measuring instrument, the operator's ability to make the measurement and environmental conditions.

An analogy that helps us understand the concepts of accuracy and precision is a dartboard. If a player throws darts and the darts land on average close to the center, then the player is considered accurate. Conversely, if the player hits on average other areas of the dartboard, then the player is less accurate. If the darts consistently land very close to each other, then the player is precise. However, if the darts land all over the dartboard, then the player is imprecise. Figure 1.1 illustrates the four cases that arise based on high/low levels of accuracy and precision, with (a) being the most desirable and (d) being the least desirable case.

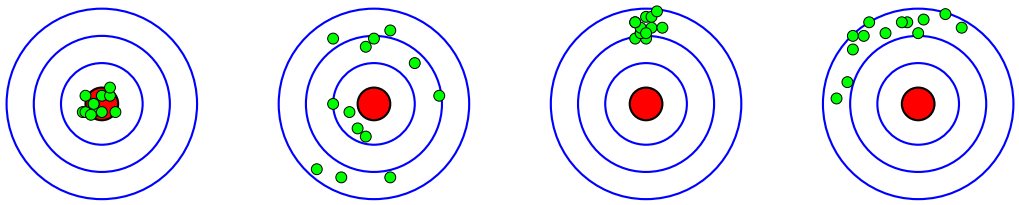

(a) (b) (c) (d)

Figure 1.1: Graphical illustration for accuracy and precision: (a) high accuracy and high precision, (b) high accuracy and low precision, (c) low accuracy and high precision, and (d) low accuracy and low precision. The centers of the circles are considered the reference points.

The error in measurement data can be caused by various factors such as the measurement device itself, the operator performing the measurement, the surrounding conditions, the time of measurement, or the items being measured, among others (Wheeler and Lyday, 1989). There are also other sources of measurement data error in industries, such as cycle-to-cycle, day-to-day, machine-to-machine, and so on (Taver, 1995).

Given the variety of factors that can cause measurement data errors, it is crucial to understand their sources for making an informed decision based on that data (Smith et al., 2007). For instance, in the three-dimensional (3D) printing industry, the calibration of

the 3D printer or the properties of the material being used can cause uncertainty in the measurement data. The failure of the manufacturer to consider the sources of error can result in the production of 3D-printed parts that are outside of the specified tolerance range. This can lead to negative consequences such as decreased product quality, increased production costs, and potentially decreased customer satisfaction and loss of business. Likewise, in chemical analyses, the accuracy of measurement devices or the conditions during data collection can be the root causes of uncertainty in measurement data, leading to reduced accuracy and precision. By gaining a comprehensive understanding of the sources of measurement data uncertainty and taking steps to minimize them, manufacturers and analysts can produce more accurate and precise results, whether they are 3D printed parts or chemical analyses, resulting in higher quality products.

A measurement system analysis is the practice of understanding and quantifying the variability in measurement data pertaining to the measurement system (Montgomery and Runger, 1993a). According to Montgomery and Runger (1993b), Burdick et al. (2003), and Majeske (2012), the main goal of most measurement system analyses is to:

(1) evaluate the measurement system's contribution to the overall variability of measurement data,
(2) identify the sources of variability within the measurement system, and
(3) determine if the measurement system is suitable for its intended purpose.

The error linked to the measurement system may stem from various factors within the measurement system. For instance, there may be multiple instruments or operators involved in collecting the data. The measurement system error can result from instrument wear and tear, operator's skill and training, or ambient conditions (Montgomery and Runger, 1993a). In many industries, a regular measurement system assessment study is performed to identify and quantify this uncertainty, as well as to pinpoint the underlying causes and address them accordingly.

1.2 Statistical properties of measurement systems

Measurement system analysis involves evaluating several statistical properties to determine the quality of a measurement system. In the manual by Automotive Industry Action Group (1995), these properties consist of bias, linearity, stability, repeatability, and reproducibility. Evaluating these properties is essential in ensuring that the measurement system is adequate. To develop these concepts, let us consider a *unit* to refer to the object or item being measured, which may be a manufactured product, a person, an animal, a physical

or chemical substance, or anything of which a characteristic is being measured. A physical quantity, property, or condition being measured is called *the measurand*.

Probability theory offers a useful framework for describing and analyzing the properties of measurement systems. Let the random variable U represent the measurand for a unit, and the random variable ϵ represent the error of the measurement system with mean δ and standard deviation σ_ϵ . One can model the actual measurement,

$$Y = U + \epsilon. \tag{1.1}$$

When the true value of the measurand is u and it is fixed, the actual measurement is modeled as,

$$Y = u + \epsilon, \tag{1.2}$$

As such, the expectation of the actual measurement is,

$$E(Y) = u + \delta. \tag{1.3}$$

The measurement of a unit is considered unbiased when the expected value of the actual measurement is equal to the true value of the measurand. This condition is met when δ is equal to zero (Vardeman and Jobe, 2016). If δ is non-zero, then the measurement bias is δ. A quantity $\delta > 0$ indicates that the measurement system overestimates the value of the measurand, while a $\delta < 0$ indicates that the measurement system underestimates the value of the measurand. Bias is a measure of the measurement system's accuracy. Figure 1.2 illustrates the measurement system bias via a schematic probability density function of Y and the elements u and δ where δ has a positive value.

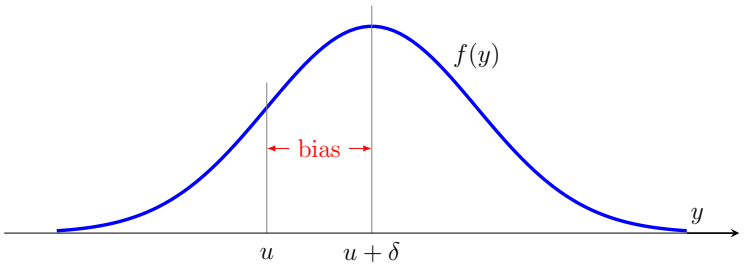

Figure 1.2: Representation of a positive bias through the probability density function of actual measurement Y, denoted as $f(y)$, the true value of the measurand, and the mean of the measurement system error.

It is desirable to reduce or minimize any biases in a measurement system, and if such biases exist, determine how they vary over the range of values being measured. The linearity property of a measurement system compares the actual measurement to the true value for different values of the measurand. According to the manual by Automotive Industry Action Group (1995) and ISO GUM (2008), the linearity property of a measurement system implies that the measurement system produces results that, on average, change at a constant rate over the range of values being measured.

Figure 1.3 shows four different examples of the linearity property, with plots (a) through (d) representing different scenarios. Plot (a) shows the ideal situation where the measurement system provides the true value of the measurand on average. Plot (b) of this figure indicates a fixed and positive bias for the measurement system, which does not depend on the measurand value. Plots (c) and (d) show situations where the difference between the measurement's expected and true values has a constant slope. Note that in (Vardeman and Jobe, 2016) a more restrictive condition for the linearity of a measurement system is considered, which corresponds to plot (b).

Another ideal property of a measurement system is that it consistently produces the same average result when used at different time frames to make measurements of the same unit with a fixed measurand. Statistical stability is the property that refers to the consistency of measurements over time. If the same measurement system produces similar average measured readings for each time frame during a length of time, it can be assessed as statistically stable (Automotive Industry Action Group, 1995). A measurement system with lower bias variation over time is considered more stable.

During the statistical stability analysis of a measurement system, the conditions to which the measurement system is exposed are a major point of discussion. For example, a measurement system that exhibits changes in its readings because of temperature fluctuations may not be considered statistically stable during those fluctuations but may be considered statistically stable once the temperature is stabilized (Automotive Industry Action Group, 1995).

Repeatability refers to the uncertainty in measurements obtained from the same measurement system when it is used multiple times over a short period, under the same conditions, to measure the same unit (Automotive Industry Action Group, 1995). For example, in a factory that produces metal parts, a measuring tool is used to measure the dimensions of each part. To assess the repeatability of the measuring tool, a single part is measured 10 times by the same operator, using the same measuring tool, and under the same conditions. If the differences between the measurements are small and within an acceptable range, then the measuring tool is considered to have good repeatability. However, if the differences be-

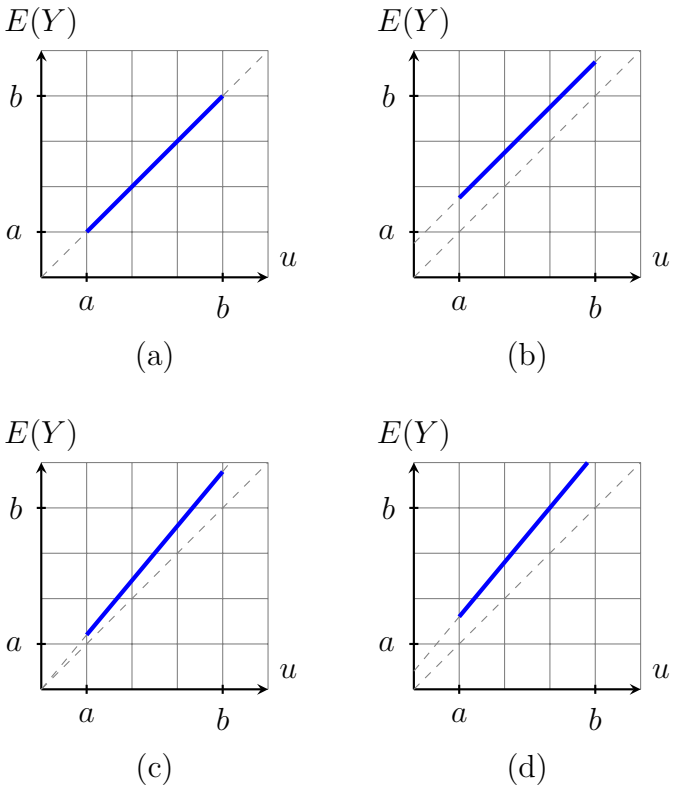

Figure 1.3: Plots of the linear relationship of the actual measurement and the values being measured. The scales of the vertical and horizontal axes are the same.

tween the measurements are large and outside of an acceptable range, then the measuring tool may be deemed poor or require maintenance to improve its repeatability.

The measurement system repeatability can be quantified under model (1.1). With a fixed true value, the variance of the actual measurement random variable is σ_ϵ^2. A measure of repeatability is the standard deviation of the actual measurement for a fixed measurand true value, determined by,

$$\sigma_{\text{repeatability}} = \sigma_\epsilon \,. \tag{1.4}$$

Figure 1.4 depicts a schematic representation of the probability density function of actual measurements for a fixed measurand u, along with the extent of imprecision resulting from the measurement system's repeatability.

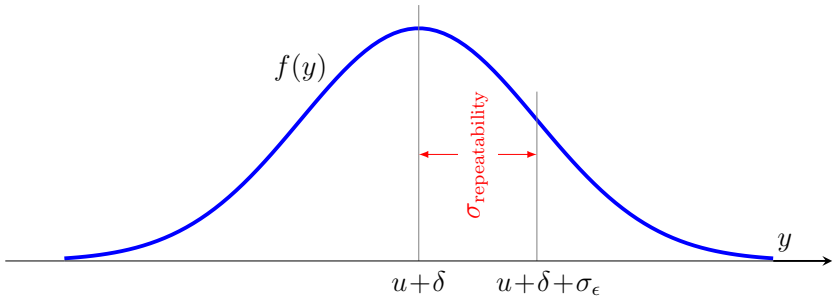

Figure 1.4: A graphical representation of the measurement system's repeatability size, depicted through the probability density function of the actual measurements. Here, δ represents the bias of the measurement system.

In some cases, there may be multiple measurement systems that are similar and could potentially be used for measuring. For instance, a particular piece of equipment could be operated by any of several operators. Reproducibility refers to the uncertainty in the measurement arising from changes in the measurement system conditions, which can be differences in either the gauge, operator or so on (Montgomery, 2020). To compare these measurement systems, one possible approach is to select a subset of available measurement systems and use them to measure a single fixed measurand (Vardeman and Jobe, 2016). In this context, the actual measurement can be modeled as,

$$Y = u + \Delta + \epsilon^*,$$

where Δ is a random variable with variance σ^2_Δ that represents the bias of the measurement system (e.g., the differences among gauges, operators, etc), and ϵ^* is a random variable with a mean of zero and variance σ^2_ϵ that represents the measurement system's imprecision error. We can assume that Δ and ϵ^* are statistically independent random variables. A measure of reproducibility is the standard deviation of the bias of measurement system (Vardeman and Jobe, 2016), determined by,

$$\sigma_{\text{reproducibility}} = \sigma_\Delta.$$

The variance of the actual measurement can be expressed as the sum of the variance due to differences between measurement systems (i.e., σ^2_Δ) and the variance due to uncertainty within a single measurement system (i.e., σ^2_ϵ) (Montgomery and Runger, 1993a). Then the

quantity,

$$\sigma_{ms} = \sqrt{\sigma_{\Delta}^2 + \sigma_{\epsilon}^2}, \tag{1.5}$$

provides an estimate of the overall uncertainty associated with the measurement system. This quantity is often used to assess the quality of a measurement system and to identify sources of variation that may need to be addressed. Figure 1.5 illustrates the relationship between σ_{ms}, $\sigma_{\text{repeatability}}$ and $\sigma_{\text{reproducibility}}$.

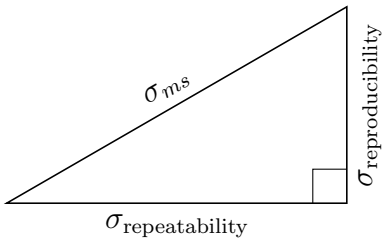

Figure 1.5: The relationship between the uncertainty in the measurement system, repeatability, and reproducibility.

1.3 Parameters for assessing measurement systems

This section provides an overview of some of the fundamental parameters involved in measurement system assessment. To begin, we assume that the characteristics of the units being measured and the error of the measurement system are statistically independent. It is well known that the total variance of the measurement data may be decomposed into two variance components (Burdick et al., 2003; Montgomery and Runger, 1993a), say

$$\sigma_t^2 = \sigma_u^2 + \sigma_{ms}^2 \tag{1.6}$$

where σ_u^2 and σ_{ms}^2 are, respectively, the variances of the units and measurement system error.

AIAG (1995) defines percentage R&R ratio as

$$\%\text{R\&R} = \frac{\sigma_{ms}}{\sigma_t} 100\% \,. \tag{1.7}$$

According to the guidelines set by AIAG (1995, Page 60), a measurement system is considered acceptable if the percentage R&R ratio is less than 10%. If the percentage R&R ratio value falls between 10% and 30%, the measurement system's acceptability will depend on factors such as the significance of the application and the cost of any necessary improvements. If the R&R ratio exceeds 30%, it is recommended to take steps to improve the measurement system.

Larsen (2002) and Burdick and Larsen (1997) note the signal-to-noise ratio as,

$$\text{SNR} = \frac{\sigma_u}{\sigma_{ms}} \cdot \tag{1.8}$$

The AIAG (1995) and Burdick et al. (2003) employ a scaled by $\sqrt{2}$ version of (1.8) as the signal-to-noise. Furthermore, this scaled version is commonly referred to as the gauge discrimination ratio which serves the purpose of determining whether the measurement process has sufficient resolution to effectively monitor the feature of interest. An approval value of 5 or greater is recommended by the AIAG, and a value less than 2 indicates that the measurement system is unacceptable for monitoring the process. Steiner and MacKay (2005, Page 97) suggest more moderate acceptability criteria where any value of SNR obtained by (1.8) exceeding 3 shows the validity of the measurement system, while a value less than 2 is considered as unacceptable.

An alternative ratio to compare the quality of a measurement system is the intra-class correlation coefficient expressed as (Mader et al., 1999; Majeske and Andrews, 2002),

$$\text{ICC} = \frac{\sigma_u^2}{\sigma_t^2} = \frac{\sigma_u^2}{\sigma_u^2 + \sigma_{ms}^2} \cdot \tag{1.9}$$

This measure of quality represents the proportion of the total variance accounted for by the variance among units. Donner and Eliasziw (1987) consider the intra-class correlation coefficient to be a measure of reliability. This ratio is indicative of the relationship between the correlation in repeated measurements on the same subject (Majeske and Andrews, 2002). When the measurement system variability is negligible relative to that of the units, the intra-class correlation coefficient is close to one. If the measurement system variability is significant compared with the variability of units, the intra-class correlation coefficient gets smaller.

The AIAG (1995) uses the precision-to-tolerance ratio (PTR) as another approval criterion, which is the ratio of two widths: the width of tolerance and the distribution of quality characteristics. If we let U and L as the upper and lower specification limits of the process, the PTR is expressed as

$$\text{PTR} = \frac{\kappa\,\sigma_{ms}}{U - L}\,, \tag{1.10}$$

where $\kappa = 5.15$ and $\kappa = 6$ are two common choices. With $\kappa = 5.15$ and $\kappa = 6$, the numerator represents the length of the interval capturing 99% and 99.73% of a normal distribution with a variance of σ^2_{ms}, respectively. The approval value of PTR in the literature differs from 0.1 to 0.3. Montgomery and Runger (1993a) suggest a value of 0.1 or less for the adequacy of a measurement system. Mader et al. (1999) mentions an approval value not greater than 0.2. Barrentine (2003) recommends that a PTR value not exceed 0.3. Meanwhile, Montgomery and Runger (1993a) note not to rely too much on PTR. It is more important that a measurement system is capable of detecting meaningful variability in units. A process with low variability can tolerate a measurement system with a higher PTR. They argued that the %R&R and the SNR are more informative measures than PTR.

1.4 Guidelines and considerations

The standard measurement system assessment plan (Montgomery and Runger, 1993a; Burdick et al., 2003) is to randomly select a number of units from the process and have each operator perform repeated measurements on each selected unit. A two-way model is frequently applied to data from this experiment that divides the measurement error into two components: a systematic error caused by the operators (reproducibility) and a repeatability error.

The number of units selected, the number of measurement trials conducted for each unit, and the number of operators involved are important design considerations. The Automotive Industry Action Group (2003) manual provides guidelines for selecting these numbers. It suggests selecting 10 units and conducting 2 to 3 measurement trials for each unit when 2 to 3 operators are involved, resulting in a total number of 40 to 90 measurements. When dealing with automated measurement systems or single-operator scenarios, the recommended number of units to select is 10, with 6 measurement trials conducted for each unit. In a similar scenario with a sample size of 60, Shainin (1992) recommends an alternative plan where a maximum of 30 units are selected, and each unit is measured

twice. For scenarios where baseline data is available, Browne, MacKay and Steiner (2010); Browne, Steiner and MacKay (2010); Stevens et al. (2013) explore various plans that configure both the number of the units and the number of repeated measurements needed to meet the desired specific specifications.

Measurement systems unaffected by operator bias or human factors such as skills, knowledge, or attitudes are commonly known as measurement systems with no operator effect. These systems are typically automated, relying on machine-controlled processes like automated gauges or scanners for conducting measurements. They hold particular significance in industries such as smart manufacturing (Suriano et al., 2015; Yang et al., 2021; Majeske, 2012), aerospace, and the automotive sector (Drouot et al., 2018; Browne et al., 2009). By treating the operator effect as negligible or nonexistent and thus excluding it from consideration, we can use a simplified one-way model to capture the inherent variabilities within the measurement system across repeated measurements. Notable studies in the field of measurement system assessment that utilize one-way models include the works of Browne et al. (2009); Browne, Steiner and MacKay (2010); Weaver et al. (2012).

1.5 Assessing multivariate and functional data measurement systems

While the measurement system assessment techniques and tools discussed earlier are useful for evaluating the measurement system of a single variable, their applicability is limited when it comes to other data types, such as multivariate and 'functional' data. Multivariate data refers to datasets that contain multiple variables or features, where these variables may exhibit relationships with one another. On the other hand, functional datasets are composed of samples from continuous and smooth functions, that vary over a continuous domain, such as time, space, or another continuous parameter. These data types, both multivariate and functional, are increasingly recognized as crucial in fields like neuroscience, environmental science, and engineering. To gain a better understanding, let us explore a few examples where the measurement system analysis is applied to these data types.

Example 1.1. *(Measurement system of the imbalance (Voelkel, 2003)). Imbalance is a frequent occurrence in machinery, causing problems such as vibration, abrasive wear, and functional issues in rotating parts like tires and discs. To address these issues, it is crucial to have an accurate measuring device that can quantify the degree of imbalance. A measurement system assessment study is valuable in this context as it helps differentiate the variation caused by the measurement system from the overall variation.*

The imbalance occurring within a single plane can be characterized as the vector connecting the expected mass center and the actual center of rotation, representing a two-dimensional property. This vector can be expressed in either a Cartesian coordinate system or a polar coordinate system. According to Voelkel (2003), conventional univariate measurement system assessment methods do not provide adequate insights for analyzing this two-dimensional data.

The example below showcases the measurement system assessment problem for a dataset consisting of samples of functional data, in the context of foot pressure analysis.

Example 1.2. *(Measurement system of plantar pressure). The study of foot pressure has garnered significant attention in biomedical and sport-related research. The primary objective of foot pressure analysis is to gain insights into normal walking patterns, track the development of walking abilities, and identify any irregular phenomena. The analysis of foot pressure has wide-ranging applications, including the design of footwear, assessment of sports performance, improvement of balance, and medical diagnostics. In the realm of healthcare, the distribution of plantar pressure can offer valuable insights into gait instability among the elderly and individuals with balance impairments. An illustrative example is the freezing of gait, which can serve as a symptom of Parkinson's disease (Shalin, 2021). This discussion underscores the critical importance of employing plantar pressure measurement systems that offer high accuracy and reliability, ensuring the validity and effectiveness of the obtained results.*

Two types of measurement systems commonly used for collecting plantar pressure are platform systems and in-shoe systems. For example, a study by Shu et al. (2010) divides the foot sole into 15 areas to study normal adult plantar pressure. Within each step, the pressure is a continuous function of time for each area of interest. Meanwhile, Shi (1993) uses data from an experiment with 34 adult participants and five steps recorded for each person to develop a functional data one-way random effect model. This model has two sources of variability: the variability between the subjects and the variability within the subjects. Estimating both variabilities is crucial for further analytical developments.

The following example serves as an illustration of the measurement system assessment problem, focusing on a dataset comprising functional data related to seat belt extraction and retraction forces in vehicles.

Example 1.3. *(Seat belt extraction and retraction forces in vehicle safety.). Seat belts, as a crucial element of safety, play a significant role in preventing fatalities, necessitating a focus on their functionality and comfort. Key to this is the assessment of extraction and retraction forces involved in fastening seat belts within a vehicle.*

The extraction force, representing the effort needed to pull the seat belt from its retracted position for fastening, and the retraction force, exerted by the seat belt mechanism to retract it after extension, are vital considerations for achieving a balance between safety and comfort. Manufacturers meticulously engineer these forces, conducting tests that output force curves in dedicated extraction/retraction force-test setups. These force curves are a result of rigorous testing, aiming to optimize extraction and retraction forces based on factors such as crash scenarios, occupant sizes, and diverse driving conditions, aligning with safety standards and regulations. However, before committing resources to these experiments, manufacturers must assess the capability of their measurement systems to accurately gauge these forces. Studies by Ruck et al. (2020) and McKendry (2023) investigate and explore this assessment challenge using a dataset of 250 force-by-distance curves.

Assessing the measurement systems for multivariate and functional data presents unique challenges, due to the complex structure of these data types (Majeske, 2008). To address the measurement system assessment for multivariate data, a straightforward approach is to analyze each variable independently and conduct separate measurement system studies. The effectiveness of this approach depends on the specific nature of the problem at hand. It can be particularly beneficial in situations where the evaluation of the measurement system is focused on individual variables, and/or when the variables exhibit either weak or no correlation. See, e.g., Esmaeeli et al. (2019). Additionally, this approach is well-suited when the variables possess distinct characteristics and requirements that are better captured by separate assessments. For instance, a study focused on human health involves measuring multiple indicators, such as heart rate, blood pressure, and body temperature. Each of these indicators has its unique characteristics and requires specific measurement devices. By independently assessing the measurement systems for each indicator, valuable insights can be gained regarding each indicator. This approach enables targeted improvements in the measurement systems for each indicator.

When features exhibit moderate to strong correlations, evaluating them as independent entities can lead to an oversight of the interactions between variables. The performance of a measurement system can be influenced by various factors that introduce errors in all feature measurements. Therefore, comprehensively evaluating the system's performance requires considering the interrelationships among variables and understanding how the system behaves under these conditions. This potential oversight of interactions between variables is demonstrated in studies conducted by Sweeney (2007) and Wang and Yang (2007).

Another potential issue arises when variables are treated independently, and the measurement system performs well for some inputs during the assessment but fails for others.

This scenario was demonstrated in a case study by Majeske (2008), which involved the measurements of four characteristics of a sheet-metal panel. The study highlighted that the presence of a few univariate quality measures that do not meet the required limitations does not imply the incapability of the multivariate measurement system. This emphasizes the need to assess the measurement system's performance as a whole, considering its behavior across all features rather than relying solely on individual assessments.

Assessing measurement systems for functional data presents even greater challenges, requiring several modifications and considerations. In functional data, individual observations are samples of functions. Typically, when a process is monitored, the measurements are recorded at discrete points, producing, possibly, a high-dimensional vector of observations. Our consideration of this class of data as a special problem is prompted by at least two factors. First, the process can be observed at a few points rather than on a high number of points. Second, the choice of sampling points can vary among functional observations. Notably, the assessment of measurement systems with functional data remains largely unexplored in the existing literature.

1.6 Roadmap of the thesis

To the best of the author's knowledge, no literature exists on assessing measurement systems when dealing with functional observations. This dissertation's primary focus is to enrich the measurement system assessment studies of multivariate measurements and extend to functional measurements. In our investigation, we observed a scarcity in literature even for multivariate data, and surprisingly, a systematic theoretical investigation for univariate measurements in measurement system analysis is also lacking. This thesis presents the methodology and theoretical framework for measurement system assessments in a consistent format. The primary emphasis is on a one-way random effect model using a balanced standard design. Continuing, the thesis is divided into the following chapters:

Chapter 2 conducts a detailed theoretical examination of measurement system assessment studies when dealing with univariate data. The chapter explores various methods employed for estimating variance components and other pertinent parameters crucial for measurement system analysis. A comprehensive scrutiny of the statistical properties of these estimators is provided, encompassing aspects such as bias, sampling variance, convergence properties, confidence intervals, and robustness issues. This foundational understanding serves as a springboard for extending these analyses to the more intricate domains of multivariate and functional data, a focal point of subsequent chapters.

In Chapter 3, we expand the scope of measurement system assessment to encompass multivariate data. The chapter begins by adapting the definitions of measurement system assessment parameters to multivariate settings, employing transformations that yield summary scalar metrics for variance-covariance matrices. Specifically, we focus on the determinant, trace, and Frobenius norm of variance-covariance matrix components. Building upon the statistical concepts and properties discussed in Chapter 2, we conduct a targeted review of existing theories related to variance-covariance component estimation in a one-way random effect model with equal replications. A key emphasis is placed on the statistical properties of the estimators of the proposed parameters in measurement system assessment, namely the signal-to-noise ratio. Our investigation includes an exploration of its convergence properties and the construction of approximate confidence intervals.

In Chapter 4, we advance our exploration by establishing a framework to investigate measurement system assessments, extending our scope to functional data types, where observed data entities are trajectories of random processes. To effectively capture the distinctive features of functional data, we expand the definition of parameters utilized in evaluating measurement systems for univariate data. This extension involves the application of a bounded operator on covariance kernels, with a specific focus on the trace and L^2 operators.

For the estimation of measurement system assessment parameters, we introduce methods to estimate covariance kernel components associated with the one-way model. Initially, we delve into a classical estimation approach without smoothing. Subsequently, we explore specialized tools in functional data analysis to obtain smooth estimates of the covariance kernel.

In Chapter 5, we conduct a detailed analysis of a real-world dataset, inherently considered as functional data. This dataset encompasses measurements of the surface roughness of printed products in the context of additive manufacturing. Our examination starts with a comprehensive analysis of this functional dataset, employing statistical methods tailored for both univariate and multivariate data types. Additionally, we leverage techniques from functional data analysis, a topic explored throughout this thesis.

Chapter 2

Measurement System Assessment Study with a Single Characteristic: A Systematic Review

2.1 Introduction

The field of measurement system assessment has seen considerable methodological advancements in the case of univariate data types. The Automotive Industry Action Group (2003) has developed various guidelines and standards for measurement system analysis that provide a comprehensive guide for conducting analysis and interpreting the results. Montgomery and Runger (1993a) demonstrate the practical aspects of designing and conducting a measurement system study, while Burdick et al. (2003) review the methods used to evaluate the capability of a measurement system with a focus on the ANOVA procedure. Additionally, Browne, MacKay and Steiner (2010), Stevens et al. (2010) and Stevens et al. (2013) offer several plans as alternatives to the standard plan for measurement system assessment. The methodologies for measurement system analysis have been extended to encompass measurement setups that involve non-numerical scales. For example, Van Wieringen and De Mast (2008) and Danila et al. (2010) demonstrate a methodology for assessing measurement systems that measure on a binary scale and evaluate units as pass or fail. In addition, Culp et al. (2018) propose a methodology for measurement system analysis with ordinal measurements, while Osthus et al. (2021) develop an approach to assess repeatability and reproducibility with count measurements. However, to the best knowledge of the author, there is still a lack of documentation on the theoretical properties of these

methods and their investigation in the literature, despite the significant methodological inclusiveness in the field.

This chapter presents a comprehensive theoretical investigation of measurement system assessment studies involving univariate data. Specifically, we examine statistical topics and properties related to the parameters of measurement system analysis, with a focus on the one-way random effect model using a balanced standard plan. Although the one-way model is advantageous for its simplicity, our investigation has revealed complexity in certain aspects. Nonetheless, the knowledge gained from this investigation is expected to serve as a solid foundation for extending these theoretical analyses to other situations, such as two-way analysis of variance and beyond. The author of this thesis is interested in exploring these areas further, but this will be beyond the scope of this thesis. So, in this thesis, we focus on the one-way random effect model only, as it is often sufficient for many practical measurement system assessment scenarios.

Additionally, by deeply exploring the one-way model, our goal is to provide a comprehensive understanding of how to assess the performance and variability of measurement systems. This knowledge will serve as a solid foundation for extending these analyses to multivariate and functional data, which will be of particular interest in Chapters 3 and 4.

This chapter is organized as follows: In Section 2.2, we present the univariate one-way ANOVA model, a statistical framework to assess the variability of the measurement system. We establish our basic notation and parameters to gauge measurement system quality. These parameters are the variance components and the ratio of variance components. These key statistical parameters are investigated in greater detail throughout this chapter. Continuing, Section 2.3, provides a preliminary analysis of the univariate one-way ANOVA model, laying the groundwork for a deeper understanding of the measurement systems. Different techniques for estimating the relevant parameters are outlined in Section 2.4. In Section 2.5, we provide a comprehensive examination of the statistical properties linked to the parameters of interest, covering the estimator's bias, sampling variance, hypothesis testing, convergence properties, and confidence intervals. In Section 2.6 we examine the robustness issues when the model is misspecified. Additionally, Section 2.7 offers supplementary materials and proofs that further enrich the chapter's contents and insights.

2.2 The univariate one-way model

We consider a setting where an experiment is being conducted with a randomly selected sample of $a > 2$ units from a population of units. Throughout this chapter, we will refer to the entity being measured in our study as a unit, and the sample size will correspond to the total number of these units. Each unit in the sample is measured $r > 1$ times. In this setting, the order in which the units are measured is determined randomly. See, e.g., (Automotive Industry Action Group, 1995, Section 3). It is assumed that the measurand remains unchanged across the repeated measurements. The model used to express the measured values is,

$$Y_{ij} = \mu + U_i + \epsilon_{ij}, \quad \text{for } i = 1, \ldots, a, \text{ and } j = 1, \ldots, r, \tag{2.1}$$

where Y_{ij} is the jth repeated measurement for the ith unit, μ is a general mean parameter, U_i represents the random main effect of unit i, and ϵ_{ij} represents the random measurement error associated with the jth replicate measurement taken from unit i. All U_i's are assumed to be independent and identically distributed (i.i.d.) $\mathcal{N}(0, \sigma_u^2)$ random variables, and all ϵ_{ij}'s are i.i.d. $\mathcal{N}(0, \sigma_\epsilon^2)$ random variables. Furthermore, for i fixed, we treat each U_i and ϵ_{ij} as being mutually independent.

Under the one-way model of (2.1), while the random variables U_i's and ϵ_{ij}'s are uncorrelated, the measurements Y_{ij}'s are not uncorrelated for all i and j. When considering repeated measurements j and j' of unit i, we have,

$$\text{Cov}(Y_{ij}, Y_{ij'}) = \sigma_u^2 \quad \text{for } j \neq j', \tag{2.2}$$

whereas for measurements of different units, one has,

$$\text{Cov}(Y_{ij}, Y_{i'j'}) = 0 \quad \text{for } i \neq i', \text{and any } j, j'. \tag{2.3}$$

As Y_{ij}'s are normally distributed random variables, the zero covariance of (2.3) signifies the independence of measurements of different units. Conversely, the repeated measurements made on each unit are dependent. In view of (2.1), measurement Y_{ij} has variance,

$$\sigma_t^2 = \sigma_u^2 + \sigma_\epsilon^2 . \tag{2.4}$$

The variance quantities σ_u^2 and σ_ϵ^2 which make up the measurement total variance σ_t^2 are called variance components.

It is desirable to have a measure to assess the quality of the measurement system. The

statistic used for this purpose is the ratio of the two aforementioned variance components,

$$\rho = \frac{\sigma_u^2}{\sigma_\epsilon^2} \cdot \tag{2.5}$$

A smaller value of ρ suggests that the dominant source of variation is the measurement error, while larger values of ρ indicate that the measurement error is not the primary cause of variation in the observed data. The parameters of measurement system assessment outlined in Chapter 1, i.e., the percentage R&R ratio, SNR, and the intra-class correlation coefficient, can be related to ρ through $\%\text{R\&R} = (1+\rho)^{-1/2} \times 100\%$, $\text{SNR} = \rho^{1/2}$, and $\text{ICC} = 1/(1+\rho^{-1})$.

2.3 Preliminary analysis

In the context of the one-way model (2.1), there are two sources of variation: the units (U) and the measurement errors (ϵ). Here, the source refers to the underlying factors or components contributing to the variation observed in measurement data (Y).

Two sums of squares that are the basis for the analysis of the variance components of the one-way model (2.1) are,

$$SS_u = r \sum_{i=1}^{a} (\overline{Y}_{i\cdot} - \overline{Y}_{\cdot\cdot})^2, \tag{2.6}$$

$$SS_\epsilon = \sum_{i=1}^{a} \sum_{j=1}^{r} (Y_{ij} - \overline{Y}_{i\cdot})^2 , \tag{2.7}$$

where $\overline{Y}_{i\cdot} = \frac{1}{r}\sum_{j=1}^{r} Y_{ij}$ is the mean of the measurements from the ith unit, and $\overline{Y}_{\cdot\cdot} = \frac{1}{ar}\sum_{i=1}^{a}\sum_{j=1}^{r} Y_{ij}$ is the overall mean of measured data. There are two means of squares,

$$MS_u = \frac{r}{a-1} \sum_{i=1}^{a} (\overline{Y}_{i\cdot} - \overline{Y}_{\cdot\cdot})^2, \tag{2.8}$$

$$MS_\epsilon = \frac{1}{a(r-1)} \sum_{i=1}^{a} \sum_{j=1}^{r} (Y_{ij} - \overline{Y}_{i\cdot})^2 . \tag{2.9}$$

The total corrected sum of squares is defined as

$$SS_t = \sum_{i=1}^{a}\sum_{j=1}^{r}(Y_{ij} - \overline{Y}_{\cdot\cdot})^2. \tag{2.10}$$

This total sum of squares can be partitioned into,

$$SS_t = SS_u + SS_\epsilon\,. \tag{2.11}$$

This classification based on the source of variation is known as the analysis of variance (ANOVA). The ANOVA classification associated with the one-way model of (2.1) is demonstrated in Table 2.1.

With the normal distribution of U_i's and ϵ_{ij}'s and their mutual independence, SS_u and SS_ϵ are two independent statistics where,

$$\frac{SS_u}{\mathrm{E}\left[MS_u\right]} \sim \chi^2_{a-1}\,, \quad \text{and} \quad \frac{SS_\epsilon}{\mathrm{E}\left[MS_\epsilon\right]} \sim \chi^2_{a(r-1)}\,. \tag{2.12}$$

The expected mean of squares terms are,

$$\mathrm{E}\left[MS_u\right] = \sigma^2_\epsilon + r\sigma^2_u \quad \text{and} \quad \mathrm{E}\left[MS_\epsilon\right] = \sigma^2_\epsilon\,. \tag{2.13}$$

The distributions of SS_u and SS_ϵ given in (2.12) lead to the result that

$$F = \frac{MS_u/\mathrm{E}\left[MS_u\right]}{MS_\epsilon/\mathrm{E}\left[MS_\epsilon\right]} = (1+r\rho)^{-1}\frac{MS_u}{MS_\epsilon} \tag{2.14}$$

has a central F-distribution with $a-1$ and $a(r-1)$ degrees of freedom.

To begin a measurement system study, Montgomery and Runger (1993a) recommend

Table 2.1: The analysis of variance classification for one-way model (2.1).

Source	Degree of freedom	Sum of squares	Mean of squares
U	$\mathrm{df}_u = a-1$	$SS_u = r\sum_{i=1}^{a}(\overline{Y}_{i\cdot} - \overline{Y}_{\cdot\cdot})^2$	$MS_u = \dfrac{SS_u}{a-1}$
ϵ	$\mathrm{df}_\epsilon = a(r-1)$	$SS_\epsilon = \sum_{i=1}^{a}\sum_{j=1}^{r}(Y_{ij} - \overline{Y}_{i\cdot})^2$	$MS_\epsilon = \dfrac{SS_\epsilon}{a(r-1)}$
Total	$ar-1$	$SS_t = \sum_{i=1}^{a}\sum_{j=1}^{r}(Y_{ij} - \overline{Y}_{\cdot\cdot})^2$	

conducting an initial analysis to investigate the factors contributing to the variation of measured data. This analysis can be achieved through a hypothesis test for σ_u^2, which we discuss in Section 2.5.3. Once the significance of this variance component is statistically tested, one can move forward to estimate the variance components.

2.4 Point estimation

The field of variance component estimation is extensively explored for the one-way model, with a wealth of literature on the subject. For a comprehensive review of methods in this domain, readers can refer to references such as Klotz et al. (1969); Sahai (1979); Khuri and Sahai (1985); Robinson (1987); Searle et al. (1992). The present section provides a concise overview of several established techniques for estimating the variance components within the context of the one-way model as defined by Equation (2.1). Specifically, we examine the ANOVA-based estimators, uniformly minimum variance unbiased estimator (UMVUE), and maximum likelihood estimator of variance components. Moreover, we utilize the common approach of plug-in estimator to obtain estimators for ratios of variance components, which are being used in the context of measurement system assessment studies.

2.4.1 ANOVA estimation

A typical procedure for estimating the variance components is through the use of the ANOVA method. The procedure is akin to the method of moments. Each sum (or mean) of the squares' expected value is a linear function of the variance components. The ANOVA estimation method involves solving these equations for σ_u^2 and σ_ϵ^2, subsequently substituting the expected means of squares with their corresponding observed values. Thus, the ANOVA estimators for σ_u^2 and σ_ϵ^2 can be derived as,

$$\widehat{\sigma_u^2} = \frac{1}{r}(MS_u - MS_\epsilon) \qquad \text{and} \qquad \widehat{\sigma_\epsilon^2} = MS_\epsilon \,. \tag{2.15}$$

These estimators are unbiased. Substituting the ANOVA estimators (2.15) outlined in (2.5), the plug-in estimator of ρ is,

$$\widehat{\rho}_{\text{ANOVA}} = \frac{1}{r}\left(\frac{MS_u}{MS_\epsilon} - 1\right). \tag{2.16}$$

One drawback of this ANOVA estimator is its potential to yield a negative estimate for the variance component σ_u^2. The estimator $\widehat{\sigma_u^2}$ obtained as in (2.15) will result in a negative value whenever $MS_u < MS_\epsilon$. Such an occurrence depends on the data characteristics. In model (2.1), the probability of such an event occurring is

$$\Pr\left(MS_u < MS_\epsilon\right) = \Pr\left(F < (1 + r\rho)^{-1}\right), \tag{2.17}$$

where random variable F has an F-distribution with $a - 1$ and $a(r - 1)$ degrees of freedom. The probability defined in (2.17) is a function of the sample size, denoted by a, and the number of measurement replications, denoted by r, which together comprise the total number of measurements $N = ar$. Additionally, it depends on the ratio of variance components denoted by ρ. A lower probability of $MS_u < MS_\epsilon$ is preferred, indicating a higher likelihood that the ANOVA estimates of variance components align with the parameter space requirements, specifically, $\sigma_u^2 \in \mathbb{R}^{0+}$, and $\sigma_\epsilon^2 \in \mathbb{R}^{+}$, where $\mathbb{R}^{0+}$ and $\mathbb{R}^{+}$ denote, respectively, the set of non-zero real numbers and positive real numbers.

To better understand the likelihood of this scenario, Figure 2.1, illustrates the relationship between the probability of $MS_u < MS_\epsilon$ and ρ across four sample sizes ($a = 5, 10, 20, 30$) and three values of replications ($r = 2, 3, 6$), a total of 12 plans. As observed in Figure 2.1, increasing the number of measurements, i.e., $N = ar$, either through larger sample sizes or increased replications, results in a reduction in the probability of $MS_u < MS_\epsilon$. Generally, larger values of ρ are more advantageous (Majeske and Andrews, 2002). A higher value of ρ corresponds to a decreased probability of $MS_u < MS_\epsilon$. It is important to note that the recommended range for ρ can vary depending on the specific context. For instance, as pointed out by Steiner and MacKay (2005), improving the measurement system is advisable if ρ falls below approximately 4.

A negative estimate of variance can be interpreted in different ways (Thompson, 1962). It might suggest that the actual value of the variance component is insignificantly different from zero, implying that the model could potentially be simplified. This assertion can gain statistical support through a hypothesis testing procedure, testing the null hypothesis $H_0 : \sigma_u^2 = 0$.

A negative variance estimate can be a consequence of insufficient data, prompting the need to incorporate more data. When assessing a measurement system, baseline (or historical) data are readily available. The use of baseline data is recommended in the literature (Steiner and MacKay, 2005, Chapter 7). The significant benefits of incorporating baseline data into measurement system assessment are quantified by Stevens et al. (2013).

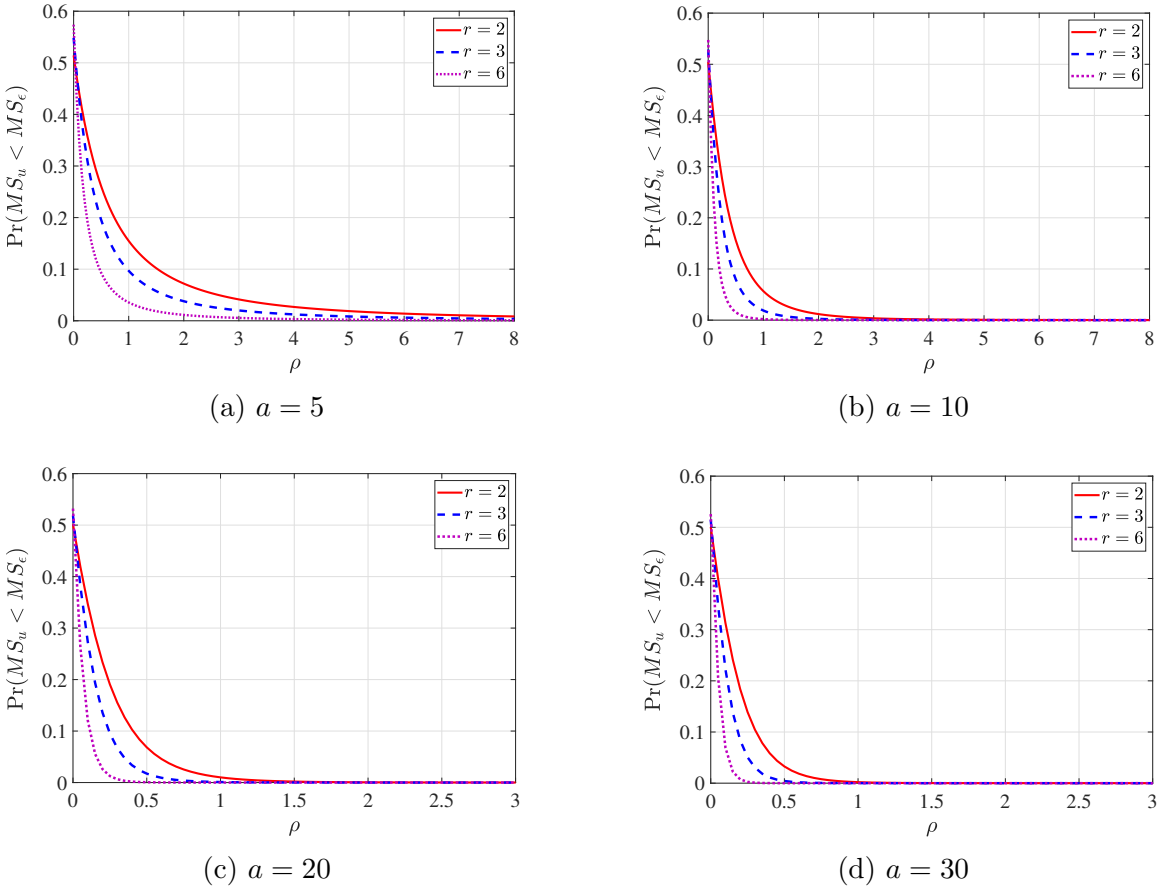

(a) $a = 5$ (b) $a = 10$

(c) $a = 20$ (d) $a = 30$

Figure 2.1: The probability of $MS_u < MS_\epsilon$ as a function of ρ for $a = 5, 10, 20, 30$ and $r = 2, 3, 6$, when the random effects U_i and measurement errors ϵ_{ij} are normally distributed.

2.4.2 Non-negative ANOVA estimation

When considering $\sigma_u^2 = 0$, the ANOVA estimator of σ_ϵ^2 is calculated as follows,

$$\widehat{\sigma_\epsilon^2} = \frac{SS_t}{ar - 1}. \tag{2.18}$$

This formula for $\widehat{\sigma_\epsilon^2}$ can be expressed as $(MS_u \mathrm{df}_u + MS_\epsilon \mathrm{df}_\epsilon)/(\mathrm{df}_u + \mathrm{df}_\epsilon)$, representing a pooled variance estimator of MS_u and MS_ϵ. In cases where $MS_u < MS_\epsilon$, it can be demonstrated that $SS_t/(ar-1) < MS_\epsilon$. Conversely, if $MS_\epsilon < MS_u$, then

$MS_\epsilon < SS_t/(ar-1)$[1]. Utilizing this relationship, the non-negative ANOVA estimators of variance components are expressed as follows,

$$\widehat{\sigma_u^2} = \max\left(0, \frac{1}{r}\left(MS_u - MS_\epsilon\right)\right), \tag{2.19a}$$

$$\widehat{\sigma_\epsilon^2} = \min\left(\frac{SS_t}{ar-1}, MS_\epsilon\right). \tag{2.19b}$$

These non-negative ANOVA estimators of variance components are no longer unbiased and they demonstrate smaller mean square errors compared to their ANOVA counterparts, as noted by Lee and Kapadia (1992).

The plug-in estimator of ρ using the non-negative estimators of variance components is given by,

$$\widehat{\rho}_{\text{NANOVA}} = \max\left(0, \frac{1}{r}\left(\frac{MS_u}{MS_\epsilon} - 1\right)\right). \tag{2.20}$$

2.4.3 Uniformly minimum variance unbiased estimators

The UMVUEs of variance components have been developed for the one-way model. Let $\boldsymbol{\theta} = (\mu, \sigma_u^2, \sigma_\epsilon^2)^\top$ be the vector of unknown parameters in model (2.1) and suppose the observed data of the measurements on unit i are arranged by $\boldsymbol{y}_i = (y_{i1}, \ldots, y_{ir})^\top$. The likelihood function of $\boldsymbol{\theta}$, as set up in (Searle et al., 1992, Chapter 3), is given by

$$\mathcal{L}(\boldsymbol{\theta}) = c(\sigma_u^2, \sigma_\epsilon^2) \exp\left\{\frac{-1}{2\sigma_\epsilon^2}\sum_{i=1}^{a}\sum_{j=1}^{r}(y_{ij} - \overline{y}_{i\cdot})^2 - \frac{1}{2(\sigma_\epsilon^2 + r\sigma_u^2)}\sum_{i=1}^{a}\sum_{j=1}^{r}(\overline{y}_{i\cdot} - \overline{y}_{\cdot\cdot})^2 - \frac{ar(\mu - \overline{y}_{\cdot\cdot})^2}{2(\sigma_\epsilon^2 + r\sigma_u^2)}\right\} \tag{2.21}$$

where $c(\sigma_u^2, \sigma_\epsilon^2) = (2\pi)^{-\frac{1}{2}ar}(\sigma_\epsilon^2)^{-\frac{1}{2}a(r-1)}(\sigma_\epsilon^2 + r\sigma_u^2)^{-\frac{a}{2}}$, and $\overline{y}_{i\cdot} = \frac{1}{r}\sum_{j=1}^{r} y_{ij}$ and $\overline{y}_{\cdot\cdot} = \frac{1}{ar}\sum_{i=1}^{a}\sum_{j=1}^{r} y_{ij}$. For a more in-depth explanation of the derivation of the likelihood function, refer to Section 2.7, where you will find additional details.

From the likelihood function structure, it can be inferred that the joint distribution of Y_{ij}'s belongs to the exponential family and the vector $(\overline{Y}_{\cdot\cdot}, MS_u, MS_\epsilon)^\top$ constitutes a jointly sufficient and complete statistic for the parameter vector $\boldsymbol{\theta} = (\mu, \sigma_u^2, \sigma_\epsilon^2)^\top$. By employing an unbiased estimator of $\boldsymbol{\theta}$, as established by Lehmann-Scheffé theorem (1950, 1955), this estimator becomes the UMVUE for $\boldsymbol{\theta}$, only depending on $(\overline{Y}_{\cdot\cdot}, MS_u, MS_\epsilon)^\top$. Note

[1]For positive values of a, b, c, and d where $\frac{a}{b} < \frac{c}{d}$, it can be shown that $\frac{a}{b} < \frac{a+c}{b+d} < \frac{c}{d}$.

that the ANOVA estimators of variance components outlined in (2.15) are unbiased, as $E(\widehat{\sigma_u^2}) = \sigma_u^2$ and $E(\widehat{\sigma_\epsilon^2}) = \sigma_\epsilon^2$. Consequently, the UMVUEs for variance components σ_u^2 and σ_ϵ^2 coincide with their respective ANOVA estimators (Graybill and Wortham, 1956).

2.4.4 Maximum likelihood estimation

Taking logarithm of $\mathcal{L}(\boldsymbol{\theta})$, the log-likelihood function of $\boldsymbol{\theta}$ is,

$$\begin{aligned}\ell(\boldsymbol{\theta}) = &-\frac{a(r-1)}{2}\ln(\sigma_\epsilon^2) - \frac{a}{2}\ln(\sigma_\epsilon^2 + r\sigma_u^2) - \frac{1}{2\sigma_\epsilon^2}\sum_{i=1}^{a}\sum_{j=1}^{r}(y_{ij} - \overline{y}_{i\cdot})^2 \\ &- \frac{1}{2(\sigma_\epsilon^2 + r\sigma_u^2)}\sum_{i=1}^{a}\sum_{j=1}^{r}(\overline{y}_{i\cdot} - \overline{y}_{\cdot\cdot})^2 - \frac{ar(\overline{y}_{\cdot\cdot} - \mu)^2}{2(\sigma_\epsilon^2 + r\sigma_u^2)} - \frac{ar}{2}\ln(2\pi)\,.\end{aligned} \tag{2.22}$$

The definition of maximum likelihood estimation necessitates the maximization of the likelihood function within the parameter space. The log-likelihood function presented in (2.22) incorporates the parameter μ through the quadratic term $(\overline{y}_{\cdot\cdot} - \mu)^2$. Given the nature of this parameter, the parameter space for μ is $\mathbb{R}$. The log-likelihood function $\ell(\boldsymbol{\theta})$ reaches its maximum when μ equals $\overline{y}_{\cdot\cdot}$.

Calculating the partial derivatives of $\ell(\boldsymbol{\theta})$ with respect to σ_u^2 and σ_ϵ^2 and subsequently solving the resulting score equations results in the following maximum likelihood estimators of variance components,

$$\widehat{\sigma_u^2} = \frac{1}{r}\big(\beta^{-1}MS_u - MS_\epsilon\big) \qquad \text{and} \qquad \widehat{\sigma_\epsilon^2} = MS_\epsilon\,, \tag{2.23}$$

where the scaling factor β is defined as $\beta = \dfrac{a}{a-1}$.

The estimators in (2.23) are considered as the maximum likelihood estimators under the condition that both $\widehat{\sigma_u^2}$ and $\widehat{\sigma_\epsilon^2}$ remain within the parameter space of σ_u^2 and σ_ϵ^2. The estimator $\widehat{\sigma_\epsilon^2} = MS_\epsilon$ is inherently positive, and thus it falls within the parameter space of σ_ϵ^2. However, the estimator $\widehat{\sigma_u^2}$, as provided in (2.23) is non-negative only if the condition $MS_u \geq \beta MS_\epsilon$ is satisfied.

If $MS_u < \beta MS_\epsilon$, the log-likelihood function $\ell(\boldsymbol{\theta})$ is maximized at the following boundary point from the parameter space,

$$\widehat{\sigma_u^2} = 0 \qquad \text{and} \qquad \widehat{\sigma_\epsilon^2} = \frac{SS_t}{ar}\,. \tag{2.24}$$

In this scenario, the pair of estimators provided in equation (2.24) serves as the maximum likelihood estimators for σ_u^2 and σ_ϵ^2, respectively (Searle et al., 1992, Chapter 3). By combining the relations (2.23) and (2.24), we can express the maximum likelihood estimators for σ_u^2 and σ_ϵ^2 as follows,

$$\widehat{\sigma_u^2} = \max\left(0\,,\,\frac{1}{r}\left(\beta^{-1}MS_u - MS_\epsilon\right)\right), \tag{2.25a}$$

$$\widehat{\sigma_\epsilon^2} = \min\left(\frac{SS_t}{ar}, MS_\epsilon\right). \tag{2.25b}$$

Substituting these maximum likelihood estimators for the variance components into the equation for ρ, the maximum likelihood estimator for ρ is determined as follows,

$$\widehat{\rho}_{\text{MLE}} = \max\left(0\,,\,\frac{1}{r}\left(\beta^{-1}\frac{MS_u}{MS_\epsilon} - 1\right)\right). \tag{2.26}$$

2.4.5 Other estimation methods

Other approaches are available for estimating the variance components. Among these, two notable approaches include the use of restricted maximum likelihood (Thompson, 1962; Patterson and Thompson, 1971) and the Bayesian framework.

The restricted maximum likelihood estimation is an adaptation of the maximum likelihood estimation method. It aims to estimate model parameters by maximizing the likelihood of the observed data while incorporating constraints on these parameters. This method is advantageous as it can yield estimates that are less biased compared to standard maximum likelihood estimates. Notably, under the assumption of normality for the random effects and balanced study plans, the solutions obtained using the restricted maximum likelihood and non-negative ANOVA estimators are identical (Corbeil and Searle, 1976).

Within the Bayesian framework, variance components are regarded as random variables characterized by a density function known as the prior density. Bayesian estimation involves utilizing the Bayes Theorem to derive a conditional probability distribution, referred to as the posterior density, taking into account the observed data. This posterior density then guides the estimation of the parameters of interest, demanding a numerical solution (Searle et al., 1992, Section 3.9). Notable examples of this approach include the works of Tiao and Tan (1965); Klotz et al. (1969); Portnoy (1971), which explore Bayes estimators of variance components within the context of the one-way model, as well as studies by Rajagopalan and Broemeling (1983); Fong et al. (2010), which extend this

methodology to a broader range of linear models. Moreover, the study by Weaver et al. (2012) showcases how the Bayesian approach offers a versatile alternative across a wide spectrum of measurement system analyses.

A summary of the estimator results discussed and reviewed in this section is presented in Table 2.2.

Table 2.2: Estimators of variance components and their ratio ρ in a one-way random effect model with balanced data.

Method	Estimators
ANOVA and UMVUE	$\widehat{\sigma_u^2} = \frac{1}{r}(MS_u - MS_\epsilon)$ $\widehat{\sigma_\epsilon^2} = MS_\epsilon$ $\widehat{\rho}_{\text{ANOVA}} = \frac{1}{r}\left(\frac{MS_u}{MS_\epsilon} - 1\right)$
Non-negative ANOVA and restricted maximum likelihood	$\widehat{\sigma_u^2} = \max\left(0, \frac{1}{r}(MS_u - MS_\epsilon)\right)$ $\widehat{\sigma_\epsilon^2} = \min\left(\frac{SS_t}{ar-1}, MS_\epsilon\right)$ $\widehat{\rho}_{\text{NANOVA}} = \max\left(0, \frac{1}{r}\left(\frac{MS_u}{MS_\epsilon} - 1\right)\right)$
Maximum likelihood	$\widehat{\sigma_u^2} = \max\left(0, \frac{1}{r}\left(\beta^{-1}MS_u - MS_\epsilon\right)\right)$ $\widehat{\sigma_\epsilon^2} = \min\left(\frac{SS_t}{ar}, MS_\epsilon\right)$ $\widehat{\rho}_{\text{MLE}} = \max\left(0, \frac{1}{r}\left(\beta^{-1}\frac{MS_u}{MS_\epsilon} - 1\right)\right)$

2.5 Theoretical properties

With the estimation of measurement system study parameters, understanding their statistical properties becomes crucial. In this section, we undertake a comprehensive examination of the statistical properties associated with the estimation of variance components and their ratio in the framework of the measurement system assessment study. Exploring these properties will provide further insights into the underlying characteristics and performance of the measurement system.

2.5.1 The expected values and bias

In our analysis of theoretical properties, we start by examining the expected value and bias linked to the estimation of the variance components and their ratio. Our focus will be on conducting a detailed examination using the estimations from ANOVA, non-negative ANOVA, and maximum likelihood methods.

A. ANOVA estimations

The ANOVA estimators of variance components provided in (2.15) are unbiased since $\mathrm{E}[MS_u] = r\sigma_u^2 + \sigma_\epsilon^2$ and $\mathrm{E}[MS_\epsilon] = \sigma_\epsilon^2$. However, this unbiasedness does not directly carry over to the estimator of ρ as defined by (2.16). The expected value of $\widehat{\rho}_{\text{ANOVA}}$ according to (2.16) is expressed as follows,

$$\begin{aligned} \mathrm{E}\left[\widehat{\rho}_{\text{ANOVA}}\right] &= \frac{1}{r}\mathrm{E}\left[\frac{MS_u}{MS_\epsilon}\right] - \frac{1}{r} \\ &= \frac{1}{r}(1 + r\rho)\mathrm{E}[F] - \frac{1}{r}\,. \end{aligned} \tag{2.27}$$

where F is a random variable that has a central F-distribution with $\mathrm{df}_u = a - 1$ and $\mathrm{df}_\epsilon = a(r-1)$ degrees of freedom. Note that the expectation of F is $\mathrm{df}_\epsilon/(\mathrm{df}_\epsilon - 2)$ where $\mathrm{df}_\epsilon > 2$. Subsequently, the expected value of $\widehat{\rho}_{\text{ANOVA}}$ can be expressed as,

$$\mathrm{E}\left[\widehat{\rho}_{\text{ANOVA}}\right] = \frac{1}{\mathrm{df}_\epsilon - 2}\left(\rho\,\mathrm{df}_\epsilon + \frac{2}{r}\right). \tag{2.28}$$

The disparity between the expected estimation values and the actual value of a parameter is considered as the bias of the estimator. In the case of $\widehat{\rho}_{\text{ANOVA}}$, the bias is expressed as

$$\text{Bias}\left[\widehat{\rho}_{\text{ANOVA}}\right] = \mathrm{E}\left[\widehat{\rho}_{\text{ANOVA}}\right] - \rho = \frac{2(1 + r\rho)}{r(\mathrm{df}_\epsilon - 2)} \tag{2.29}$$

This equation demonstrates that $\widehat{\rho}_{\text{ANOVA}}$ consistently exhibits a positive bias and the bias tends to zero as the sample size or the number of replications increases.

The relative bias, expressed in percentage, is used to measure the accuracy of an estimator for estimating ρ. It can be calculated using the following relation

$$\left(\frac{\mathrm{E}\left[\widehat{\rho}\right]}{\rho} - 1\right) \times 100\,. \tag{2.30}$$

Figure 2.2 depicts a comparison of the percentage relative bias of $\widehat{\rho}_{\text{ANOVA}}$ with respect to ρ across various study plans, characterized by different combinations of sample size and number of replication measurements.

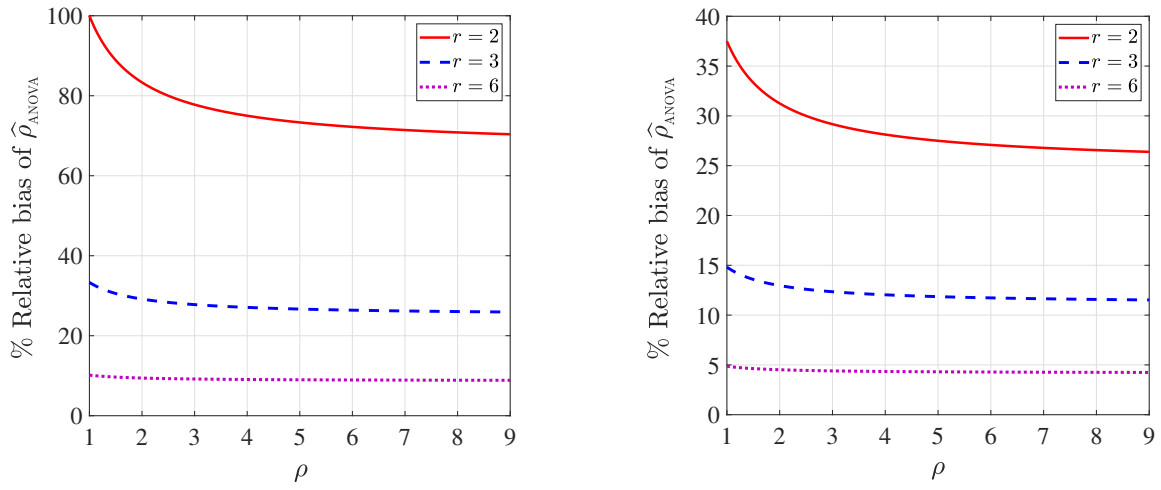

(a) $a = 5$

(b) $a = 10$

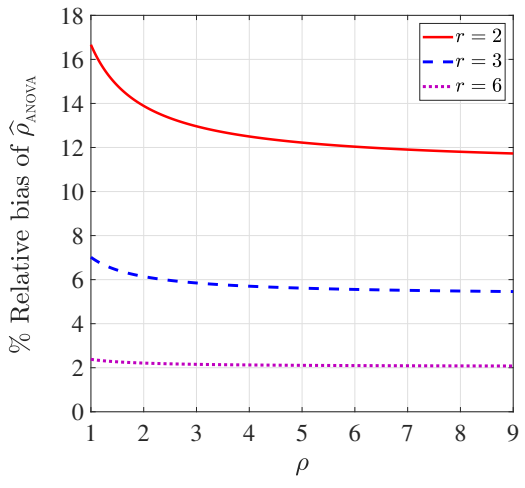

(c) $a = 20$

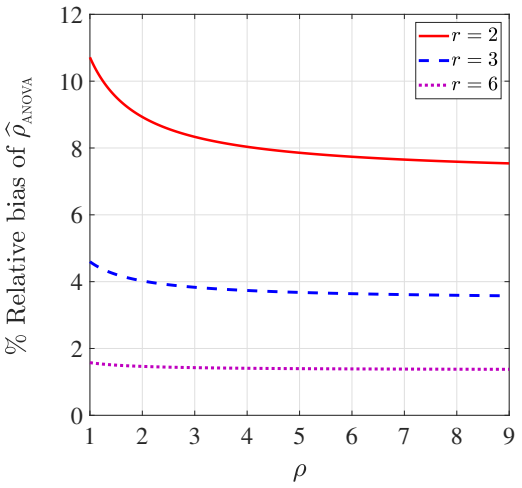

(d) $a = 30$

Figure 2.2: The percentage relative bias of $\widehat{\rho}_{\text{ANOVA}}$ with respect to ρ in a one-way random effect model.

It is worth noting that any reasonable measurement system typically has $\rho > 1$ (Browne, Steiner and MacKay, 2010), and therefore we focus on $\rho > 1$ in our study. Each figure comprises four distinct sample sizes, specifically with $a = 5, 10, 20, 30$. For each sample size, we consider three different numbers of measurement replication, including $r = 2, 3, 6$. As illustrated in Figure 2.2, an increase in either the sample size or the number of replications results in a reduction of bias in the estimation of $\widehat{\rho}_{\text{ANOVA}}$.

Figure 2.3 illustrates a scenario where the total number of measurements remains constant at $N = 60$ across four study plans. While the plan characterized by $a = 10$ and $r = 6$ is noteworthy due to its recommendation by AIAG (2003) for single-operator measurement systems, it's important to highlight that the plan with $a = 6$ and $r = 10$ demonstrates a lower relative bias for the estimation of $\widehat{\rho}_{\text{ANOVA}}$ compared to the other plans. This reduction in bias can primarily be attributed to its higher degrees of freedom for error and the larger number of replications.

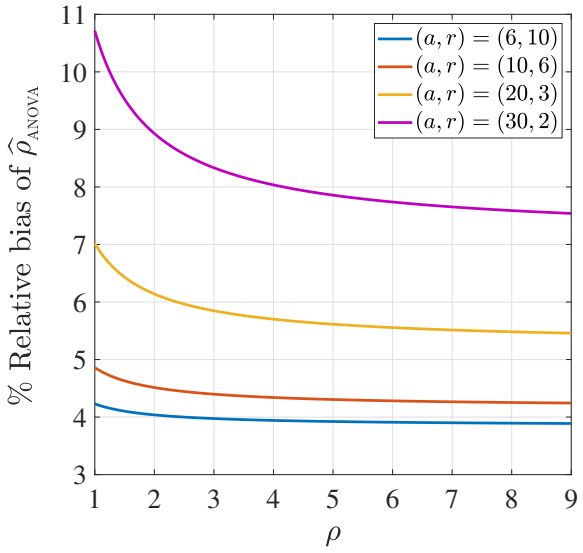

Figure 2.3: The percentage relative bias of $\widehat{\rho}_{\text{ANOVA}}$ as a function of ρ in a one-way random effect model with $N = 60$ measurements.

B. Maximum likelihood and non-negative ANOVA

Identifying the bias of maximum likelihood and non-negative ANOVA estimators can be challenging since their estimations of σ_u^2 and σ_ϵ^2 depend on the relationship between MS_u

and MS_ϵ. Specifically, the expected values of σ_u^2, σ_ϵ^2, and ρ depend on the probability of the event that the estimates lie on the boundary of the parameter space. This probability using the maximum likelihood estimation method is determined by,

$$p_\circ = \Pr\left(\frac{MS_u}{MS_\epsilon} < \beta\right) = \Pr\left(F < \beta(1+r\rho)^{-1}\right), \tag{2.31}$$

where F is the random variable, as characterized in (2.14). The expected values of the maximum likelihood estimators $\widehat{\sigma_u^2}$ and $\widehat{\sigma_\epsilon^2}$ are determined by

$$\mathrm{E}\left[\widehat{\sigma_u^2}\right] = \frac{1}{r}(1-p_\circ)\,\mathrm{E}\left[\beta^{-1}MS_u - MS_\epsilon \,\middle|\, \frac{MS_u}{MS_\epsilon} \geq \beta\right], \tag{2.32}$$

$$\mathrm{E}\left[\widehat{\sigma_\epsilon^2}\right] = (1-p_\circ)\,\mathrm{E}\left[MS_\epsilon \middle| \frac{MS_u}{MS_\epsilon} \geq \beta\right] + \frac{p_\circ}{ar}\mathrm{E}\left[SS_t \middle| \frac{MS_u}{MS_\epsilon} < \beta\right], \tag{2.33}$$

and the expected value of $\widehat{\rho}_{\text{MLE}}$ is,

$$\mathrm{E}\left[\widehat{\rho}_{\text{MLE}}\right] = \frac{1}{r}(1-p_\circ)\,\mathrm{E}\left[\beta^{-1}\frac{MS_u}{MS_\epsilon} - 1 \,\middle|\, \frac{MS_u}{MS_\epsilon} \geq \beta\right]. \tag{2.34}$$

We can determine the expectation of $\widehat{\rho}_{\text{MLE}}$ through,

$$\mathrm{E}\left[\widehat{\rho}_{\text{MLE}}\right] = \frac{1}{r}(1-p_\circ)\,\mathrm{E}\left[\beta^{-1}(1+r\rho)F - 1 \mid F \geq \beta(1+r\rho)^{-1}\right]. \tag{2.35}$$

The distribution of $\widehat{\rho}_{\text{MLE}}$ can be verified as a truncated F-distribution with $a-1$ and $a(r-1)$ degrees of freedom. A more explicit expression for the moments of this distribution is provided by Nadarajah and Kotz (2008), involving the use of the Gauss hyper-geometric function.

The expected values of the maximum likelihood estimators $\widehat{\sigma_u^2}$, $\widehat{\sigma_\epsilon^2}$, and $\widehat{\rho}_{\text{MLE}}$ cannot be obtained analytically due to the complexity of the equations. Consequently, assessing the bias associated with these estimates presents challenges in analytical determination, and thus numerical evaluations are necessary.

The properties of the estimators from the non-negative ANOVA and maximum likelihood methods are very similar in model (2.1). In fact, by substituting β with 1 in equations (2.31) and (2.35), we can first deduce the probability that the non-negative ANOVA estimations lie on the boundary and subsequently compute $\mathrm{E}\left[\widehat{\rho}_{\text{NANOVA}}\right]$.

In Figures 2.4 and 2.5, we depict the percentage relative bias of $\widehat{\rho}_{\text{MLE}}$ and $\widehat{\rho}_{\text{ANOVA}}$ relative to ρ across various combinations of a and r as shown in Figure 2.2. From Figure 2.4, the estimate of ρ_{MLE} exhibits a positive bias when $r = 2$, while it demonstrates a negative bias

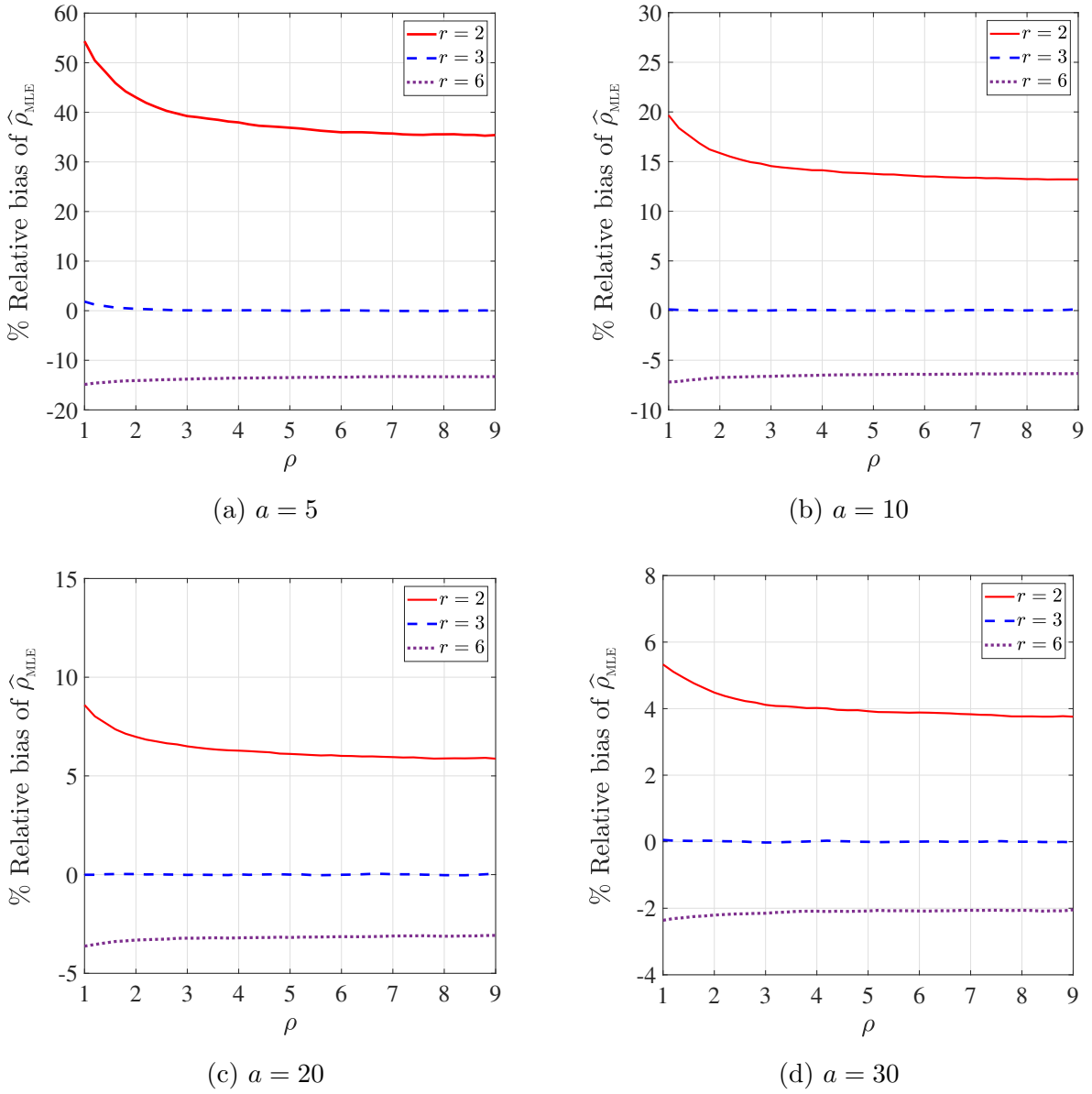

(a) $a = 5$ (b) $a = 10$

(c) $a = 20$ (d) $a = 30$

Figure 2.4: The percentage relative bias of $\widehat{\rho}_{\text{MLE}}$ with respect to ρ in a one-way random effect model, where the random effects of U and ϵ are normally distributed.

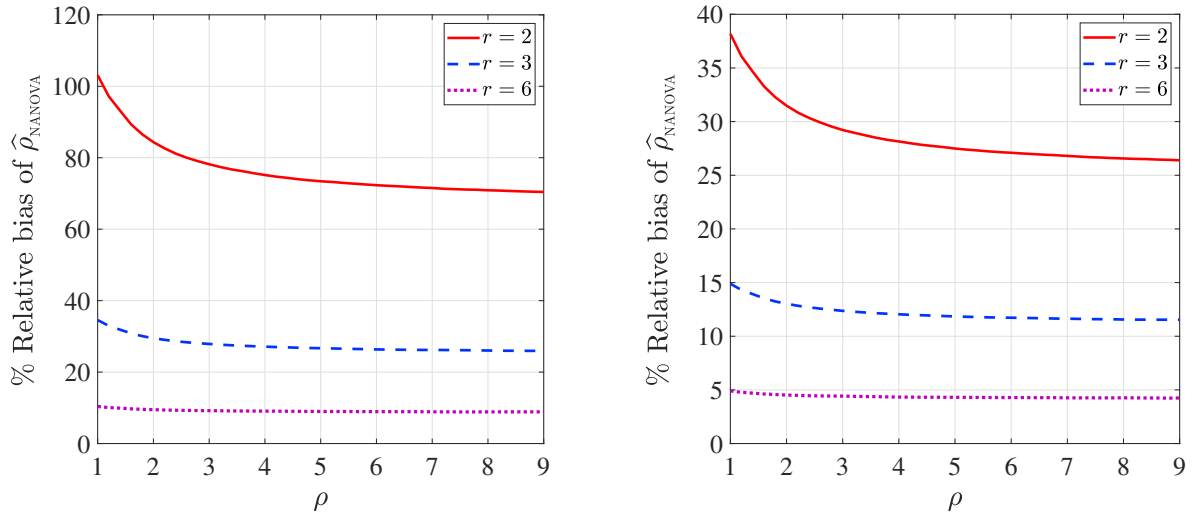

(a) $a = 5$ (b) $a = 10$

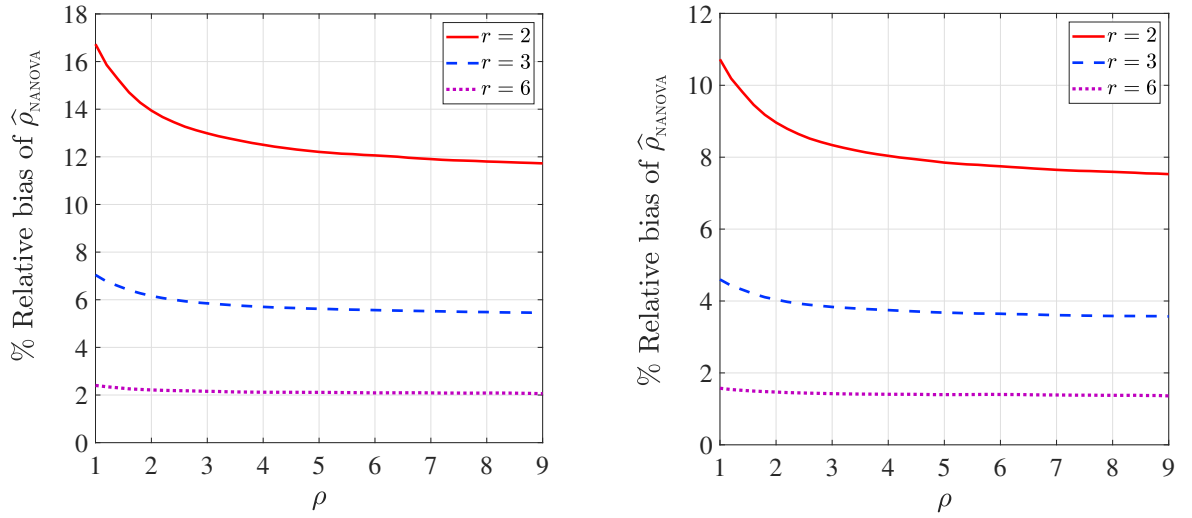

(c) $a = 20$ (d) $a = 30$

Figure 2.5: The percentage relative bias of $\widehat{\rho}_{\text{NANOVA}}$ with respect to ρ in a one-way random effect model, where the random effects of U and ϵ are normally distributed.

when $r = 6$. Interestingly, when $r = 3$, the bias remains approximately zero across all the studied sample sizes, which is a desirable characteristic. Plot (d) of Figure 2.4 with $a = 30$ illustrates the larger sample size situation, where the relative bias exhibits a narrower range, indicating reduced variability across different numbers of measurement replications. Comparing the plots of Figures 2.4 and 2.5, $\widehat{\rho}_{\text{MLE}}$ generally exhibits smaller bias across plans with smaller numbers of measurement replication, e.g., 2 and 3 replications. However, $\widehat{\rho}_{\text{NANOVA}}$ has a smaller relative bias than $\widehat{\rho}_{\text{MLE}}$, in absolute value, when $r = 6$.

Figure 2.6 illustrates the percentage relative bias of $\widehat{\rho}_{\text{MLE}}$ and $\widehat{\rho}_{\text{NANOVA}}$ for four study plans with a constant total number of measurements $N = 60$. We note that $\widehat{\rho}_{\text{MLE}}$ exhibits negligible bias, close to zero, with $a = 20$ and $r = 3$, while $\widehat{\rho}_{\text{NANOVA}}$ achieves its least bias when $a = 6$ and $r = 10$.

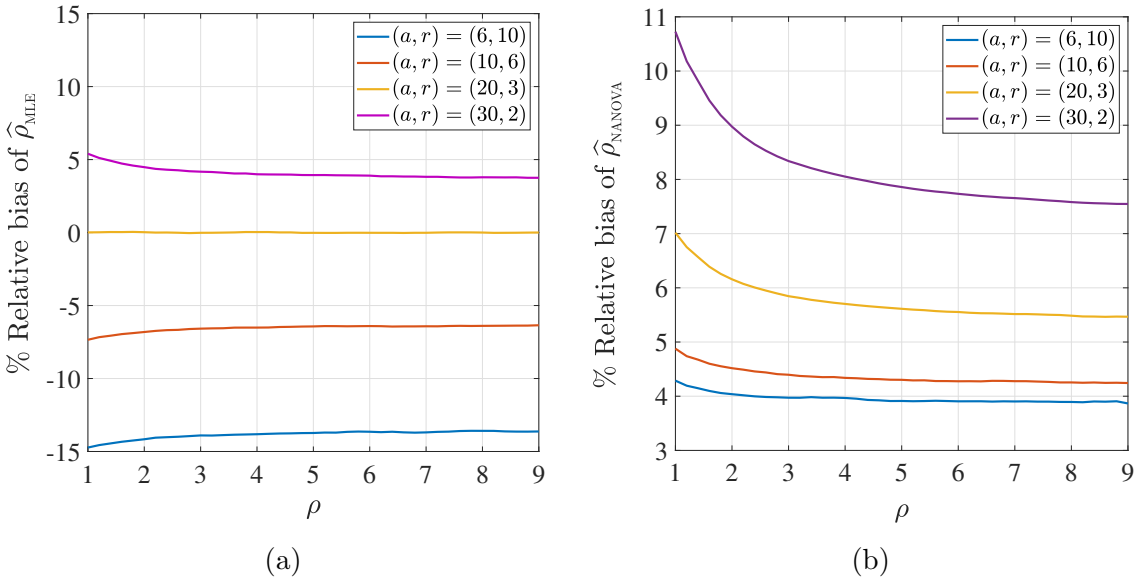

Figure 2.6: The percentage relative bias of (a) $\widehat{\rho}_{\text{MLE}}$ and (b) $\widehat{\rho}_{\text{NANOVA}}$ as a function of ρ in a one-way random effect model with $N = 60$ measurements.

2.5.2 Sampling variance

A. ANOVA estimations

The variances of the mean of squares terms MS_u and MS_ϵ, which follow multiples of chi-squared distributions with $\mathrm{df}_u = a-1$ and $\mathrm{df}_\epsilon = a(r-1)$ degrees of freedom, are obtained as (Searle et al., 1992),

$$\mathrm{Var}\left[MS_u\right] = \frac{2\left(\mathrm{E}\left[MS_u\right]\right)^2}{a-1} \quad \text{and} \quad \mathrm{Var}\left[MS_\epsilon\right] = \frac{2\left(\mathrm{E}\left[MS_\epsilon\right]\right)^2}{a(r-1)}\,. \tag{2.36}$$

Given the independence of MS_u and MS_ϵ under the normality assumption, we can express the variances of $\widehat{\sigma_u^2}$ and $\widehat{\sigma_\epsilon^2}$, using the ANOVA estimation method for a sample size of a and replication r as follows

$$\mathrm{Var}\left[\widehat{\sigma_u^2}\right] = \frac{2}{r^2}\left\{\frac{(\sigma_\epsilon^2 + r\sigma_u^2)^2}{a-1} + \frac{\sigma_\epsilon^4}{a(r-1)}\right\}, \tag{2.37}$$

$$\mathrm{Var}\left[\widehat{\sigma_\epsilon^2}\right] = \frac{2\,\sigma_\epsilon^4}{a(r-1)}\,. \tag{2.38}$$

The variance of $\widehat{\rho}_{\text{ANOVA}}$, as defined in (2.16), can be computed by,

$$\begin{aligned}\mathrm{Var}\left[\widehat{\rho}_{\text{ANOVA}}\right] &= \frac{1}{r^2}\,\mathrm{Var}\left[\frac{MS_u}{MS_\epsilon}\right] \\ &= \frac{(1+r\rho)^2}{r^2}\,\mathrm{Var}\left[F\right],\end{aligned} \tag{2.39}$$

where the random variable F is defined in (2.14). Then, the variance of random variable F is,

$$\mathrm{Var}\left[F\right] = \frac{2\,\mathrm{df}_\epsilon^2\left(\mathrm{df}_\epsilon + \mathrm{df}_u - 2\right)}{\mathrm{df}_u\left(\mathrm{df}_\epsilon - 2\right)^2\left(\mathrm{df}_\epsilon - 4\right)}\,, \tag{2.40}$$

where $\mathrm{df}_\epsilon > 4$, and does not exist otherwise. This condition on df_ϵ restricts the sample size a and the number of measurement replications r. For example, when $r = 2$, the sample size a should be greater than or equal to 5. Plugging (2.40) in (2.39), the variance of $\widehat{\rho}_{\text{ANOVA}}$ is

obtained as,

$$\mathrm{Var}\left[\widehat{\rho}_{\text{ANOVA}}\right] = \frac{2(1+r\rho)^2\,\mathrm{df}_\epsilon^2\,(\mathrm{df}_\epsilon + \mathrm{df}_u - 2)}{r^2\mathrm{df}_u\,(\mathrm{df}_\epsilon - 2)^2\,(\mathrm{df}_\epsilon - 4)}\,, \tag{2.41}$$

B. Maximum likelihood and non-negative ANOVA

First, we study the variance of $\widehat{\sigma_u^2}$ and $\widehat{\sigma_\epsilon^2}$ using their maximum likelihood estimations. For $\widehat{\sigma_u^2}$,

$$\begin{aligned}\mathrm{Var}\left[\widehat{\sigma_u^2}\right] &= \mathrm{E}\left[\left(\widehat{\sigma_u^2}\right)^2\right] - \left(\mathrm{E}\left[\widehat{\sigma_u^2}\right]\right)^2 \\ &= \tfrac{1}{r^2}(1-p_\circ)\mathrm{E}\left[\left(\beta^{-1}MS_u - MS_\epsilon\right)^2 \,\middle|\, \frac{MS_u}{MS_\epsilon} \geq \beta\right] - \left(\mathrm{E}\left[\widehat{\sigma_u^2}\right]\right)^2,\end{aligned} \tag{2.42}$$

where $\mathrm{E}\left[\widehat{\sigma_u^2}\right]$ is explained in (2.32). For $\widehat{\sigma_\epsilon^2}$,

$$\begin{aligned}\mathrm{Var}\left[\widehat{\sigma_\epsilon^2}\right] &= \mathrm{E}\left[\left(\widehat{\sigma_\epsilon^2}\right)^2\right] - \left(\mathrm{E}\left[\widehat{\sigma_\epsilon^2}\right]\right)^2 \\ &= (1-p_\circ)\mathrm{E}\left[MS_\epsilon^2 \,\middle|\, \frac{MS_u}{MS_\epsilon} \geq \beta\right] + \frac{p_\circ}{a^2r^2}\,\mathrm{E}\left[SS_t^2 \,\middle|\, \frac{MS_u}{MS_\epsilon} < \beta\right] - \left(\mathrm{E}\left[\widehat{\sigma_\epsilon^2}\right]\right)^2.\end{aligned} \tag{2.43}$$

where $\mathrm{E}\left[\widehat{\sigma_\epsilon^2}\right]$ is outlined in (2.33). In a similar fashion, we can determine the variance of $\widehat{\rho}_{\text{MLE}}$ through

$$\mathrm{Var}\left[\widehat{\rho}_{\text{MLE}}\right] = \mathrm{E}\left[\widehat{\rho}^2_{\text{MLE}}\right] - \left(\mathrm{E}\left[\widehat{\rho}_{\text{MLE}}\right]\right)^2,$$

where,

$$\mathrm{E}\left[\widehat{\rho}^2_{\text{MLE}}\right] = \tfrac{1}{r^2}(1-p_\circ)\mathrm{E}\left[\left(\beta^{-1}(1+r\rho)F - 1\right)^2 \mid F \geq \beta(1+r\rho)^{-1}\right], \tag{2.44}$$

and $\mathrm{E}\left[\widehat{\rho}_{\text{MLE}}\right]$ is given in (2.35).

We can express the finite-sample variance properties of $\widehat{\sigma_u^2}$ and $\widehat{\sigma_\epsilon^2}$ using non-negative ANOVA estimators, as well as $\widehat{\rho}_{\text{NANOVA}}$, in a similar manner by setting β to 1.

A relative standard error (SE), expressed as a percentage, is calculated to compare the

finite-sample variance of the ρ estimations using the following formula

$$\frac{\sqrt{\text{Var}\left[\widehat{\rho}\right]}}{\rho} \times 100\,. \tag{2.45}$$

In Figure 2.7, the plots illustrate the relative standard error (SE) as a function of ρ for estimates of both $\widehat{\rho}_{\text{NANOVA}}$ and $\widehat{\rho}_{\text{MLE}}$. These plots represent various study plans, each with a total of 60 measurements. From the comparison we observe that $\widehat{\rho}_{\text{MLE}}$ consistently exhibits lower variance than $\widehat{\rho}_{\text{NANOVA}}$ across the studied plans. Additionally, the smallest relative SE of $\widehat{\rho}_{\text{MLE}}$ is achieved when the study plan consists of a sample size of 20 with 3 measurement replications.

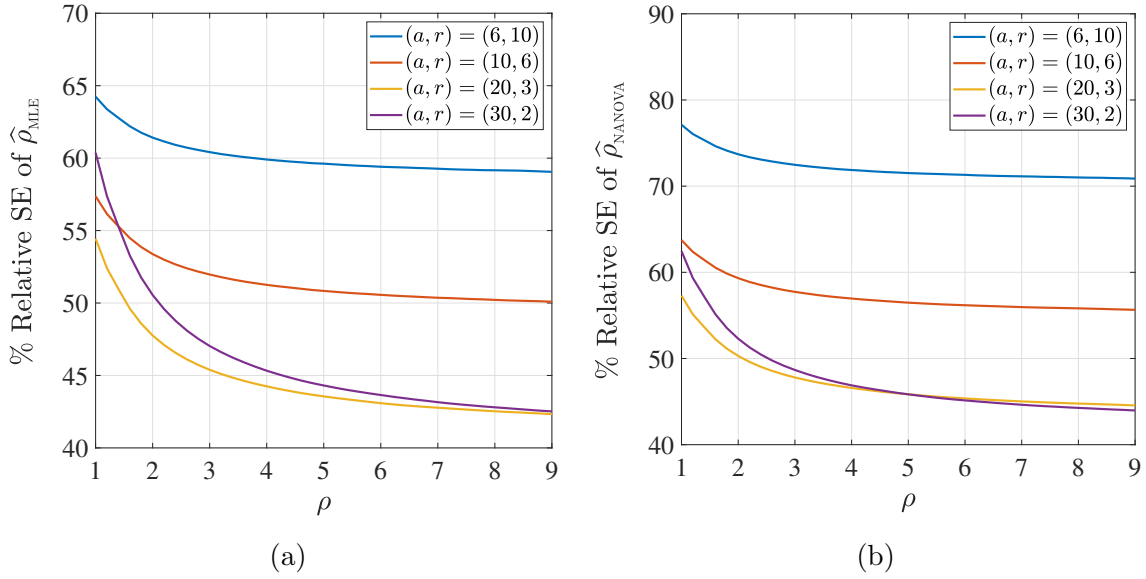

Figure 2.7: The percentage relative SE of (a) $\widehat{\rho}_{\text{MLE}}$ and (b) $\widehat{\rho}_{\text{NANOVA}}$ as a function of ρ in a one-way random effect model with $N = 60$ measurements.

2.5.3 Test of hypothesis

Point estimates provide insight into the magnitude of the assessment parameters for measurement system study, but they do not convey enough information about the precision of these estimates. For example, if a point estimate for the measurement system variability exceeds expectations, hypothesis testing can help determine if it is significantly larger than

a particular hypothesis. Conversely, a small point estimate for the signal-to-noise ratio (or the parameter ρ) might indicate an inadequate measurement system. Utilizing statistical hypothesis tests enables us to make probabilistic statements and assess the significance of these parameters (Burdick, 1994; Montgomery and Runger, 1993a).

To assess the statistical significance of estimated values and make informed decisions about the measurement system, we will explore three specific hypothesis tests within the context of model (2.1), as listed below.

i) $H_0 : \sigma_u^2 = 0$ vs $H_0 : \sigma_u^2 > 0$,
ii) $H_0 : \sigma_\epsilon \leq \sigma_0$ vs $H_a : \sigma_\epsilon > \sigma_0$,
iii) $H_0 : \rho \leq \rho_0$ vs $H_a : \rho > \rho_0$.

An essential question in the field of measurement system analysis is whether the variability in measurement data can be attributed to variability among units (Montgomery and Runger, 1993a). To investigate this, a hypothesis test can be conducted for σ_u^2 with the null hypothesis $H_0 : \sigma_u^2 = 0$.

We employ the statistic MS_u/MS_ϵ to assess whether the variance component σ_u^2 is negligible compared to σ_ϵ^2. Under hypothesis $H_0 : \sigma_u^2 = 0$, the statistic MS_u/MS_ϵ follows an F-distribution with df_u and df_ϵ degrees of freedom. A large observed value of this statistic provides evidence that the variance component σ_u^2 significantly affects the observed data. The p-value for testing $H_0 : \sigma_u^2 = 0$ can be obtained as,

$$p\text{-value} = 1 - \Pr\left(F < \frac{r\sum_{i=1}^{a}(y_{i\cdot} - \overline{y}_{\cdot\cdot})^2/(a-1)}{\sum_{i=1}^{a}\sum_{j=1}^{r}(y_{ij} - \overline{y}_{i\cdot})^2/(N-a)}\right), \tag{2.46}$$

Another common query in measurement system assessment studies is whether the measurement system exhibits a low variability that remains below a certain threshold (Burdick and Larsen, 1997). In such cases, a hypothesis test can be carried out with the null hypothesis $H_0 : \sigma_\epsilon \leq \sigma_0$ and the alternative hypothesis $H_a : \sigma_\epsilon > \sigma_0$, where σ_0 represents an acceptable threshold.

To test the hypothesis $H_0 : \sigma_\epsilon \leq \sigma_0$, we utilize SS_ϵ/σ_0^2 as the test statistic. If $\sigma_\epsilon = \sigma_0$, this statistic has the same distribution as $X = SS_\epsilon/\sigma_\epsilon^2$, which follows a chi-square distribution with df_ϵ degrees of freedom. Typically, a large observed value of SS_ϵ provides evidence in favor of $\sigma_\epsilon > \sigma_0$. The p-value for the test can be computed as

$$p\text{-value} = 1 - \Pr\left(X < \frac{1}{\sigma_0^2}\sum_{i=1}^{a}\sum_{j=1}^{r}(y_{ij} - \overline{y}_{i\cdot})^2\right). \tag{2.47}$$

In measurement system analysis, it may be necessary to conduct a hypothesis test to examine whether the relative size of the variance components due to the units and measurement system is greater than a certain level, denoted as ρ_0 (Donner and Eliasziw, 1987; Steiner and MacKay, 2005). In this case, we formulate the null hypothesis as $H_0 : \rho \leq \rho_0$, with the alternative hypothesis $H_a : \rho > \rho_0$.

For this hypothesis test, we use the test statistic $(1 + r\rho_0)^{-1} MS_u/MS_\epsilon$. If $\rho = \rho_0$, this test statistic follows an F-distribution with degrees of freedom df_u and df_ϵ. A large observed value of $(1 + r\rho_0)^{-1} MS_u/MS_\epsilon$ provides evidence in favour of the alternative hypothesis $H_a : \rho > \rho_0$. The p-value for this hypothesis test is calculated as

$$p\text{-value} = 1 - \Pr\left(F < \frac{r \sum_{i=1}^{a} (y_{i\cdot} - \overline{y}_{\cdot\cdot})^2}{(1 + r\rho_0) \sum_{i=1}^{a} \sum_{j=1}^{r} (y_{ij} - \overline{y}_{i\cdot})^2} \right). \tag{2.48}$$

2.5.4 Convergence properties

This section focuses on the convergence behavior of the estimates of σ_u^2, σ_ϵ^2, and the ratio of these components as the number of measurements $N = ar$ increases in the one-way model (2.1). We will examine if the estimators of these components are consistent, and investigate their convergence in distribution.

We analyze the asymptotic characteristics of the estimates in three situations, where the sample size (a) and/or the replication number (r) increase:

($\mathcal{S}1$) $a \to \infty$ and r is fixed,
($\mathcal{S}2$) $a \to \infty$ and $r \to \infty$,
($\mathcal{S}3$) $r \to \infty$ and a is fixed.

In each case, the total number of measurements, denoted as $N = ar$, increases due to the growth in either the sample size, replication number, or both. We lead off the analysis by examining the asymptotic behavior of the maximum likelihood estimates. This knowledge will provide us with a foundation for analyzing and interpreting the convergence properties of ANOVA-based estimators.

In Theorem 2.1, we provide insight into the convergence behavior for the maximum likelihood estimates of variance components σ_u^2 and σ_ϵ^2 in the one-way random effect model (2.1) for asymptotic situation $\mathcal{S}1$.

Theorem 2.1. *Let $\widehat{\sigma_\epsilon^2}$ and $\widehat{\sigma_u^2}$ be the maximum likelihood estimates. Then with a fixed number of measurement replications r and as $a \to \infty$, the following convergence properties hold:*

a) $\widehat{\sigma_\epsilon^2} \xrightarrow{a.s} \sigma_\epsilon^2$, *provided that* $\mathrm{E}\left[\epsilon_{ij}^2\right] < \infty$,

b) $\widehat{\sigma_u^2} \xrightarrow{a.s} \sigma_u^2$, *provided that* $\mathrm{E}\left[U_i^2\right] < \infty$ *and* $\mathrm{E}\left[\epsilon_{ij}^2\right] < \infty$,

c) *Within the context of the normal distributional setting of model (2.1) and under the condition that* σ_u^2 *is positive,*

$$\sqrt{a}\begin{pmatrix} \widehat{\sigma_\epsilon^2} - \sigma_\epsilon^2 \\ \widehat{\sigma_u^2} - \sigma_u^2 \end{pmatrix} \xrightarrow{d} \mathcal{N}\left(\mathbf{0}, \begin{pmatrix} \sigma_{11} & \sigma_{12} \\ \sigma_{21} & \sigma_{22} \end{pmatrix}\right),$$

where the elements of the covariance matrix are given by

$$\sigma_{11} = \frac{2\,\sigma_\epsilon^4}{r-1}, \quad \sigma_{12} = \frac{-2\,\sigma_\epsilon^4}{r(r-1)},$$
$$\textit{and} \;\; \sigma_{22} = 2(\sigma_u^2 + r^{-1}\sigma_\epsilon^2)^2 + \frac{2\sigma_\epsilon^4}{r^2(r-1)}.$$

Proof. See the supplementary materials in Section 2.7. □

It is noteworthy that the almost sure convergence properties established in Theorem 2.1 hold under only the assumptions of independence and identical distributions of all U_i's and all ϵ_{ij}'s, as well as the finiteness of their second moments. Specifically, the validity of the results is not affected by the distributions of U_i's and ϵ_{ij}'s. Furthermore, without assuming the distributions of U_i and ϵ_{ij}'s, part (c) of Theorem 2.1 still guarantees convergence to a normal distribution as long as U_i^2 and ϵ_{ij}^2 have finite variances. However, the covariance matrix will be different and it depends on the distributions of U_i's and ϵ_{ij}'s.

In Theorem 2.2, we analyze the convergence properties of $\widehat{\rho}_{\mathrm{MLE}}$ in the asymptotic situation that the sample size a grows large.

Theorem 2.2. *As* $a \to \infty$ *and for any fixed number of measurement replications* r*, we have*

a) $\widehat{\rho}_{\mathrm{MLE}} \xrightarrow{a.s} \rho$, *provided that* $\mathrm{E}\left[\epsilon_{ij}^2\right]$ *and* $\mathrm{E}\left[U_{ij}^2\right]$ *are finite,*

b) $\sqrt{a}\,(\widehat{\rho}_{\mathrm{MLE}} - \rho) \xrightarrow{d} \mathcal{N}\left(0, \sigma_\rho^2\right)$ *where* $\sigma_\rho^2 = \frac{2}{r^2}\left[(1+r\rho)^2 + \frac{1}{r-1}\right]$*, under the condition that* σ_u^2 *is positive.*

Proof. Applying Slutskey's theorem to parts (a) and (b) of Theorem 2.1 concludes part (a). Applying Slutskey's theorem to the marginal asymptotic distribution of the estimator for the variance component σ_u^2, together with the estimator for σ_ϵ^2 converging almost surely to the true value σ_ϵ^2, concludes part (b). □

Corollary 2.1, which addresses the convergence of $\widehat{\sigma_u^2}$, $\widehat{\sigma_\epsilon^2}$ and $\widehat{\rho}_{\text{MLE}}$ as both the sample size and number of measurement replications become large, is derived from the results established in Theorems 2.1 and 2.2.

Corollary 2.1. *Under the condition of $\sigma_u^2 > 0$ and the normality distribution assumption of model (2.1), as $a \to \infty$ and $r \to \infty$ then,*

a) *The joint distribution of $\left(\widehat{\sigma_\epsilon^2}, \widehat{\sigma_u^2}\right)^\top$ converges as follows,*

$$\sqrt{a}\begin{pmatrix}\sqrt{r}\left(\widehat{\sigma_\epsilon^2} - \sigma_\epsilon^2\right)\\ \widehat{\sigma_u^2} - \sigma_u^2\end{pmatrix} \xrightarrow{d} \mathcal{N}\left(\mathbf{0}, \begin{pmatrix}2\sigma_\epsilon^4 & 0\\ 0 & 2\sigma_u^4\end{pmatrix}\right),$$

b) $\sqrt{a}\left(\widehat{\rho}_{\text{MLE}} - \rho\right) \xrightarrow{d} \mathcal{N}\left(0, 2\rho^2\right)$.

Therefore, $a^{-1/2}$ is the rate of convergence of $\widehat{\rho}_{\text{MLE}}$. Next, we analyze the asymptotics for the situation $\mathcal{S}3$.

Theorem 2.3. *Given a fixed sample size, as $r \to \infty$ the following convergence properties hold:*

a) $\widehat{\sigma_\epsilon^2} \xrightarrow{a.s} \sigma_\epsilon^2$, *provided that* $\mathrm{E}\left[\epsilon_{ij}^2\right] < \infty$,

b) $\sqrt{ar}\left(\widehat{\sigma_\epsilon^2} - \sigma_\epsilon^2\right) \xrightarrow{d} \mathcal{N}\left(0, \tau_\epsilon^2\right)$, *where* $\tau_\epsilon^2 = \mathrm{Var}\left[\epsilon_{ij}^2\right]$, *provided that* $\tau_\epsilon^2 < \infty$,

c) $\frac{a}{\sigma_u^2}\widehat{\sigma_u^2} \xrightarrow{d} \chi_{a-1}^2$, *provided that σ_u^2 is positive.*

d) $\frac{a}{\rho}\widehat{\rho}_{\text{MLE}} \xrightarrow{d} \chi_{a-1}^2$, *provided that σ_u^2 is positive.*

Proof. See the supplementary materials. □

Combining the results from Theorems 2.1 to 2.3 leads to the conclusion that the probability of obtaining an estimate on the boundary of the parameter space is zero when the number of measurements grows large, as specified in Theorem 2.4.

Theorem 2.4. *As the number of measurements $N \to \infty$ and under the conditions specified by model (2.1), both non-negative ANOVA and maximum likelihood methods approach zero probability of estimates lying on the boundaries of the parameter space.*

Proof. Refer to the supplementary materials. □

2.5.5 Confidence intervals

We explore the construction of confidence intervals for the variance components σ_u^2 and σ_ϵ^2 as well as the parameter ρ involved in the measurement system assessment study. Under the conditions of the one-way model (2.1), exact confidence intervals for σ_ϵ^2 and ρ can be found (Scheffé, 1959, Page 229). However, for the variance component σ_u^2, exact confidence intervals are not readily available. We will demonstrate the process of obtaining approximate confidence intervals using results from large sample theories.

A. Exact confidence intervals

Under the normality assumption of ϵ_{ij} in the one-way random effect model of (2.1), we have $SS_\epsilon/\sigma_\epsilon^2 \sim \chi^2_{a(r-1)}$ leading to the derivation of the exact $(1-\alpha)100\%$ confidence interval for σ_ϵ^2 as follows,

$$\mathcal{CI}_{\sigma_\epsilon^2} = \left[\frac{SS_\epsilon}{\chi^2_{a(r-1),1-\alpha/2}}, \frac{SS_\epsilon}{\chi^2_{a(r-1),\,\alpha/2}}\right], \tag{2.49}$$

where $\chi^2_{\nu,1-\alpha/2}$ and $\chi^2_{\nu,\alpha/2}$ are, respectively, the upper and lower critical values of a chi-squared distribution with ν degrees of freedom at the $\frac{\alpha}{2}$-level.

Under the assumptions of normality and independence of U_i's and ϵ_{ij}'s, the exact confidence interval can be obtained for the ratio of variance components σ_u^2 and σ_ϵ^2. From (2.14), it is observed that $(1+r\rho)^{-1}\frac{MS_u}{MS_\epsilon}$ follows an F-distribution with $a-1$ and $a(r-1)$ degrees of freedom. Therefore, the exact $(1-\alpha)100\%$ confidence interval for ρ is defined by,

$$\mathcal{CI}_\rho = \left[\frac{1}{r}\left(\frac{MS_u/MS_\epsilon}{F_{a-1,\,a(r-1),1-\alpha/2}} - 1\right), \frac{1}{r}\left(\frac{MS_u/MS_\epsilon}{F_{a-1,\,a(r-1),\,\alpha/2}} - 1\right)\right]. \tag{2.50}$$

Here $F_{a-1,\,a(r-1),\,1-\alpha/2}$ and $F_{a-1,\,a(r-1),\,\alpha/2}$ are, respectively, the upper and lower critical values of an F-distribution with $a-1$ and $a(r-1)$ degrees of freedom at the $\frac{\alpha}{2}$-level.

B. Approximate confidence intervals

An exact confidence interval for σ_u^2 is not available. We can construct large sample intervals, as suggested by Montgomery and Runger (1993b); Borror et al. (1997).

Using the result of Theorem 2.1, we can establish a Wald-type confidence interval for σ_u^2. The quantity $\sqrt{a}\,(\widehat{\sigma_u^2} - \sigma_u^2)/\sqrt{\widehat{\sigma_{22}}}$ is asymptotically pivotal, which leads to the following

Wald-type confidence interval for σ_u^2 at $1-\alpha$ level,

$$\left[\widehat{\sigma_u^2} - \frac{z_{1-\alpha/2}\sqrt{\widehat{\sigma_{22}}}}{\sqrt{a}}, \widehat{\sigma_u^2} + \frac{z_{1-\alpha/2}\sqrt{\widehat{\sigma_{22}}}}{\sqrt{a}}\right]. \tag{2.51}$$

However, the above Wald confidence interval of σ_u^2 is not range preserving, as the lower bound could be negative. To address this issue, we can define the negative bounds to be zero, resulting in the interval

$$\mathcal{CI}_{\sigma_u^2,\text{Wald}} = \left[\max\left(0, \widehat{\sigma_u^2} - \frac{z_{1-\alpha/2}\sqrt{\widehat{\sigma_{22}}}}{\sqrt{a}}\right), \widehat{\sigma_u^2} + \frac{z_{1-\alpha/2}\sqrt{\widehat{\sigma_{22}}}}{\sqrt{a}}\right]. \tag{2.52}$$

To construct a confidence interval that preserves the range for σ_u^2, we can construct a Wald confidence interval for the log-transformation on $\widehat{\sigma_u^2}$. Subsequently, we invert the limits to approximate a confidence interval for σ_u^2. Applying the delta method to the limiting distribution outcome of Theorem 2.1 yields the following asymptotic convergence result,

$$\sqrt{a}\left\{\log\left(\widehat{\sigma_u^2}\right) - \log\left(\sigma_u^2\right)\right\} \xrightarrow{\text{d}} \mathcal{N}\left(0, \frac{\sigma_{22}}{\sigma_u^4}\right), \tag{2.53}$$

as $a \to \infty$. Consequently $\sqrt{a}\left\{\log(\widehat{\sigma_u^2}) - \log(\sigma_u^2)\right\}\widehat{\sigma_u^2}/\sqrt{\widehat{\sigma_{22}}}$ is asymptotically pivotal, where $\widehat{\sigma_u^2} > 0$. This leads to the following $(1-\alpha)100\%$ confidence interval for σ_u^2,

$$\mathcal{CI}_{\sigma_u^2,\log} = \left[\exp\left\{\log(\widehat{\sigma_u^2}) - \frac{z_{1-\alpha/2}\sqrt{\widehat{\sigma_{22}}}}{\widehat{\sigma_u^2}\sqrt{a}}\right\}, \exp\left\{\log(\widehat{\sigma_u^2}) + \frac{z_{1-\alpha/2}\sqrt{\widehat{\sigma_{22}}}}{\widehat{\sigma_u^2}\sqrt{a}}\right\}\right]. \tag{2.54}$$

We note that when the number of measurements or the signal-to-noise ratio is small, the log-transform confidence interval of σ_u^2 may not offer a reasonable approximation, partly due to the increased likelihood of obtaining an estimate of $\widehat{\sigma_u^2}$ close to zero. Ebadi et al. (2023) demonstrate that using the Cornish–Fisher expansion to adjust the percentiles can yield favorable results. Further investigation into this matter is a potential avenue for future research.

We can construct a large sample confidence interval for σ_u^2, based on the result of Theorem 2.3. This asymptotic confidence interval, with $(1-\alpha)100\%$ coverage probability for σ_u^2, is established as follows

$$\mathcal{CI}_{\sigma_u^2,\text{chi}} = \left[\frac{a\widehat{\sigma_u^2}}{\chi^2_{a-1,\,1-\alpha/2}}, \frac{a\widehat{\sigma_u^2}}{\chi^2_{a-1,\,\alpha/2}}\right]. \tag{2.55}$$

A summary of the three approximate confidence interval bounds for σ_u^2 discussed in this section is presented in Table 2.3.

Table 2.3: Relations of approximate confidence intervals on σ_u^2 for the one-way random effect model based on its asymptotic distributions.

Interval	Lower limit	Upper limit
$\mathcal{CI}_{\sigma_u^2,\text{Wald}}$	$\max\left(0, \widehat{\sigma_u^2} - \frac{z_{1-\alpha/2}\sqrt{\widehat{\sigma_{22}}}}{\sqrt{a}}\right)$	$\widehat{\sigma_u^2} + \frac{z_{1-\alpha/2}\sqrt{\widehat{\sigma_{22}}}}{\sqrt{a}}$
$\mathcal{CI}_{\sigma_u^2,\log}$	$\exp\left\{\log(\widehat{\sigma_u^2}) - \frac{z_{1-\alpha/2}\sqrt{\widehat{\sigma_{22}}}}{\widehat{\sigma_u^2}\sqrt{a}}\right\}$	$\exp\left\{\log(\widehat{\sigma_u^2}) + \frac{z_{1-\alpha/2}\sqrt{\widehat{\sigma_{22}}}}{\widehat{\sigma_u^2}\sqrt{a}}\right\}$
$\mathcal{CI}_{\sigma_u^2,\text{chi}}$	$\frac{a\,\widehat{\sigma_u^2}}{\chi^2_{a-1,\,1-\alpha/2}}$	$\frac{a\,\widehat{\sigma_u^2}}{\chi^2_{a-1,\,\alpha/2}}$

C. Comparison of confidence intervals

We conducted Monte Carlo simulation studies to assess the performance of the three confidence intervals for σ_u^2 as listed in Table 2.3. These simulations considered six combinations of a and r while maintaining a constant total of $N = 96$ measurements. For each (a, r) combination, we investigated three distinct sets of variances: $(\sigma_u^2, \sigma_\epsilon^2) = (0.5, 1)$, $(0.5, 0.5)$, and $(0.5, 0.1)$, representing low, moderate, and high signal-to-noise ratio scenarios, respectively. In each scenario, we generated 5×10^5 simulated datasets, where U_i and ϵ_{ij} independently followed normal distributions with variances σ_u^2 and σ_ϵ^2. These scenarios were chosen to assess the confidence intervals' performance under varying levels of variance signal-to-noise ratio and various combinations of a and r.

We assessed the coverage probability of each confidence interval by measuring how frequently it accurately included the true value of σ_u^2. When calculating the results for the log-transformed confidence interval, we focused on samples with $\widehat{\sigma_u^2} > 0.01$. To gauge the likelihood of this scenario, Table 2.4 provides the $\Pr(\widehat{\sigma_u^2} < 0.01)$ values for the scenarios under study.

Tables 2.5 and 2.6 display the outcomes of our numerical investigation regarding the 90% and 95% asymptotic confidence intervals and the average length of these intervals, respectively. In these tables, we have highlighted in blue the highest simulated coverage probability among the three. We noted that the log-transformed confidence intervals for σ_u^2

Table 2.4: $\Pr(\widehat{\sigma_u^2} < 0.01)$ with $N = 96$ measurements.

	(a, r)					
$(\sigma_u^2, \sigma_\epsilon^2)$	$(6, 16)$	$(8, 12)$	$(12, 8)$	$(24, 4)$	$(32, 3)$	$(48, 2)$
$(0.5, 1)$	2.15×10^{-2}	1.18×10^{-2}	5.36×10^{-3}	3.72×10^{-3}	5.27×10^{-3}	1.25×10^{-2}
$(0.5, 0.5)$	6.55×10^{-3}	2.26×10^{-3}	4.20×10^{-4}	4.0×10^{-05}	8.0×10^{-5}	1.90×10^{-4}
$(0.5, 0.1)$	7.90×10^{-4}	9.0×10^{-5}	0	0	0	0

generally provide better coverage compared to the Wald-type intervals. However, it is important to highlight that these confidence intervals tend to produce less reliable percentiles in scenarios with a low signal-to-noise ratio or a small number of measurement replications. In such cases, the interval length tends to increase significantly. In scenarios with moderate to high signal-to-noise ratio situations, $\mathcal{CI}_{\sigma_u^2,\log}$ demonstrates superior performance over $\mathcal{CI}_{\sigma_u^2,\text{chi}}$ in attaining the target coverage level when dealing with large sample sizes. Conversely, when replication numbers are larger, $\mathcal{CI}_{\sigma_u^2,\text{chi}}$ exhibits better performance.

2.6 Robustness issues

In this section, we briefly explore the robustness issues of the procedures introduced in this chapter for univariate measurement system assessment. A comprehensive investigation of robustness is deferred to future work.

We consider the scenario where the distribution of the measurement errors deviates from the assumed model and ϵ_{ij}'s follow a contaminated normal distribution,

$$\epsilon_{ij} \sim (1 - \lambda)\,\mathcal{N}(0, \sigma_\epsilon^2) + \lambda\, H, \quad \text{for } \; i = 1, \ldots, a, \; \text{and } \; j = 1, \ldots, r. \tag{2.56}$$

Here, λ denotes the contamination ratio, and H represents the contamination distribution. Under this model, ϵ_{ij}'s are drawn from the assumed normal distributed $\mathcal{N}(0, \sigma_\epsilon^2)$ with probability $1 - \lambda$, and from the distribution H with a probability λ.

Table 2.5: Simulated 90% confidence intervals for σ_u^2 with $\alpha = 0.1$ and $N = 96$ measurements.

(a) $\sigma_u^2 = 0.5$, $\sigma_\epsilon^2 = 1$

	Coverage probability			Mean interval width		
(a, r)	$\mathcal{CI}_{\sigma_u^2,\text{Wald}}$	$\mathcal{CI}_{\sigma_u^2,\log}$	$\mathcal{CI}_{\sigma_u^2,\text{chi}}$	$\mathcal{CI}_{\sigma_u^2,\text{Wald}}$	$\mathcal{CI}_{\sigma_u^2,\log}$	$\mathcal{CI}_{\sigma_u^2,\text{chi}}$
$(6, 16)$	0.687	0.903	0.828	0.851	1.148	1.906
$(8, 12)$	0.735	0.919	0.818	0.825	1.063	1.334
$(12, 8)$	0.786	0.941	0.790	0.765	1.131	0.902
$(24, 4)$	0.846	0.962	0.701	0.690	1.802×10^2	0.540
$(32, 3)$	0.866	0.959	0.646	0.682	6.832×10^4	0.450
$(48, 2)$	0.891	0.943	0.533	0.713	1.599×10^{11}	0.354

(b) $\sigma_u^2 = 0.5$, $\sigma_\epsilon^2 = 0.5$

	Coverage probability			Mean interval width		
(a, r)	$\mathcal{CI}_{\sigma_u^2,\text{Wald}}$	$\mathcal{CI}_{\sigma_u^2,\log}$	$\mathcal{CI}_{\sigma_u^2,\text{chi}}$	$\mathcal{CI}_{\sigma_u^2,\text{Wald}}$	$\mathcal{CI}_{\sigma_u^2,\log}$	$\mathcal{CI}_{\sigma_u^2,\text{chi}}$
$(6, 16)$	0.687	0.822	0.864	0.828	1.004	1.929
$(8, 12)$	0.735	0.847	0.859	0.778	0.895	1.350
$(12, 8)$	0.785	0.872	0.845	0.693	0.765	0.912
$(24, 4)$	0.842	0.901	0.799	0.573	0.612	0.546
$(32, 3)$	0.859	0.913	0.766	0.541	0.577	0.454
$(48, 2)$	0.881	0.939	0.695	0.522	3.633	0.358

(c) $\sigma_u^2 = 0.5$, $\sigma_\epsilon^2 = 0.1$

	Coverage probability			Mean interval width		
(a, r)	$\mathcal{CI}_{\sigma_u^2,\text{Wald}}$	$\mathcal{CI}_{\sigma_u^2,\log}$	$\mathcal{CI}_{\sigma_u^2,\text{chi}}$	$\mathcal{CI}_{\sigma_u^2,\text{Wald}}$	$\mathcal{CI}_{\sigma_u^2,\log}$	$\mathcal{CI}_{\sigma_u^2,\text{chi}}$
$(6, 16)$	0.687	0.798	0.893	0.800	0.931	1.949
$(8, 12)$	0.735	0.827	0.892	0.732	0.821	1.363
$(12, 8)$	0.785	0.852	0.889	0.631	0.682	0.921
$(24, 4)$	0.840	0.878	0.880	0.478	0.498	0.550
$(32, 3)$	0.855	0.885	0.875	0.425	0.439	0.458
$(48, 2)$	0.871	0.893	0.863	0.364	0.372	0.361

Table 2.6: Simulated 95% confidence intervals for σ_u^2 with $N = 96$ measurements.

(a) $\sigma_u^2 = 0.5$, $\sigma_\epsilon^2 = 1$

	Coverage probability			Mean interval width		
(a, r)	$\mathcal{CI}_{\sigma_u^2,\text{Wald}}$	$\mathcal{CI}_{\sigma_u^2,\text{log}}$	$\mathcal{CI}_{\sigma_u^2,\text{chi}}$	$\mathcal{CI}_{\sigma_u^2,\text{Wald}}$	$\mathcal{CI}_{\sigma_u^2,\text{log}}$	$\mathcal{CI}_{\sigma_u^2,\text{chi}}$
$(6, 16)$	0.728	0.992	0.889	0.936	1.566	2.740
$(8, 12)$	0.776	0.991	0.882	0.929	1.570	1.809
$(12, 8)$	0.827	0.991	0.860	0.893	3.248	1.164
$(24, 4)$	0.889	0.984	0.781	0.813	9.957×10^3	0.667
$(32, 3)$	0.910	0.980	0.726	0.802	1.246×10^7	0.551
$(48, 2)$	0.940	0.967	0.611	0.833	6.611×10^{14}	0.430

(b) $\sigma_u^2 = 0.5$, $\sigma_\epsilon^2 = 0.5$

	Coverage probability			Mean interval width		
(a, r)	$\mathcal{CI}_{\sigma_u^2,\text{Wald}}$	$\mathcal{CI}_{\sigma_u^2,\text{log}}$	$\mathcal{CI}_{\sigma_u^2,\text{chi}}$	$\mathcal{CI}_{\sigma_u^2,\text{Wald}}$	$\mathcal{CI}_{\sigma_u^2,\text{log}}$	$\mathcal{CI}_{\sigma_u^2,\text{chi}}$
$(6, 16)$	0.728	0.895	0.921	0.911	1.282	2.773
$(8, 12)$	0.776	0.913	0.918	0.897	1.126	1.831
$(12, 8)$	0.826	0.934	0.908	0.823	0.950	1.177
$(24, 4)$	0.885	0.959	0.870	0.683	0.756	0.675
$(32, 3)$	0.903	0.969	0.842	0.644	0.834	0.556
$(48, 2)$	0.927	0.977	0.776	0.621	8.364×10^1	0.433

(c) $\sigma_u^2 = 0.5$, $\sigma_\epsilon^2 = 0.1$

	Coverage probability			Mean interval width		
(a, r)	$\mathcal{CI}_{\sigma_u^2,\text{Wald}}$	$\mathcal{CI}_{\sigma_u^2,\text{log}}$	$\mathcal{CI}_{\sigma_u^2,\text{chi}}$	$\mathcal{CI}_{\sigma_u^2,\text{Wald}}$	$\mathcal{CI}_{\sigma_u^2,\text{log}}$	$\mathcal{CI}_{\sigma_u^2,\text{chi}}$
$(6, 16)$	0.728	0.861	0.944	0.892	1.178	2.802
$(8, 12)$	0.776	0.886	0.944	0.870	1.024	1.848
$(12, 8)$	0.826	0.911	0.942	0.752	0.840	1.188
$(24, 4)$	0.882	0.932	0.936	0.570	0.604	0.680
$(32, 3)$	0.898	0.938	0.932	0.507	0.530	0.561
$(48, 2)$	0.916	0.945	0.923	0.433	0.447	0.437

We performed Monte Carlo simulation studies using contaminated data. In the data generation process, we considered two contamination distributions for H:

(a) normal distribution $\mathcal{N}(0, 9\sigma_\epsilon^2)$,
(b) scaled central t-distribution with 5 degrees of freedom and scaling factor $3\sigma_\epsilon$.

Contamination ratio λ was set at 0.05 and 0.1. We explored four plans with (a, r) as follows: $(10, 6), (15, 4), (20, 3)$, and $(30, 2)$, resulting in a total number of 60 measurements. The true value of σ_u^2 was fixed at 0.5, and we investigated $\sigma_\epsilon^2 = 1, 0.5$, and 0.1, corresponding to low, moderate, and high signal-to-noise ratio settings. Table 2.7 shows the coverage probability of the 90% confidence interval of ρ based on 5×10^5 random trials for both cases of the contamination distributions.

In both contamination scenarios, it becomes apparent that the coverage probability deviates from the nominal level, resulting in under coverage. Specifically, with an increase in the contamination ratio λ from 5% to 10%, the coverage probability drops below 80% in settings with moderate and high signal-to-noise ratios. The Monte Carlo study results underscore the significant impact of heavy-tail distribution for contamination, such as the t-distribution, on the confidence interval of ρ. Notably, the majority of coverage probabilities fall below 70% for a 10% contamination ratio.

Table 2.7: Simulated coverage probability of the nominal 90% confidence intervals for ρ under various settings of a and r with $\sigma_u^2 = 0.5$: (a) $H \sim \mathcal{N}(0, 9\sigma_\epsilon^2)$, (b) $H \sim 3\,\sigma_\epsilon t(5)$.

(a) $H \sim \mathcal{N}(0, 9\sigma_\epsilon^2)$

	$\lambda = 5\%$			$\lambda = 10\%$		
(a, r)	$\rho = 0.5$	$\rho = 1$	$\rho = 5$	$\rho = 0.5$	$\rho = 1$	$\rho = 5$
$(10, 6)$	0.876	0.862	0.844	0.835	0.802	0.757
$(15, 4)$	0.868	0.846	0.812	0.821	0.768	0.689
(20.3)	0.867	0.839	0.792	0.820	0.755	0.647
$(30, 2)$	0.873	0.841	0.774	0.835	0.762	0.617

(b) $H \sim 3\,\sigma_\epsilon t(5)$

	$\lambda = 5\%$			$\lambda = 10\%$		
(a, r)	$\rho = 0.5$	$\rho = 1$	$\rho = 5$	$\rho = 0.5$	$\rho = 1$	$\rho = 5$
$(10, 6)$	0.850	0.820	0.785	0.783	0.720	0.643
$(15, 4)$	0.838	0.794	0.738	0.766	0.675	0.560
(20.3)	0.839	0.786	0.711	0.768	0.661	0.515
$(30, 2)$	0.853	0.792	0.690	0.798	0.677	0.487

2.7 Supplementary materials

This section includes the supplementary materials associated with Chapter 2.

A. Further details on the derivation of the likelihood function

Let $\boldsymbol{Y}_i = (Y_{i1}, \ldots, Y_{ir})^\top$ denote a random vector consisting of all r repeated measurements on unit i for $i = 1, \ldots, a$. Under the assumptions of one-way model (2.1), $\boldsymbol{Y}_1, \boldsymbol{Y}_2 \ldots, \boldsymbol{Y}_a$ are i.i.d. multivariate $\mathcal{N}(\mu \mathbf{1}_r, \boldsymbol{\Sigma})$ random vectors, where $\mathbf{1}_r$ is a column vector with r elements of 1, and $\boldsymbol{\Sigma}$ is defined by,

$$\boldsymbol{\Sigma} = \sigma_\epsilon^2 \boldsymbol{I}_r + \sigma_u^2 \boldsymbol{J}_r \,. \tag{2.57}$$

Here, $\boldsymbol{I}_n$ is the $n \times n$ identity matrix and $\boldsymbol{J}_n = \mathbf{1}_n \mathbf{1}_n^\top$ is an $n \times n$ matrix with elements 1. The likelihood of observing sample $\boldsymbol{y}_1, \ldots, \boldsymbol{y}_a$ is,

$$\mathcal{L}(\boldsymbol{\theta}; \boldsymbol{y}_1, \ldots, \boldsymbol{y}_a) = \prod_{i=1}^{a} (2\pi)^{-\frac{r}{2}} |\boldsymbol{\Sigma}|^{-\frac{1}{2}} \exp\left(-\frac{1}{2} (\boldsymbol{y}_i - \mathbf{1}_r \mu)^T \boldsymbol{\Sigma}^{-1} (\boldsymbol{y}_i - \mathbf{1}_r \mu) \right) \tag{2.58}$$

With $\boldsymbol{\Sigma}$ given in (2.57) involving a special form, its determinant and inverse matrix are obtained as[2],

$$|\boldsymbol{\Sigma}| = (\sigma_\epsilon^2)^{r-1} (\sigma_\epsilon^2 + r\sigma_S^2) \,, \tag{2.59}$$

and

$$\boldsymbol{\Sigma}^{-1} = \frac{1}{\sigma_\epsilon^2} \left(\boldsymbol{I}_r - \frac{\sigma_u^2}{\sigma_\epsilon^2 + r\sigma_S^2} \boldsymbol{J}_r \right) . \tag{2.60}$$

Plugging in the expressions for $|\boldsymbol{\Sigma}|$ and $\boldsymbol{\Sigma}^{-1}$, we can re-express the likelihood function presented in equation (2.58) as follows,

$$\mathcal{L}(\boldsymbol{\theta}; \boldsymbol{y}_1, \ldots, \boldsymbol{y}_a) = c(\sigma_u^2, \sigma_\epsilon^2) \exp\left(-\frac{1}{2\sigma_\epsilon^2} \sum_{i=1}^{a} (\boldsymbol{y}_i - \mathbf{1}_r \mu)^T \left(\boldsymbol{I}_r - \frac{\sigma_u^2}{\sigma_\epsilon^2 + r\sigma_u^2} \boldsymbol{J}_r \right) (\boldsymbol{y}_i - \mathbf{1}_r \mu) \right) , \tag{2.61}$$

[2] If $\mathbf{A} = c\boldsymbol{I}_n + \mathbf{u}\mathbf{v}^T$, then $|\mathbf{A}| = c^n (1 + \frac{1}{c} \mathbf{u}^T \mathbf{v})$ and $\mathbf{A}^{-1} = \frac{1}{c} \left(\boldsymbol{I}_n - \frac{\mathbf{u}\mathbf{v}^T}{c + \mathbf{v}^T \mathbf{u}} \right)$.

with $c(\sigma_u^2, \sigma_\epsilon^2)$ being defined as,

$$c(\sigma_u^2, \sigma_\epsilon^2) = (2\pi)^{-\frac{1}{2}ar}(\sigma_\epsilon^2)^{-\frac{1}{2}a(r-1)}(\sigma_\epsilon^2 + r\sigma_u^2)^{-\frac{1}{2}a}.$$

The term inside the exponential function can be arranged in order to display SS_u and SS_ϵ, as follows,

$$\begin{aligned}
&\frac{1}{2\sigma_\epsilon^2}\sum_{i=1}^{a}(\boldsymbol{y}_i - \mathbf{1}_r\mu)^T\left(\boldsymbol{I}_r - \frac{\sigma_u^2}{\sigma_\epsilon^2 + r\sigma_u^2}\boldsymbol{J}_r\right)(\boldsymbol{y}_i - \mathbf{1}_r\mu) \\
&\qquad = \frac{1}{\sigma_\epsilon^2}\sum_{i=1}^{a}\sum_{j=1}^{r}(y_{ij} - \mu)^2 - \frac{\sigma_u^2}{\sigma_\epsilon^2(\sigma_\epsilon^2 + r\sigma_u^2)}\sum_{i=1}^{a}(\boldsymbol{y}_i - \mu\mathbf{1}_r)^T\mathbf{1}\mathbf{1}_r^T(\boldsymbol{y}_i - \mu\mathbf{1}_r) \\
&\qquad = \frac{1}{\sigma_\epsilon^2}\sum_{i=1}^{a}\sum_{j=1}^{r}(y_{ij} - \overline{y}_{i\cdot} + \overline{y}_{i\cdot} - \mu)^2 - \frac{r^2\sigma_u^2}{\sigma_\epsilon^2(\sigma_\epsilon^2 + r\sigma_u^2)}\sum_{i=1}^{a}(\overline{y}_{i\cdot} - \mu)^2 \\
&\qquad = \frac{1}{\sigma_\epsilon^2}\sum_{i=1}^{a}\sum_{j=1}^{r}(y_{ij} - \overline{y}_{i\cdot})^2 + \frac{r}{\sigma_\epsilon^2}\sum_{i=1}^{a}(\overline{y}_{i\cdot} - \mu)^2 - \frac{r^2\sigma_u^2}{\sigma_\epsilon^2(\sigma_\epsilon^2 + r\sigma_u^2)}\sum_{i=1}^{a}(\overline{y}_{i\cdot} - \mu)^2 \\
&\qquad = \frac{SS_\epsilon}{\sigma_\epsilon^2} + \frac{r}{\sigma_\epsilon^2 + r\sigma_u^2}\sum_{i=1}^{a}(\overline{y}_{i\cdot} - \overline{y}_{\cdot\cdot} + \overline{y}_{\cdot\cdot} - \mu)^2 \\
&\qquad = \frac{SS_\epsilon}{\sigma_\epsilon^2} + \frac{SS_u}{\sigma_\epsilon^2 + r\sigma_u^2} + \frac{ra}{\sigma_\epsilon^2 + r\sigma_u^2}(\overline{y}_{\cdot\cdot} - \mu)^2.
\end{aligned}$$

which leads to the expected outcome.

B. Proof of convergence properties

To prove convergence properties outlined in Section 2.5, we rely on a set of lemmas that establish the convergence of sample moments. Specifically, Lemma 2.1 (Lehmann, 1999, Section 2.1) provides the necessary information on the consistency of sample moments, and Lemma 2.2 (Lehmann, 1999, Section 2.4) presents the asymptotic normality results of sample variance.

Lemma 2.1. ***(Consistency of sample moments).*** *Let $X_1, \ldots, X_n$ be i.i.d. random variables with mean ξ and finite k–th absolute moment $\mathrm{E}\left[|X_i|^k\right]$, so the k-th central moment $M_k = \mathrm{E}\left[(X_i - \xi)^k\right]$ exists. Then the k-th sample moment $\widehat{M_k} = \frac{1}{n}\sum_{i=1}^{n}(X_i - \overline{X})^k$ converges to M_k almost sure as $n \to \infty$.*

Lemma 2.2. ***(Asymptotic normality of sample variance).*** *Suppose that* $X_1, \ldots, X_n$ *are i.i.d. random variables such that* $\mathrm{E}[X_i] = \xi$, $\mathrm{Var}[X_i] = \sigma^2$, *and* $\mathrm{Var}[(X_i - \mu)^2] = \tau^2 < \infty$ *hold. Let* $S^2 = \frac{1}{n}\sum_{i=1}^{n}(X_i - \overline{X})^2$. *Then,*

$$\sqrt{n}(S^2 - \sigma^2) \xrightarrow{d} \mathcal{N}(0, \tau^2)$$

as $n \to \infty$.

Using these lemmas, we can now proceed to establish the convergence properties of the estimators introduced in Section 2.5.

Proof of Theorem 2.1

(a) Recall that

$$\widehat{\sigma_\epsilon^2} = MS_\epsilon = \frac{1}{a(r-1)}\sum_{i=1}^{a}\sum_{j=1}^{r}(Y_{ij} - \overline{Y}_{i\cdot})^2.$$

The random variable $Y_{ij} - \overline{Y}_{i\cdot}$ can be expressed as $\epsilon_{ij} - \overline{\epsilon}_{i\cdot}$ where $\overline{\epsilon}_{i\cdot} = \frac{1}{r}\sum_{j=1}^{r}\epsilon_{ij}$. Assuming independent random variables ϵ_{ij}'s with zero mean and finite second moment σ_ϵ^2, it can be shown that the second moment for the random variable $\epsilon_{ij} - \overline{\epsilon}_{i\cdot}$ is $\mathrm{E}[(\epsilon_{ij} - \overline{\epsilon}_{i\cdot})^2] = \frac{r-1}{r}\sigma_\epsilon^2$. Because all ϵ_{ij}'s are identically distributed too, random variables $\sum_{j=1}^{r}(\epsilon_{1j} - \overline{\epsilon}_{1\cdot})^2$, $\sum_{j=1}^{r}(\epsilon_{2j} - \overline{\epsilon}_{2\cdot})^2, \ldots$ are independent, identically distributed, and have finite mean,

$$E\left[\sum_{j=1}^{r}(\epsilon_{ij} - \overline{\epsilon}_{i\cdot})^2\right] = (r-1)\sigma_\epsilon^2, \quad \text{for } \; i = 1, \ldots, a. \tag{2.62}$$

By the strong law of large numbers when we get,

$$\frac{1}{a}\sum_{i=1}^{a}\sum_{j=1}^{r}(\epsilon_{ij} - \overline{\epsilon}_{i\cdot})^2 \xrightarrow{\text{a.s}} (r-1)\sigma_\epsilon^2, \tag{2.63}$$

as $a \to \infty$ and for any fixed number of r. This completes the proof for part (a).

(b) The maximum likelihood estimate of σ_u^2 is given by,

$$\begin{aligned}\widehat{\sigma_u^2} &= \frac{1}{r}\big(\beta^{-1}MS_u - MS_\epsilon\big),\\ &= \frac{1}{a}\sum_{i=1}^{a}(\overline{Y}_{i\cdot} - \overline{Y}_{\cdot\cdot})^2 - \frac{1}{ar(r-1)}\sum_{i=1}^{a}\sum_{j=1}^{r}(Y_{ij} - \overline{Y}_{i\cdot})^2.\end{aligned}$$

The random variable generated by $\overline{Y}_{i\cdot}$ can be represented as $\mu + U_i + \bar{\epsilon}_{i\cdot}$. Assuming that all U_i's and all ϵ_{ij}'s are i.i.d., we can conclude that the random variables $\overline{Y}_{1\cdot}$, $\overline{Y}_{2\cdot}, \ldots$ are identically distributed and independent with mean μ and the variance of $\sigma_u^2 + r^{-1}\sigma_\epsilon^2$. Applying Lemma 2.1 to $\overline{Y}_{1\cdot}$, $\overline{Y}_{2\cdot}, \ldots$ we obtain that,

$$\frac{1}{a}\sum_{i=1}^{a}(\overline{Y}_{i\cdot} - \overline{Y}_{\cdot\cdot})^2 \xrightarrow{\text{a.s}} \sigma_u^2 + \frac{\sigma_\epsilon^2}{r}, \tag{2.64}$$

as $a \to \infty$. Combining this with the result from part (a) that $MS_\epsilon \to \sigma_\epsilon^2$ almost surely, we conclude that

$$\widehat{\sigma_u^2} \xrightarrow{\text{a.s}} \sigma_u^2 > 0, \quad \text{as } a \to \infty, \tag{2.65}$$

which means that the estimator $\widehat{\sigma_u^2}$ converges almost surely to the true value of σ_u^2 as $a \to \infty$, value of r.

(c) To prove this, we begin with the equation,

$$\sqrt{a}\begin{pmatrix}\widehat{\sigma_\epsilon^2} - \sigma_\epsilon^2\\ \widehat{\sigma_u^2} - \sigma_u^2\end{pmatrix} = \sqrt{a}\begin{pmatrix}\frac{1}{a(r-1)}\sum_{i=1}^{a}\sum_{j=1}^{r}(Y_{ij} - \overline{Y}_{i\cdot})^2 - \sigma_\epsilon^2\\ \frac{1}{a}\sum_{i=1}^{a}(\overline{Y}_{i\cdot} - \overline{Y}_{\cdot\cdot})^2 - \frac{1}{ar(r-1)}\sum_{i=1}^{a}\sum_{j=1}^{r}(Y_{ij} - \overline{Y}_{i\cdot})^2 - \sigma_u^2\end{pmatrix}. \tag{2.66}$$

This equation can be expressed as the sum of two vectors,

$$\frac{1}{\sqrt{a}}\sum_{i=1}^{a}\begin{pmatrix}\frac{1}{(r-1)}\sum_{j=1}^{r}(Y_{ij} - \overline{Y}_{i\cdot})^2 - \sigma_\epsilon^2\\ \frac{-1}{r(r-1)}\sum_{j=1}^{r}(Y_{ij} - \overline{Y}_{i\cdot})^2 + \frac{\sigma_\epsilon^2}{r}\end{pmatrix} \quad \text{and} \quad \frac{1}{\sqrt{a}}\sum_{i=1}^{a}\begin{pmatrix}0\\ (\overline{Y}_{i\cdot} - \overline{Y}_{\cdot\cdot})^2 - \sigma_u^2 - \frac{\sigma_\epsilon^2}{r}\end{pmatrix}. \tag{2.67}$$

The multivariate central limit theorem indicates that, as $a \to \infty$,

$$\frac{1}{\sqrt{a}}\sum_{i=1}^{a}\begin{pmatrix}\frac{1}{r-1}\sum_{j=1}^{r}(Y_{ij} - \overline{Y}_{i\cdot})^2 - \sigma_\epsilon^2\\ \frac{-1}{r(r-1)}\sum_{j=1}^{r}(Y_{ij} - \overline{Y}_{i\cdot})^2 + \frac{\sigma_\epsilon^2}{r}\end{pmatrix} \xrightarrow{\text{d}} \mathcal{N}\left(\mathbf{0}, \tau_1^2\begin{pmatrix}1 & -r^{-1}\\ -r^{-1} & r^{-2}\end{pmatrix}\right), \tag{2.68}$$

where τ_1^2 is the variance of $\frac{1}{r-1}\sum_{j=1}^{r}(Y_{ij}-\overline{Y}_{i\cdot})^2$, given by

$$\tau_1^2 = \frac{1}{(r-1)^2}\,\mathrm{Var}\left[\sum_{j=1}^{r}(\epsilon_{ij}-\overline{\epsilon}_{i\cdot})^2\right]. \tag{2.69}$$

Furthermore, the asymptotic distribution of a sample variance indicates that,

$$\sqrt{a}\left(\frac{1}{a}\sum_{i=1}^{a}\left(\overline{Y}_{i\cdot}-\overline{Y}_{\cdot\cdot}\right)^2-\sigma_u^2-\frac{\sigma_\epsilon^2}{r}\right)\xrightarrow{\mathrm{d}}\mathcal{N}(0,\,\tau_2^2) \tag{2.70}$$

as $a\to\infty$ where τ_2^2 is the variance of $(\overline{Y}_{i\cdot}-\mu)^2$, expressed by,

$$\tau_2^2 = \mathrm{Var}\left[(U_i+\overline{\epsilon}_{i\cdot})^2\right].$$

In the case of the one-way model (2.1) with normal distribution assumptions, we have

$$\tau_1^2 = \frac{2\sigma_\epsilon^4}{r-1}, \tag{2.71}$$

$$\tau_2^2 = 2(\sigma_u^2+r^{-1}\sigma_\epsilon^2)^2. \tag{2.72}$$

In addition, the random vectors presented in (2.67) are independent. Combining these results leads to the expected outcome, and hence, the proof is complete.

Proof of Theorem 2.3

(a) Consider the following equation for $\widehat{\sigma_\epsilon^2}$,

$$\widehat{\sigma_\epsilon^2} = \frac{1}{a(r-1)}\sum_{i=1}^{a}\sum_{j=1}^{r}(\epsilon_{ij}-\overline{\epsilon}_{i\cdot})^2.$$

The random variables ϵ_{ij}'s are i.i.d.. Applying Lemma 2.1 to ϵ_{i1}, ϵ_{i2}, ..., we obtain

$$\frac{1}{r}\sum_{j=1}^{r}(\epsilon_{ij}-\overline{\epsilon}_{i\cdot})^2\xrightarrow{\text{a.s}}\sigma_\epsilon^2 \tag{2.73}$$

as $r \to \infty$ and for any fixed number of units. By summing the above result for all units, we obtain

$$\frac{1}{ar}\sum_{i=1}^{a}\sum_{j=1}^{r}(\epsilon_{ij}-\bar{\epsilon}_{i\cdot})^2 \xrightarrow{\text{a.s}} \sigma_\epsilon^2 \qquad \text{as } r\to\infty \text{ and } \forall a\,. \tag{2.74}$$

Therefore, $\widehat{\sigma_\epsilon^2} \xrightarrow{\text{a.s}} \sigma_\epsilon^2$ as $r \to \infty$.

(b) Starting from the asymptotic normality of the sample variance in Lemma 2.2, we have,

$$\sqrt{r}\left(\frac{1}{r}\sum_{j=1}^{r}(\epsilon_{ij}-\bar{\epsilon}_{i\cdot})^2-\sigma_\epsilon^2\right)\xrightarrow{\text{d}}\mathcal{N}(0,\,\tau_\epsilon^2), \quad \text{as } r\to\infty. \tag{2.75}$$

Since $\sum_{j=1}^{r}(\epsilon_{1j}-\bar{\epsilon}_{1\cdot})^2$, $\sum_{j=1}^{r}(\epsilon_{2j}-\bar{\epsilon}_{2\cdot})^2, \ldots$ are independent random variables that are normally distributed as r increases, their sum will also be normally distributed. Thus, using the properties of the normal distribution, we get

$$\sqrt{ar}\left(\frac{1}{ar}\sum_{i=1}^{a}\sum_{j=1}^{a}(\epsilon_{ij}-\bar{\epsilon}_{i\cdot})^2-\sigma_\epsilon^2\right)\xrightarrow{\text{d}}\mathcal{N}(0,\,\tau_\epsilon^2), \quad \text{as } r\to\infty. \tag{2.76}$$

which concludes the result.

(c) To prove this part, we start by expressing the maximum likelihood estimate of σ_u^2 as,

$$\widehat{\sigma_u^2}=\frac{1}{a}\sum_{i=1}^{a}\left(\overline{Y}_{i\cdot}-\overline{Y}_{\cdot\cdot}\right)^2-\frac{1}{r}MS_\epsilon \tag{2.77}$$

We know that the random variable $\sum_{i=1}^{a}\left(\overline{Y}_{i\cdot}-\overline{Y}_{\cdot\cdot}\right)^2/(\sigma_u^2+r^{-1}\sigma_\epsilon^2)$ follows a chi-squared distribution with $a-1$ degrees of freedom assuming the normal distribution of random effects. Therefore, $a^{-1}\sum_{i=1}^{a}\left(\overline{Y}_{i\cdot}-\overline{Y}_{\cdot\cdot}\right)^2$ has a gamma distribution with shape parameter $(a-1)/2$ and scale parameter $2(\sigma_u^2+r^{-1}\sigma_\epsilon^2)/a$ [3]. Moreover, part (b) of this theorem implies

[3] If $X \sim \chi_\nu^2$ and $c > 0$, then the random variable cX follows a gamma distribution with a shape parameter of $\nu/2$ and a scale parameter of $2c$.

that $MS_\epsilon = O_p\left(r^{-1/2}\right)$, which allows us to express (2.77) as

$$\widehat{\sigma_u^2} = \text{Gamma}\left(\frac{a-1}{2}, 2a^{-1}\left(\sigma_u^2 + r^{-1}\sigma_\epsilon^2\right)\right) + o_p(1). \tag{2.78}$$

Here, Gamma(κ, θ) denotes the gamma distribution with shape parameter κ and scale parameter θ. Since $r^{-1}\sigma_\epsilon^2$ converges to zero as $r \to \infty$, we have that $\widehat{\sigma_u^2}$ converges in distribution to a gamma distribution with shape parameter $(a-1)/2$ and scale parameter $2\sigma_u^2/a$, as $r \to \infty$, i.e.,

$$\widehat{\sigma_u^2} \xrightarrow{\text{d}} \text{Gamma}\left(\frac{a-1}{2}, 2a^{-1}\sigma_u^2\right). \tag{2.79}$$

which is the expected convergence result.

Proof of Theorem 2.4

In the limit case where the sample size a tends towards infinity, we established in Theorems 2.1 and 2.2 that $\widehat{\sigma_u^2}$ converges to σ_u^2, $\widehat{\sigma_\epsilon^2}$ converges to σ_ϵ^2, and $\widehat{\rho}_{\text{MLE}}$ converges to ρ. In addition, $\beta \to 1$ and the estimates obtained through the maximum likelihood method and (non-negative) ANOVA are identical.

In the scenario where the replication number r approaches infinity the estimates take different forms: $\widehat{\sigma_u^2} \to \sum_{i=1}^a \left(\overline{y}_{i\cdot} - \overline{y}_{\cdot\cdot}\right)^2/a$, $\widehat{\sigma_\epsilon^2} \to \sigma_\epsilon^2$, and $\widehat{\rho}_{\text{MLE}} \to \sum_{i=1}^a (\overline{y}_{i\cdot} - \overline{y}_{\cdot\cdot})^2/(a\sigma_\epsilon^2)$, using the maximum likelihood method. With (non-negative) ANOVA method, the estimates can be slightly different: $\widehat{\sigma_u^2} \to \sum_{i=1}^a \left(\overline{y}_{i\cdot} - \overline{y}_{\cdot\cdot}\right)^2/(a-1)$, $\widehat{\sigma_\epsilon^2} \to \sigma_\epsilon^2$, and $\widehat{\rho}_{\text{(N)ANOVA}}$ approaches $\sum_{i=1}^a \left(\overline{y}_{i\cdot} - \overline{y}_{\cdot\cdot}\right)^2/((a-1)\sigma_\epsilon^2)$. In either case, all of these estimates fall within the parameter space for the respective parameters.

Chapter 3

Measurement System Assessment Study for Multiple Characteristics

3.1 Introduction and background

When extending the measurement system assessment study to include multivariate data, we are confronted with the inherent complexity of their variability structure. In this context, the evaluation of the measurement system's performance and capability presents distinct challenges. To the best of the author's knowledge, the literature on this topic is sparse and not as developed as the univariate case.

Addressing the challenge of quantifying a measurement system's performance often involves summarizing complex variance-covariance matrices into a single scalar value. One approach, by Voelkel (2003), represents the summary measure of a variance-covariance matrix for bivariate data through the diameter of a circle. The circle is calculated to include, with a pre-specified probability, the mass of the corresponding bivariate normal distribution. In a different approach, Majeske (2008) investigates this problem by developing confidence regions in the form of ellipsoids, considering the assumption of random variables following a multivariate normal distribution. Wang and Yang (2007) and Wang (2013) utilize principal component analysis (PCA) to identify significant components and compute a composite summary index for the measurement system performance. The proposed index is typically calculated as the geometric mean of measurement system assessment parameters, such as the R&R ratio and PTR, for the selected principal components. Expanding on this methodology, Peruchi et al. (2014) refine the PCA-based method by introducing a summary measure through the weighted arithmetic mean and weighted geometric mean,

applied to the R&R ratios of the selected principal components. Marques et al. (2020) and de Almeida et al. (2020) explore applying factor analysis methods, particularly suited for multivariate cases where variables can be grouped into distinct categories, called factors, such that there is typically a high correlation between variables within the same group and moderate to low correlation between variables of different groups. Subsequently, a univariate measurement system analysis would be performed for each factor. These diverse approaches offer insights into summarizing and evaluating the performance of measurement systems in the context of multivariate data, each with its advantages and applicability.

In this study, our goal is to offer scalar metrics for assessing measurement systems of multivariate data. By doing so, we aim to equip practitioners with metrics that are simpler and more interpretable. This approach streamlines the interpretation process and supports more informed decision-making regarding measurement system performance.

Our study examines the applicability of several scalar measures for summarizing variance-covariance components in the context of measurement system assessment. Specifically, we explore variants of the following measures of a variance-covariance matrix:

- ❏ Generalized variance
- ❏ Trace
- ❏ Frobenius norm (or vector variance)

Each scalar measure corresponds to a distinct operation, offering unique insights into the characteristics of the variance-covariance matrix. They serve as particular generalized means of the eigenvalues, providing deeper information about the structure and behaviour of variances and covariances.

The generalized variance is a measure linked to the volume (or hyper-volume) bounded by the contours of the multivariate normal density function. Along with its variants, it holds significant importance in monitoring multivariate process variability. Noteworthy works by Alt and Smith (1988), Djauhari (2005), Montgomery (2020), and the comprehensive literature review by Ebadi et al. (2022) demonstrate the success of this measure in capturing variability. Despite its appealing features, the generalized variance has certain limitations. One notable limitation is that if the variance-covariance matrix is rank deficient, the generalized variance becomes zero. This constraint imposes a significant constraint on its applicability, requiring the variance-covariance matrix to be non-singular. Additionally, when the number of variables is greater than 2, obtaining the statistical properties of the sample generalized variance, e.g., its exact distribution or moments (Huwang et al., 2007), can be challenging.

On the other hand, the trace of a variance-covariance matrix provides an alternative approach to describing multivariate dispersion by summing the variances of all vari-

ables (Huwang et al., 2007; González and Sánchez, 2010). In a comprehensive literature review by Ajadi et al. (2021), an overview of selected articles that employ the trace measure as a summary statistic for the estimated covariance matrix is presented. Unlike the generalized variance, the trace represents a linear mapping, which enhances its appeal for variance component models. However, a criticism raised is that the trace measure does not consider the covariances among random variables when computing the overall measure (Ajadi et al., 2021).

Another measure of multivariate variability is the vector variance, which characterizes the overall variability of a variance-covariance matrix by considering the trace of its squared form, thus incorporating all the elements of the covariance structure (Djauhari, 2007; Djauhari et al., 2008). The trace and vector variance measures are equal to zero if and only if the distribution is degenerate at the mean vector.

The assessment of measurement systems for multivariate data relies on estimating two variance-covariance matrices: one associated with the measurement system and the other corresponding to the units. A widely employed technique for their estimation is the unbiased estimation of the variance-covariance components through multivariate analysis of variance (MANOVA), as demonstrated in numerous studies focusing on measurement system assessment (Majeske, 2008; Peruchi et al., 2016; Shi et al., 2016; Esmaeeli et al., 2019). This procedure entails subtracting positive-definite matrices, occasionally leading to estimated variance-covariance matrices that may not be non-negative definite. In a different approach, Bayesian methods have been applied to computationally evaluate variance-covariance matrices in this context (Hamada, 2016).

This chapter focuses on assessing measurement systems applied to multivariate data, aiming to build upon the statistical procedures and concepts discussed in Chapter 2. Our particular emphasis lies in exploring the one-way random effect model with an equal number of replications. In this setting, the unbiased estimate of the units' variance-covariance matrix may not necessarily be non-negative definite. This issue and potential methods to address it have been extensively noted in the literature, including the works by Anderson (1984); Amemiya (1985); Anderson et al. (1986); Srivastava and Kubokawa (1999); Kubokawa and Tsai (2006); Duan et al. (2023). To ensure a non-negative estimate of the units' variance-covariance matrix while also obtaining a positive-definite estimate of measurement error variance-covariance matrix, we follow the approach proposed by Anderson (1984) and consider the maximum likelihood estimation for the subsequent analyses.

3.1.1 Contributions and outlines

We make the following contributions in this chapter:

1. We extend the definition of parameters used to assess measurement systems to encompass multivariate data. Specifically, we explore using the generalized variance, the trace, and the Frobenius norm to effectively summarize the variance-covariance matrices.
2. We conduct a selective review of existing theories on the estimation of variance-covariance components within a one-way random effect model with equal replications.
3. We explore the convergence properties of variance-covariance components obtained through the maximum likelihood estimation method.
4. We concentrate on one of the proposed parameters in measurement system assessment—the signal-to-noise ratio. Our investigation encompasses an exploration of its convergence properties and the construction of approximate confidence intervals. Our systematic inference procedure can be seamlessly extended to other proposed measurement system assessment parameters introduced in this chapter.
5. We conduct a comparative analysis of the application of three transformations, i.e., the generalized variance, the trace, and the Frobenius norm, in their asymptotic properties.

The structure of this chapter is as follows: In Section 3.2, we present the framework of the multivariate one-way model for studying measurement systems. We establish our fundamental notation and parameters essential for evaluating multivariate data measurement systems. Section 3.3 provides an initial exploration of the one-way model, offering insights to prepare for our in-depth study. Estimating the parameters of measurement system assessment involves estimating the variance-covariance components. In Section 3.4, we study various existing methods for estimating these crucial quantities. In Section 3.5, we investigate the convergence properties of the estimators of variance-covariance components and the signal-to-noise ratio. In Section 3.6, several confidence intervals of the signal-to-noise ratio are discussed. The results of our simulation studies are presented in Section 3.7. In Section 3.8, we offer prospects on the topics covered in this chapter. Additionally, Section 3.9 provides supplementary materials and proofs, further enhancing the chapter's content and insights.

3.1.2 Notation

We introduce some notation that will be used throughout this chapter.

The identity matrix of size n is denoted by $\boldsymbol{I}_n$, $\boldsymbol{J}_n$ represents an $n \times n$ matrix with all entries equal to one, while $\mathbf{1}_n$ is a column vector of size n consisting of ones. For a given matrix $\boldsymbol{A} = (a_{ij})$, the notation $|\boldsymbol{A}|$, $\|\boldsymbol{A}\|_F$, and $\mathrm{tr}(\boldsymbol{A})$ represent its determinant, Frobenius norm, and trace, respectively. If a symmetric matrix $\boldsymbol{A}$ is positive definite, positive semi-definite, or negative definite, we write $\boldsymbol{A} \succ 0$, $\boldsymbol{A} \succeq 0$, or $\boldsymbol{A} \prec 0$, respectively. The notation $\mathrm{vec}(\boldsymbol{A})$ refers to the vector obtained by stacking the columns of matrix $\boldsymbol{A}$ on top of one another. The symbol $\boldsymbol{A} \otimes \boldsymbol{B}$ indicates the Kronecker product of two matrices $\boldsymbol{A}$ and $\boldsymbol{B}$. For a scalar-valued differentiable function f, the gradient of f with respect to $\boldsymbol{A}$ is denoted by $\nabla f(\boldsymbol{A}) = \partial f(\boldsymbol{A})/\partial \boldsymbol{A}$. For a symmetric $n \times n$ matrix $\boldsymbol{A} = (a_{ij})$, we define $\boldsymbol{\Gamma}(\boldsymbol{A}) = \big(\boldsymbol{\Gamma}_{ij}(\boldsymbol{A})\big)$ a block matrix, of size $n^2 \times n^2$, where each block $\boldsymbol{\Gamma}_{ij}(\boldsymbol{A})$ for $i, j = 1, \ldots, n$ is given by,

$$\boldsymbol{\Gamma}_{ij}(\boldsymbol{A}) = \begin{pmatrix} a_{ij}a_{11} + a_{i1}a_{j1} & \ldots & a_{ij}a_{1n} + a_{in}a_{j1} \\ \vdots & \ddots & \vdots \\ a_{ij}a_{n1} + a_{i1}a_{jn} & \ldots & a_{ij}a_{nn} + a_{in}a_{jn} \end{pmatrix}. \tag{3.1}$$

3.2 Model and performance metrics

To analyze the capability of a measurement system that measures multiple characteristics, an experiment is conducted by randomly selecting a sample of $a > 2$ units from the available population. Each unit in the sample consists of p features, where $p \leq a$, and each feature is measured $r \geq 2$ times. The following model is employed to represent the measured data and for subsequent analyses,

$$\boldsymbol{Y}_{ij} = \boldsymbol{\mu} + \boldsymbol{U}_i + \boldsymbol{\epsilon}_{ij}, \quad \text{for } i = 1, \ldots, a, \text{ and } j = 1, \ldots, r. \tag{3.2}$$

Here, $\boldsymbol{Y}_{ij}$, $\boldsymbol{\mu}$, $\boldsymbol{U}_i$, and $\boldsymbol{\epsilon}_{ij}$ are all p–dimensional column vectors. Measurement vector $\boldsymbol{Y}_{ij}$ contains the measurements of all p features for unit i at the jth repeated measurement, $\boldsymbol{\mu}$ is the vector of general mean, while $\boldsymbol{U}_i$ represents the vector of random effect for unit i, and $\boldsymbol{\epsilon}_{ij}$ represents the random measurement error for unit i at the jth replication. All $\boldsymbol{U}_i$'s are i.i.d. multivariate $\mathcal{N}(\mathbf{0}, \boldsymbol{\Sigma}_u)$ random vectors, and all $\boldsymbol{\epsilon}_{ij}$'s are i.i.d. multivariate $\mathcal{N}(\mathbf{0}, \boldsymbol{\Sigma}_\epsilon)$ random vectors. Furthermore, each pair of $\boldsymbol{U}_i$ and $\boldsymbol{\epsilon}_{ij}$ is mutually independent.

In the context of multivariate one-way random effect model (3.2), the variance-covariance

matrix of measurement vector $\boldsymbol{Y}_{ij}$ is expressed as,

$$\boldsymbol{\Sigma}_t = \boldsymbol{\Sigma}_u + \boldsymbol{\Sigma}_\epsilon \,. \tag{3.3}$$

A key parameter used to assess the capability of a measurement system in univariate measurement system assessment studies is the signal-to-noise ratio. This parameter is determined by the ratio of two components, associated with the variability of the units being measured and the variability of the measurement system itself. It helps identify whether the measurement system constitutes the dominant source of variation in the measurements.

In this study, we extend the parameter's definition to multivariate data by summarizing the variance-covariance matrices $\boldsymbol{\Sigma}_u$ and $\boldsymbol{\Sigma}_\epsilon$ using a scalar function and comparing the ratio between them. The statistic for this purpose is defined as follows,

$$\rho_{\mathscr{V}} = \frac{\mathscr{V}(\boldsymbol{\Sigma}_u)}{\mathscr{V}(\boldsymbol{\Sigma}_\epsilon)} \,. \tag{3.4}$$

Here, $\mathscr{V} : \mathbb{R}^{p\times p} \to \mathbb{R}$ is a continuous smooth transformation that quantifies the variability of the variance-covariance matrix. When $p = 1$, the covariance matrix is reduced to a variance value, and $\mathscr{V}(\cdot)$ is defined such that $\mathscr{V}(\sigma_u^2) = \sigma_u^2$ and $\mathscr{V}(\sigma_\epsilon^2) = \sigma_\epsilon^2$, resulting in $\rho = \sigma_u^2/\sigma_\epsilon^2$. Note that the definition of SNR (signal-to-noise ratio), outlined in (1.8) for univariate measurements, is a square root transformation of ρ. In this chapter, we exclusively work with $\rho_{\mathscr{V}}$ and refer to it as the signal-to-noise ratio. The square root transformation of $\rho_{\mathscr{V}}$ is denoted as $\text{SNR}_{\mathscr{V}}$, where $\text{SNR}_{\mathscr{V}} = [\mathscr{V}(\boldsymbol{\Sigma}_u)/\mathscr{V}(\boldsymbol{\Sigma}_\epsilon)]^{1/2}$.

Applying this framework, we set up the counterparts of the percentage R&R ratio and the intra-class correlation coefficient for multivariate data, as follows,

$$\%\text{R\&R}_{\mathscr{V}} = \left[\frac{\mathscr{V}(\boldsymbol{\Sigma}_\epsilon)}{\mathscr{V}(\boldsymbol{\Sigma}_u + \boldsymbol{\Sigma}_\epsilon)}\right]^{1/2} \times 100\% \,, \tag{3.5}$$

$$\text{ICC}_{\mathscr{V}} = \frac{\mathscr{V}(\boldsymbol{\Sigma}_u)}{\mathscr{V}(\boldsymbol{\Sigma}_u + \boldsymbol{\Sigma}_\epsilon)} \,. \tag{3.6}$$

We will examine the following specific transformations of the variance-covariance matrix to quantify data concentration using summary statistics.

A. Generalized variance

The generalized variance is defined as the determinant of the variance-covariance matrix.

Using the generalized variance, we can calculate the signal-to-noise ratio as,

$$\rho_{\text{gv}} = \left|\boldsymbol{\Sigma}_u \boldsymbol{\Sigma}_\epsilon^{-1}\right|^{\frac{1}{p}}. \tag{3.7}$$

This statistic allows us to quantify and compare the variability of the variance-covariance matrices $\boldsymbol{\Sigma}_u$ and $\boldsymbol{\Sigma}_\epsilon$ by taking the geometric mean of their eigenvalues. It also represents the geometric mean of the eigenvalues of $\boldsymbol{\Sigma}_u \boldsymbol{\Sigma}_\epsilon^{-1}$, providing a measure that captures both the variability and the relationship between these matrices. Note that (3.7) corresponds to the performance criterion proposed by Majeske (2008), based on the volume of ellipsoid contours related to a non-singular multivariate normal distribution.
Using this convention, we can proceed to calculate the percentage R&R ratio and the intra-class correlation coefficient as follows,

$$\%\text{R\&R}_{\text{gv}} = \left|\boldsymbol{\Sigma}_\epsilon \left(\boldsymbol{\Sigma}_u + \boldsymbol{\Sigma}_\epsilon\right)^{-1}\right|^{\frac{2}{p}} \times 100\%\,, \tag{3.8}$$

$$\text{ICC}_{\text{gv}} = \left|\boldsymbol{\Sigma}_u \left(\boldsymbol{\Sigma}_u + \boldsymbol{\Sigma}_\epsilon\right)^{-1}\right|^{\frac{1}{p}}. \tag{3.9}$$

B. Trace

The alternative statistic for assessing the signal-to-noise ratio can be defined using the trace of $\boldsymbol{\Sigma}_u$ and $\boldsymbol{\Sigma}_\epsilon$, as follows

$$\rho_{\text{tr}} = \frac{\text{tr}\left(\boldsymbol{\Sigma}_u\right)}{\text{tr}\left(\boldsymbol{\Sigma}_\epsilon\right)}, \tag{3.10}$$

The trace of a matrix is equivalent to the average of the eigenvalues of that matrix. This form enables the comparison between the variance-covariance matrices $\boldsymbol{\Sigma}_u$ and $\boldsymbol{\Sigma}_\epsilon$ based on their average eigenvalues.
Using the trace, we establish the counterparts of the percentage R&R ratio and the intra-class correlation coefficient for multivariate data, as follows,

$$\%\text{R\&R}_{\text{tr}} = \left[\frac{\text{tr}(\boldsymbol{\Sigma}_\epsilon)}{\text{tr}(\boldsymbol{\Sigma}_u) + \text{tr}(\boldsymbol{\Sigma}_\epsilon)}\right]^{1/2} \times 100\%\,, \tag{3.11}$$

$$\text{ICC}_{\text{tr}} = \frac{\text{tr}(\boldsymbol{\Sigma}_u)}{\text{tr}(\boldsymbol{\Sigma}_u) + \text{tr}(\boldsymbol{\Sigma}_\epsilon)}\,. \tag{3.12}$$

The percentage R&R ratio and the intra-class correlation coefficient can be related to

ρ_{tr} through the following relationships,

$$\%\text{R\&R}_{\text{tr}} = \left(1 + \rho_{\text{tr}}\right)^{-1/2} \times 100\%\,, \tag{3.13}$$

$$\text{ICC}_{\text{tr}} = \left(1 + \rho_{\text{tr}}^{-1}\right)^{-1}. \tag{3.14}$$

C. Frobenius norm

By considering the Frobenius norm of the variance-covariance matrices $\boldsymbol{\Sigma}_u$, $\boldsymbol{\Sigma}_\epsilon$, and $\boldsymbol{\Sigma}_t$, we obtain the following measures for the signal-to-noise ratio, the percentage R&R ratio, and the intra-class correlation coefficients,

$$\rho_{_F} = \frac{\|\boldsymbol{\Sigma}_u\|_{_F}}{\|\boldsymbol{\Sigma}_\epsilon\|_{_F}}\,, \tag{3.15}$$

$$\%\text{R\&R}_{_F} = \left[\frac{\|\boldsymbol{\Sigma}_\epsilon\|_{_F}}{\|\boldsymbol{\Sigma}_u + \boldsymbol{\Sigma}_\epsilon\|_{_F}}\right]^{1/2} \times 100\%\,, \tag{3.16}$$

$$\text{ICC}_{_F} = \frac{\|\boldsymbol{\Sigma}_u\|_{_F}}{\|\boldsymbol{\Sigma}_u + \boldsymbol{\Sigma}_\epsilon\|_{_F}}\,, \tag{3.17}$$

where $\|\boldsymbol{\Sigma}\|_{_F}^2 = \|\text{vec}\,(\boldsymbol{\Sigma})\|^2 = \text{tr}\,(\boldsymbol{\Sigma}^2)$. This form enables a comparison between the variance-covariance matrices based on the sum of the squares of all elements of these variance-covariance matrices or, in other words, based on the quadratic mean of all their eigenvalues.

3.3 Preliminary analysis

For the multivariate one-way model (3.2), the two matrices of the sum of squares and cross-products that capture the variation between groups and within groups are, respectively, given as follows,

$$\boldsymbol{SS}_u = r \sum_{i=1}^{a} (\overline{\boldsymbol{Y}}_{i\cdot} - \overline{\boldsymbol{Y}}_{\cdot\cdot})(\overline{\boldsymbol{Y}}_{i\cdot} - \overline{\boldsymbol{Y}}_{\cdot\cdot})^\top, \tag{3.18}$$

$$\boldsymbol{SS}_\epsilon = \sum_{i=1}^{a} \sum_{j=1}^{r} (\boldsymbol{Y}_{ij} - \overline{\boldsymbol{Y}}_{i\cdot})(\boldsymbol{Y}_{ij} - \overline{\boldsymbol{Y}}_{i\cdot})^\top. \tag{3.19}$$

Here, $\overline{\boldsymbol{Y}}_{i\cdot} = \frac{1}{r}\sum_{j=1}^{r}\boldsymbol{Y}_{ij}$ represents the mean vector of measurements for the ith unit, calculated as the average of r measurements for that unit. Alternatively, $\overline{\boldsymbol{Y}}_{\cdot\cdot} = \frac{1}{ar}\sum_{i=1}^{a}\sum_{j=1}^{r}\boldsymbol{Y}_{ij}$ is the overall sample mean vector of the measurements, calculated as the average of all measurements in the experiment. The matrices of the mean of squares and cross-products corresponding to $\boldsymbol{SS}_u$ and $\boldsymbol{SS}_\epsilon$ are given by,

$$\boldsymbol{MS}_u = \frac{\boldsymbol{SS}_u}{\mathrm{df}_u} = \frac{r}{a-1}\sum_{i=1}^{a}(\overline{\boldsymbol{Y}}_{i\cdot} - \overline{\boldsymbol{Y}}_{\cdot\cdot})(\overline{\boldsymbol{Y}}_{i\cdot} - \overline{\boldsymbol{Y}}_{\cdot\cdot})^\top, \tag{3.20}$$

$$\boldsymbol{MS}_\epsilon = \frac{\boldsymbol{SS}_\epsilon}{\mathrm{df}_\epsilon} = \frac{1}{a(r-1)}\sum_{i=1}^{a}\sum_{j=1}^{r}(\boldsymbol{Y}_{ij} - \overline{\boldsymbol{Y}}_{i\cdot})(\boldsymbol{Y}_{ij} - \overline{\boldsymbol{Y}}_{i\cdot})^\top, \tag{3.21}$$

where $\mathrm{df}_u = a-1$ and $\mathrm{df}_\epsilon = a(r-1)$. Table 3.1 displays the multivariate analysis of variance classification.

The matrices $\boldsymbol{MS}_u$ and $\boldsymbol{MS}_\epsilon$ possess certain properties that are relevant for their interpretation. Specifically, $\boldsymbol{MS}_u$ is a positive-semi definite symmetric matrix, which means that all of its eigenvalues are non-negative real numbers, while $\boldsymbol{MS}_\epsilon$ is a positive-definite symmetric matrix, which implies that all of its eigenvalues are strictly positive real numbers. Additionally, assuming the normality distribution for $\boldsymbol{U}_i$'s and $\boldsymbol{\epsilon}_{ij}$'s and their mutual independence, $\boldsymbol{MS}_u$ and $\boldsymbol{MS}_\epsilon$ are two independent matrices, where

$$\boldsymbol{SS}_u \sim \mathscr{W}\left(\boldsymbol{\Sigma}_\epsilon + r\boldsymbol{\Sigma}_u, a-1\right) \quad \text{and} \quad \boldsymbol{SS}_\epsilon \sim \mathscr{W}\left(\boldsymbol{\Sigma}_\epsilon, a(r-1)\right). \tag{3.22}$$

Here, $\mathscr{W}(\boldsymbol{\Sigma}, n)$ refers to a central Wishart distribution with scale matrix $\boldsymbol{\Sigma}$ and n degrees of freedom. If $a \leq p$, $\boldsymbol{SS}_u$ and $\boldsymbol{SS}_\epsilon$ no longer have a density. However, their distributions are defined, taking values in a lower-dimension subspace of $p \times p$ matrices (Uhlig, 1994;

Table 3.1: The multivariate analysis of variance classification for the multivariate one-way model.

Source	Degree of freedom	Sum of squares and products	Mean of squares and products
U	$\mathrm{df}_u = a-1$	$\boldsymbol{SS}_u = r\sum_{i=1}^{a}(\overline{\boldsymbol{Y}}_{i\cdot} - \overline{\boldsymbol{Y}}_{\cdot\cdot})(\overline{\boldsymbol{Y}}_{i\cdot} - \overline{\boldsymbol{Y}}_{\cdot\cdot})^\top$	$\boldsymbol{MS}_u = \dfrac{\boldsymbol{SS}_u}{a-1}$
ϵ	$\mathrm{df}_\epsilon = a(r-1)$	$\boldsymbol{SS}_\epsilon = \sum_{i=1}^{a}\sum_{j=1}^{r}(\boldsymbol{Y}_{ij} - \overline{\boldsymbol{Y}}_{i\cdot})(\boldsymbol{Y}_{ij} - \overline{\boldsymbol{Y}}_{i\cdot})^\top$	$\boldsymbol{MS}_\epsilon = \dfrac{\boldsymbol{SS}_\epsilon}{a(r-1)}$
Total	$ar-1$	$\boldsymbol{SS}_t = \sum_{i=1}^{a}\sum_{j=1}^{r}(\boldsymbol{Y}_{ij} - \overline{\boldsymbol{Y}}_{\cdot\cdot})(\boldsymbol{Y}_{ij} - \overline{\boldsymbol{Y}}_{\cdot\cdot})^\top$	

Srivastava, 2003). In this chapter, we assume that $a > p$, allowing us to find the expected values of $\boldsymbol{MS}_u$ and $\boldsymbol{MS}_\epsilon$ as follows

$$\mathrm{E}\left[\boldsymbol{MS}_u\right] = \boldsymbol{\Sigma}_\epsilon + r\boldsymbol{\Sigma}_u \quad \text{and} \quad \mathrm{E}\left[\boldsymbol{MS}_\epsilon\right] = \boldsymbol{\Sigma}_\epsilon\,. \tag{3.23}$$

To initiate the measurement system study for multivariate data, we can extend the recommendation of Montgomery and Runger (1993a) for univariate data by conducting an initial analysis to investigate the factors contributing to the variability in the measured data. For the one-way model described in Section 3.2, we can test whether the unit's effect on the measured data is significant. Specifically, we set the null hypothesis of no unit's effect as $H_0 : \boldsymbol{\Sigma}_u = \mathbf{0}$. Various tests are available for this analysis, and further insights into these tests can be found in references such as (Sugiura and Nagao, 1968; Rao, 1983; Krzanowski and Marriott, 1994) and (Anderson, 2003, Section 10.6).

3.4 Point estimation

To estimate the signal-to-noise ratio, the percentage gauge R&R ratio, and the intra-class correlation coefficient, one can estimate the variance-covariance matrices $\boldsymbol{\Sigma}_u$ and $\boldsymbol{\Sigma}_\epsilon$ and then apply the plug-in estimators,

$$\widehat{\rho}_{\mathscr{V}} = \frac{\mathscr{V}\left(\widehat{\boldsymbol{\Sigma}}_u\right)}{\mathscr{V}\left(\widehat{\boldsymbol{\Sigma}}_\epsilon\right)}\,, \tag{3.24}$$

$$\widehat{\%\mathrm{R\&R}}_{\mathscr{V}} = \left[\frac{\mathscr{V}(\widehat{\boldsymbol{\Sigma}}_\epsilon)}{\mathscr{V}(\widehat{\boldsymbol{\Sigma}}_u + \widehat{\boldsymbol{\Sigma}}_\epsilon)}\right]^{1/2} \times 100\%\,, \tag{3.25}$$

$$\widehat{\mathrm{ICC}}_{\mathscr{V}} = \frac{\mathscr{V}(\widehat{\boldsymbol{\Sigma}}_u)}{\mathscr{V}(\widehat{\boldsymbol{\Sigma}}_u + \widehat{\boldsymbol{\Sigma}}_\epsilon)}\,. \tag{3.26}$$

We will briefly discuss some existing methods for analytically estimating the variance-covariance matrices in the one-way random effect model with a balanced design setting.

3.4.1 Multivariate ANOVA estimation

The procedure for multivariate ANOVA, also known as MANOVA, is similar to the univariate ANOVA. Specifically, the expected value of each empirical matrix of sums (or means)

of squares and cross-products is a linear function of the variance-covariance matrices. To estimate $\boldsymbol{\Sigma}_u$ and $\boldsymbol{\Sigma}_\epsilon$, one can solve the equations in (3.23) for these matrices, and replace $\mathrm{E}[\boldsymbol{MS}_u]$, and $\mathrm{E}[\boldsymbol{MS}_\epsilon]$ with their empirical versions. This procedure results in the multivariate ANOVA estimators as follows,

$$\widehat{\boldsymbol{\Sigma}}_u = \frac{1}{r}\left(\boldsymbol{MS}_u - \boldsymbol{MS}_\epsilon\right) \quad \text{and} \quad \widehat{\boldsymbol{\Sigma}}_\epsilon = \boldsymbol{MS}_\epsilon\,. \tag{3.27}$$

The parameter space for variance-covariance matrices specifies that the estimator of $\boldsymbol{\Sigma}_\epsilon$ should be a symmetric positive definite matrix, while the estimator of $\boldsymbol{\Sigma}_u$ should be a symmetric positive semi-definite matrix. The ANOVA estimation of $\boldsymbol{\Sigma}_\epsilon$ always remains within the parameter space of $\boldsymbol{\Sigma}_\epsilon$. The ANOVA estimator of $\boldsymbol{\Sigma}_u$ can, at times, fall outside the parameter space, yielding inadmissible results such as negative variances and potential failure to be positive semi-definite. These issues may lead to computational difficulties or result in invalid inferences

The probability of $\widehat{\boldsymbol{\Sigma}}_u \succeq 0$, in the one-way model, depends on the distribution of the smallest root of the equation

$$|\boldsymbol{MS}_u - \delta \boldsymbol{MS}_\epsilon| = 0\,, \tag{3.28}$$

which may also be expressed as $\left|\boldsymbol{MS}_u \boldsymbol{MS}_\epsilon^{-1} - \delta \boldsymbol{I}\right| = 0$ (Hill and Thompson, 1978). To illustrate this, let

$$\boldsymbol{MS}_u = \mathbf{Z}\boldsymbol{D}\mathbf{Z}^\top \quad \text{and} \quad \boldsymbol{MS}_\epsilon = \mathbf{Z}\mathbf{Z}^\top, \tag{3.29}$$

where $\mathbf{Z}$ is a $p \times p$ matrix, $\boldsymbol{D} = \mathrm{diag}(\delta_1, \ldots, \delta_p)$ and $\delta_1 \geq \delta_2 \geq \ldots \geq \delta_p > 0$ are the roots of (3.28). Therefore, $\widehat{\boldsymbol{\Sigma}}_u = r^{-1}\mathbf{Z}(\boldsymbol{D} - \boldsymbol{I})\mathbf{Z}^\top$, and it is positive definite if $\delta_p \geq 1$.

To evaluate $\Pr(\delta_p \geq 1)$, we need the distribution of the smallest eigenvalue of $\boldsymbol{MS}_u \boldsymbol{MS}_\epsilon^{-1}$. Here, $\boldsymbol{MS}_u$ and $\boldsymbol{MS}_\epsilon^{-1}$ are independent Wishart matrices. The ratio of two independently distributed Wishart random matrices and the behavior of its eigenvalues, which generalize the univariate statistic of the F-distribution, is of fundamental importance in multivariate analysis. The works of Pillai (1965); Venables et al. (1974); Hill and Thompson (1978); Bhargava and Disch (1982); Johnstone (2009); Hashiguchi et al. (2018) have contributed to this subject. The distributions of the eigenvalues of $\boldsymbol{MS}_u \boldsymbol{MS}_\epsilon^{-1}$ rely only on $\boldsymbol{\Sigma}_u \boldsymbol{\Sigma}_\epsilon^{-1}$, rather than the individual elements of $\boldsymbol{\Sigma}_u$ and $\boldsymbol{\Sigma}_\epsilon$.

To get a better understanding of the likelihood of $\widehat{\boldsymbol{\Sigma}}_u \succ 0$, consider the case where $\boldsymbol{\Sigma}_u$ and $\boldsymbol{\Sigma}_\epsilon$ are diagonal matrices, and the signal-to-noise ratio is the same for all individual

variables such that $\boldsymbol{\Sigma}_u \boldsymbol{\Sigma}_\epsilon^{-1} = \rho \boldsymbol{I}$. Let $\boldsymbol{S}_1$ and $\boldsymbol{S}_2$ be defined as

$$\boldsymbol{S}_1 = a(r-1)\boldsymbol{M}\boldsymbol{S}_\epsilon \quad \text{and} \quad \boldsymbol{S}_2 = \lambda^{-1}(a-1)\boldsymbol{M}\boldsymbol{S}_u \,,$$

where $\lambda = 1 + r\rho$, and it is also the solution of $|(\boldsymbol{\Sigma}_\epsilon + r\boldsymbol{\Sigma}_u)\boldsymbol{\Sigma}_\epsilon^{-1} - \lambda \boldsymbol{I}| = 0$. As a result, $\boldsymbol{S}_1 \sim \mathscr{W}(\boldsymbol{\Sigma}_\epsilon, a(r-1))$ and $\boldsymbol{S}_2 \sim \mathscr{W}(\boldsymbol{\Sigma}_\epsilon, a-1)$. Let κ_1 be the largest eigenvalue of $\boldsymbol{S}_1(\boldsymbol{S}_1 + \boldsymbol{S}_2)^{-1}$. Then, κ_1 satisfies $|\boldsymbol{S}_1 - \kappa_1(\boldsymbol{S}_1 + \boldsymbol{S}_2)| = 0$. This implies that the smallest root of $|\boldsymbol{M}\boldsymbol{S}_u - \delta \boldsymbol{M}\boldsymbol{S}_\epsilon| = 0$ can be determined as,

$$\delta_p = \frac{a(r-1)(1-\kappa_1)\lambda}{\kappa_1(a-1)} \,.$$

Then, the probability that $\widehat{\boldsymbol{\Sigma}}_u$ is not positive definite can be computed through,

$$\Pr(\delta_p < 1) = 1 - \Pr\left(\kappa_1 < \frac{\mathrm{df}_\epsilon \lambda}{\mathrm{df}_u + \mathrm{df}_\epsilon \lambda}\right) \cdot \tag{3.30}$$

The generalization of this result to cases where $\boldsymbol{\Sigma}_u$ and $\boldsymbol{\Sigma}_\epsilon$ are not necessarily restricted to be diagonal is discussed by Hill and Thompson (1978). Several methods that facilitate the calculation of the cumulative distribution function of κ_1 can be found in (Johnstone, 2009) and the references there.

In Figure 3.1, the plots depict the probability of $\delta_p < 1$, according to (3.30), as a function of ρ for different values of p ranging from 3 to 8. These plots consider a plan with $a = 10$ and $r = 6$. As the dimensionality p increases, the likelihood of $\delta_p < 1$ also increases.

The increasing likelihood of $\delta_p < 1$ with higher dimensionality underscores that when dealing with multiple inputs for each sample, the probability of the MANOVA estimator of $\boldsymbol{\Sigma}_u$ not being positive definite becomes more significant. This observation suggests exploring alternative estimator types. In the following sections, we investigate the UMVUE and maximum likelihood estimations.

3.4.2 UMVUEs

Suppose the vector $\boldsymbol{\mu}$ and matrices $\boldsymbol{\Sigma}_u$ and $\boldsymbol{\Sigma}_\epsilon$ are the unknown parameters. Using the notation $\boldsymbol{y}_{ij}$ for the observed value of the random vector $\boldsymbol{Y}_{ij}$, the likelihood function for $\boldsymbol{\mu}$,

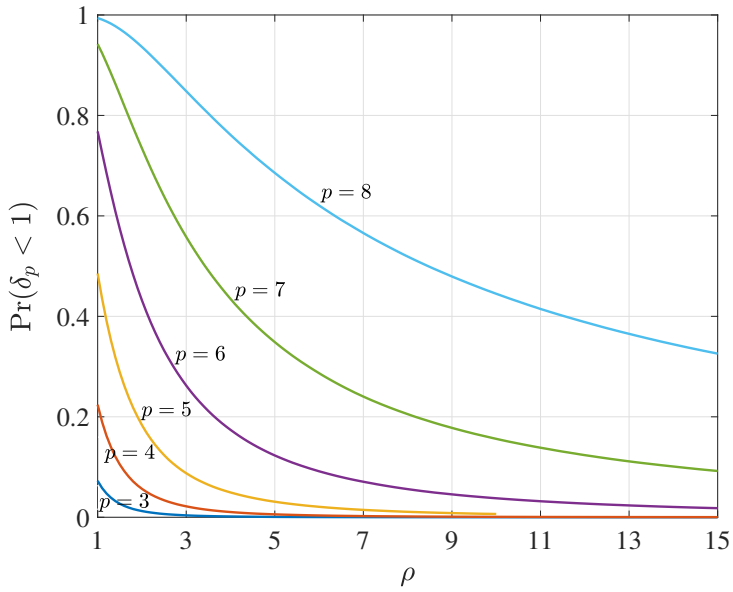

Figure 3.1: Probability of $\delta_p < 1$ with respect to the signal-to-noise ratio ρ for $a = 10$ and $r = 6$, with $\boldsymbol{\Sigma}_u = \rho \boldsymbol{I}$ and $\boldsymbol{\Sigma}_\epsilon = \boldsymbol{I}$.

$\boldsymbol{\Sigma}_u$, and $\boldsymbol{\Sigma}_\epsilon$, as developed by Anderson et al. (1986), is expressed as follows,

$$\mathcal{L}(\boldsymbol{\mu}, \boldsymbol{\Sigma}_u, \boldsymbol{\Sigma}_\epsilon) = c(\boldsymbol{\Sigma}_u, \boldsymbol{\Sigma}_\epsilon) \exp\left(-\frac{1}{2}\text{tr}\left(\boldsymbol{G}\boldsymbol{\Sigma}_\epsilon^{-1}\right) - \frac{1}{2}\text{tr}\left(\boldsymbol{H}(\boldsymbol{\Sigma}_\epsilon + r\boldsymbol{\Sigma}_u)^{-1}\right) - \frac{ar}{2}(\overline{\boldsymbol{y}}_{\cdot\cdot} - \boldsymbol{\mu})^\top(\boldsymbol{\Sigma}_\epsilon + r\boldsymbol{\Sigma}_u)^{-1}(\overline{\boldsymbol{y}}_{\cdot\cdot} - \boldsymbol{\mu})\right), \tag{3.31}$$

where

$$c(\boldsymbol{\Sigma}_u, \boldsymbol{\Sigma}_\epsilon) = (2\pi)^{-\frac{apr}{2}} |\boldsymbol{\Sigma}_\epsilon|^{-\frac{a(r-1)}{2}} |\boldsymbol{\Sigma}_\epsilon + r\boldsymbol{\Sigma}_u|^{-\frac{a}{2}},$$

$$\boldsymbol{H} = r\sum_{i=1}^{a}(\overline{\boldsymbol{y}}_{i\cdot} - \overline{\boldsymbol{y}}_{\cdot\cdot})(\overline{\boldsymbol{y}}_{i\cdot} - \overline{\boldsymbol{y}}_{\cdot\cdot})^\top, \quad \text{and} \quad \boldsymbol{G} = \sum_{i=1}^{a}\sum_{j=1}^{r}(\boldsymbol{y}_{ij} - \overline{\boldsymbol{y}}_{i\cdot})(\boldsymbol{y}_{ij} - \overline{\boldsymbol{y}}_{i\cdot})^\top,$$

with $\overline{\boldsymbol{y}}_{i\cdot} = \frac{1}{r}\sum_{j=1}^{r}\boldsymbol{y}_{ij}$ and $\overline{\boldsymbol{y}}_{\cdot\cdot} = \frac{1}{ar}\sum_{i=1}^{a}\sum_{j=1}^{r}\boldsymbol{y}_{ij}$. For further detailed insights into the derivation of this likelihood function, we refer the reader to the supplementary materials provided in Section 3.9.

The procedure for obtaining the UMVUEs of $\boldsymbol{\mu}$, $\boldsymbol{\Sigma}_u$, and $\boldsymbol{\Sigma}_\epsilon$ is similar to their univariate

counterparts. The relationship of $\mathcal{L}(\boldsymbol{\mu}, \boldsymbol{\Sigma}_u, \boldsymbol{\Sigma}_\epsilon)$, as outlined in (3.31), signifies that the joint distribution of $\boldsymbol{Y}_{ij}$'s belongs to the multi-parameter exponential family. Additionally, $\overline{\boldsymbol{Y}}_{\cdot\cdot}$, $\boldsymbol{MS}_u$, and $\boldsymbol{MS}_\epsilon$ together form the complete and sufficient statistics for $\boldsymbol{\mu}$, $\boldsymbol{\Sigma}_u$, and $\boldsymbol{\Sigma}_\epsilon$. Consequently, the UMVUEs for both $\boldsymbol{\Sigma}_u$ and $\boldsymbol{\Sigma}_\epsilon$ align with their corresponding MANOVA estimators.

3.4.3 Maximum likelihood estimation

To address the issue of obtaining non-positive definite estimators in MANOVA, we need a procedure that ensures the covariance matrix estimators remain within their parameter space. Klotz and Putter (1969); Anderson (1984) and Rao and Heckler (1998) have explored the derivation of maximum likelihood estimation of $\boldsymbol{\Sigma}_u$ and $\boldsymbol{\Sigma}_\epsilon$ constrained to their parameter space for the one-way model. Since many of the results in our study rely on these estimations, we provide a brief overview here.

Taking logarithm from (3.31), the log–likelihood function of $\boldsymbol{\mu}, \boldsymbol{\Sigma}_u$ and $\boldsymbol{\Sigma}_\epsilon$ is obtained as follows,

$$\begin{aligned}\ell(\boldsymbol{\mu}, \boldsymbol{\Sigma}_u, \boldsymbol{\Sigma}_\epsilon) = &-\frac{apr}{2}\ln(2\pi) - \frac{a(r-1)}{2}\ln(|\boldsymbol{\Sigma}_\epsilon|) - \frac{a}{2}\ln(|\boldsymbol{\Sigma}_\epsilon + r\boldsymbol{\Sigma}_u|) - \frac{1}{2}\mathrm{tr}(\boldsymbol{G}\boldsymbol{\Sigma}_\epsilon^{-1}) \\ &-\frac{1}{2}\mathrm{tr}\left(\boldsymbol{H}(\boldsymbol{\Sigma}_\epsilon + r\boldsymbol{\Sigma}_u)^{-1}\right) - \frac{ar}{2}(\overline{\boldsymbol{y}}_{\cdot\cdot} - \boldsymbol{\mu})^\top(\boldsymbol{\Sigma}_\epsilon + r\boldsymbol{\Sigma}_u)^{-1}(\overline{\boldsymbol{y}}_{\cdot\cdot} - \boldsymbol{\mu})\,.\end{aligned} \tag{3.32}$$

Maximum likelihood estimation methods require us to maximize the likelihood function within the defined parameter space. Initially, we consider maximizing $\ell(\boldsymbol{\mu}, \boldsymbol{\Sigma}_u, \boldsymbol{\Sigma}_\epsilon)$ with respect to $\boldsymbol{\mu}$, where $\mathbb{R}^p$ is the parameter space for $\boldsymbol{\mu}$. The likelihood function of (3.32) interacts with $\boldsymbol{\mu}$ only through the quadratic form $(\overline{\boldsymbol{y}}_{\cdot\cdot} - \boldsymbol{\mu})^\top(\boldsymbol{\Sigma}_\epsilon + r\boldsymbol{\Sigma}_u)^{-1}(\overline{\boldsymbol{y}}_{\cdot\cdot} - \boldsymbol{\mu})$. It is easy to see that setting $\boldsymbol{\mu} = \overline{\boldsymbol{y}}_{\cdot\cdot}$ maximizes the likelihood function for any fixed $\boldsymbol{\Sigma}_u$ and $\boldsymbol{\Sigma}_\epsilon$, making $\overline{\boldsymbol{Y}}_{\cdot\cdot}$ the maximum likelihood estimator for $\boldsymbol{\mu}$.

Next, we investigate the maximum likelihood estimators for the covariance matrices $\boldsymbol{\Sigma}_u$ and $\boldsymbol{\Sigma}_\epsilon$. Let $\mathbf{Q}$ be an orthogonal $p \times p$ matrix, and $\boldsymbol{\Lambda} = \mathrm{diag}(\lambda_1, \ldots, \lambda_p)$, with $\lambda_1 \geq \lambda_2 \geq \ldots \geq \lambda_p \geq 0$, such that,

$$\boldsymbol{MS}_\epsilon^{-\frac{1}{2}}\boldsymbol{MS}_u\boldsymbol{MS}_\epsilon^{-\frac{1}{2}} = \beta\,\mathbf{Q}\boldsymbol{\Lambda}\mathbf{Q}^\top, \tag{3.33}$$

where $\beta = \dfrac{a}{a-1}$. We define $\mathbf{Z} = \boldsymbol{MS}_\epsilon^{\frac{1}{2}}\mathbf{Q}$. Then, we can express $\boldsymbol{MS}_u$ and $\boldsymbol{MS}_\epsilon$ as

$$\boldsymbol{MS}_u = \beta\,\mathbf{Z}\boldsymbol{\Lambda}\mathbf{Z}^\top \quad \text{and} \quad \boldsymbol{MS}_\epsilon = \mathbf{Z}\mathbf{Z}^\top, \tag{3.34}$$

Using this decomposition pair, we get

$$\beta^{-1}\boldsymbol{MS}_u - \boldsymbol{MS}_\epsilon = \mathbf{Z}(\boldsymbol{\Lambda} - \boldsymbol{I}_p)\mathbf{Z}^\top . \tag{3.35}$$

If all λ_i's are greater than or equal to unity, then $\beta^{-1}\boldsymbol{MS}_u - \boldsymbol{MS}_\epsilon$ is non-negative definite, and the maximum likelihood estimators of $\boldsymbol{\Sigma}_u$ and $\boldsymbol{\Sigma}_\epsilon$ are derived as follows,

$$\widehat{\boldsymbol{\Sigma}}_u = \frac{1}{r}\left(\beta^{-1}\boldsymbol{MS}_u - \boldsymbol{MS}_\epsilon\right) \quad \text{and} \quad \widehat{\boldsymbol{\Sigma}}_\epsilon = \boldsymbol{MS}_\epsilon . \tag{3.36}$$

If some of the λ_i's are less than 1, then $\beta^{-1}\boldsymbol{MS}_u - \boldsymbol{MS}_\epsilon$ is not non-negative definite. For univariate data, this indicates negativity. However, for multivariate data, a matrix that is not non-negative definite can be indefinite. Let k be the number of eigenvalues λ_i's greater than unity. Then, the remaining $p-k$ eigenvalues $\lambda_{k+1}, \ldots, \lambda_p$ are less than unity. To partition $\mathbf{Z}$ and $\boldsymbol{\Lambda}$, we first define $\boldsymbol{\Lambda}_1$ as a diagonal matrix with the first k eigenvalues $\lambda_1, \ldots, \lambda_k$ and $\boldsymbol{\Lambda}_2$ as a diagonal matrix with the remaining $p-k$ eigenvalues $\lambda_{k+1}, \ldots, \lambda_p$. We also define $\mathbf{Z}_1$ as the $p \times k$ sub-matrix of $\mathbf{Z}$ corresponding to the first k columns and $\mathbf{Z}_2$ as the $p \times (p-k)$ sub-matrix corresponding to the remaining columns of $\mathbf{Z}$. With this notation, we can write,

$$\mathbf{Z} = \begin{pmatrix} \mathbf{Z}_1 & \mathbf{Z}_2 \end{pmatrix} \quad \text{and} \quad \boldsymbol{\Lambda} = \begin{pmatrix} \boldsymbol{\Lambda}_1 & \mathbf{0} \\ \mathbf{0} & \boldsymbol{\Lambda}_2 \end{pmatrix}.$$

It is possible to decompose (3.35) as follows,

$$\beta^{-1}\boldsymbol{MS}_u - \boldsymbol{MS}_\epsilon = \mathbf{Z}_1(\boldsymbol{\Lambda}_1 - \boldsymbol{I}_k)\mathbf{Z}_1^\top + \boldsymbol{\Omega}, \tag{3.37}$$

where $\boldsymbol{\Omega}$ is defined as

$$\boldsymbol{\Omega} = \mathbf{Z}_2(\boldsymbol{\Lambda}_2 - \mathbf{I}_{p-k})\mathbf{Z}_2^\top . \tag{3.38}$$

This decomposition expresses $\beta^{-1}\boldsymbol{MS}_u - \boldsymbol{MS}_\epsilon$ as the sum of $\mathbf{Z}_1(\boldsymbol{\Lambda}_1 - \boldsymbol{I}_k)\mathbf{Z}_1^\top \succeq 0$ and $\boldsymbol{\Omega} \prec 0$. The term $\mathbf{Z}_1(\boldsymbol{\Lambda}_1 - \boldsymbol{I}_k)\mathbf{Z}_1^\top$, representing the non-negative definite contribution to the decomposition, can be considered as the estimator of $r\boldsymbol{\Sigma}_u$. It has been shown in (Anderson, 1984, Section 7) that the maximum likelihood estimators for the variance-covariance matrices $\boldsymbol{\Sigma}_u$ and $\boldsymbol{\Sigma}_\epsilon$ are given by,

$$\widehat{\boldsymbol{\Sigma}}_u = \frac{1}{r}\left(\beta^{-1}\boldsymbol{MS}_u - \boldsymbol{MS}_\epsilon - \boldsymbol{\Omega}\right) \quad \text{and} \quad \widehat{\boldsymbol{\Sigma}}_\epsilon = \boldsymbol{MS}_\epsilon + \frac{\boldsymbol{\Omega}}{r} . \tag{3.39}$$

Of particular significance is the fact that these estimators are obtained by adjusting the

estimators given in (3.36) using the term $\boldsymbol{\Omega}$. To establish that $\widehat{\boldsymbol{\Sigma}}_\epsilon$ in (3.39) is positive definite too, we can write $\widehat{\boldsymbol{\Sigma}}_\epsilon$ as,

$$\widehat{\boldsymbol{\Sigma}}_\epsilon = \mathbf{Z}_1\mathbf{Z}_1^\top + \frac{1}{r}\mathbf{Z}_2\boldsymbol{\Lambda}_2\mathbf{Z}_2^\top + \frac{r-1}{r}\,\mathbf{Z}_2\mathbf{Z}_2^\top,$$

in which all terms are positive definite matrices. Therefore, $\widehat{\boldsymbol{\Sigma}}_\epsilon \succ 0$. On the other hand, $\widehat{\boldsymbol{\Sigma}}_u \succeq 0$ and its rank is determined by k, the number of eigenvalues of $\boldsymbol{\Lambda}$ greater than one. If all eigenvalues λ_i's are less than 1, the maximum likelihood estimates for the variance-covariance matrices $\boldsymbol{\Sigma}_u$ and $\boldsymbol{\Sigma}_\epsilon$ are obtained as follows,

$$\widehat{\boldsymbol{\Sigma}}_u = \mathbf{0} \quad \text{and} \quad \widehat{\boldsymbol{\Sigma}}_\epsilon = \frac{\boldsymbol{SS}_t}{ar}\,. \tag{3.40}$$

The estimation procedure described above yields a maximum likelihood estimate of $\boldsymbol{\Sigma}_u$ whose rank is determined by the available sample data. However, there are cases where prior knowledge or considerations regarding the true rank of $\boldsymbol{\Sigma}_u$ are available. Even when the true rank is unknown, statistical tests are available to make inferences about the rank of $\boldsymbol{\Sigma}_u$ (Anderson, 1989; Anderson and Amemiya, 1991; Amemiya et al., 1990). Hence, it may be desirable in some situations to obtain an estimator of $\boldsymbol{\Sigma}_u$ that is both non-negative definite and constrained to have a pre-specified rank, denoted as m where $m < p$. By imposing this constraint, the variation of the units can be characterized in a lower-dimensional linear space, with a maximum dimension of m. To estimate the covariance matrix $\boldsymbol{\Sigma}_u$ with a specified reduced rank of m, the integer k that is used to partition $\boldsymbol{\Lambda}$ can be determined as the minimum of m and the number of λ_i's greater than one.

3.4.4 Other estimation methods

Various alternative approaches are available for estimating the variance-covariance components of the multivariate one-way model (3.2), which are constrained within the parameter space.

One such method, known as bending and originally proposed by Hayes and Hill (1981), involves the modification of eigenvalues derived from $\boldsymbol{MS}_\epsilon^{-1}\boldsymbol{MS}_u$. This technique has found extensive application in the field of genetics and biomedical contexts. Another estimation method discussed by Amemiya (1985), is based on restricted maximum likelihood estimation. It involves minimizing an objective function that incorporates $\mathcal{L}(\boldsymbol{\mu}, \boldsymbol{\Sigma}_u, \boldsymbol{\Sigma}_\epsilon)$ alongside a penalty term. Employing this method, the estimators for $\boldsymbol{\Sigma}_u$ and $\boldsymbol{\Sigma}_\epsilon$ are

defined as follows,

$$\widehat{\boldsymbol{\Sigma}}_u = \frac{1}{r}\left(\boldsymbol{MS}_u - \boldsymbol{MS}_\epsilon - \boldsymbol{\Omega}\right) \quad \text{and} \quad \widehat{\boldsymbol{\Sigma}}_\epsilon = \boldsymbol{MS}_\epsilon + \frac{a-1}{ar-1}\,\boldsymbol{\Omega}\,. \tag{3.41}$$

In a similar context, Meyer and Kirkpatrick (2010) propose alternative estimators for variance-covariance matrices, employing a penalized maximum likelihood approach, which can be computationally intensive. Srivastava and Kubokawa (1999) and Kubokawa and Tsai (2006) discuss several estimators for the variance-covariance matrices by minimizing entropy loss functions. However, the statistical properties of their suggested estimators require cumbersome investigation.

3.5 Convergence properties

To examine the asymptotic properties of the outcome estimates, we consider three scenarios in which either the sample size, replication numbers, or both become large:

($\mathcal{S}1$) $a \to \infty$ and r is fixed,
($\mathcal{S}2$) $r \to \infty$ and a is fixed,
($\mathcal{S}3$) $r \to \infty$ and $a \to \infty$.

We analyze these scenarios by examining estimators obtained through the maximum likelihood method as well.

$\mathcal{S}1$. Asymptotic behaviors when increasing the sample size a

Theorem 3.1 provides insights into the asymptotic properties of $\widehat{\boldsymbol{\Sigma}}_u$ and $\widehat{\boldsymbol{\Sigma}}_\epsilon$ in the context of asymptotic scenario $\mathcal{S}1$. According to Remadi and Amemiya (1994), having some knowledge of the rank of $\boldsymbol{\Sigma}_u$ with a sufficiently large probability is crucial for correctly inferring the distribution convergence in this asymptotic case. This knowledge can be acquired through a hypothesis test expressed in terms of the rank of $\boldsymbol{\Sigma}_u$.

Theorem 3.1. *As the replication number r remains fixed and $a \to \infty$, the estimators $\widehat{\boldsymbol{\Sigma}}_u$ and $\widehat{\boldsymbol{\Sigma}}_\epsilon$ from the maximum likelihood method exhibit the following asymptotic properties:*

a) $\widehat{\boldsymbol{\Sigma}}_\epsilon \xrightarrow{a.s} \boldsymbol{\Sigma}_\epsilon$, *given that* $\boldsymbol{\epsilon}_{ij}$*'s are i.i.d. random vectors with* $\mathrm{E}\left[\|\boldsymbol{\epsilon}_{ij}\|^2\right] < \infty$.

b) $\widehat{\boldsymbol{\Sigma}}_u \xrightarrow{a.s} \boldsymbol{\Sigma}_u$, *provided that both* $\boldsymbol{U}_{ij}$*'s and* $\boldsymbol{\epsilon}_{ij}$*'s are i.i.d. random vectors such that* $\mathrm{E}\left[\|\boldsymbol{U}_i\|^2\right] < \infty$ *and* $\mathrm{E}\left[\|\boldsymbol{\epsilon}_{ij}\|^2\right] < \infty$, *and* $\boldsymbol{\epsilon}_{ij}$*'s are independent of* $\boldsymbol{U}_{ij}$*'s.*

c) *Under the normality assumption of i.i.d. random vectors* $\boldsymbol{U}_i$ *and* $\boldsymbol{\epsilon}_{ij}$*, and given that* $\boldsymbol{\Sigma}_u \succ 0$*, the joint distribution of* $\widehat{\boldsymbol{\Sigma}}_\epsilon$ *and* $\widehat{\boldsymbol{\Sigma}}_u$ *satisfies,*

$$\sqrt{a}\,\mathrm{vec}\begin{pmatrix}\widehat{\boldsymbol{\Sigma}}_\epsilon - \boldsymbol{\Sigma}_\epsilon \\ \widehat{\boldsymbol{\Sigma}}_u - \boldsymbol{\Sigma}_u\end{pmatrix} \to \mathcal{N}\left(\boldsymbol{0}, \begin{pmatrix}\boldsymbol{\Sigma}_{11} & \boldsymbol{\Sigma}_{12} \\ \boldsymbol{\Sigma}_{21} & \boldsymbol{\Sigma}_{22}\end{pmatrix}\right).$$

The blocks of the covariance matrix of the limiting distribution are given by,

$$\boldsymbol{\Sigma}_{11} = \frac{1}{r-1}\boldsymbol{\Gamma}(\boldsymbol{\Sigma}_\epsilon)\,, \quad \boldsymbol{\Sigma}_{12} = \frac{-1}{r(r-1)}\boldsymbol{\Gamma}(\boldsymbol{\Sigma}_\epsilon)\,,$$
$$\boldsymbol{\Sigma}_{22} = \boldsymbol{\Gamma}\left(\boldsymbol{\Sigma}_u + \tfrac{1}{r}\boldsymbol{\Sigma}_\epsilon\right) + \frac{1}{r^2(r-1)}\boldsymbol{\Gamma}\left(\boldsymbol{\Sigma}_\epsilon\right)\,,$$

where $\boldsymbol{\Gamma}(\cdot)$ *denotes the covariance operator as defined in* (3.1)*.*

Proof. See the supplementary materials. □

Without specifying a particular distribution for $\boldsymbol{U}_i$ and $\boldsymbol{\epsilon}_{ij}$, part (c) of Theorem 3.1 still ensures convergence to a normal distribution, provided that both sequences $\boldsymbol{U}_i$ and $\boldsymbol{\epsilon}_{ij}$ are i.i.d. random vectors of finite fourth moments.

In Theorem 3.2, we investigate the convergence characteristics of $\widehat{\rho}_{\mathscr{V}}$ as the sample size tends towards infinity.

Theorem 3.2. *As* $a \to \infty$*, and with any fixed replication number, we have the following convergence results:*

a) $\widehat{\rho}_{\mathscr{V}} \xrightarrow{a.s} \rho_{\mathscr{V}}$*, provided that* $\mathrm{E}\left[\|\boldsymbol{U}_i\|^2\right] < \infty$ *and* $\mathrm{E}\left[\|\boldsymbol{\epsilon}_{ij}\|^2\right] < \infty$*,*

b) *Within the conditions defined in Theorem 3.1, part (c), we have*

$$\sqrt{a}\begin{pmatrix}\mathscr{V}(\widehat{\boldsymbol{\Sigma}}_\epsilon) - \mathscr{V}(\boldsymbol{\Sigma}_\epsilon) \\ \mathscr{V}(\widehat{\boldsymbol{\Sigma}}_u) - \mathscr{V}(\boldsymbol{\Sigma}_u)\end{pmatrix} \xrightarrow{d} \mathcal{N}\left(\boldsymbol{0}, \begin{pmatrix}\sigma_{11} & \sigma_{12} \\ \sigma_{21} & \sigma_{22}\end{pmatrix}\right),$$

where

$$\sigma_{11} = \frac{2}{r-1}\|\nabla\mathscr{V}(\boldsymbol{\Sigma}_\epsilon)\boldsymbol{\Sigma}_\epsilon\|_F^2\,, \quad \sigma_{12} = \frac{-2}{r(r-1)}\left\{\mathrm{tr}\left(\nabla\mathscr{V}(\boldsymbol{\Sigma}_\epsilon)\boldsymbol{\Sigma}_\epsilon\nabla\mathscr{V}(\boldsymbol{\Sigma}_u)\boldsymbol{\Sigma}_\epsilon\right)\right\},$$
$$\sigma_{22} = 2\,\|\nabla\mathscr{V}(\boldsymbol{\Sigma}_u)\left(\boldsymbol{\Sigma}_u + \tfrac{1}{r}\boldsymbol{\Sigma}_\epsilon\right)\|_F^2 + \frac{2}{r^2(r-1)}\|\nabla\mathscr{V}(\boldsymbol{\Sigma}_u)\boldsymbol{\Sigma}_\epsilon\|_F^2\,.$$

c) *Under the constraint defined in Theorem 3.1, part (c),* $\sqrt{a}\left\{\widehat{\rho}_{\mathscr{V}} - \rho_{\mathscr{V}}\right\} \xrightarrow{d} \mathcal{N}\big(0, \sigma_\rho^2\big)$, *where*

$$\sigma_\rho^2 = \frac{\rho_{\mathscr{V}}^2 \sigma_{11} - 2\rho_{\mathscr{V}}\sigma_{12} + \sigma_{22}}{\{\mathscr{V}(\boldsymbol{\Sigma}_\epsilon)\}^2}\,.$$

Proof. See the supplementary materials. □

Using the result of Theorem 3.2, we proceed to derive the asymptotic variances σ_{11} and σ_{22}, along with the asymptotic covariance σ_{12}, by exploring the three selections of the matrix transformation $\mathscr{V}(\cdot)$ outlined in Section 3.2.

a. Generalized variance

Assuming $\boldsymbol{\Sigma}_u$ is full rank, let $\mathscr{V}(\boldsymbol{\Sigma}) = \big|\boldsymbol{\Sigma}\big|^{\frac{1}{p}}$. The gradient of $\big|\boldsymbol{\Sigma}\big|$ is $\boldsymbol{\Sigma}^{-1}$. Then, $\nabla\mathscr{V}(\boldsymbol{\Sigma})$ is $\frac{1}{p}\big|\boldsymbol{\Sigma}\big|^{\frac{1}{p}}\boldsymbol{\Sigma}^{-1}$. Thus,

$$\begin{aligned}\sigma_{11} = \frac{2}{p(r-1)}\big|\boldsymbol{\Sigma}_\epsilon\big|^{\frac{2}{p}}\,, \quad \sigma_{12} = \frac{-2}{p^2 r(r-1)}\big|\boldsymbol{\Sigma}_\epsilon\boldsymbol{\Sigma}_u\big|^{\frac{1}{p}}\operatorname{tr}\big(\boldsymbol{\Sigma}_u^{-1}\boldsymbol{\Sigma}_\epsilon\big)\,,\\ \sigma_{22} = \frac{2}{p}\big|\boldsymbol{\Sigma}_u\big|^{\frac{2}{p}}\left\{1 + \frac{2}{pr}\operatorname{tr}\big(\boldsymbol{\Sigma}_u^{-1}\boldsymbol{\Sigma}_\epsilon\big) + \frac{1}{pr(r-1)}\|\boldsymbol{\Sigma}_u^{-1}\boldsymbol{\Sigma}_\epsilon\|_F^2\right\}.\end{aligned} \tag{3.42}$$

b. Trace

When we let $\mathscr{V}(\boldsymbol{\Sigma}) = \operatorname{tr}(\boldsymbol{\Sigma})$, the gradient of $\mathscr{V}(\boldsymbol{\Sigma})$ is the identity matrix. Consequently,

$$\begin{aligned}\sigma_{11} = \frac{2}{r-1}\operatorname{tr}\left(\boldsymbol{\Sigma}_\epsilon^2\right), \qquad \sigma_{12} = \frac{-2}{r(r-1)}\operatorname{tr}\left(\boldsymbol{\Sigma}_\epsilon^2\right),\\ \sigma_{22} = 2\operatorname{tr}\left\{\left(\boldsymbol{\Sigma}_u + \tfrac{1}{r}\boldsymbol{\Sigma}_\epsilon\right)^2\right\} + \frac{2}{r(r-1)}\frac{1}{r}\operatorname{tr}\left(\boldsymbol{\Sigma}_\epsilon^2\right).\end{aligned} \tag{3.43}$$

c. Frobenius norm

When $\mathscr{V}(\boldsymbol{\Sigma}) = \|\boldsymbol{\Sigma}\|_F$, the gradient of $\mathscr{V}(\boldsymbol{\Sigma})$ is given by $\nabla\mathscr{V}(\boldsymbol{\Sigma}) = \boldsymbol{\Sigma}/\|\boldsymbol{\Sigma}\|_F$. This leads to,

$$\begin{aligned}\sigma_{11} = \frac{2}{r-1}\,, \quad \sigma_{12} = \frac{-2}{r(r-1)}\left\{\operatorname{tr}(\boldsymbol{\Sigma}_\epsilon^3\boldsymbol{\Sigma}_u)\right\}/\|\boldsymbol{\Sigma}_\epsilon\|_F\|\boldsymbol{\Sigma}_u\|_F\,,\\ \sigma_{22} = 2\,\|\boldsymbol{\Sigma}_u(\boldsymbol{\Sigma}_u + \tfrac{1}{r}\boldsymbol{\Sigma}_\epsilon)\|_F^2/\|\boldsymbol{\Sigma}_u\|_F^2 + \frac{2}{r(r-1)}\left\{\frac{1}{r}\,\|\boldsymbol{\Sigma}_u\boldsymbol{\Sigma}_\epsilon\|_F^2\right\}/\|\boldsymbol{\Sigma}_u\|_F^2\,.\end{aligned} \tag{3.44}$$

$\mathcal{S}2$. Asymptotic behaviors when increasing the replications r

In the asymptotic case $\mathcal{S}1$, complexities arise in the distributional convergence due to the rank restrictions. Shifting our focus to the second asymptotic scenario, $\mathcal{S}2$, where the replication number increases, we first provide a detailed analysis of the convergence properties of $\widehat{\boldsymbol{\Sigma}}_u$ and $\widehat{\boldsymbol{\Sigma}}_\epsilon$. Theorem 3.3 concentrates on this scenario.

Theorem 3.3. *Suppose the sample size a is fixed. As $r \to \infty$, the following asymptotic properties hold,*

a) $\widehat{\boldsymbol{\Sigma}}_\epsilon \xrightarrow{a.s} \boldsymbol{\Sigma}_\epsilon$, *provided that* $\mathrm{E}\left[\|\boldsymbol{\epsilon}_{ij}\|^2\right] < \infty$.

b) $\sqrt{ar}\,\mathrm{vec}\big(\widehat{\boldsymbol{\Sigma}}_\epsilon - \boldsymbol{\Sigma}_\epsilon\big) \xrightarrow{\mathrm{d}} \mathcal{N}\big(\mathbf{0}, \boldsymbol{\Gamma}(\boldsymbol{\Sigma}_\epsilon)\big)$, *provided that $\boldsymbol{\epsilon}_{ij}$'s are normally distributed.*

c) $a\,\widehat{\boldsymbol{\Sigma}}_u \xrightarrow{d} \mathcal{W}(\boldsymbol{\Sigma}_u, a-1)$, *provided that $\boldsymbol{U}_i$'s and $\boldsymbol{\epsilon}_{ij}$'s are normally distributed i.i.d. random vectors.*

d) *The estimates $\widehat{\boldsymbol{\Sigma}}_\epsilon$ and $\widehat{\boldsymbol{\Sigma}}_u$ tend to be statistically independent.*

Proof. Refer to the supplementary materials for the proof. □

Analyzing the asymptotic distribution of $\widehat{\rho}_{\mathcal{V}}$ in case $\mathcal{S}2$ incorporates a transformation of a random matrix following a Wishart distribution. The literature contains well-established results regarding the distribution of some transformations of a Wishart matrix. For detailed information on the trace and the sample generalized variance transformations of a Wishart matrix, readers can refer to Jensen (1970); Anderson (2003); Gupta and Nagar (2000); Pham-Gia et al. (2015). We will provide a brief overview of some of these results.

Let us consider $\boldsymbol{S} = (s_{ij})$, a random matrix that follows a Wishart distribution $\mathcal{W}(\boldsymbol{\Sigma}, n)$ where $\boldsymbol{\Sigma} = (\sigma_{ij})$. In general, when $\boldsymbol{\Sigma}$ is not a diagonal matrix, the distribution of $\mathrm{tr}(\boldsymbol{S})$ becomes quite complex, involving zonal polynomials (Gupta and Nagar, 2000, Section 1.5). A detailed description of this distribution and its moments is provided in (Muirhead, 1982, Theorem 8.3.4). In a special case where $\boldsymbol{\Sigma}$ is a scaled identity matrix, i.e., $\boldsymbol{\Sigma} = \sigma^2\boldsymbol{I}$, the quantity $\mathrm{tr}(\boldsymbol{S})/\sigma^2$ follows a chi-square distribution. In a more general case where $\boldsymbol{\Sigma}$ is a diagonal matrix, each quantity s_{ii}/σ_{ii} follows a chi-squared distribution, and these variables are independent. In this instance, $\mathrm{tr}(\boldsymbol{S})$ can be expressed as a linear combination of independent central chi-square random variables. In a bivariate setting, this yields a mixture of Gamma distributions.

As for the determinant of $\boldsymbol{S}$, its distribution involves the product of chi-squared distributed random variables (Anderson, 2003). The discussion highlights the associated complexities when it comes to the asymptotic distribution of parameter $\widehat{\rho}_{\mathcal{V}}$.

$\mathcal{S}3$. Asymptotic behavior when increasing the sample size a and replications r

Turning our attention to the third asymptotic scenario $\mathcal{S}3$, Theorem 3.4 specially addresses this scenario, providing straightforward asymptotic distribution results of $\widehat{\boldsymbol{\Sigma}}_u$ and $\widehat{\boldsymbol{\Sigma}}_\epsilon$ and $\widehat{\rho}_{\mathscr{V}}$ in this setting.

Theorem 3.4. *Under the normality assumptions on sequences $\boldsymbol{U}_i$ and $\boldsymbol{\epsilon}_{ij}$, and provided that $\boldsymbol{\Gamma}(\boldsymbol{\Sigma}_u) \succ 0$, we have as $a \to \infty$ and $r \to \infty$,*

a) *The joint distribution of $\widehat{\boldsymbol{\Sigma}}_u$ and $\widehat{\boldsymbol{\Sigma}}_\epsilon$ converges as follows,*

$$\sqrt{a}\,\mathrm{vec}\begin{pmatrix}\sqrt{r}\left(\widehat{\boldsymbol{\Sigma}}_\epsilon - \boldsymbol{\Sigma}_\epsilon\right)\\ \widehat{\boldsymbol{\Sigma}}_u - \boldsymbol{\Sigma}_u\end{pmatrix} \to \mathcal{N}\left(\mathbf{0}, \begin{pmatrix}\boldsymbol{\Gamma}(\boldsymbol{\Sigma}_\epsilon) & \mathbf{0}\\ \mathbf{0} & \boldsymbol{\Gamma}(\boldsymbol{\Sigma}_u)\end{pmatrix}\right).$$

b) $\sqrt{a}\left\{\widehat{\rho}_{\mathscr{V}} - \rho_{\mathscr{V}}\right\} \xrightarrow{d} \mathcal{N}\left(0, \sigma_\rho^2\right)$ *where*

$$\sigma_\rho^2 = 2\left(\frac{\left\|\nabla\mathscr{V}(\boldsymbol{\Sigma}_u)\boldsymbol{\Sigma}_u\right\|_F}{\mathscr{V}(\boldsymbol{\Sigma}_\epsilon)}\right)^2.$$

Proof. See the supplementary materials for the proof. □

In Section 3.2, we proposed three different transformations for quantifying the signal-to-noise ratio. In Theorem 3.5, we conduct a comparative analysis of their asymptotic properties.

Theorem 3.5. *As $a \to \infty$ and $r \to \infty$, and when considering the relative values of $\mathscr{V}(\widehat{\boldsymbol{\Sigma}}_\epsilon)$, $\mathscr{V}(\widehat{\boldsymbol{\Sigma}}_u)$, and $\widehat{\rho}_{\mathscr{V}}$, the following ranking holds among the three matrix transformations:*

a) *The generalized variance transformation yields the smallest asymptotic variances.*
b) *The Frobenius norm transformation results in the highest asymptotic variances.*

Proof. Refer to the supplementary materials. □

3.6 Confidence intervals

We leverage the result of Theorem 3.2 and establish Wald-type confidence intervals for $\mathscr{V}(\boldsymbol{\Sigma}_\epsilon)$, $\mathscr{V}(\boldsymbol{\Sigma}_u)$, and $\rho_{\mathscr{V}}$. Here, we will detail the procedure for constructing confidence

intervals for $\rho_{\mathscr{V}}$, noting that the procedures for establishing confidence intervals for $\mathscr{V}(\boldsymbol{\Sigma}_\epsilon)$ and $\mathscr{V}(\boldsymbol{\Sigma}_u)$ follow a similar approach.

The quantity $\sqrt{a}\{\widehat{\rho}_{\mathscr{V}} - \rho_{\mathscr{V}}\}/\sigma_\rho$ is asymptotically pivotal, which leads to the following Wald-type confidence interval for $\rho_{\mathscr{V}}$ at $1-\alpha$ level,

$$\left[\widehat{\rho}_{\mathscr{V}} - \frac{z_{1-\alpha/2}\widehat{\sigma_\rho}}{\sqrt{a}},\, \widehat{\rho}_{\mathscr{V}} + \frac{z_{1-\alpha/2}\widehat{\sigma_\rho}}{\sqrt{a}}\right]. \tag{3.45}$$

In the aforementioned Wald-type confidence interval, the lower bound can be negative. Thus, the direct construction of the confidence interval for $\rho_{\mathscr{V}}$ based on $\widehat{\rho}_{\mathscr{V}}$ does not preserve the range. To address this, we can simply set any negative lower bounds to zero, resulting in the interval

$$\mathcal{CI}_{\rho,\,\text{Wald}} = \left[\max\left(0,\, \widehat{\rho}_{\mathscr{V}} - \frac{z_{1-\alpha/2}\widehat{\sigma_\rho}}{\sqrt{a}}\right),\, \widehat{\rho}_{\mathscr{V}} + \frac{z_{1-\alpha/2}\widehat{\sigma_\rho}}{\sqrt{a}}\right]. \tag{3.46}$$

To create a confidence interval of $\rho_{\mathscr{V}}$ that preserves the range, we can utilize a log transformation on $\rho_{\mathscr{V}}$ based on the result of Theorem 3.2. This transformation yields the following result,

$$\sqrt{a}\left\{\log(\widehat{\rho}_{\mathscr{V}}) - \log(\rho_{\mathscr{V}})\right\} \xrightarrow{\text{d}} \mathcal{N}\Big(0,\, \frac{\sigma_\rho^2}{\rho_{\mathscr{V}}^2}\Big), \tag{3.47}$$

as $a \to \infty$. Consequently $\sqrt{a}\,\widehat{\rho}_{\mathscr{V}}\big\{\log(\widehat{\rho}_{\mathscr{V}}) - \log(\rho_{\mathscr{V}})\big\}/\widehat{\sigma}_\rho$ is asymptotically pivotal, where $\widehat{\rho}_{\mathscr{V}} > 0$. This leads to the following confidence interval for $\rho_{\mathscr{V}}$,

$$\mathcal{CI}_{\rho,\,\log} = \left[\exp\left\{\log(\widehat{\rho}_{\mathscr{V}}) - \frac{z_{1-\alpha/2}\widehat{\sigma_\rho}}{\widehat{\rho}_{\mathscr{V}}\sqrt{a}}\right\},\, \exp\left\{\log(\widehat{\rho}_{\mathscr{V}}) + \frac{z_{1-\alpha/2}\widehat{\sigma_\rho}}{\widehat{\rho}_{\mathscr{V}}\sqrt{a}}\right\}\right]. \tag{3.48}$$

3.7 Simulation studies

We conducted numerical studies to examine the finite sample statistical properties of three signal-to-noise ratio estimators, namely $\widehat{\rho}_{\text{gv}}$, $\widehat{\rho}_{\text{tr}}$, and $\widehat{\rho}_{_F}$. Our investigation focuses on a one-way model with three variables, that is $p = 3$. We kept the mean vector $\boldsymbol{\mu}$ at zero. In our analysis, we considered two models for the variance-covariance matrices:

- **Model 1:** In this model, we assume $\boldsymbol{\Sigma}_u = \rho\boldsymbol{I}$ and $\boldsymbol{\Sigma}_\epsilon = \boldsymbol{I}$. Here, all three variables of the measurand are uncorrelated, and the marginal signal-to-noise ratio values are

identical for each variable, each equal to ρ. Additionally, with all three transformations, that are the generalized variance, the trace, and the Frobenius norm, the signal-to-noise ratio quantity consistently maintains the value of ρ.

– **Model 2:** We introduced more complexity by specifying $\boldsymbol{\Sigma}_u$ as the following non-diagonal matrix,

$$\boldsymbol{\Sigma}_u = \alpha \begin{pmatrix} 0.9 & 0.5 & 0.5 \\ 0.5 & 2.0 & 0.3 \\ 0.5 & 0.3 & 3.0 \end{pmatrix}, \tag{3.49}$$

while maintaining $\boldsymbol{\Sigma}_\epsilon = \boldsymbol{I}$. In this scenario, the variables being measured are correlated, and the marginal signal-to-noise ratio values vary among the variables. The eigenvalues of $\boldsymbol{\Sigma}_u$ are proportional to 0.649, 2.000, and 3.250. The parameter α in this model is adjusted based on the desired signal-to-noise ratio $\rho_{\mathscr{V}}$.

For each design, we generated 10^5 simulated datasets in which the random variables $\boldsymbol{U}_i$ and $\boldsymbol{\epsilon}_{ij}$ followed multivariate normal distributions with variance-covariance matrices $\boldsymbol{\Sigma}_u$ and $\boldsymbol{\Sigma}_\epsilon$, respectively.

Figures 3.2 and 3.3 display the percentage relative bias and the percentage relative standard error (SE) results for $\widehat{\rho}_{\text{gv}}$, $\widehat{\rho}_{\text{tr}}$, and $\widehat{\rho}_{_F}$ with respect to their true values, ρ_{gv}, ρ_{tr}, and $\rho_{_F}$, over a continuous range from 1 to 9. These comparisons are made under four different configurations of (a, r) : $(16, 6), (24, 4), (32, 3)$, and $(48, 2)$, while maintaining a constant total of 96 measurements. The results for Model 1 are presented in Figure 3.2 and the results for Model 2 are shown in Figure 3.3.

For both Model 1 and Model 2, as the sample size of the plans increases, the three estimators of the signal-to-noise ratio show reduced bias. Notably, in the case of a plan with $a = 48$ and $r = 2$, the smallest relative bias is observed across all three estimators of the signal-to-noise ratio for both models.

In these studies, the estimators $\widehat{\rho}_{\text{gv}}$ and $\widehat{\rho}_{\text{tr}}$ exhibit a negative relative bias for both models, indicating underestimation across the range of signal-to-noise ratios from 1 to 9. We observe that $\widehat{\rho}_{\text{gv}}$ has the most substantial percentage bias level for a small to moderate range of signal-to-noise ratios quantities, while $\widehat{\rho}_{_F}$ exhibits the smallest bias.

Plots (b), (d), and (f) in Figures 3.2 and 3.3 indicate that the plan with $a = 48$ and $r = 2$ generally results in the lowest relative bias and SE, especially for scenarios with moderate to high signal-to-noise ratio levels.

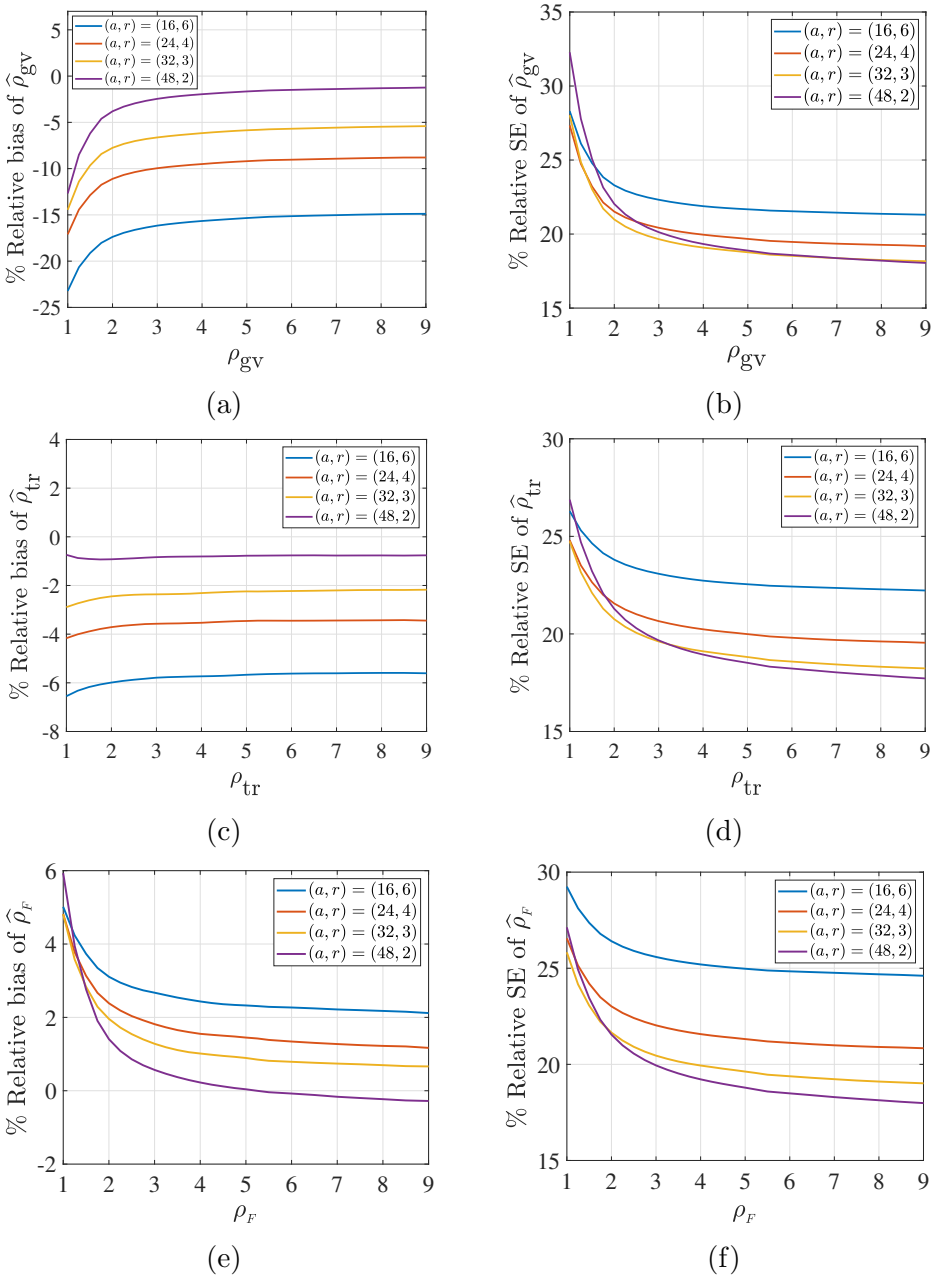

Figure 3.2: The percentage relative bias and the percentage relative SE of $\widehat{\rho}_{\text{gv}}$, $\widehat{\rho}_{\text{tr}}$, and $\widehat{\rho}_{F}$, for Model 1 with $N = 96$ measurements.

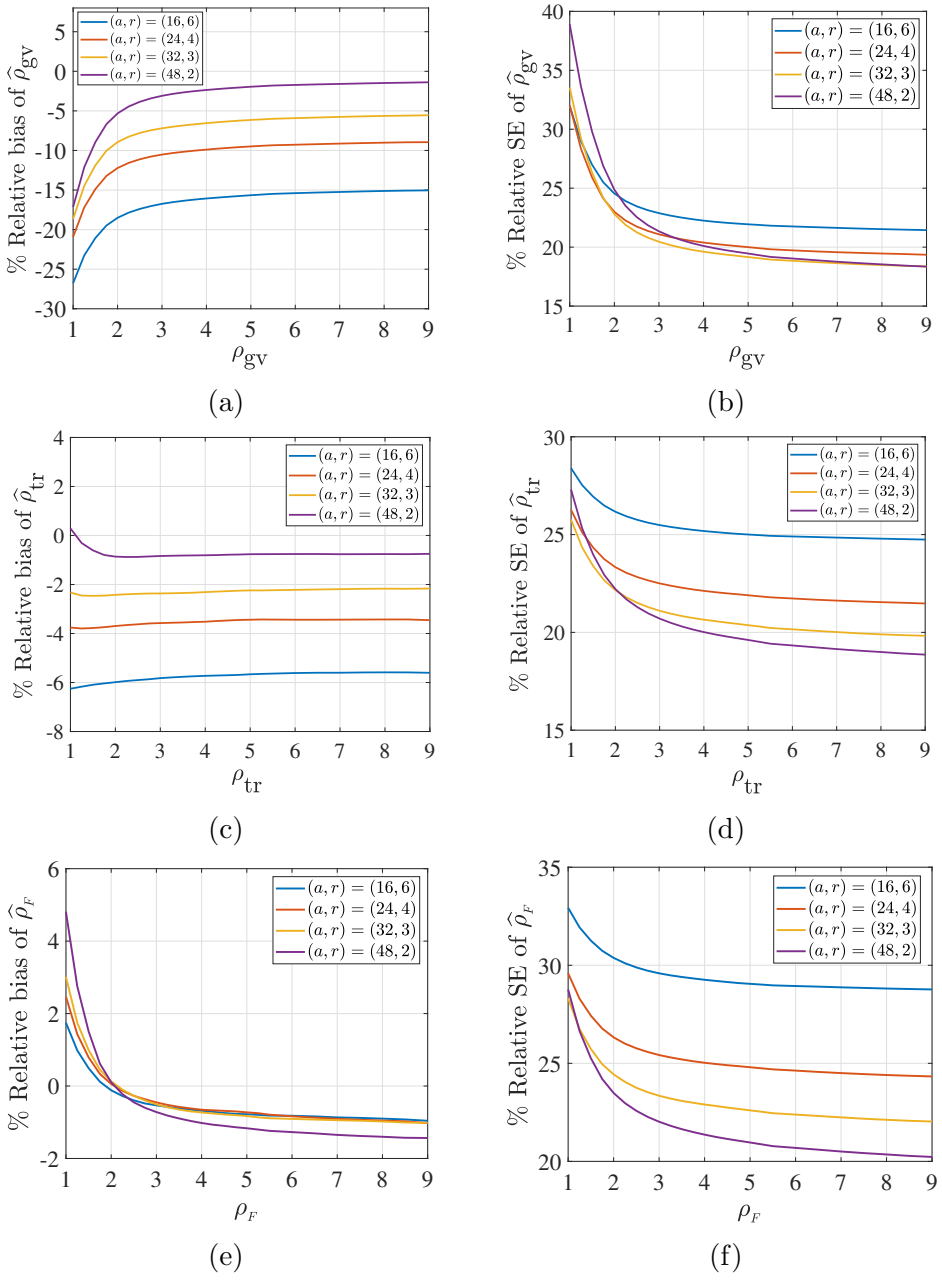

Figure 3.3: The percentage relative bias and the percentage relative SE of $\widehat{\rho}_{\rm gv}$, $\widehat{\rho}_{\rm tr}$, and $\widehat{\rho}_{F}$, for Model 2 with $N = 96$ measurements.

3.8 Discussion and prospects

The concept of using a single summary number as a measure of variability for multidimensional observations is supported by several compelling reasons. Firstly, a single summary number offers simplicity and ease of understanding, making it more accessible for individuals involved in process monitoring and decision-making. By condensing the information into a single value, it eliminates the complexity of interpreting multiple numbers and provides a concise representation of the variability. Furthermore, this approach ingeniously reduces the multivariate problem to a univariate one, facilitating comparisons across different observations. This reduction to a single number summary streamlines the assessment of the measurement system for multivariate data. However, it is important to acknowledge the potential risks associated with representing the quality measure of multivariate characteristics with a single number. The misuse or misinterpretation of this summary measure can lead to flawed conclusions or inappropriate actions. We also remind ourselves that the classical approval levels were designed to be used for a single variable, rather than a vector of variables. The approval criteria for multivariate parameters in measurement system assessment studies are currently under investigation in our ongoing and future work.

3.9 Supplementary materials

This section contains the proofs of the theoretical results and supplementary materials related to Chapter 3.

A. Further details on the derivation of likelihood function (3.31)

To make the random vectors more amenable to maximum likelihood estimation, we reformat them by combining the vectors $\boldsymbol{Y}_{i1}, \ldots, \boldsymbol{Y}_{ir}$ into a single extended vector $\boldsymbol{Y}_i = (\boldsymbol{Y}_{i1}^\top, \ldots, \boldsymbol{Y}_{ir}^\top)^\top$. Assuming normality and independence of the random vectors in the multivariate one-way model (3.2), $\boldsymbol{Y}_1, \boldsymbol{Y}_2, \ldots, \boldsymbol{Y}_a$ are i.i.d. multivariate $\mathcal{N}(\mathbf{1}_r \otimes \boldsymbol{\mu}, \boldsymbol{\Sigma})$ random vectors where $\boldsymbol{\Sigma}$ is defined by

$$\boldsymbol{\Sigma} = \boldsymbol{I}_r \otimes \boldsymbol{\Sigma}_\epsilon + \boldsymbol{J}_r \otimes \boldsymbol{\Sigma}_u \,. \tag{3.50}$$

Let $\boldsymbol{y}_i$ denote the observed value of $\boldsymbol{Y}_i$. The likelihood of observing $\boldsymbol{y}_1, \ldots, \boldsymbol{y}_a$ is,

$$\mathcal{L}(\boldsymbol{\mu}, \boldsymbol{\Sigma}_u, \boldsymbol{\Sigma}_\epsilon; \boldsymbol{y}_1, \ldots, \boldsymbol{y}_a) = \prod_{i=1}^{a} (2\pi)^{-\frac{pr}{2}} |\boldsymbol{\Sigma}|^{-\frac{1}{2}} \exp\Big(-\frac{1}{2} (\boldsymbol{y}_i - \mathbf{1}_r \otimes \boldsymbol{\mu})^\top \boldsymbol{\Sigma}^{-1} (\boldsymbol{y}_i - \mathbf{1}_r \otimes \boldsymbol{\mu}) \Big). \tag{3.51}$$

Since $\boldsymbol{\Sigma}$ has the special structure described in (3.50), we can calculate its determinant and inverse matrix as follows,

$$|\boldsymbol{\Sigma}| = |\boldsymbol{\Sigma}_\epsilon|^{r-1} |\boldsymbol{\Sigma}_\epsilon + r\boldsymbol{\Sigma}_u| \,, \tag{3.52}$$

and

$$\boldsymbol{\Sigma}^{-1} = \boldsymbol{I}_r \otimes \boldsymbol{\Sigma}_\epsilon^{-1} - \boldsymbol{J}_r \otimes \left(\boldsymbol{\Sigma}_\epsilon^{-1} \boldsymbol{\Sigma}_u (\boldsymbol{\Sigma}_\epsilon + r\boldsymbol{\Sigma}_u)^{-1} \right) . \tag{3.53}$$

By substituting the expressions for $|\boldsymbol{\Sigma}|$ and $\boldsymbol{\Sigma}^{-1}$, we can rewrite the likelihood function in (3.51) as,

$$\mathcal{L}(\boldsymbol{\mu}, \boldsymbol{\Sigma}_u, \boldsymbol{\Sigma}_\epsilon; \boldsymbol{y}_1, \ldots, \boldsymbol{y}_a) =$$
$$c(\boldsymbol{\Sigma}_u, \boldsymbol{\Sigma}_\epsilon) \exp\Big(-\frac{1}{2} \sum_{i=1}^{a} (\boldsymbol{y}_i - \mathbf{1}_r \otimes \boldsymbol{\mu})^\top \left\{ \boldsymbol{I}_r \otimes \boldsymbol{\Sigma}_\epsilon^{-1} - \boldsymbol{J}_r \otimes \left(\boldsymbol{\Sigma}_\epsilon^{-1} \boldsymbol{\Sigma}_u (\boldsymbol{\Sigma}_\epsilon + r\boldsymbol{\Sigma}_u)^{-1} \right) \right\} (\boldsymbol{y}_i - \mathbf{1}_r \otimes \boldsymbol{\mu}) \Big), \tag{3.54}$$

where

$$c(\boldsymbol{\Sigma}_u, \boldsymbol{\Sigma}_\epsilon) = (2\pi)^{-\frac{apr}{2}} |\boldsymbol{\Sigma}_\epsilon|^{-\frac{a(r-1)}{2}} |\boldsymbol{\Sigma}_\epsilon + r\boldsymbol{\Sigma}_u|^{-\frac{a}{2}} .$$

The exponential term in $\mathcal{L}(\boldsymbol{y}_1, \ldots, \boldsymbol{y}_a; \boldsymbol{\mu}, \boldsymbol{\Sigma}_u, \boldsymbol{\Sigma}_\epsilon)$ can be manipulated to yield matrices of sums of squares and products $\boldsymbol{SS}_u$ and $\boldsymbol{SS}_\epsilon$ in the likelihood expression. Specifically, we can write,

$$\begin{aligned}
&\sum_{i=1}^{a} (\boldsymbol{y}_i - \mathbf{1}_r \otimes \boldsymbol{\mu})^\top \left\{ \boldsymbol{I}_r \otimes \boldsymbol{\Sigma}_\epsilon^{-1} - \boldsymbol{J}_r \otimes \left(\boldsymbol{\Sigma}_\epsilon^{-1} \boldsymbol{\Sigma}_u (\boldsymbol{\Sigma}_\epsilon + r\boldsymbol{\Sigma}_u)^{-1} \right) \right\} (\boldsymbol{y}_i - \mathbf{1}_r \otimes \boldsymbol{\mu}) \\
&\qquad = \sum_{i=1}^{a} (\boldsymbol{y}_i - \mathbf{1}_r \otimes \boldsymbol{\mu})^\top (\boldsymbol{I}_r \otimes \boldsymbol{\Sigma}_\epsilon^{-1}) (\boldsymbol{y}_i - \mathbf{1}_r \otimes \boldsymbol{\mu}) \qquad (3.55) \\
&\qquad - \sum_{i=1}^{a} (\boldsymbol{y}_i - \mathbf{1}_r \otimes \boldsymbol{\mu})^\top \left\{ \boldsymbol{J}_r \otimes \left(\boldsymbol{\Sigma}_\epsilon^{-1} \boldsymbol{\Sigma}_u (\boldsymbol{\Sigma}_\epsilon + r\boldsymbol{\Sigma}_u)^{-1} \right) \right\} (\boldsymbol{y}_i - \mathbf{1}_r \otimes \boldsymbol{\mu}) .
\end{aligned}$$

Looking at the right-hand side of equation (3.55), we can write the first term as follows,

$$\begin{aligned}
&\sum_{i=1}^{a} (\boldsymbol{y}_i - \mathbf{1}_r \otimes \boldsymbol{\mu})^\top (\boldsymbol{I}_r \otimes \boldsymbol{\Sigma}_\epsilon^{-1}) (\boldsymbol{y}_i - \mathbf{1}_r \otimes \boldsymbol{\mu}) \\
&\qquad = \sum_{i=1}^{a} \sum_{j=1}^{r} (\boldsymbol{y}_{ij} - \boldsymbol{\mu})^\top \boldsymbol{\Sigma}_\epsilon^{-1} (\boldsymbol{y}_{ij} - \boldsymbol{\mu}) \\
&\qquad = \sum_{i=1}^{a} \sum_{j=1}^{r} (\boldsymbol{y}_{ij} - \overline{\boldsymbol{y}}_{i\cdot} + \overline{\boldsymbol{y}}_{i\cdot} - \boldsymbol{\mu})^\top \boldsymbol{\Sigma}_\epsilon^{-1} (\boldsymbol{y}_{ij} - \overline{\boldsymbol{y}}_{i\cdot} + \overline{\boldsymbol{y}}_{i\cdot} - \boldsymbol{\mu}) \\
&\qquad = \sum_{i=1}^{a} \sum_{j=1}^{r} (\boldsymbol{y}_{ij} - \overline{\boldsymbol{y}}_{i\cdot})^\top \boldsymbol{\Sigma}_\epsilon^{-1} (\boldsymbol{y}_{ij} - \overline{\boldsymbol{y}}_{i\cdot}) + r \sum_{i=1}^{a} (\overline{\boldsymbol{y}}_{i\cdot} - \boldsymbol{\mu})^\top \boldsymbol{\Sigma}_\epsilon^{-1} (\overline{\boldsymbol{y}}_{i\cdot} - \boldsymbol{\mu}) \\
&\qquad = \operatorname{tr}\left(\boldsymbol{G} \boldsymbol{\Sigma}_\epsilon^{-1} \right) + r \sum_{i=1}^{a} (\overline{\boldsymbol{y}}_{i\cdot} - \boldsymbol{\mu})^\top \boldsymbol{\Sigma}_\epsilon^{-1} (\overline{\boldsymbol{y}}_{i\cdot} - \boldsymbol{\mu}) , \qquad (3.56)
\end{aligned}$$

Continuing with the second term on the right-hand side of (3.55), we have

$$\begin{aligned}
&\sum_{i=1}^{a}(\boldsymbol{y}_i-\mathbf{1}_r\otimes\boldsymbol{\mu})^\top\left\{\boldsymbol{J}_r\otimes\left(\boldsymbol{\Sigma}_\epsilon^{-1}\boldsymbol{\Sigma}_u(\boldsymbol{\Sigma}_\epsilon+r\boldsymbol{\Sigma}_u)^{-1}\right)\right\}(\boldsymbol{y}_i-\mathbf{1}_r\otimes\boldsymbol{\mu})\\
&\qquad=\sum_{i=1}^{a}(\boldsymbol{y}_i-\mathbf{1}_r\otimes\boldsymbol{\mu})^\top(\mathbf{1}_r\otimes\boldsymbol{I}_p)\left(\boldsymbol{\Sigma}_\epsilon^{-1}\boldsymbol{\Sigma}_u(\boldsymbol{\Sigma}_\epsilon+r\boldsymbol{\Sigma}_u)^{-1}\right)(\mathbf{1}_r\otimes\boldsymbol{I}_p)^\top(\boldsymbol{y}_i-\mathbf{1}_r\otimes\boldsymbol{\mu})\\
&\qquad=r^2\sum_{i=1}^{a}(\overline{\boldsymbol{y}}_{i\cdot}-\boldsymbol{\mu})^\top\boldsymbol{\Sigma}_\epsilon^{-1}\boldsymbol{\Sigma}_u(\boldsymbol{\Sigma}_\epsilon+r\boldsymbol{\Sigma}_u)^{-1}(\overline{\boldsymbol{y}}_{i\cdot}-\boldsymbol{\mu})\,. \qquad (3.57)
\end{aligned}$$

Combining the expressions in (3.56) and (3.57), we obtain,

$$\begin{aligned}
&\mathrm{tr}(\boldsymbol{S}\boldsymbol{S}_\epsilon\boldsymbol{\Sigma}_\epsilon^{-1})+r\sum_{i=1}^{a}(\overline{\boldsymbol{y}}_{i\cdot}-\boldsymbol{\mu})^\top\boldsymbol{\Sigma}_\epsilon^{-1}(\overline{\boldsymbol{y}}_{i\cdot}-\boldsymbol{\mu})-r^2\sum_{i=1}^{a}(\overline{\boldsymbol{y}}_{i\cdot}-\boldsymbol{\mu})^\top\boldsymbol{\Sigma}_\epsilon^{-1}\boldsymbol{\Sigma}_u(\boldsymbol{\Sigma}_\epsilon+r\boldsymbol{\Sigma}_u)^{-1}(\overline{\boldsymbol{y}}_{i\cdot}-\boldsymbol{\mu})\\
&\quad=\mathrm{tr}\left(\boldsymbol{G}\boldsymbol{\Sigma}_\epsilon^{-1}\right)+r\sum_{i=1}^{a}(\overline{\boldsymbol{y}}_{i\cdot}-\boldsymbol{\mu})^\top\boldsymbol{\Sigma}_\epsilon^{-1}\left\{\boldsymbol{I}_p-r\boldsymbol{\Sigma}_u(\boldsymbol{\Sigma}_\epsilon+r\boldsymbol{\Sigma}_u)^{-1}\right\}(\overline{\boldsymbol{y}}_{i\cdot}-\boldsymbol{\mu})\\
&\quad=\mathrm{tr}\left(\boldsymbol{G}\boldsymbol{\Sigma}_\epsilon^{-1}\right)+r\sum_{i=1}^{a}(\overline{\boldsymbol{y}}_{i\cdot}-\boldsymbol{\mu})^\top(\boldsymbol{\Sigma}_\epsilon+r\boldsymbol{\Sigma}_u)^{-1}(\overline{\boldsymbol{y}}_{i\cdot}-\boldsymbol{\mu})\,, \qquad (3.58)
\end{aligned}$$

where the sum term in the last equality can be expressed as

$$\begin{aligned}
&\sum_{i=1}^{a}(\overline{\boldsymbol{y}}_{i\cdot}-\boldsymbol{\mu})^\top(\boldsymbol{\Sigma}_\epsilon+r\boldsymbol{\Sigma}_u)^{-1}(\overline{\boldsymbol{y}}_{i\cdot}-\boldsymbol{\mu})\\
&\qquad=\sum_{i=1}^{a}(\overline{\boldsymbol{y}}_{i\cdot}-\overline{\boldsymbol{y}}_{\cdot\cdot}+\overline{\boldsymbol{y}}_{\cdot\cdot}-\boldsymbol{\mu})^\top(\boldsymbol{\Sigma}_\epsilon+r\boldsymbol{\Sigma}_u)^{-1}(\overline{\boldsymbol{y}}_{i\cdot}-\overline{\boldsymbol{y}}_{\cdot\cdot}+\overline{\boldsymbol{y}}_{\cdot\cdot}-\boldsymbol{\mu})\\
&\qquad=\frac{1}{r}\mathrm{tr}(\boldsymbol{H}(\boldsymbol{\Sigma}_\epsilon+r\boldsymbol{\Sigma}_u)^{-1})+a\,(\overline{\boldsymbol{y}}_{\cdot\cdot}-\boldsymbol{\mu})^\top(\boldsymbol{\Sigma}_\epsilon+r\boldsymbol{\Sigma}_u)^{-1}(\overline{\boldsymbol{y}}_{\cdot\cdot}-\boldsymbol{\mu})\,. \qquad (3.59)
\end{aligned}$$

This results in the likelihood function of (3.54) to be expressed as,

$$\begin{aligned}
&\mathcal{L}(\boldsymbol{\mu},\boldsymbol{\Sigma}_u,\boldsymbol{\Sigma}_\epsilon)=\\
&c(\boldsymbol{\Sigma}_u,\boldsymbol{\Sigma}_\epsilon)\exp\left(-\tfrac{1}{2}\mathrm{tr}\left(\boldsymbol{G}\boldsymbol{\Sigma}_\epsilon^{-1}\right)-\tfrac{1}{2}\mathrm{tr}\left(\boldsymbol{H}(\boldsymbol{\Sigma}_\epsilon+r\boldsymbol{\Sigma}_u)^{-1}\right)-\tfrac{ar}{2}(\overline{\boldsymbol{y}}_{\cdot\cdot}-\boldsymbol{\mu})^\top(\boldsymbol{\Sigma}_\epsilon+r\boldsymbol{\Sigma}_u)^{-1}(\overline{\boldsymbol{y}}_{\cdot\cdot}-\boldsymbol{\mu})\right).
\end{aligned}$$

B. Proof of convergence properties

We start by reviewing some relevant materials that will assist in our proofs. Lemma 3.1 (Anderson, 2003, Section 3.4) provides essential information regarding the consistency of the

multivariate sample covariance matrix. Subsequently, Lemma 3.2 (Anderson, 2003, Section 3.4) presents the asymptotic normality results of a sample covariance matrix.

Lemma 3.1. ***(Consistency of sample covariance matrix).*** *Suppose* $\boldsymbol{X}_1, \ldots, \boldsymbol{X}_n$ *are i.i.d. random vectors with a mean* $\mathrm{E}[\boldsymbol{X}] = \boldsymbol{\xi}$ *and finite variance-covariance matrix* $\mathrm{E}\left[(\boldsymbol{X}-\boldsymbol{\xi})(\boldsymbol{X}-\boldsymbol{\xi})^\top\right] = \boldsymbol{\Sigma}$. *Then, the sample covariance matrix* $\boldsymbol{S} = \frac{1}{n-1}\sum_{i=1}^n (\boldsymbol{X}_i - \overline{\boldsymbol{X}})(\boldsymbol{X}_i - \overline{\boldsymbol{X}})^\top$ *converges to* $\boldsymbol{\Sigma}$ *almost surely as* $n \to \infty$, *provided that each element of* $\boldsymbol{X}_i$*'s has finite second moment.*

Lemma 3.2. ***(Asymptotic normality of sample covariance matrix).*** *Consider a sample of independent p-dimensional random vectors* $\boldsymbol{X}_1, \ldots, \boldsymbol{X}_n$, *drawn from a multivariate normal distribution* $\mathcal{N}(\boldsymbol{\xi}, \boldsymbol{\Sigma})$. *Let* $\boldsymbol{S} = \frac{1}{n-1}\sum_{i=1}^n (\boldsymbol{X}_i - \overline{\boldsymbol{X}})(\boldsymbol{X}_i - \overline{\boldsymbol{X}})^\top$. *Then,*

$$\sqrt{n}\, vec\,(\boldsymbol{S} - \boldsymbol{\Sigma}) \xrightarrow{d} \mathcal{N}\big(\boldsymbol{0}, \boldsymbol{\Gamma}(\boldsymbol{\Sigma})\big),$$

as $n \to \infty$, *where* $\boldsymbol{\Gamma}(\boldsymbol{\Sigma}) = \big(\boldsymbol{\Gamma}_{ij}(\boldsymbol{\Sigma})\big)$ *and* $\big(\boldsymbol{\Gamma}_{ij}(\boldsymbol{\Sigma})\big)_{k\ell} = \sigma_{ij}\sigma_{k\ell} + \sigma_{i\ell}\sigma_{kj}$ *for* $i, j, k, \ell = 1, \ldots, n$.

In Lemma 3.2, without assuming normality, if $\boldsymbol{X}_1, \ldots, \boldsymbol{X}_n$ are i.i.d. random vectors with finite fourth moments, $\sqrt{n}\,\mathrm{vec}\,(\boldsymbol{S} - \boldsymbol{\Sigma})$ will still follow an asymptotically normal distribution with a mean of $\boldsymbol{0}$. However, it's important to note that the specific covariance structure of this limiting distribution depends on the fourth-order moments of $\boldsymbol{X}_1, \ldots, \boldsymbol{X}_n$.

The following lemma is used in the derivation procedure of several theorems and results, in this chapter.

Lemma 3.3. *Let* $\boldsymbol{A} = (a_{ij})$, $\boldsymbol{B} = (b_{ij})$, *and* $\boldsymbol{C} = (c_{ij})$ *be symmetric* $p \times p$ *matrices, and* $\boldsymbol{\Gamma}(\cdot)$ *be defined as in* (3.1). *Then we have,*

a) $\{\mathrm{vec}\,(\boldsymbol{A})\}^\top \boldsymbol{\Gamma}(\boldsymbol{B})\mathrm{vec}\big(\boldsymbol{C}\big) = 2\,\mathrm{tr}\,(\boldsymbol{ABCB})\,.$

b) *When* $\boldsymbol{A} = \boldsymbol{C}$, *we have:* $\{\mathrm{vec}\,(\boldsymbol{A})\}^\top \boldsymbol{\Gamma}(\boldsymbol{B})\mathrm{vec}\big(\boldsymbol{A}\big) = 2\|\boldsymbol{AB}\|_F^2\,.$

Proof. We can derive the result as follows,

$$\begin{aligned}
\{\mathrm{vec}\,(\boldsymbol{A})\}^\top \boldsymbol{\Gamma}(\boldsymbol{B})\mathrm{vec}\big(\boldsymbol{C}\big) &= \sum_{i=1}^p \sum_{j=1}^p \sum_{k=1}^p \sum_{\ell=1}^p a_{ik}\big(b_{ij}b_{k\ell} + b_{i\ell}b_{jk}\big)c_{j\ell} \\
&= 2\sum_{i=1}^p \sum_{j=1}^p \sum_{k=1}^p \sum_{\ell=1}^p a_{ik}\, b_{k\ell}\, c_{\ell j}\, b_{ji} \\
&= 2\,\mathrm{tr}(\boldsymbol{ABCB}).
\end{aligned}$$

Substituting $\boldsymbol{C} = \boldsymbol{A}$ into the expression, we have,

$$\begin{aligned}\{\mathrm{vec}\,(\boldsymbol{A})\}^{\top}\,\boldsymbol{\Gamma}(\boldsymbol{B})\mathrm{vec}\big(\boldsymbol{A}\big) &= 2\,\mathrm{tr}(\boldsymbol{ABAB}) \\ &= 2\,\mathrm{tr}\left((\boldsymbol{AB})^2\right) \\ &= 2\,\|\boldsymbol{AB}\|_F^2\,.\end{aligned}$$

This establishes the results as claimed in the lemma. □

Now, we can proceed to prove the convergence properties of the estimators introduced in Section 3.5.

Proof of Theorem 3.1

(a) Consider the maximum likelihood estimator $\widehat{\boldsymbol{\Sigma}}_\epsilon = \boldsymbol{MS}_\epsilon + \frac{\boldsymbol{\Omega}}{r}$. Since $\boldsymbol{\Omega} = O_p(a^{-1/2})$ according to Remadi and Amemiya (1993, 1994), we can express $\widehat{\boldsymbol{\Sigma}}_\epsilon$ as

$$\widehat{\boldsymbol{\Sigma}}_\epsilon = \boldsymbol{MS}_\epsilon + O_p\left(r^{-1}a^{-1/2}\right). \tag{3.60}$$

The next step involves demonstrating $\boldsymbol{MS}_\epsilon \xrightarrow{\text{a.s}} \boldsymbol{\Sigma}_\epsilon$ as $a \to \infty$. Recall that,

$$\boldsymbol{MS}_\epsilon = \frac{1}{a(r-1)}\sum_{i=1}^{a}\sum_{j=1}^{r}(\boldsymbol{Y}_{ij} - \overline{\boldsymbol{Y}}_{i\cdot})(\boldsymbol{Y}_{ij} - \overline{\boldsymbol{Y}}_{i\cdot})^{\top}.$$

The random vector $\boldsymbol{Y}_{ij} - \overline{\boldsymbol{Y}}_{i\cdot}$ can be equivalently expressed as $\boldsymbol{\epsilon}_{ij} - \overline{\boldsymbol{\epsilon}}_{i\cdot}$ where $\overline{\boldsymbol{\epsilon}}_{i\cdot} = \frac{1}{r}\sum_{j=1}^{r}\boldsymbol{\epsilon}_{ij}$. Considering the independent random vectors $\boldsymbol{\epsilon}_{ij}$'s with a mean of zero and covariance matrix $\mathrm{E}\left[\boldsymbol{\epsilon}_{ij}\boldsymbol{\epsilon}_{ij}^{\top}\right] = \boldsymbol{\Sigma}_\epsilon$, we can demonstrate that,

$$\mathrm{E}\left[(\boldsymbol{\epsilon}_{ij} - \overline{\boldsymbol{\epsilon}}_{i\cdot})\,(\boldsymbol{\epsilon}_{ij} - \overline{\boldsymbol{\epsilon}}_{i\cdot})^{\top}\right] = \frac{r-1}{r}\,\boldsymbol{\Sigma}_\epsilon\,.$$

Furthermore, since $\boldsymbol{\epsilon}_{ij}$'s are identically distributed vectors, then $\sum_{j=1}^{r}(\boldsymbol{\epsilon}_{1j} - \overline{\boldsymbol{\epsilon}}_{1\cdot})\,(\boldsymbol{\epsilon}_{1j} - \overline{\boldsymbol{\epsilon}}_{1\cdot})^{\top}$, $\sum_{j=1}^{r}(\boldsymbol{\epsilon}_{2j} - \overline{\boldsymbol{\epsilon}}_{2\cdot})\,(\boldsymbol{\epsilon}_{2j} - \overline{\boldsymbol{\epsilon}}_{2\cdot})^{\top}$, and so on, are i.i.d. random matrices with an expected value of $(r-1)\boldsymbol{\Sigma}_\epsilon$. Then, By the strong law of large numbers, we obtain,

$$\frac{1}{a}\sum_{i=1}^{a}\sum_{j=1}^{r}(\boldsymbol{\epsilon}_{ij} - \overline{\boldsymbol{\epsilon}}_{i\cdot})\,(\boldsymbol{\epsilon}_{ij} - \overline{\boldsymbol{\epsilon}}_{i\cdot})^{\top} \xrightarrow{\text{a.s}} (r-1)\boldsymbol{\Sigma}_\epsilon\,, \tag{3.61}$$

for any fixed number of replications. Consequently, we can conclude that $\boldsymbol{MS}_\epsilon \xrightarrow{\text{a.s}} \boldsymbol{\Sigma}_\epsilon$ as $a \to \infty$.

(b) Given that $\boldsymbol{\Omega} = O_p(a^{-1/2})$, we can express $\widehat{\boldsymbol{\Sigma}}_u$ as follows,

$$\widehat{\boldsymbol{\Sigma}}_u = \frac{1}{r}\left(\beta^{-1}\boldsymbol{MS}_u - \boldsymbol{MS}_\epsilon\right) + O_p\left(r^{-1}a^{-1/2}\right). \tag{3.62}$$

Next, we demonstrate the convergence of the term $\beta^{-1}\boldsymbol{MS}_u$ to $r\boldsymbol{\Sigma}_u + \boldsymbol{\Sigma}_\epsilon$ as $a \to \infty$. The random variable generated by $\overline{\boldsymbol{Y}}_{i\cdot}$ can be represented equivalently as $\boldsymbol{\mu}+\boldsymbol{U}_i+\overline{\boldsymbol{\epsilon}}_{i\cdot}$. Under the assumption that all $\boldsymbol{U}_i$'s and all $\boldsymbol{\epsilon}_{ij}$'s are i.i.d., we can conclude that the random variables $\overline{\boldsymbol{Y}}_{1\cdot}$, $\overline{\boldsymbol{Y}}_{2\cdot}, \ldots$ are i.i.d. with a mean of $\boldsymbol{\mu}$ and covariance matrix $\boldsymbol{\Sigma}_u + r^{-1}\boldsymbol{\Sigma}_\epsilon$. By applying Lemma 3.1 to $\overline{\boldsymbol{Y}}_{1\cdot}$, $\overline{\boldsymbol{Y}}_{2\cdot}, \ldots$, we obtain the following convergence result,

$$\frac{1}{a}\sum_{i=1}^{a}(\overline{\boldsymbol{Y}}_{i\cdot} - \overline{\boldsymbol{Y}}_{\cdot\cdot})(\overline{\boldsymbol{Y}}_{i\cdot} - \overline{\boldsymbol{Y}}_{\cdot\cdot})^\top \xrightarrow{\text{a.s}} \boldsymbol{\Sigma}_u + \frac{1}{r}\boldsymbol{\Sigma}_\epsilon \tag{3.63}$$

as $a \to \infty$. This implies that $\beta^{-1}\boldsymbol{MS}_u \xrightarrow{\text{a.s}} r\boldsymbol{\Sigma}_u + \boldsymbol{\Sigma}_\epsilon$ as $a \to \infty$. Combining this result with the convergence result from part (a) of this theorem, where $\boldsymbol{MS}_\epsilon \to \boldsymbol{\Sigma}_\epsilon$ almost surely as $a \to \infty$, we can conclude that $\widehat{\boldsymbol{\Sigma}}_u \xrightarrow{\text{a.s}} \boldsymbol{\Sigma}_u$ as $a \to \infty$.

(c) To prove this, we begin with,

$$\begin{aligned}\sqrt{a}\,\text{vec}\begin{pmatrix}\widehat{\boldsymbol{\Sigma}}_\epsilon - \boldsymbol{\Sigma}_\epsilon \\ \widehat{\boldsymbol{\Sigma}}_u - \boldsymbol{\Sigma}_u\end{pmatrix} &= \frac{1}{\sqrt{a}}\sum_{i=1}^{a}\text{vec}\begin{pmatrix}\frac{1}{(r-1)}\sum_{j=1}^{r}(\boldsymbol{Y}_{ij} - \overline{\boldsymbol{Y}}_{i\cdot})(\boldsymbol{Y}_{ij} - \overline{\boldsymbol{Y}}_{i\cdot})^\top - \boldsymbol{\Sigma}_\epsilon \\ \frac{-1}{r(r-1)}\sum_{j=1}^{r}(\boldsymbol{Y}_{ij} - \overline{\boldsymbol{Y}}_{i\cdot})(\boldsymbol{Y}_{ij} - \overline{\boldsymbol{Y}}_{i\cdot})^\top + \frac{1}{r}\boldsymbol{\Sigma}_\epsilon\end{pmatrix} \\ &\quad + \frac{1}{\sqrt{a}}\sum_{i=1}^{a}\text{vec}\begin{pmatrix}\boldsymbol{0} \\ (\overline{\boldsymbol{Y}}_{i\cdot} - \overline{\boldsymbol{Y}}_{\cdot\cdot})(\overline{\boldsymbol{Y}}_{i\cdot} - \overline{\boldsymbol{Y}}_{\cdot\cdot})^\top - \boldsymbol{\Sigma}_u - \frac{1}{r}\boldsymbol{\Sigma}_\epsilon\end{pmatrix},\end{aligned} \tag{3.64}$$

where the two random vectors on the right-hand side are independent. The multivariate central limit theorem indicates that, as $a \to \infty$,

$$\frac{1}{\sqrt{a}}\sum_{i=1}^{a}\text{vec}\begin{pmatrix}\frac{1}{(r-1)}\sum_{j=1}^{r}(\boldsymbol{Y}_{ij} - \overline{\boldsymbol{Y}}_{i\cdot})(\boldsymbol{Y}_{ij} - \overline{\boldsymbol{Y}}_{i\cdot})^\top - \boldsymbol{\Sigma}_\epsilon \\ \frac{-1}{r(r-1)}\sum_{j=1}^{r}(\boldsymbol{Y}_{ij} - \overline{\boldsymbol{Y}}_{i\cdot})(\boldsymbol{Y}_{ij} - \overline{\boldsymbol{Y}}_{i\cdot})^\top + \frac{1}{r}\boldsymbol{\Sigma}_\epsilon\end{pmatrix} \xrightarrow{\text{d}} \mathcal{N}\left(\boldsymbol{0}, \boldsymbol{\Sigma}_1\right),$$

where $\boldsymbol{\Sigma}_1$ is defined as,

$$\boldsymbol{\Sigma}_1 = \frac{1}{r-1}\begin{pmatrix}1 & -r^{-1} \\ -r^{-1} & r^{-2}\end{pmatrix} \otimes \boldsymbol{\Gamma}(\boldsymbol{\Sigma}_\epsilon). \tag{3.65}$$

Furthermore, the asymptotic normality of a sample covariance matrix, as in Lemma 3.2, indicates that

$$\sqrt{a}\,\mathrm{vec}\Big(\frac{1}{a}\sum_{i=1}^{a}(\overline{\boldsymbol{Y}}_{i\cdot}-\overline{\boldsymbol{Y}}_{\cdot\cdot})(\overline{\boldsymbol{Y}}_{i\cdot}-\overline{\boldsymbol{Y}}_{\cdot\cdot})^{\top}-\boldsymbol{\Sigma}_u-\frac{1}{r}\boldsymbol{\Sigma}_\epsilon\Big)\xrightarrow{\mathrm{d}}\mathcal{N}\left(\mathbf{0},\boldsymbol{\Gamma}\left(\boldsymbol{\Sigma}_u+\tfrac{1}{r}\boldsymbol{\Sigma}_\epsilon\right)\right)\,. \tag{3.66}$$

Combining these results leads to the expected outcome.

Proof of Theorem 3.2

The validity of results in part (a) can be established by applying the continuous mapping theorem to $\widehat{\boldsymbol{\Sigma}}_\epsilon$ and $\widehat{\boldsymbol{\Sigma}}_u$, and leveraging the asymptotic results provided in Theorem 3.1.

(b) Applying the multivariate Delta method to the limiting distribution result in part (c) of Theorem 3.1, we have,

$$\sqrt{a}\begin{pmatrix}\mathscr{V}(\widehat{\boldsymbol{\Sigma}}_\epsilon)-\mathscr{V}(\boldsymbol{\Sigma}_\epsilon)\\ \mathscr{V}(\widehat{\boldsymbol{\Sigma}}_u)-\mathscr{V}(\boldsymbol{\Sigma}_u)\end{pmatrix}\to\mathcal{N}\left(\mathbf{0},\begin{pmatrix}\sigma_{11}&\sigma_{12}\\ \sigma_{21}&\sigma_{22}\end{pmatrix}\right)$$

in distribution where

$$\begin{aligned}\sigma_{11}&=\nabla\left\{\mathrm{vec}(\mathscr{V}(\boldsymbol{\Sigma}_\epsilon))\right\}^{\top}\boldsymbol{\Sigma}_{11}\nabla\mathrm{vec}\left(\mathscr{V}(\boldsymbol{\Sigma}_\epsilon)\right),\\ \sigma_{12}&=\nabla\left\{\mathrm{vec}(\mathscr{V}(\boldsymbol{\Sigma}_\epsilon))\right\}^{\top}\boldsymbol{\Sigma}_{12}\nabla\mathrm{vec}\left(\mathscr{V}(\boldsymbol{\Sigma}_u)\right),\\ \sigma_{22}&=\nabla\left\{\mathrm{vec}(\mathscr{V}(\boldsymbol{\Sigma}_u))\right\}^{\top}\boldsymbol{\Sigma}_{22}\nabla\mathrm{vec}\left(\mathscr{V}(\boldsymbol{\Sigma}_u)\right).\end{aligned} \tag{3.67}$$

In the above expressions, $\boldsymbol{\Sigma}_{11}$, $\boldsymbol{\Sigma}_{12}$, and $\boldsymbol{\Sigma}_{22}$ are matrices as given in Theorem 3.1.

To proceed with the proof, we substitute the relations $\boldsymbol{\Sigma}_{11}$, $\boldsymbol{\Sigma}_{12}$, and $\boldsymbol{\Sigma}_{22}$ in the expressions for σ_{11}, σ_{12}, and σ_{22}. By applying the result from part (a) of Lemma 3.3, where we have $\left\{\mathrm{vec}\left(\boldsymbol{A}\right)\right\}^{\top}\boldsymbol{\Gamma}(\boldsymbol{B})\mathrm{vec}\big(\boldsymbol{C}\big)=2\,\mathrm{tr}(\boldsymbol{ABCB})$, alongside the relation $\nabla\mathrm{vec}(\mathscr{V}(\boldsymbol{\Sigma}))=\mathrm{vec}\left(\nabla\mathscr{V}(\boldsymbol{\Sigma})\right)$, we obtain the following expressions,

$$\begin{aligned}\sigma_{11}&=\frac{2}{r(r-1)}\left\{\mathrm{tr}\big(r\left\{\nabla\mathscr{V}(\boldsymbol{\Sigma}_\epsilon)\boldsymbol{\Sigma}_\epsilon\right\}^2\big\}\right.,\\ \sigma_{12}&=\frac{-2}{r(r-1)}\left\{\mathrm{tr}\big(\nabla\mathscr{V}(\boldsymbol{\Sigma}_\epsilon)\boldsymbol{\Sigma}_\epsilon\nabla\mathscr{V}(\boldsymbol{\Sigma}_u)\boldsymbol{\Sigma}_\epsilon\big\}\right.,\\ \sigma_{22}&=2\,\mathrm{tr}\big(\left\{\nabla\mathscr{V}(\boldsymbol{\Sigma}_u)\left(\boldsymbol{\Sigma}_u+\tfrac{1}{r}\boldsymbol{\Sigma}_\epsilon\right)\right\}^2\big)+\frac{2}{r^2(r-1)}\left\{\mathrm{tr}\big(\left\{\nabla\mathscr{V}(\boldsymbol{\Sigma}_u)\boldsymbol{\Sigma}_\epsilon\right\}^2\big)\right\}.\end{aligned} \tag{3.68}$$

Furthermore, by using the relation $\mathrm{tr}(\boldsymbol{A}^2) = \|\boldsymbol{A}\|_F^2$ for a symmetric matrix $\boldsymbol{A}$, we can express σ_{11} and σ_{22} equivalently as follows,

$$\begin{aligned}\sigma_{11} &= \frac{2}{(r-1)}\|\nabla\mathscr{V}(\boldsymbol{\Sigma}_\epsilon)\boldsymbol{\Sigma}_\epsilon\|_F^2\,,\\ \sigma_{22} &= 2\,\|\nabla\mathscr{V}(\boldsymbol{\Sigma}_u)\left(\boldsymbol{\Sigma}_u + \tfrac{1}{r}\boldsymbol{\Sigma}_\epsilon\right)\|_F^2 + \frac{2}{r^2(r-1)}\|\nabla\mathscr{V}(\boldsymbol{\Sigma}_u)\boldsymbol{\Sigma}_\epsilon\|_F^2\,.\end{aligned} \tag{3.69}$$

(c) Let the bivariate function g be defined as $g(x,y) = y/x$. Applying the Delta method to the limiting distribution in part (b) with $g\left(\mathscr{V}(\boldsymbol{\Sigma}_\epsilon), \mathscr{V}(\boldsymbol{\Sigma}_u)\right)$, as $a \to \infty$, we find that $\sqrt{a}\,\{\widehat{\rho} - \rho\} \to \mathcal{N}(0, \sigma_\rho^2)$, where σ_ρ^2 is determined by

$$\sigma_\rho^2 = \boldsymbol{u}^\top \begin{pmatrix}\sigma_{11} & \sigma_{12}\\ \sigma_{21} & \sigma_{22}\end{pmatrix}\boldsymbol{u}\,, \tag{3.70}$$

and

$$\boldsymbol{u} = \left(\frac{\partial g\left(\mathscr{V}(\boldsymbol{\Sigma}_\epsilon), \mathscr{V}(\boldsymbol{\Sigma}_u)\right)}{\partial\mathscr{V}(\boldsymbol{\Sigma}_\epsilon)}, \frac{\partial g\left(\mathscr{V}(\boldsymbol{\Sigma}_\epsilon), \mathscr{V}(\boldsymbol{\Sigma}_u)\right)}{\partial\mathscr{V}(\boldsymbol{\Sigma}_u)}\right)^\top = \frac{1}{\mathscr{V}(\boldsymbol{\Sigma}_\epsilon)}\begin{pmatrix}-\rho\\ 1\end{pmatrix}. \tag{3.71}$$

Performing the algebraic calculations, we have,

$$\sigma_\rho^2 = \frac{\rho^2\sigma_{11} - 2\rho\sigma_{12} + \sigma_{22}}{\{\mathscr{V}(\boldsymbol{\Sigma}_\epsilon)\}^2}\,. \tag{3.72}$$

Proof of Theorem 3.3

(a) We begin with the relationship $\widehat{\boldsymbol{\Sigma}}_\epsilon = \boldsymbol{M}\boldsymbol{S}_\epsilon + O_p(r^{-1}a^{-1/2})$. As the replication number becomes large, the second term tends to zero. Therefore, we can proceed with the proof by demonstrating that $\boldsymbol{M}\boldsymbol{S}_\epsilon$ converges to $\boldsymbol{\Sigma}_\epsilon$ almost surely. Applying Lemma 3.1 to the sequence of random vectors $\boldsymbol{\epsilon}_{i1}, \boldsymbol{\epsilon}_{i2}, \ldots$, we have,

$$\frac{1}{r-1}\sum_{j=1}^{r}(\boldsymbol{\epsilon}_{ij} - \overline{\boldsymbol{\epsilon}}_{i\cdot})(\boldsymbol{\epsilon}_{ij} - \overline{\boldsymbol{\epsilon}}_{i\cdot})^\top \xrightarrow{\text{a.s.}} \boldsymbol{\Sigma}_\epsilon\,, \tag{3.73}$$

as $r \to \infty$, for each $i = 1, \ldots, a$. By summing up the result of (3.73) across all units, we obtain

$$\boldsymbol{MS}_\epsilon = \frac{1}{a(r-1)} \sum_{i=1}^{a} \sum_{j=1}^{r} (\boldsymbol{\epsilon}_{ij} - \overline{\boldsymbol{\epsilon}}_{i\cdot})(\boldsymbol{\epsilon}_{ij} - \overline{\boldsymbol{\epsilon}}_{i\cdot})^\top \xrightarrow{\text{a.s}} \boldsymbol{\Sigma}_\epsilon \,, \tag{3.74}$$

as $r \to \infty$ for any sample size. Therefore, $\widehat{\boldsymbol{\Sigma}}_\epsilon \xrightarrow{\text{a.s}} \boldsymbol{\Sigma}_\epsilon$ as $r \to \infty$.

(b) We aim to establish the proof of this part by showing that,

$$\sqrt{ar}\, \text{vec}\left(\boldsymbol{MS}_\epsilon - \boldsymbol{\Sigma}_\epsilon\right) \xrightarrow{\text{d}} \mathcal{N}\big(\mathbf{0}, \boldsymbol{\Gamma}(\boldsymbol{\Sigma}_\epsilon)\big), \tag{3.75}$$

as $r \to \infty$. Applying Lemma 3.2, which describes the asymptotic normality of the sample covariance matrix, we have,

$$\sqrt{r}\, \text{vec}\Big(\frac{1}{r-1} \sum_{j=1}^{r} (\boldsymbol{\epsilon}_{ij} - \overline{\boldsymbol{\epsilon}}_{i\cdot})(\boldsymbol{\epsilon}_{ij} - \overline{\boldsymbol{\epsilon}}_{i\cdot})^\top - \boldsymbol{\Sigma}_\epsilon\Big) \xrightarrow{\text{d}} \mathcal{N}\big(\mathbf{0}, \boldsymbol{\Gamma}(\boldsymbol{\Sigma}_\epsilon)\big), \tag{3.76}$$

as $r \to \infty$. Since $(\boldsymbol{\epsilon}_{1j} - \overline{\boldsymbol{\epsilon}}_{1\cdot})(\boldsymbol{\epsilon}_{1j} - \overline{\boldsymbol{\epsilon}}_{1\cdot})^\top$, $(\boldsymbol{\epsilon}_{2j} - \overline{\boldsymbol{\epsilon}}_{2\cdot})(\boldsymbol{\epsilon}_{2j} - \overline{\boldsymbol{\epsilon}}_{2\cdot})^\top$, and so on, are independent random matrices that follow a normal distribution when vectorized, and assuming a sufficiently large replication number, their summation will also exhibit a normal distribution, in asymptotic case. This implies the convergence in (3.75) as $r \to \infty$.

(c) To demonstrate the result of this part, we examine the relationship of the maximum likelihood estimate of $\boldsymbol{\Sigma}_u$, given by,

$$\widehat{\boldsymbol{\Sigma}}_u = \frac{1}{a} \sum_{i=1}^{a} (\overline{\boldsymbol{Y}}_{i\cdot} - \overline{\boldsymbol{Y}}_{\cdot\cdot})(\overline{\boldsymbol{Y}}_{i\cdot} - \overline{\boldsymbol{Y}}_{\cdot\cdot})^\top - \frac{1}{r} \left(\boldsymbol{MS}_\epsilon - \boldsymbol{\Omega}\right). \tag{3.77}$$

We proceed to establish the distributional convergence of the first term in (3.77). Recall that the sequence of $\overline{\boldsymbol{Y}}_{1\cdot}$, $\overline{\boldsymbol{Y}}_{2\cdot}, \ldots$ are i.i.d. random vectors with a covariance matrix of $\boldsymbol{\Sigma}_u + r^{-1}\boldsymbol{\Sigma}_\epsilon$. Consequently, under the assumption of normally distributed random variables, the sum $\sum_{i=1}^{a} (\overline{\boldsymbol{Y}}_{i\cdot} - \overline{\boldsymbol{Y}}_{\cdot\cdot})(\overline{\boldsymbol{Y}}_{i\cdot} - \overline{\boldsymbol{Y}}_{\cdot\cdot})^\top$ follows a Wishart distribution $\mathcal{W}\left(\boldsymbol{\Sigma}_u + r^{-1}\boldsymbol{\Sigma}_\epsilon, a-1\right)$. As $r \to \infty$, the first term in (3.77) converges to $a^{-1}\mathcal{W}(\boldsymbol{\Sigma}_u, a-1)$. Moreover, the remaining terms are $O_p(1/r)$ which allows us to express $\widehat{\boldsymbol{\Sigma}}_u$ as,

$$\widehat{\boldsymbol{\Sigma}}_u = \frac{1}{a} \mathcal{W}\left(\boldsymbol{\Sigma}_u, a-1\right) + o_p(1), \tag{3.78}$$

as $r \to \infty$.

(d) The independence of the asymptotic relationships of $\widehat{\boldsymbol{\Sigma}}_\epsilon$ and $\widehat{\boldsymbol{\Sigma}}_u$ follows from their relationships expressed in terms of independent statistics.

Proof of Theorem 3.4

Part (a) of Theorem 3.4, which addresses the convergence of $\widehat{\boldsymbol{\Sigma}}_u$ and $\widehat{\boldsymbol{\Sigma}}_\epsilon$, can be deducted from the results presented in Theorem 3.1. Here, we provide a concise proof by demonstrating the asymptotic normality of $\widehat{\boldsymbol{\Sigma}}_u$. The next steps concerning the asymptotic normality of $\boldsymbol{\Sigma}_\epsilon$ and its independence from $\widehat{\boldsymbol{\Sigma}}_u$ in their asymptotic behaviors are identical to that presented in parts (b) and (d) of Theorem 3.3.

From Theorem 3.3, we have that $\widehat{\boldsymbol{\Sigma}}_u = \frac{1}{a}\sum_{i=1}^{a}(\overline{\boldsymbol{Y}}_{i\cdot} - \overline{\boldsymbol{Y}}_{\cdot\cdot})(\overline{\boldsymbol{Y}}_{i\cdot} - \overline{\boldsymbol{Y}}_{\cdot\cdot})^\top + O_p(r^{-1}a^{-1/2})$. Using the asymptotic normality of a sample covariance matrix, as stated in Lemma 3.2, we find that,

$$\sqrt{a}\,\mathrm{vec}\Big(\frac{1}{a}\sum_{i=1}^{a}(\overline{\boldsymbol{Y}}_{i\cdot} - \overline{\boldsymbol{Y}}_{\cdot\cdot})(\overline{\boldsymbol{Y}}_{i\cdot} - \overline{\boldsymbol{Y}}_{\cdot\cdot})^\top - \boldsymbol{\Sigma}_u - \frac{1}{r}\boldsymbol{\Sigma}_\epsilon\Big) \xrightarrow{\mathrm{d}} \mathcal{N}\left(\mathbf{0}, \boldsymbol{\Gamma}\left(\boldsymbol{\Sigma}_u + \tfrac{1}{r}\boldsymbol{\Sigma}_\epsilon\right)\right), \tag{3.79}$$

as $a \to \infty$, leading to

$$\sqrt{a}\,\mathrm{vec}\Big(\frac{1}{a}\sum_{i=1}^{a}(\overline{\boldsymbol{Y}}_{i\cdot} - \overline{\boldsymbol{Y}}_{\cdot\cdot})(\overline{\boldsymbol{Y}}_{i\cdot} - \overline{\boldsymbol{Y}}_{\cdot\cdot})^\top - \boldsymbol{\Sigma}_u\Big) \xrightarrow{\mathrm{d}} \mathcal{N}\left(\mathbf{0}, \boldsymbol{\Gamma}\left(\boldsymbol{\Sigma}_u\right)\right), \tag{3.80}$$

as both $a \to \infty$ and $r \to \infty$. This implies the asymptotic relation of $\widehat{\boldsymbol{\Sigma}}_u$ as the sample size and replications number both tend to infinity.

(b) Applying the multivariate Delta method to the result in part (a), we find that the joint distribution of $\mathscr{V}(\widehat{\boldsymbol{\Sigma}}_\epsilon)$ and $\mathscr{V}(\widehat{\boldsymbol{\Sigma}}_\epsilon)$ converges as follows,

$$\sqrt{a}\begin{pmatrix}\sqrt{r}\left(\mathscr{V}(\widehat{\boldsymbol{\Sigma}}_\epsilon) - \mathscr{V}(\boldsymbol{\Sigma}_\epsilon)\right)\\ \mathscr{V}(\widehat{\boldsymbol{\Sigma}}_u) - \mathscr{V}(\boldsymbol{\Sigma}_u)\end{pmatrix} \xrightarrow{\mathrm{d}} \mathcal{N}\left(\mathbf{0}, \begin{pmatrix}\hbar_{\mathscr{V}}(\boldsymbol{\Sigma}_\epsilon) & 0\\ 0 & \hbar_{\mathscr{V}}(\boldsymbol{\Sigma}_u)\end{pmatrix}\right), \tag{3.81}$$

as $a \to \infty$ and $r \to \infty$ where $\hbar_{\mathscr{V}}(\boldsymbol{\Sigma}) = 2\left\|\nabla\mathscr{V}(\boldsymbol{\Sigma})\boldsymbol{\Sigma}\right\|_F^2 = 2\,\mathrm{tr}\big(\left\{\nabla\mathscr{V}(\boldsymbol{\Sigma})\boldsymbol{\Sigma}\right\}^2\big)$.

Using the marginal asymptotic distribution of $\mathscr{V}(\widehat{\boldsymbol{\Sigma}}_u)$, together with $\mathscr{V}(\widehat{\boldsymbol{\Sigma}}_\epsilon) \xrightarrow{\mathrm{a.s}} \mathscr{V}(\boldsymbol{\Sigma}_\epsilon)$ and the Slutsky's theorem, concludes the expected result.

Proof of Theorem 3.5

Based on Theorem 3.4, the relative values of $\mathscr{V}(\widehat{\boldsymbol{\Sigma}}_\epsilon)$, $\mathscr{V}(\widehat{\boldsymbol{\Sigma}}_u)$, and $\widehat{\rho}_{\mathscr{V}}$, converge as follows,

$$\sqrt{ar}\left\{\frac{\mathscr{V}(\widehat{\boldsymbol{\Sigma}}_\epsilon)}{\mathscr{V}(\boldsymbol{\Sigma}_\epsilon)}-1\right\}\xrightarrow{\mathrm{d}}\mathcal{N}\left(0,\mathscr{u}_{\mathscr{V}}(\boldsymbol{\Sigma}_\epsilon)\right), \tag{3.82}$$

$$\sqrt{a}\left\{\frac{\mathscr{V}(\widehat{\boldsymbol{\Sigma}}_u)}{\mathscr{V}(\boldsymbol{\Sigma}_u)}-1\right\}\xrightarrow{\mathrm{d}}\mathcal{N}\left(0,\mathscr{u}_{\mathscr{V}}(\boldsymbol{\Sigma}_u)\right), \tag{3.83}$$

$$\sqrt{a}\left\{\frac{\widehat{\rho}_{\mathscr{V}}}{\rho_{\mathscr{V}}}-1\right\}\xrightarrow{\mathrm{d}}\mathcal{N}\left(0,\mathscr{u}_{\mathscr{V}}(\boldsymbol{\Sigma}_u)\right), \tag{3.84}$$

where $\mathscr{u}_{\mathscr{V}}(\boldsymbol{\Sigma})=2\left[\frac{\|\nabla\mathscr{V}(\boldsymbol{\Sigma})\boldsymbol{\Sigma}\|_F}{\mathscr{V}(\boldsymbol{\Sigma})}\right]^2$. For the three cases of $\mathscr{V}(\boldsymbol{\Sigma})=\left|\boldsymbol{\Sigma}\right|^{\frac{1}{p}}$, $\mathscr{V}(\boldsymbol{\Sigma})=\mathrm{tr}(\boldsymbol{\Sigma})$, and $\mathscr{V}(\boldsymbol{\Sigma})=\|\boldsymbol{\Sigma}\|_F$, the corresponding asymptotic variances are derived, respectively, as follows,

$$\mathscr{u}_{\mathrm{gv}}(\boldsymbol{\Sigma})=\frac{2}{p}, \tag{3.85}$$

$$\mathscr{u}_{\mathrm{tr}}(\boldsymbol{\Sigma})=2\left\|\frac{\boldsymbol{\Sigma}}{\mathrm{tr}(\boldsymbol{\Sigma})}\right\|_F^2, \tag{3.86}$$

$$\mathscr{u}_{F}(\boldsymbol{\Sigma})=\frac{2\,\mathrm{tr}(\boldsymbol{\Sigma}^4)}{\{\mathrm{tr}(\boldsymbol{\Sigma}^2)\}^2}. \tag{3.87}$$

Thus, to proceed with the proof the theorem, we need the following inequality,

$$\frac{1}{p}\leq\frac{\mathrm{tr}(\boldsymbol{\Sigma}^2)}{\{\mathrm{tr}(\boldsymbol{\Sigma})\}^2}\leq\frac{\mathrm{tr}(\boldsymbol{\Sigma}^4)}{\{\mathrm{tr}(\boldsymbol{\Sigma}^2)\}^2}, \tag{3.88}$$

which should hold for any symmetric positive semi-definite matrix $\boldsymbol{\Sigma}$. To verify the inequalities in (3.88), we proceed by showing that

$$\frac{1}{p}\leq\frac{\alpha_1^2+\cdots+\alpha_n^2}{(\alpha_1+\cdots+\alpha_n)^2}\leq\frac{\alpha_1^4+\cdots+\alpha_n^4}{(\alpha_1^2+\cdots+\alpha_n^2)^2}, \tag{3.89}$$

where $\alpha_1,\ldots,\alpha_n$ are all positive numbers.

The first inequality in (3.89) directly follows from the Cauchy-Schwarz inequality. To establish the second inequality, we introduce new variables $z_i=\alpha_i/\sqrt{\sum_{i=1}^n\alpha_i^2}$ for

$i = 1, \ldots, n$, allowing us to express the second inequality as

$$\frac{z_1^2 + \cdots + z_n^2}{(z_1 + \cdots + z_n)^2} \leqslant \frac{z_1^4 + \cdots + z_n^4}{(z_1^2 + \cdots + z_n^2)^2} \,. \tag{3.90}$$

Here, $0 < z_i \leq 1$ for $i = 1, \ldots, n$ and $\sum_{i=1}^n z_i^2 = 1$. Therefore, we only need to confirm that,

$$1 \leqslant f(z_1, \ldots, z_n) \,, \tag{3.91}$$

where the function $f(z_1, \ldots, z_n)$ is defined as,

$$f(z_1, \ldots, z_n) = (z_1 + \cdots + z_n)^2 \left(z_1^4 + \cdots + z_n^4\right) \,. \tag{3.92}$$

This function is symmetric with respect to its variables. The minimum of $f(z_1, \ldots, z_n)$ occurs when all variables are equal (Waterhouse, 1983). Given the condition that $\sum_{i=1}^n z_i^2 = 1$, the minimum of (3.92) occurs when $z_1 = \cdots = z_n = 1/\sqrt{n}$, at which point the value of $f(z_1, \ldots, z_n)$ becomes 1. This completes the proof.

Chapter 4

Measurements System Assessment Study for Functional Datasets

4.1 Introduction and background

In Chapters 2 and 3, we addressed the assessment of measurement systems when dealing with conventional data types, such as samples of scalar random variables or random vectors. However, many real-world manufacturing processes often involve more complex and dynamic measurement data, requiring sophisticated approaches to analysis. In this chapter, we take a step further by extending the analysis of measurement systems to encompass functional data type that consists of observations of continuous random functions across a defined domain.

In the manufacturing industry, functional datasets are becoming increasingly available in various fields. For instance, within the realm of surface quality assessment, functional datasets play a significant role in capturing a wide spectrum of surface characteristics. These include roughness, waviness, finish, texture, geometric compliance, and shape deformation, measured along a continuous path or area. Notable examples can be found in references such as (Jin et al., 2020; Yang et al., 2021; Mozaffari et al., 2021; Jin et al., 2023). The prevalence of such datasets underscores the necessity for advanced analytical approaches that can comprehensively address uncertainties stemming from the measurement system and other contributing factors in the context of functional data.

The statistical methodologies for analyzing functional datasets are referred to as functional data analysis. Comprehensive insights into this field are presented by Bosq (2000);

Ramsay and Silverman (2005); Zhang (2013); Horváth and Kokoszka (2012); Wang et al. (2016); Srivastava and Klassen (2016); Wang et al. (2016).

Functional data, due to their inherent nature of being infinite-dimensional objects, introduce challenges to their analysis. They can be treated as sample paths or realizations of a stochastic process. The Karhunen–Loève theorem provides a representation of stochastic processes in L^2 space. This representation is obtained by extracting functional principal components from the covariance kernel of these stochastic processes. In practical applications, this representation is often truncated to a selected number of the initial expansion terms to approximate the stochastic processes. This operation of estimating the principal components and selecting a subset of them as functional bases is widely known as functional principal component analysis (FPCA). Employing this framework, a stochastic process in L^2 space can be characterized by a finite-dimensional vector including the random principal component scores. For an in-depth exploration of this subject, we refer the reader to notable works by Ramsay and Silverman (2002, 2005); Yao et al. (2005); Ferraty and Vieu (2006); Hall et al. (2006); Hall (2010); Horváth and Kokoszka (2012); Shang (2014). Other relevant contributions to the field of FPCA include James et al. (2000); Di et al. (2009); Jolliffe and Cadima (2016).

One of the fundamental challenges that naturally emerges in functional data analysis is the estimation of mean and covariance functions. This task holds significance not only in its own right but also plays a pivotal role for FPCA and the broader context of measurement systems analysis when dealing with functional data. Classical estimators from multivariate statistics, such as the sample mean and covariance matrix, may not provide reasonable smoothed estimations in this scenario. The effectiveness of these estimators can be influenced by diverse sampling plans under which data are collected, ranging from dense to sparse and from regular to irregular settings (Horváth and Kokoszka, 2012; Zhang and Wang, 2016; Nie et al., 2022). Moreover, functional data involve complex temporal or spatial dependencies and are often susceptible to noise contamination. These factors collectively suggest the need for distinct statistical approaches when analyzing functional data (Yao et al., 2005).

Several methods and modifications have been proposed to infuse smoothness into the estimation process. These techniques consider conditions of smoothness, including the requirement of possessing several continuous derivatives (Ramsay and Silverman, 2005). In the works by Besse et al. (1997); Cardot (2000); Wahba (1990), non-parametric spline-based techniques are employed to estimate a smooth curve for each sample path of the functional data within a variety of sampling settings.

In the literature concerning the estimation of mean and covariance functions, one

category is founded on a form of the penalized least-squares method. To estimate the mean function, Rice and Silverman (1991) suggest a least-squares approach that maintains smoothness up to the second derivation. This method is applied within an identical sampling setting, where data are collected at the same locations across all functions. Cai and Yuan (2011), on the other hand, adapt the penalized least-squares method. They control the level of smoothness using (L^2 norm of) the n-th derivative of functions, considering both regular and irregular sampling settings. In a different context, Cai and Yuan (2010) employ the penalized least-squares method to estimate the covariance function within the framework of reproducing kernel Hilbert space (RKHS).

Within the spectrum of methodologies, another significant category for the estimation of mean and covariance functions is based on kernel smoothing techniques (Yao et al., 2005; Hall et al., 2006; Li and Hsing, 2010; Zhang, 2013; Zhang and Wang, 2016). A widely used kernel method is the local linear smoothing, which locally fits a straight line across all points within the function's domain.

In the realm of functional data, a collection of functional observations often exhibits consistent shape features, with potential random distortions in observation time, distance, or any other continuous parameter (Kneip and Gasser, 1992; Ramsay and Silverman, 2005). This temporal variation, or warping, constitutes a significant source of variability in functional data, distinguishing it from more conventional data formats. The process of aligning functional observations to mitigate such variations is known as registration. For a summary of major functional data registration methods, refer to (Marron et al., 2014).

In current real-world scenarios involving measurement system studies, a notable absence exists: a standardized procedure for measurement system assessment tailored to the class of functional data. This chapter aims to bridge this gap by introducing specific methodologies for such scenarios. Unlike the classical methods adopted from multivariate data analysis, our approach utilizes and benefits from the specialized tools of functional data analysis that are purpose-built for effectively addressing the intricacies of these datasets.

4.1.1 Contributions and outlines

In this chapter, we make the following contributions:

1. We establish a framework for studying measurement systems involving functional data using a one-way ANOVA model.
2. We extend the definition of parameters used in assessing measurement systems of univariate data to effectively capture the distinctive characteristics of functional data. This extension involves utilizing a bounded operator on covariance kernels.

We focus on the trace and the L^2 operators of covariance kernels. We illustrate how, by employing these operators, the parameters for measurement system assessment can be expressed in terms of the underlying eigenvalues.

3. To estimate the measurement system assessment parameters, we first provide methods to estimate covariance kernel components associated with the one-way model. We employ a regularization approach within the framework of RKHS to obtain smooth and reliable estimates of the covariance kernels.

The organization of this chapter is outlined as follows: After establishing the basic notation, Section 4.2 introduces the setup and framework of the one-way ANOVA model for a measurement system study involving functional data. This section provides a comprehensive overview of fundamental definitions and properties related to the model components. Section 4.3 offers a detailed review of the structure of variability in the functional one-way model. In Section 4.4, parameters for assessing the measurement systems of functional data are established and defined. Section 4.5 is dedicated to the estimation procedure. It reviews a basic estimation technique without smoothing and then employs a regularization method within the framework of RKHS to estimate two smooth covariance functions corresponding to the random effects in the model. Moving forward, Section 4.6 presents the results of numerical studies conducted. In Section 4.7, prospects for further research are discussed. Additional resources and supplementary materials are outlined in Section 4.8.

4.1.2 Basic notation and conventions

This chapter employs the following notation and conventions: We use $\mathcal{D}$ to denote a finite interval. The L^2 norm of a function $f(x)$, with $x \in \mathcal{D}$, is denoted as $\|f\|_{L^2}$, where,

$$\|f\|_{L^2} = \left[\int_{\mathcal{D}} f^2(x)\,\mathrm{d}x\right]^{1/2}.$$

If $\|f\|_{L^2} < \infty$, we refer to f, as a squared integrable function. In this case, we can express $f(x) \in \mathscr{L}^2(\mathcal{D})$, where $\mathscr{L}^2(\mathcal{D})$ represents the Hilbert space comprising all squared integrable functions over $\mathcal{D}$. The associated inner product of $\mathscr{L}^2(\mathcal{D})$ is defined as,

$$\langle f, g\rangle_{\mathscr{L}^2(\mathcal{D})} = \int_{\mathcal{D}} f(x)g(x)\,\mathrm{d}x,$$

where both functions f and g belong to $\mathscr{L}^2(\mathcal{D})$. The notation $f^{(n)}$ refers to the n-th derivative of the function f.

If $f(x_1, x_2)$ is a bivariate function and $x_1, x_2 \in \mathscr{D}$, notations $\mathrm{tr}(f)$ and $\|f\|_{L^2}$ represent the trace and the L^2 norm of f, respectively, given by

$$\mathrm{tr}(f) = \int_{\mathscr{D}} f(x, x)\, \mathrm{d}x\,,$$
$$\|f\|_{L^2} = \left[\iint_{\mathscr{D}\times\mathscr{D}} f^2(x_1, x_2)\, \mathrm{d}x_1\, \mathrm{d}x_2\right]^{1/2}.$$

A symmetric bivariate function $f(x_1, x_2)$ is considered positive-semi-definite if, for any $x_1, x_2, \ldots, x_n \in \mathscr{D}$ and $a_1, \ldots, a_n \in \mathbb{R}$, the following inequality holds for all n,

$$\sum_{i=1}^{n}\sum_{j=1}^{n} a_i a_j f(x_i, x_j) \geq 0\,,$$

and positive definite if '$>$' holds, where $a_1, \ldots, a_n$ are not all zero.

4.2 One-way model setup

Suppose an experiment is being conducted, where a sample of 'a' units is randomly selected from the population of units. The measurand represents a continuous feature or attribute of the units, which is a function of the independent variable x, where x belongs to a connected interval $\mathscr{D} \subset \mathbb{R}$. Each sample unit undergoes multiple measurements, with $r > 1$ repetitions. We treat the replication measurements of each unit sample as a single group. The underlying model employed to represent the measurement data is given by,

$$Y_{ij}(x) = \mu(x) + U_i(x) + \epsilon_{ij}(x), \quad \text{for } i = 1, \ldots, a, \text{ and } j = 1, \ldots, r, \tag{4.1}$$

where $x \in \mathscr{D}$. In this model, $Y_{ij}(x)$ represents the measured value of the attribute for the ith unit at location x and in the jth replicate. The term $\mu(\cdot)$ denotes the overall mean function, which represents the expected behavior of the attribute over the interval $\mathscr{D}$. The component $U_i(\cdot)$ represents the random function associated with the main effect of unit i, and $\epsilon_{ij}(\cdot)$ is the random function corresponding to the measurement error of unit i at the jth replication measurement.

All U_i's are independent realizations of the stochastic process U, and all ϵ_{ij}'s are independent realizations of the stochastic process ϵ. These stochastic processes, U and ϵ, are characterized by the following assumptions: First, without loss of generality, we assume

that U and ϵ are centered on zero, meaning that for any point $x \in \mathscr{D}$, $\mathrm{E}[U(x)] = 0$ and $\mathrm{E}[\epsilon(x)] = 0$. Secondly, U and ϵ are second–order processes, indicating that $\mathrm{E}[|U(x)|^2] < \infty$ and $\mathrm{E}[|\epsilon(x)|^2] < \infty$, for all $x \in \mathscr{D}$. Furthermore, stochastic processes U and ϵ are mutually independent.

From the second-order property of processes U and ϵ, it can be inferred that these processes are stochastic elements of $\mathscr{L}^2(\mathscr{D})$, equipped with the Borel σ-algebra, and squared integrable. This indicates that,

$$\mathrm{E}\big[\|U\|_{L^2}^2\big] = \mathrm{E}\left[\int_{\mathscr{D}} U^2(x)\,\mathrm{d}x\right] < \infty, \tag{4.2a}$$

$$\mathrm{E}\big[\|\epsilon\|_{L^2}^2\big] = \mathrm{E}\left[\int_{\mathscr{D}} \epsilon^2(x)\,\mathrm{d}x\right] < \infty\,. \tag{4.2b}$$

The squared integrability condition of $U(\cdot)$ and $\epsilon(\cdot)$, as outlined in (4.2), enables the calculation and analysis of their variances and covariances. The covariance kernels (or covariance functions) of the stochastic processes U and ϵ are defined as follows,

$$C_u(x_1, x_2) = \mathrm{E}\left[U(x_1)\,U(x_2)\right], \tag{4.3a}$$

$$C_\epsilon(x_1, x_2) = \mathrm{E}\left[\epsilon(x_1)\,\epsilon(x_2)\right], \tag{4.3b}$$

respectively, where $x_1, x_2 \in \mathscr{D}$. The covariance kernel C_u is positive semi-definite, while C_ϵ is positive definite. Both C_u and C_ϵ are squared integrable; that is,

$$\iint_{\mathscr{D}\,\mathscr{D}} C_u^2(x_1, x_2)\,\mathrm{d}x_1\,\mathrm{d}x_2 < \infty, \tag{4.4a}$$

$$\iint_{\mathscr{D}\,\mathscr{D}} C_\epsilon^2(x_1, x_2)\,\mathrm{d}x_1\,\mathrm{d}x_2 < \infty. \tag{4.4b}$$

Consequently, both C_u and C_ϵ are Hilbert–Schmidt kernels of $\mathscr{L}^2(\mathscr{D} \times \mathscr{D})$. For an in-depth exploration of these properties of covariance kernels, refer to (Horváth and Kokoszka, 2012, Chapter 2).

In the functional one-way random effects model (4.1), the covariance kernel of the measurement Y_{ij} is expressed as,

$$C_t(x_1, x_2) = C_u(x_1, x_2) + C_\epsilon(x_1, x_2)\,. \tag{4.5}$$

By using the properties of the L^2 norm, it can be demonstrated that C_t is also squared

integrable, establishing it as a Hilbert-Schmidt kernel of $\mathscr{L}^2(\mathscr{D} \times \mathscr{D})$. The constituent parts C_u and C_ϵ of the covariance kernel C_t are individually denoted as covariance kernel components.

4.3 Spectral analysis

This section provides a comprehensive review of the structure of the variability of stochastic processes U and ϵ in model 4.1.

The covariance operators $A_u : \mathscr{L}^2(\mathscr{D}) \to \mathscr{L}^2(\mathscr{D})$ and $A_\epsilon : \mathscr{L}^2(\mathscr{D}) \to \mathscr{L}^2(\mathscr{D})$ associated with C_u and C_ϵ can be expressed as the following integral operators,

$$A_u f(\cdot) = \int_{\mathscr{D}} C_u(\cdot\,, x) f(x)\,\mathrm{d}x, \tag{4.6a}$$

$$A_\epsilon f(\cdot) = \int_{\mathscr{D}} C_\epsilon(\cdot\,, x) f(x)\,\mathrm{d}x. \tag{4.6b}$$

Since $\mathscr{D}$ is a bounded interval and C_u and C_ϵ are Hilbert-Schmidt kernels, the covariance operators A_u and A_ϵ are both compact and self-adjoint operators on the Hilbert space $\mathscr{L}^2(\mathscr{D})$. Applying the spectral theorem for compact and self-adjoint operators, we ascertain the existence of two sequences of basis functions in $\mathscr{L}^2(\mathscr{D})$. One sequence, denoted as $\Psi_1, \Psi_2, \ldots$, encompasses the eigenfunctions of A_u. Correspondingly, the other sequence, denoted as $\Phi_1, \Phi_2, \ldots$, comprises the eigenfunctions of A_ϵ. For $x \in \mathscr{D}$, these sequences satisfy

$$A_u \Psi_k(x) = \lambda_{uk} \Psi_k(x), \tag{4.7a}$$

$$A_\epsilon \Phi_\nu(x) = \lambda_{\epsilon\nu} \Phi_\nu(x), \tag{4.7b}$$

where eigenvalues $\lambda_{u1} \geq \lambda_{u2} \geq \cdots \geq 0$ and $\lambda_{\epsilon 1} \geq \lambda_{\epsilon 2} \geq \cdots \geq 0$.

According to Mercer's theorem, which relates the spectral expansion of an operator to the representation of the corresponding kernel, the covariance kernels C_u and C_ϵ can be expressed as

$$C_u(x_1, x_2) = \sum_{k \geq 1} \lambda_{uk} \Psi_k(x_1) \Psi_k(x_2), \tag{4.8a}$$

$$C_\epsilon(x_1, x_2) = \sum_{\nu \geq 1} \lambda_{\epsilon\nu} \Phi_\nu(x_1) \Phi_\nu(x_2). \tag{4.8b}$$

Motivated by these representations, the covariance kernels C_u and C_ϵ possess the following properties

$$\operatorname{tr}(C_u) = \int_{\mathscr{D}} C_u(x,x)\,\mathrm{d}x = \sum_{k\geq 1} \lambda_{uk} < \infty, \tag{4.9a}$$

$$\operatorname{tr}(C_\epsilon) = \int_{\mathscr{D}} C_\epsilon(x,x)\,\mathrm{d}x = \sum_{\nu\geq 1} \lambda_{\epsilon\nu} < \infty, \tag{4.9b}$$

and

$$\|C_u\|_{L^2}^2 = \iint_{\mathscr{D}\,\mathscr{D}} C_u^2(x_1,x_2)\,\mathrm{d}x_1\,\mathrm{d}x_2 = \sum_{k\geq 1} \lambda_{uk}^2 < \infty, \tag{4.10a}$$

$$\|C_\epsilon\|_{L^2}^2 = \iint_{\mathscr{D}\,\mathscr{D}} C_\epsilon^2(x_1,x_2)\,\mathrm{d}x_1\,\mathrm{d}x_2 = \sum_{\nu\geq 1} \lambda_{\epsilon\nu}^2 < \infty. \tag{4.10b}$$

These equations highlight that the trace and L^2 norm of the covariance kernels of stochastic processes U and ϵ are finite and can be expressed solely in terms of the associated eigenvalues.

Moving forward, we focus on designing parameters for the assessment of the measurement system of functional data. The spectral analysis of stochastic processes U and ϵ enables us to articulate the measurement system assessment parameters, leveraging the spectral properties of covariance kernel components C_u and C_ϵ .

4.4 Parameters for assessing measurement systems

In Chapter 1, we presented an overview of fundamental parameters related to the assessment of a measurement system for a single variable. In Chapter 3, we extended these considerations to multivariate data, summarizing variance-covariance matrices using a scalar function. In this chapter, we further extend our study to define the functional versions of these parameters. Building upon the notion in Chapter 3, we proceed to summarize the covariance kernels. This procedure involves the use of a continuous bounded operator $\mathscr{T} : \mathscr{L}^2(\mathscr{D}\times\mathscr{D}) \to \mathbb{R}$ that acts on a covariance kernel and produces a positive real number.

Applying this framework, we set up the counterparts of the signal-to-noise ratio, the percentage R&R ratio, and the intra-class correlation coefficient for functional data, re-

spectively, as follows,

$$\mathrm{SNR}_{\mathcal{T}} = \left[\frac{\mathcal{T}C_u}{\mathcal{T}C_\epsilon}\right]^{1/2}, \tag{4.11}$$

$$\%\mathrm{R\&R}_{\mathcal{T}} = \left[\frac{\mathcal{T}C_\epsilon}{\mathcal{T}C_t}\right]^{1/2} \times 100\%\,, \tag{4.12}$$

$$\mathrm{ICC}_{\mathcal{T}} = \frac{\mathcal{T}C_u}{\mathcal{T}C_t}\,. \tag{4.13}$$

We examine the following special mappings of the covariance kernels to quantify the dispersion of functional data.

A. Trace

By defining the operator $\mathcal{T}$ as the trace of covariance kernel, the signal-to-noise ratio, the percentage R&R ratio, and the intra-class correlation coefficient for functional data are expressed as follows,

$$\mathrm{SNR}_{\mathrm{tr}} = \left[\frac{\mathrm{tr}(C_u)}{\mathrm{tr}(C_\epsilon)}\right]^{1/2}, \tag{4.14}$$

$$\%\mathrm{R\&R}_{\mathrm{tr}} = \left[\frac{\mathrm{tr}(C_\epsilon)}{\mathrm{tr}(C_t)}\right]^{1/2} \times 100\%\,, \tag{4.15}$$

$$\mathrm{ICC}_{\mathrm{tr}} = \frac{\mathrm{tr}(C_u)}{\mathrm{tr}(C_t)}\,. \tag{4.16}$$

Following the spectral analysis of stochastic processes U and ϵ and using the linear property of the trace operator, these parameters can alternatively be calculated using the eigenvalues associated with the covariance kernels, in the form of

$$\mathrm{SNR}_{\mathrm{tr}} = \left[\frac{\sum_{k\geq 1}\lambda_{uk}}{\sum_{\nu\geq 1}\lambda_{\epsilon\nu}}\right]^{1/2}, \tag{4.17}$$

$$\%\mathrm{R\&R}_{\mathrm{tr}} = \left[\frac{\sum_{\nu\geq 1}\lambda_{\epsilon\nu}}{\sum_{k\geq 1}\lambda_{uk}+\sum_{\nu\geq 1}\lambda_{\epsilon\nu}}\right]^{1/2} \times 100\%\,, \tag{4.18}$$

$$\mathrm{ICC}_{\mathrm{tr}} = \frac{\sum_{k\geq 1}\lambda_{uk}}{\sum_{k\geq 1}\lambda_{uk}+\sum_{\nu\geq 1}\lambda_{\epsilon\nu}}\,. \tag{4.19}$$

Since expectation commutes with bounded (continues) linear operators, we have,

$$\mathrm{E}\left[\|U\|_{L^2}^2\right] = \int_{\mathscr{D}} C_u(x,x)\,\mathrm{d}x, \tag{4.20a}$$

$$\mathrm{E}\left[\|\epsilon\|_{L^2}^2\right] = \int_{\mathscr{D}} C_\epsilon(x,x)\,\mathrm{d}x\,. \tag{4.20b}$$

These equations imply that the expected L^2 norm of the stochastic processes U and ϵ is equal to the trace of the covariance kernels associated with each of these processes. From the independence of the stochastic processes U and ϵ, it can be deduced that

$$\mathrm{E}\left[\|U+\epsilon\|_{L^2}^2\right] = \int_{\mathscr{D}} C_t(x,x)\,\mathrm{d}x\,. \tag{4.21}$$

Equations (4.20) and (4.21) highlight that the parameters for assessing the measurement system, as outlined in (4.14), effectively quantify the relative variability between the processes U and ϵ concerning their expected L^2 norms.

B. L^2 norm

By defining the operator $\mathscr{T}$ as the L^2 norm of the covariance kernel, we can establish the signal-to-noise ratio, percentage R&R ratio, and intra-class correlation coefficients for functional data as follows,

$$\mathrm{SNR}_{L^2} = \left[\frac{\|C_u\|_{L^2}}{\|C_\epsilon\|_{L^2}}\right]^{1/2}, \tag{4.22}$$

$$\%\mathrm{R\&R}_{L^2} = \left[\frac{\|C_\epsilon\|_{L^2}}{\|C_t\|_{L^2}}\right]^{1/2} \times 100\%\,, \tag{4.23}$$

$$\mathrm{ICC}_{L^2} = \frac{\|C_u\|_{L^2}}{\|C_t\|_{L^2}}\,. \tag{4.24}$$

Additionally, the signal-to-noise ratio can be calculated as,

$$\mathrm{SNR}_{L^2} = \left[\frac{\sum_{k\geq 1}\lambda_{uk}^2}{\sum_{\nu\geq 1}\lambda_{\epsilon\nu}^2}\right]^{1/4}. \tag{4.25}$$

The L^2 norm operator is not linear in the sense of preserving the addition.

4.5 Estimation procedure

From (4.11), to estimate the parameters for measurement system assessment, one can estimate the covariance kernels C_u and C_ϵ and then apply the following plug-in estimators,

$$\widehat{\mathrm{SNR}}_{\mathcal{T}} = \left[\frac{\mathcal{T}\widehat{C_u}}{\mathcal{T}\widehat{C_\epsilon}}\right]^{1/2}, \tag{4.26a}$$

$$\widehat{\%\mathrm{R\&R}}_{\mathcal{T}} = \left[\frac{\mathcal{T}\widehat{C_\epsilon}}{\mathcal{T}\widehat{C_t}}\right]^{1/2} \times 100\%\,, \tag{4.26b}$$

$$\widehat{\mathrm{ICC}}_{\mathcal{T}} = \frac{\mathcal{T}\widehat{C_u}}{\mathcal{T}\widehat{C_t}}\,, \tag{4.26c}$$

where $\widehat{C_t} = \widehat{C_u} + \widehat{C_\epsilon}$.

As we proceed to the following sections, we will explore fundamental approaches for estimating the covariance kernels C_u and C_ϵ. The discussion will unfold, covering a basic estimation method and extending to more a sophisticated technique involving smoothing procedures.

4.5.1 Basic estimation without smoothing

For the functional one-way model (4.1), we can define several sample means and covariance functions, without involving smoothing.

Two sample mean functions associated with this model are the group sample mean function and the global sample mean function. Specifically, at point x within the interval $\mathcal{D}$, the group sample mean function for the ith unit is calculated as follows,

$$\overline{Y}_{i\cdot}(x) = \frac{1}{r}\sum_{j=1}^{r} Y_{ij}(x)\,. \tag{4.27}$$

The global sample mean function of the measurements, considering all units and replicated

measurements, is given by

$$\overline{Y}_{\cdot\cdot}(x) = \frac{1}{ar}\sum_{i=1}^{a}\sum_{j=1}^{r} Y_{ij}\,(x)\,. \tag{4.28}$$

There are two bivariate functions, the sum of squares and cross products, capturing the between-groups and within-groups variations. They are defined, respectively, as follows,

$$SS_u(x_1,x_2) = r\sum_{i=1}^{a}\left[\overline{Y}_{i\cdot}(x_1) - \overline{Y}_{\cdot\cdot}(x_1)\right]\left[\left(\overline{Y}_{i\cdot}(x_2) - \overline{Y}_{\cdot\cdot}(x_2)\right]\right., \tag{4.29}$$

$$SS_\epsilon(x_1,x_2) = \sum_{i=1}^{a}\sum_{j=1}^{r}\left[Y_{ij}(x_1) - \overline{Y}_{i\cdot}(x_1)\right]\left[(Y_{ij}(x_2) - \overline{Y}_{i\cdot}(x_2)\right]\right., \tag{4.30}$$

where $x_1, x_2 \in \mathfrak{D}$. The bivariate functions of the mean of squares and products corresponding are given by,

$$MS_u(x_1,x_2) = \frac{SS_u(x_1,x_2)}{a-1} = \frac{r}{a-1}\sum_{i=1}^{a}\left[\overline{Y}_{i\cdot}(x_1) - \overline{Y}_{\cdot\cdot}(x_1)\right]\left[\left(\overline{Y}_{i\cdot}(x_2) - \overline{Y}_{\cdot\cdot}(x_2)\right]\right., \tag{4.31}$$

$$MS_\epsilon(x_1,x_2) = \frac{SS_\epsilon(x_1,x_2)}{a(r-1)} = \frac{1}{a(r-1)}\sum_{i=1}^{a}\sum_{j=1}^{r}\left[Y_{ij}(x_1) - \overline{Y}_{i\cdot}(x_1)\right]\left[(Y_{ij}(x_2) - \overline{Y}_{i\cdot}(x_2)\right]\right., \tag{4.32}$$

Table 4.1 displays the functional analysis of variance, also known as FANOVA, classification.

Table 4.1: The analysis of variance classification for the functional one-way model with stochastic effects.

Source	Degree of freedom	Sum of squares and products	Mean of squares and products
U	$\mathrm{df}_u = a-1$	$SS_u(x_1,x_2) = r\sum_{i=1}^{a}\left[\overline{Y}_{i\cdot}(x_1) - \overline{Y}_{\cdot\cdot}(x_1)\right]\left[(\overline{Y}_{i\cdot}(x_2) - \overline{Y}_{\cdot\cdot}(x_2)\right]$	$MS_u(x_1,x_2) = \dfrac{SS_u(x_1,x_2)}{a-1}$
ϵ	$\mathrm{df}_\epsilon = a(r-1)$	$SS_\epsilon(x_1,x_2) = \sum_{i=1}^{a}\sum_{j=1}^{r}\left[Y_{ij}(x_1) - \overline{Y}_{i\cdot}(x_1)\right]\left[(Y_{ij}(x_2) - \overline{Y}_{i\cdot}(x_2)\right]$	$MS_\epsilon(x_1,x_2) = \dfrac{SS_\epsilon(x_1,x_2)}{a(r-1)}$
Total	$ar-1$	$SS_t(x_1,x_2) = \sum_{i=1}^{a}\sum_{j=1}^{r}\left[Y_{ij}(x_1 - \overline{Y}_{\cdot\cdot}(x_1)\right]\left[Y_{ij}(x_2 - \overline{Y}_{\cdot\cdot}(x_2)\right]$	

Under the assumptions outlined for the one-way model (4.1), it can be shown that,

$$\mathrm{E}\left[MS_u(x_1, x_2)\right] = C_\epsilon(x_1, x_2) + r\, C_u\left(x_1, x_2\right), \tag{4.33a}$$

$$\mathrm{E}\left[MS_\epsilon(x_1, x_2)\right] = C_\epsilon\left(x_1, x_2\right). \tag{4.33b}$$

Through the use of the above equations, the unbiased estimators of C_u and C_ϵ are obtained as

$$\widehat{C_u}(x_1, x_2) = \frac{1}{r}\left(MS_u(x_1, x_2) - MS_\epsilon(x_1, x_2)\right), \tag{4.34a}$$

$$\widehat{C_\epsilon}(x_1, x_2) = MS_\epsilon(x_1, x_2). \tag{4.34b}$$

In practice, the observed data consists of sample values of functions $Y_{ij}(\cdot)$ collected at a finite number of discrete points. The sampling arrangement can take the form of either regular or irregular grids. In a regular grid setting, data from all functions are collected at identical points across all subjects and replications. Conversely, for an irregular sampling method, the sampling locations and the number of samples collected per function may vary between functions.

The unbiased estimators of covariance kernels presented in (4.34) require that the sampling method be regular across all functional observations. Given that the observations consist of a finite number of discrete points, the estimators of covariance kernels in (4.34) are considered unbiased at this finite set of points, rather than across the entire range $\mathscr{D}$.

4.5.2 Estimation with smoothing

To estimate the covariance kernels of processes U and ϵ within the context of one-way ANOVA model 4.1, we apply a regularization approach using RKHS framework, following the methodology outlined in (Cai and Yuan, 2010). Given the foundational role of RKHS in our research, we offer a brief review of the terms, definitions, and key properties associated with RKHS in the supplementary materials of Section 4.8. For a more comprehensive exploration of RKHS, we recommend referring to Aronszajn (1950); Wahba (1990).

We begin by reviewing the required conditions for covariance kernels to be included in an RKHS. We assume that the sample paths of U and ϵ exhibit smoothness, each belonging to a specific RKHS. If the process U resides in the RKHS with the reproducing kernel K_u, denoted as $\mathcal{H}(K_u)$, and satisfies $\mathrm{E}\left[\|U\|^2_{\mathcal{H}(K_u)}\right] < \infty$, then it is established that the covariance kernel C_u is a member of the tensor product Hilbert space $\mathcal{H}(K_u \otimes K_u)$ (Cai and Yuan, 2010, Theorem 1). Likewise, assuming that the process ϵ belongs to the Hilbert

space $\mathcal{H}(K_\epsilon)$ and satisfies $\mathrm{E}\left[\|\epsilon\|^2_{\mathcal{H}(K_\epsilon)}\right] < \infty$, the covariance function C_ϵ is a member of the tensor product Hilbert space $\mathcal{H}(K_\epsilon \otimes K_\epsilon)$. For brevity in notation, we henceforth assume $K_u = K_\epsilon = K$. This result can be applied to derive estimates for C_ϵ and C_u within the framework of $\mathcal{H}(K \otimes K)$.

Next, we investigate the regularization method to derive smooth estimates of covariance kernels C_ϵ and C_u . This process involves formulating an optimization problem utilizing a generic input function B, where B serves as an initial non-smooth estimate of the covariance kernel we aim to estimate. The regularization problem is stated as follows,

$$\min_{C \in \mathcal{H}(K \otimes K)} \left\{ \mathscr{L}(B, C) + \lambda \|C\|^2_{\mathcal{H}(K \otimes K)} \right\}. \tag{4.35}$$

Here, $\mathscr{L}(B, C)$ quantifies the discrepancy between the estimated covariance kernel C and the initial estimate B, at a finite number of discrete points. The term $\|C\|^2_{\mathcal{H}(K \otimes K)}$ serves as a penalization term that encourages smoothness in the solution for desirable properties. The parameter $\lambda > 0$ acts as a tuning parameter, controlling the trade-off between fidelity to the data and smoothness of the estimated covariance kernel. The specific value of λ can be determined through techniques like cross-validation, or information criteria such as AIC or BIC. See, e.g., (Hastie et al., 2009).

We employ a least squares method to find the member of $\mathcal{H}(K \otimes K)$ that best fits the initial estimate B, while the smoothness level is controlled by parameter λ. To proceed, we adopt a regular discrete sampling setting where data from all units and replications are collected at m identical points, namely $s_1, \ldots, s_m$. The loss function $\mathscr{L}(B, C)$ in problem (4.35) is the residuals sum of squares, computed as,

$$\mathscr{L}(B, C) = \sum_{k_1=1}^{m} \sum_{k_2=1}^{m} \left(B(s_{k_1}, s_{k_2}) - C(s_{k_1}, s_{k_2}) \right)^2. \tag{4.36}$$

To derive the specific form of the initial estimate B, we take advantage of the relationships among MS_u, MS_ϵ, and the covariance kernels C_u and C_ϵ, as detailed in (4.33). For the estimation of C_ϵ, the initial estimate B is defined as follow,

$$B(s_{k_1}, s_{k_2}) = MS_\epsilon(s_{k_1}, s_{k_2}) = \frac{1}{a(r-1)} \sum_{i=1}^{a} \sum_{j=1}^{r} \left[Y_{ij}(s_{k_1}) - \overline{Y}_{i\cdot}(s_{k_1}) \right] \left[Y_{ij}(s_{k_2}) - \overline{Y}_{i\cdot}(s_{k_2}) \right]. \tag{4.37}$$

Here, (s_{k_1}, s_{k_2}) are selected from the sampling grid where $k_1 = 1, \ldots, m$, and $k_2 = 1, \ldots, m$.

On the other hand, when adopting the following expression for the input function B,

$$B(s_{k_1}, s_{k_2}) = \frac{1}{r} MS_u(s_{k_1}, s_{k_2}) = \frac{1}{a-1} \sum_{i=1}^{a} \left[\overline{Y}_{i\cdot}(s_{k_1}) - \overline{Y}_{\cdot\cdot}(s_{k_1})\right] \left[\overline{Y}_{i\cdot}(s_{k_2}) - \overline{Y}_{\cdot\cdot}(s_{k_2})\right] , \tag{4.38}$$

the outcome of serves as an estimator for $C_u + r^{-1}C_\epsilon$, from which we can deduce the estimator of C_u.

The well-posedness of the regularization problem (4.35) ensures a unique solution that depends stably on the input data (Tikhonov and Arsenin, 1977). Although the problem is formulated within an infinite-dimensional subspace, the *representer theorem* guarantees the existence of a finite-dimensional representation for the solution.

By the representer theorem, and following a similar approach as described in (Wahba, 1990, Theorem 1.3.1), the minimizer of the regularization problem (4.35) under the regular discrete sampling is assumed to have the form,

$$C(x_1, x_2) = \sum_{k_1=1}^{m} \sum_{k_2=1}^{m} a_{k_1 k_2} K(x_1, s_{k_1}) K(x_2, s_{k_2}), \tag{4.39}$$

for any $x_1, x_2 \in \mathcal{D}$, where the coefficients $a_{k_1 k_2} \in \mathbb{R}$ need to be estimated. From the reproducing property of the RKHS of $\mathcal{H}(K) \otimes \mathcal{H}(K)$, it follows that $K(x_1, s_{k_1})K(x_2, s_{k_2}) = K \otimes K((x_1, x_2), (s_{k_1}, s_{k_j}))$. In the representation given in (4.39), the covariance kernel C is expressed in terms of basis functions, which are derived from the tensor product of kernel sections centered on the sampling grid points (s_{k_1}, s_{k_2}).

For a function C that admits the representation (4.39), its squared RKHS norm $\|C\|^2_{\mathcal{H}(K\otimes K)}$ can be derived as,

$$\begin{aligned} \|C\|^2_{\mathcal{H}(K\otimes K)} &= \sum_{k_1=1}^{m} \sum_{k_2=1}^{m} \sum_{\ell_1=1}^{m} \sum_{\ell_2=1}^{m} a_{k_1 k_2} a_{\ell_1 \ell_2} K(s_{k_1}, s_{\ell_1}) K(s_{k_2}, s_{\ell_2}) \\ &= \mathbf{a}^\top (\boldsymbol{K} \otimes \boldsymbol{K})\, \mathbf{a}\,, \end{aligned} \tag{4.40}$$

where

$$\mathbf{a} = \left(a_{11}, a_{12}, \ldots, a_{1m}, a_{21}, \ldots, a_{mm}\right)^\top ,$$

and $\boldsymbol{K} \in \mathbb{R}^{m\times m}$ is the positive semi-definite kernel matrix, with the entry in row k_1 and column k_2 evaluated as $K(s_{k_1}, s_{k_2})$.

Define the vector of the initial estimates as

$$\mathbf{b} = \big(B(s_1, s_1), B(s_1, s_2), \ldots, B(s_1, s_m), B(s_2, s_1), \ldots, B(s_m, s_m)\big)^\top .$$

Now, the regularization problem $\min_{C \in \mathcal{H}(K \otimes K)} \left\{ \mathscr{L}(B, C) + \lambda \|C\|^2_{\mathcal{H}(K \otimes K)} \right\}$ is equivalent to,

$$\min_{\mathbf{a}} \|\mathbf{b} - (\boldsymbol{K} \otimes \boldsymbol{K})\, \mathbf{a}\|^2 + \lambda\, \mathbf{a}^\top (\boldsymbol{K} \otimes \boldsymbol{K})\, \mathbf{a}\,. \tag{4.41}$$

The solution for coefficients vector $\mathbf{a}$ is given by

$$\widehat{\mathbf{a}} = \boldsymbol{H}^{-1}\mathbf{b}\,. \tag{4.42}$$

where $\boldsymbol{H} = \boldsymbol{K} \otimes \boldsymbol{K} + \lambda\, \boldsymbol{I}$.

Remark 4.1. *The extension of the aforementioned outcome becomes more versatile by enriching the RKHS with offset terms from a parametric subspace denoted as $\mathcal{N}_0$. This enrichment leads to an estimator for the covariance function composed of two terms: one term is from $\mathcal{H}(K \otimes K)$ and the other belongs to $\mathcal{N}_0$. Assuming a regular discrete sampling setting, the estimator for the covariance function takes the following form,*

$$\widetilde{C}(x_1, x_2) = \sum_{i=1}^{m} \sum_{j=1}^{m} a_{ij} K(x_1, s_i) K(x_2, s_j) + \sum_{p=1}^{n_0} d_p \vartheta_p\,(x_1, x_2)\,, \tag{4.43}$$

where $x_1, x_2 \in \mathcal{D}$, and $\{\vartheta_1, \ldots, \vartheta_{n_0}\}$ are the basis functions of $\mathcal{N}_0$.

To account for the impact of the penalization function on the terms from the parametric space (Duchon, 1977), the regularization problem for estimating $\widetilde{C}$ can be expressed as,

$$\min_{\mathbf{a},\, \mathbf{d}} \|\mathbf{b} - (\boldsymbol{K} \otimes \boldsymbol{K})\, \mathbf{a} - \boldsymbol{\varphi}\, \mathbf{d}\|^2 + \lambda\, \mathbf{a}^\top (\boldsymbol{K} \otimes \boldsymbol{K})\, \mathbf{a}\,. \tag{4.44}$$

where,

$$\boldsymbol{\varphi} = (\boldsymbol{\vartheta}_1, \ldots, \boldsymbol{\vartheta}_{n_0})\,, \quad \mathbf{d} = \big(d_1, \ldots, d_{n_0}\big)^\top ,$$
$$\boldsymbol{\vartheta}_p = \big(\vartheta_p(s_1, s_1), \vartheta_p(s_1, s_2), \ldots, \vartheta_p(s_1, s_m), \vartheta_p(s_2, s_1), \ldots, \vartheta_p(s_m, s_m)\big)^\top ,$$

for $p = 1, \ldots, n_0$. The solutions for vectors $\mathbf{a}$ and $\mathbf{d}$ that minimize (4.44) are, respectively,

estimated by,

$$\widehat{\mathbf{a}} = \boldsymbol{H}^{-1}\left(\boldsymbol{I} - \boldsymbol{\varphi}(\boldsymbol{\varphi}^\top \boldsymbol{H}^{-1}\boldsymbol{\varphi})^{-1}\boldsymbol{\varphi}^\top \boldsymbol{H}^{-1}\right)\mathbf{b}\,, \tag{4.45}$$

$$\widehat{\mathbf{d}} = \left(\boldsymbol{\varphi}^\top \boldsymbol{H}^{-1}\boldsymbol{\varphi}\right)^{-1}\boldsymbol{\varphi}^\top \boldsymbol{H}^{-1}\mathbf{b}\,. \tag{4.46}$$

The vector of fitted values to the data is

$$(\boldsymbol{K}\otimes\boldsymbol{K})\,\widehat{\mathbf{a}} + \boldsymbol{\varphi}\,\widehat{\mathbf{d}} = \boldsymbol{S}\,\mathbf{b}\,, \tag{4.47}$$

where $\boldsymbol{S}$ *is the projection operator,*

$$\boldsymbol{S} = (\boldsymbol{K}\otimes\boldsymbol{K})\boldsymbol{H}^{-1}\left(\boldsymbol{I} - \boldsymbol{\varphi}(\boldsymbol{\varphi}^\top \boldsymbol{H}^{-1}\boldsymbol{\varphi})^{-1}\boldsymbol{\varphi}^\top \boldsymbol{H}^{-1}\right) + \boldsymbol{\varphi}\left(\boldsymbol{\varphi}^\top \boldsymbol{H}^{-1}\boldsymbol{\varphi}\right)^{-1}\boldsymbol{\varphi}^\top \boldsymbol{H}^{-1}\,. \tag{4.48}$$

This extension opens avenues for more comprehensive analysis, as we shall explore in the subsequent section of this chapter.

4.6 Simulation study

We conducted simulation studies to demonstrate the implementation of the methodology developed in this chapter and to illustrate its performance in finite sample settings. We considered $\mathcal{D} = [0,1]$ and designated the RKHS $\mathcal{H}$ as the second-order Sobolev-Hilbert space $\mathcal{W}_2^2$. This space is precisely defined in the supplementary materials of Section 4.8. The reproducing kernel associated with $\mathcal{W}_2^2$ is given by,

$$K(x_1,x_2) = \frac{1}{4}B_2(x_1)B_2(x_2) - \frac{1}{24}B_4(\,|x_1-x_2|\,)\,, \tag{4.49}$$

where $B_n(\cdot)$ is the n-th Bernoulli polynomial (see, e.g., Wahba (1990)). For the parametric space, we selected $\mathcal{N}_0 = \text{span}\{1, x_1, x_2, x_1x_2, x_1^2, x_2^2\}$.

Motivated by the numerical example of Mostafaiy et al. (2019), we generated the mean function μ and the stochastic processes U and ϵ as follows,

$$\mu(x) = \textstyle\sum_{k=2}^{10} 4(-1)^{k+1}k^{-2}\Psi_k(x)\,, \tag{4.50a}$$

$$U(x) = \textstyle\sum_{k=1}^{10}(-1)^{k+1}k^{-2}\zeta_k\Psi_k(x)\,, \tag{4.50b}$$

$$\epsilon(x) = \textstyle\sum_{\nu=1}^{5}\frac{1}{2}(-1)^{\nu+1}\nu^{-2}\xi_\nu\Phi_\nu(x)\,, \tag{4.50c}$$

where the basis functions $\Psi_k(\cdot)$ and $\Phi_\nu(\cdot)$ are given by

$$\Psi_k(x) = \begin{cases} 1 & \text{for } k = 1\,, \\ \sqrt{2}\,\cos(k\pi x) & \text{for } 2 \le k \le 10\,, \end{cases} \tag{4.51a}$$

$$\Phi_\nu(x) = \sqrt{2}\,\sin(\nu\pi x)\,, \qquad \text{for } \nu = 1, \ldots, 5\,. \tag{4.51b}$$

The random variables $\zeta_1, \ldots, \zeta_{10}$ and $\xi_1, \ldots, \xi_5$ are independently sampled from the uniform distribution on $[-\sqrt{3}, \sqrt{3}\,]$. It can be verified the covariance functions C_u and C_ϵ are

$$C_u(x_1, x_2) = \textstyle\sum_{k=1}^{10} \lambda_{uk} \Psi_k(x_1) \Psi_k(x_2)\,, \tag{4.52a}$$

$$C_\epsilon(x_1, x_2) = \textstyle\sum_{\nu=1}^{5} \lambda_{\epsilon\nu} \Phi_\nu(x_1) \Phi_\nu(x_2)\,, \tag{4.52b}$$

where $\lambda_{uk} = k^{-4}$ and $\lambda_{\epsilon\nu} = 4^{-1}\nu^{-4}$, for $k = 1, \ldots, 10$ and $\nu = 1, \ldots, 5$.

To generate the trajectories of the random measurement function Y_{ij}'s, we independently generated sample paths U_i's and ϵ_{ij}'s for $i = 1, \ldots, a$ and $j = 1, \ldots, r$. Subsequently, the function Y_{ij} was constructed using the functional one-way model described in (4.1). We considered a simulated scenario with a sample size of 10 and 6 replications. Figure 4.1 (a-c) illustrates the simulated mean function $\mu(\cdot)$, the sample paths of the units main effect $U_i(\cdot)$, and the measurement error $\epsilon_{ij}(\cdot)$ for $i = 1, \ldots, 10$ and $r = 1, \ldots, 6$. Plot (d) of this figure depicts the composite functions obtained by combining these three terms across all samples and replications, i.e., $Y_{ij}\,(\cdot)$. Each function is represented with a distinct color for visual clarity in these panels.

The tuning parameter λ plays an important role in the efficiency of the resulting estimates of covariance functions and, consequently, in the parameters of the measurement system assessment study. Employing a grid search, we estimated the value of the tuning parameter using the generalized cross-validation (GCV) method. The GCV function is defined as follows,

$$\text{GCV} = \frac{\|\,(\boldsymbol{I} - \boldsymbol{S})\,\mathbf{b}\|^2}{\left(1 - m^{-2}\text{tr}(\boldsymbol{S})\right)^2}\,, \tag{4.53}$$

where $\boldsymbol{S}$ represents the projection matrix characterized in (4.48).

The sampling frequency was set to $m = 4$ and 8, where each trajectory of Y_{ij} is sampled at m fixed points, spaced by a distance of $\frac{1}{m-1}$ within the interval $[0, 1]$. Applying the estimation method outlined in this chapter to the simulated dataset, we obtain smooth estimates of the covariance kernel components. Figure 4.2 presents a 3D visualization comparing the true covariance functions C_u and C_ϵ with their respective estimates at

varying sampling frequencies. Significantly, at a higher sampling frequency, the estimates more effectively capture the underlying modes of variability within C_u and C_ϵ . For a more detailed insight, Figure 4.3 illustrates the estimates of the first two basis functions for both C_u and C_ϵ, alongside the corresponding true basis functions for comparison. This visual examination highlights the method's capability to capture the main characteristics of covariance function components, even with as few as 4 samples per function.

The values of the percentage R&R ratio, the signal-to-noise ratio, and intra-class correlation coefficient values are detailed in Table 4.2, utilizing both the trace and L^2 norm of the covariance functions. Panel (a) presents the true values, while panel (b) showcases the estimated values.

Following the same criteria as employed in univariate measurement system assessment studies for approving the measurement system, where an R&R ratio greater than 30% suggests the need for improvement, it is recommended to enhance the measurement system. For the signal-to-noise ratio, Steiner and MacKay (2005) suggest improvement when the ratio falls between 2 and 3. Consequently, improving such a measurement system is recommended based on these considerations.

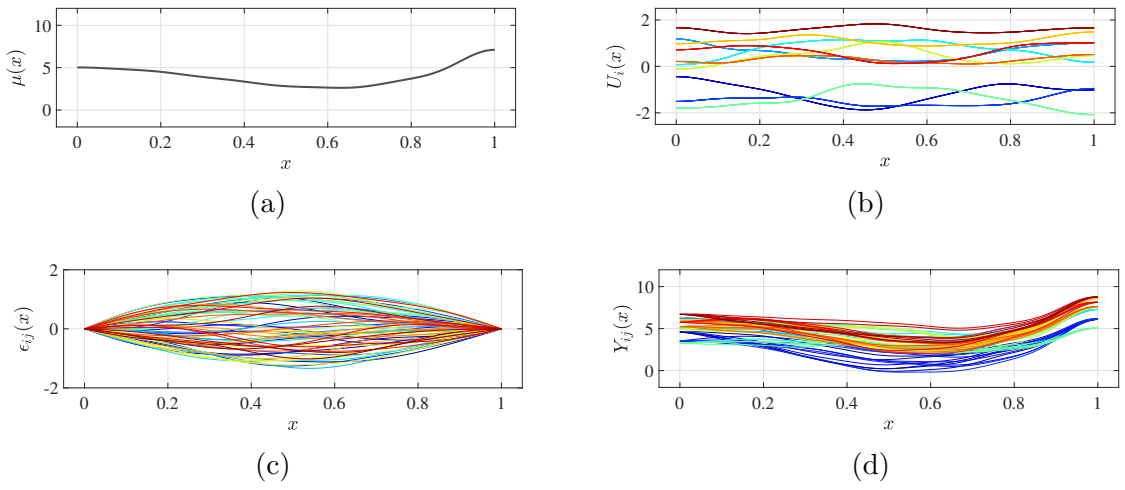

Figure 4.1: Simulated functions $\mu(x)$, $U_i(x)$, $\epsilon_{ij}(x)$, and $Y_{ij}(x)$, for $a = 10$ and $r = 6$.

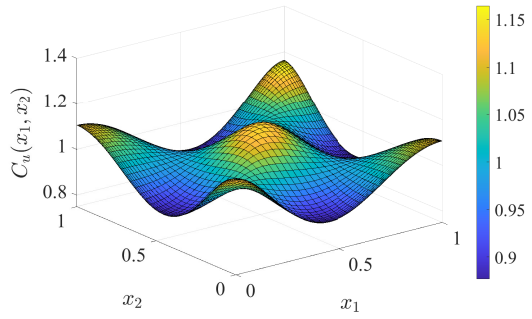

(a) True covariance function C_u.

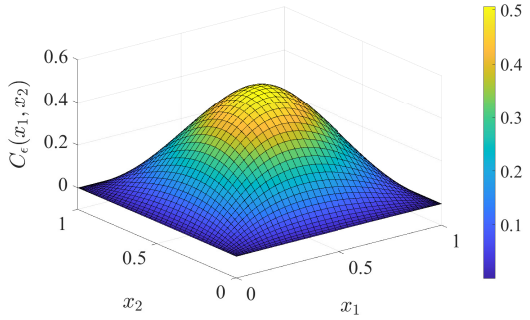

(b) True covariance function C_ϵ.

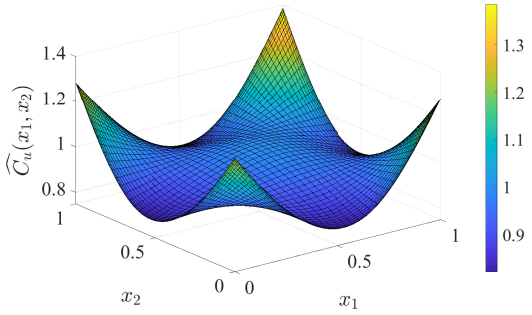

(c) $m = 4$

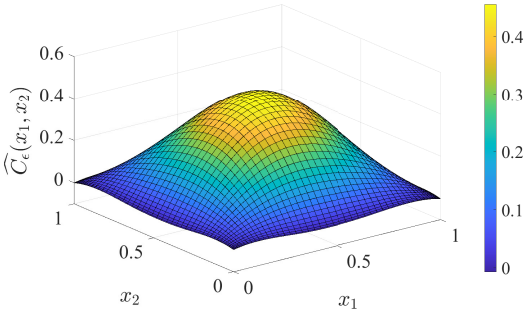

(d) $m = 4$

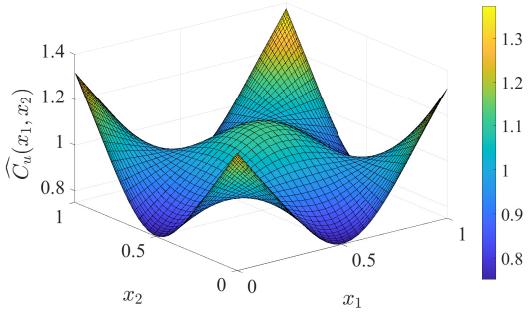

(e) $m = 8$

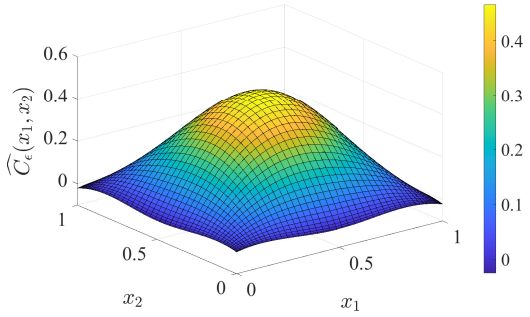

(f) $m = 8$

Figure 4.2: True covariance functions of C_u and C_ϵ (the top panels) and their smooth estimates for a sampling frequency $m = 4$ (the middle panels) and $m = 8$ (the bottom panels), in a one-way random effect model with $a = 10$ and $r = 6$.

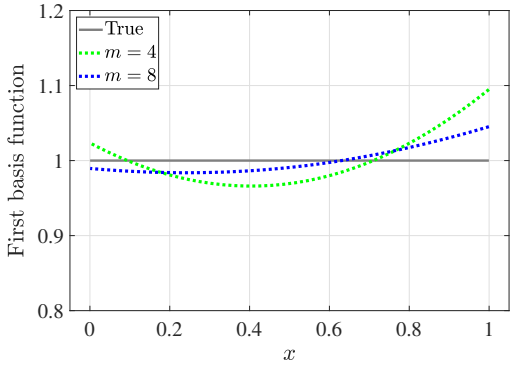

(a) Ψ_1 and its estimates.

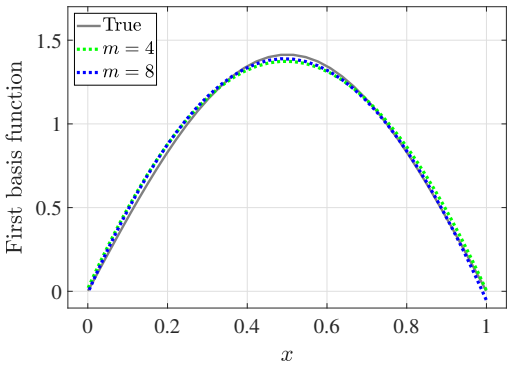

(b) Φ_1 and its estimates.

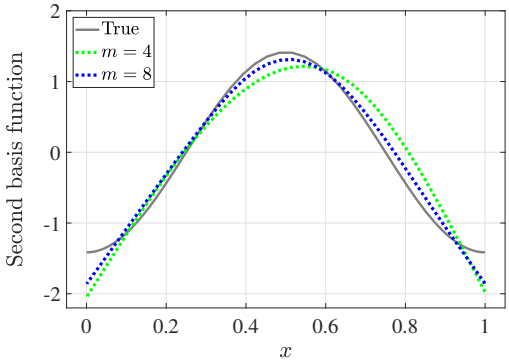

(c) Ψ_2 and its estimates.

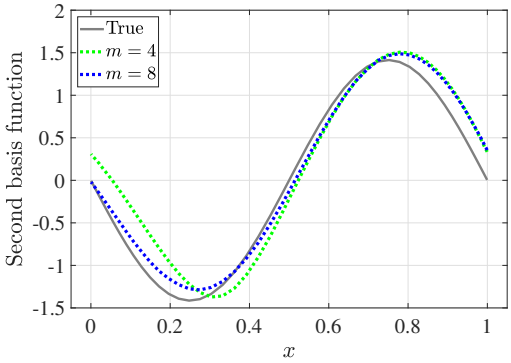

(d) Φ_2 and its estimates.

Figure 4.3: Smooth estimation of the first and second basis functions of C_u (left panels) and C_ϵ (right panels), for sampling frequencies $m = 4$ and 8. The solid lines represent the true basis functions.

Table 4.2: The values of the percentage R&R ratio, the signal-to-noise ratio, and intra-class correlation coefficient, using the trace and L^2 norm of covariance functions: (a) true values, (b) estimated values.

(a)

Trace			L_2 norm		
$\%\text{R\&R}_{\text{tr}}$	SNR_{tr}	ICC_{tr}	$\text{R\&R}_{L^2}$	SNR_{L^2}	ICC_{L^2}
% 44.69	2.00	0.80	% 45.39	2.00	0.82

(b)

	Trace			L_2 norm		
m	$\widehat{\%\text{R\&R}}_{\text{tr}}$	$\widehat{\text{SNR}}_{\text{tr}}$	$\widehat{\text{ICC}}_{\text{tr}}$	$\widehat{\%\text{R\&R}}_{L^2}$	$\widehat{\text{SNR}}_{L^2}$	$\widehat{\text{ICC}}_{L^2}$
4	% 44.69	2.00	0.80	% 45.19	2.01	0.82
8	% 43.74	2.06	0.81	% 44.67	2.04	0.83

4.7 Prospects for further research

While this chapter primarily focuses on scenarios where functional data samples are collected using regular grid points, it is important to emphasize that the regularization approach for estimating continuous covariance kernels within the RKHS framework is not restricted to cases with a regular grid. The algorithm for estimation relies on a smoothing procedure, enabling us to effectively capture underlying patterns within the functional data. This approach facilitates the learning of continuous covariance kernels based on a finite set of training samples, and it can be adapted for irregular sampling grids as well.

We consider our current work to be valuable for gaining insightful perspectives and as a practical guide for addressing the measurement system assessment of functional data, using a FANOVA model. However, we acknowledge the need to establish cutoff values for the parameters in the measurement system assessment study, a point that currently lacks clarity. This aspect is under investigation in our ongoing and future work.

Functional data can extend into more intricate domains, such as multivariate functional data or spatial random fields (Martínez-Hernández and Genton, 2020; Koner and Staicu, 2023). A prime example of this data type is found in the field of additive manufacturing, where the variable of interest pertains to the surface characteristics of manufactured parts, shape, or a combination of these. When investigating this phenomenon, scientific inquiries often revolve around the repeatability and reproducibility of the measurement system.

We believe that the tools and techniques presented in this chapter open new avenues for research and the development of methodologies to analyze the measurement systems of these complex datasets.

In this thesis, we explored the measurement system analysis of functional data in a Hilbert space. We examined the so-called vertical or amplitude variations of the functional data, which involves shifting observations up or down. It is also possible for functional data to inherit other modes of variability.

Another mode can be the warping, which leads to the phase variability of functional observations. To get a better understanding, consider a template function $\mu(x)$ defined on domain $\mathscr{D} \subset \mathbb{R}$. A model for the representation of a function when subjected to the warping effect is given by

$$y(x) = a(x)(\mu \circ h(x)) + \varepsilon(x), \tag{4.54}$$

where $x \in \mathscr{D}$. In this model, $y(x)$ represents the measured value of the template function at location x, $h(x)$ is the warping effect, which satisfies some properties, $a(\cdot) \in \mathbb{R}^+$ and $\varepsilon(\cdot)$ are the scaling and vertical translations, respectively. The composition $\mu \circ h(\cdot)$ characterizes $\mu(h(\cdot))$ and represents the warping of $\mu(\cdot)$ by $h(\cdot)$. The effect of this warping function is relocating the values of $\mu(\cdot)$ horizontally. The warping function, therefore, does not change the amplitude values directly. That being said, warping only affects the phase, i.e., the value of location, (or time).

While classical tools for functional data analysis in the Hilbert space $\mathscr{L}^2(\mathscr{D})$ work well when functional data observations are perfectly aligned, they have limitations, such as the lack of isometry, as for two functions $f_1(x), f_2(x) \in \mathscr{L}^2(\mathscr{D})$, in general

$$\|f_1 - f_2\|_{L^2} \neq \|f_1 \circ h - f_2 \circ h\|_{L^2}.$$

The lack of isometry results that Hilbert space tools are inadequate in capturing the warping effect accurately and do not provide a suitable distance metric.

The framework of elastic functional data (Srivastava et al., 2010), offers the tools to represent and analyze this mode of variation, when present in functional data. In this framework, the Riemannian geometry and Fisher-Rao metric are to achieve a proper distance metric (Srivastava et al., 2011). The strength of using this framework is paramount in predicting the underlying template function under random warping, scaling, and vertical translation.

4.8 Supplementary materials

In this section, we have included the supplementary materials that accompany Chapter 4.

A. Reproducing kernel Hilbert spaces

Let $\mathcal{H}$ be a real Hilbert space of functions defined on the interval $\mathcal{D}$, equipped with an inner product $\langle \cdot, \cdot \rangle_{\mathcal{H}}$. The space $\mathcal{H}$ is termed an RKHS if there exists a symmetric positive-definite function $K(\cdot, \cdot)$ on $\mathcal{D} \times \mathcal{D}$, known as the reproducing kernel of $\mathcal{H}$, satisfying the following properties for every $x \in \mathcal{D}$ and $f \in \mathcal{H}$,

i) $K(x, \cdot) \in \mathcal{H}$,
ii) $f(x) = \langle f(\cdot), K(x, \cdot) \rangle_{\mathcal{H}}$.

The second property, referred to as the reproducing property, states that the evaluation of a function at a point can be represented as an inner product with the corresponding reproducing kernel. It is important to note that the reproducing kernel is a positive semi-definite function. We denote the Hilbert space associated with the reproducing kernel function K as $\mathcal{H}(K)$. The Moore-Aronszajn theorem (1950) establishes a one-to-one correspondence between an RKHS of functions and the reproducing kernel, such that each RKHS is uniquely associated with a specific kernel K.

A concrete example of an RKHS is the Sobolev-Hilbert space $\mathcal{W}_2^n$ with $n \in \mathbb{N}$. This space consists of all functions $f \in \mathscr{L}^2([0, 1])$ that satisfy the following conditions

i) $f, f^{(1)}, \ldots, f^{(n-1)}$ are absolutely continuous,
ii) $f^{(n)} \in \mathscr{L}^2([\,0, 1])$.

When $\mathcal{W}_2^n$ is endowed with the squared norm given by

$$\|f\|_{\mathcal{W}_2^n}^2 = \sum_{k=0}^{n-1} \left(\int_0^1 f^{(k)}(x) \mathrm{d}x \right)^2 + \int_0^1 \left(f^{(n)}(x) \right)^2 \mathrm{d}x, \tag{4.55}$$

the space $\mathcal{W}_2^n$ becomes an RKHS with a reproducing kernel expressed as

$$K_n(x_1, x_2) = \frac{1}{(n!)^2} B_n(x_1) B_n(x_2) - \frac{(-1)^n}{(2n)!} B_{2n}\left(|x_1 - x_2| \right). \tag{4.56}$$

Consider the reproducing kernel K in the context of Mercer's theorem. Assuming that

the reproducing kernel K is squared integrable, it can be expressed as

$$K(x_1, x_2) = \sum_{k \geq 1} \rho_k \varphi_k(x_1) \varphi_k(x_2) \,, \tag{4.57}$$

where $\rho_1, \rho_2, \ldots$ are non-negative constants, and $\varphi_1(\cdot), \varphi_2(\cdot), \ldots$ represent a sequence of orthonormal basis functions of $\mathscr{L}^2(\mathscr{D})$. According to (Wahba, 1990, Lemma 1.1.1), a function $f \in \mathscr{L}^2(\mathscr{D})$ belongs to RKHS of $\mathcal{H}(K)$ if and only if the following condition is met,

$$\|f\|^2_{\mathcal{H}(K)} = \sum_{k \geq 1} \frac{f_k^2}{\rho_k} < \infty \,, \tag{4.58}$$

where $f_k = \langle f, \varphi_k \rangle_{\mathscr{L}^2(\mathscr{D})}$. This condition validates the eligibility of a function for inclusion in the RKHS of $\mathcal{H}(K)$, where the reproducing kernel K is defined as per (4.57).

The tensor product Hilbert space is defined as follows: Let $\mathcal{H}_1$ and $\mathcal{H}_2$ be two Hilbert spaces defined on $\mathscr{D}$, equipped with the corresponding inner product operations $\langle \cdot, \cdot \rangle_{\mathcal{H}_1}$ and $\langle \cdot, \cdot \rangle_{\mathcal{H}_2}$. For functions $f \in \mathcal{H}_1$ and $g \in \mathcal{H}_2$, the tensor product of f and g is defined as $f \otimes g(x_1, x_2) = f(x_1) g(x_2)$, where $x_1, x_2 \in \mathscr{D}$. Let V denote the vector space generated by all such tensors. By defining the following inner product for vector space V,

$$\langle f_1 \otimes g_1, f_2 \otimes g_2 \rangle = \langle f_1, f_2 \rangle_{\mathcal{H}_1} \langle g_1, g_2 \rangle_{\mathcal{H}_2} \,, \tag{4.59}$$

where $f_1, f_2 \in \mathcal{H}_1$ and $g_1, g_2 \in \mathcal{H}_2$, the vector space V is complete, thereby making V a Hilbert space. This Hilbert space is referred to as the tensor product Hilbert space of $\mathcal{H}_1$ and $\mathcal{H}_2$, denoted by $\mathcal{H}_1 \otimes \mathcal{H}_2$, and the associated inner product is denoted as $\langle \cdot, \cdot \rangle_{\mathcal{H}_1 \otimes \mathcal{H}_2}$.

For an RKHS $\mathcal{H}(K)$, it can be shown that the tensor product Hilbert space $\mathcal{H}(K) \otimes \mathcal{H}(K)$ is itself an RKHS. Let us consider two functions f and g that are elements of an RKHS $\mathcal{H}(K)$ defined on $\mathscr{D}$. For every $x_1, x_2 \in \mathscr{D}$, the following relationship holds,

$$\begin{aligned} f \otimes g(x_1, x_2) &= \langle f(\cdot), (x_1, \cdot) \rangle_{\mathcal{H}(K)} \, \langle g(\cdot), K(x_2, \cdot) \rangle_{\mathcal{H}(K)} \\ &= \langle f \otimes g, K(x, \cdot) \otimes K(y, \cdot) \rangle_{\mathcal{H}(K) \otimes \mathcal{H}(K)} \,. \end{aligned} \tag{4.60}$$

This equation implies that the reproducing property remains intact for an RKHS with the reproducing kernel $K \otimes K$, which is given by,

$$K \otimes K((x_1, x_2), (y_1, y_2)) = K(x_1, y_1) K(x_2, y_2) \,. \tag{4.61}$$

We can demonstrate the condition under which a bivariate function f on $\mathscr{D} \times \mathscr{D}$ can be included in the tensor product space $\mathcal{H}(K) \otimes \mathcal{H}(K)$, where K is the reproducing kernel expressed as per (4.57). According to Cai and Yuan (2010), a bivariate function $f \in \mathscr{L}^2(\mathscr{D} \times \mathscr{D})$ belongs to the tensor product Hilbert space $\mathcal{H}(K) \otimes \mathcal{H}(K)$, if and only if the following condition is met,

$$\|f\|^2_{\mathcal{H}(K \otimes K)} = \sum_{k \geq 1} \sum_{\ell \geq 1} \frac{f^2_{k\ell}}{\rho_k \rho_\ell} < \infty \,, \tag{4.62}$$

where $f_{k\ell}$ is defined as,

$$f_{k\ell} = \iint_{\mathscr{D} \times \mathscr{D}} f(x_1, x_2) \varphi_k(x_1) \varphi_\ell(x_2) \mathrm{d}x_1 \mathrm{d}x_2 \,. \tag{4.63}$$

This condition verifies the eligibility of a bivariate function for inclusion in the RKHS $\mathcal{H}(K \otimes K)$.

B. The Representer theorem

The following Representer theorem is due to Kimeldorf and Wahba (1971), and the generalized result is due to Schölkopf et al. (2001).

Theorem 4.1. ***(Nonparametric Representer theorem).*** *Consider a nonempty set $\mathfrak{X}$, a positive-definite real-valued kernel K on $\mathfrak{X} \times \mathfrak{X}$, with the corresponding RKHS of $\mathcal{H}(K)$. Let $(x_1, y_1), \ldots, (x_n, y_n) \in \mathfrak{X} \times \mathbb{R}$ be the training sample, $g(\cdot)$ is a strictly increasing real-valued function on $\mathbb{R}^+$, an arbitrary error function $E : (\mathfrak{X} \times \mathbb{R}^2)^n \to \mathbb{R} \cup \{\infty\}$, which collectively define the following regularized risk function,*

$$E\left\{(x_1, y_1, f(x_1)), \ldots, (x_n, y_n, f(x_n))\right\} + g(\|f\|) \,.$$

Any function $f \in \mathcal{H}(K)$ minimizing the above risk function, admits a representation of the form,

$$f(\cdot) = \sum_{i=1}^{n} a_i K(\cdot, x_i) \,,$$

where $a_i \in \mathbb{R}$.

It is possible to generalize the above result further, by enriching the RKHS through the addition of offset terms, which are not subject to penalization.

Theorem 4.2. ***(Parametric Representer theorem).*** *In addition to the assumptions of the previous theorem, suppose we are given a subspace $\mathcal{N}_0$ that is the span of $\{\vartheta_1, \ldots, \vartheta_{n_\circ}\}$, where $\vartheta_1, \ldots, \vartheta_{n_\circ}$ are real-valued basis functions on $\mathfrak{X}$. We consider functions of the form $\tilde{f} = f + h$, with $f \in \mathcal{H}(K)$ and $h \in \mathcal{N}_0$. Any function $\tilde{f}$ minimizing the regularized risk,*

$$E\left((x_1, y_1, \tilde{f}(x_1), \ldots, (x_n, y_n, \tilde{f}(x_n))\right) + g(\|f\|)\,.$$

admits a representation of the form

$$\tilde{f}(\cdot) = \sum_{i=1}^{n} a_i K(\cdot, x_i) + \sum_{p=1}^{n_0} d_p \vartheta_p(\cdot)\,,$$

where $a_i, d_p \in \mathbb{R}$.

Chapter 5

Case Study Application

In this chapter, we apply the three methodologies discussed throughout this thesis to analyze a real-world dataset of surface texture indicators from an additive manufacturing process.

The case study involves a functional dataset acquired from the *Multi-Scale Additive Manufacturing Lab*. This dataset comprises measurements of two indicators reflecting the surface roughness of printed products. While the specific focus may not align perfectly with the measurement system assessment outlined in this thesis, we chose this dataset because of its relevance. It serves as a valuable demonstration to showcase the versatility of the methodologies presented in this thesis, although the case study itself does not address a measurement system assessment problem. This chapter presents a comprehensive analysis of this additive manufacturing dataset, covering statistical methods for analyzing univariate and multivariate data types, along with functional data analysis techniques.

5.1 Experiment setup and data acquisition

An experiment was conducted over five days, with each day corresponding to an individual manufacturing cycle. During each cycle, three items were printed, all derived from the same computer-aided design and utilizing the same setup on the manufacturing platform. Consequently, a total of 15 items were printed throughout the experiment. A confocal laser scanning microscope was employed for precise data acquisition, facilitating high-resolution profilometry data collection. The key surface texture characteristics used to measure roughness are the *arithmetic mean height* and *maximum height*, denoted as S_a

and S_z, respectively. In a given area A, they are defined as follows

$$S_a = \frac{1}{A} \int |z(x, y)| \, \mathrm{d}x \, \mathrm{d}y \,, \tag{5.1}$$

$$S_z = \max_A z(x, y) + \min_A |z(x, y)| \,, \tag{5.2}$$

where $z(x, y)$ represents the height at the location (x, y). To learn more about the scanner and its surface roughness measurement methods, interested readers can visit https://www.keyence.com/support/user/laser-microscope-documents/.

The surface data profile includes measurements of arithmetic mean heights and maximum heights, collected from 14 consistently identical locations across all manufactured items. Figure 5.1 provides a visual illustration of this dataset. In Figure 5.1(a), the observed values of S_a for all five cycles and printed parts are shown with respect to their respective locations, with observations connected together. Printed parts within the same day are represented using the same color. Similarly, Figure 5.1(b) displays the observed values of S_z for all 15 parts. A full listing of the dataset is provided in the supplementary materials of Section 5.4. Our goal is to assess and compare day-to-day and item-to-item variations contributing to surface roughness variability.

5.2 Surface texture model

This is an analysis of variance problem involving 5 days (5 cycles) and 3 printed items each day. The variables are the roughness measurements S_a and S_z, which can be potentially observed over continuous domains. Therefore, we can treat them as functional observations. We require a FANOVA that includes a smoothing technique and considers the sparsity, such as those discussed in Chapter 4. The underlying model for the texture roughness indicator at location x is given by,

$$Y_{ij}(x) = \mu(x) + D_i(x) + \epsilon_{ij}(x), \quad \text{for } i = 1, \ldots, 5, \text{ and } j = 1, \ldots, 3, \tag{5.3}$$

where $x \in \mathcal{D}$, and $\mathcal{D}$ is a continuous domain initially spanning $[0, 14]$. In this model, $Y_{ij}(x)$ represents the measured value of the roughness for the jth printed item in the ith cycle at location x, $\mu(\cdot)$ denotes the overall mean function which represents the average roughness. The term D_i represents the random effect function specific to day (or cycle) i, and $\epsilon_{ij}(\cdot)$ is the random function specific to the jth printed item during cycle i.

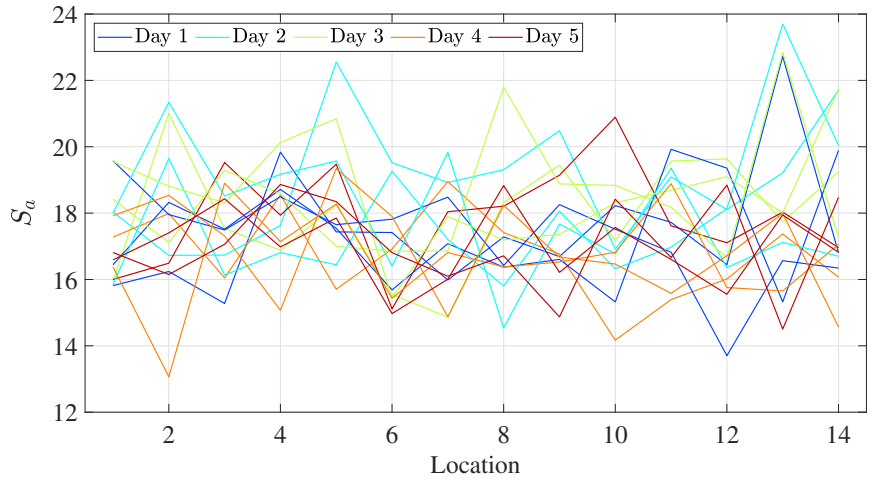

(a)

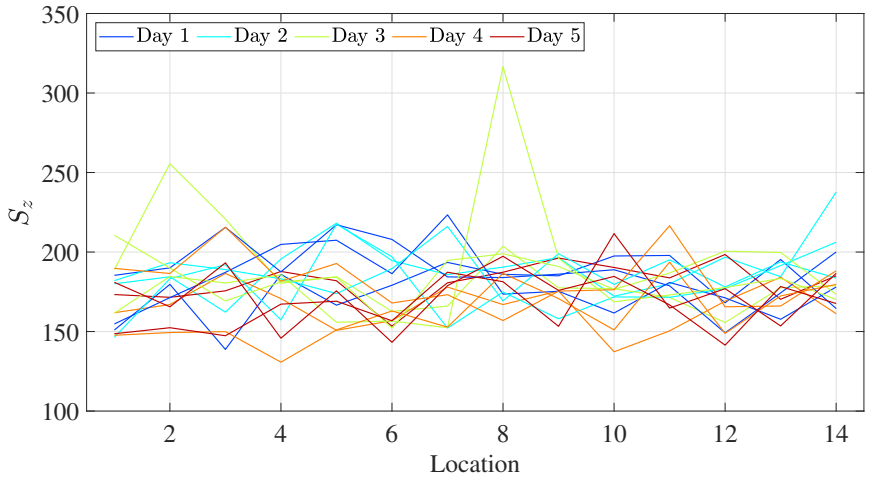

(b)

Figure 5.1: Illustration of additive manufacturing dataset values for roughness indicators: the arithmetic mean height (top panel) and maximum height (bottom panel).

Throughout this thesis, we have consistently denoted ϵ_{ij} as the measurement error in the context of measurement system assessment. In the context of this specific case study, ϵ_{ij} refers to the *item's error*. Despite this specific designation, we continue to use the term *measurement error* to represent the item's error in our discussions.

5.2.1 Point-wise analysis

We initially applied a one-way ANOVA model, detailed in Chapter 2, to the roughness measurements at all 14 locations. In this analysis, the roughness measurement at each location was treated as an individual random variable, resulting in 14 distinct analyses. We tested the significance of the variance associated with the day's effect by calculating the p-value for each of the 14 variables, as described in (2.46). In 12 locations for S_a and 9 locations for S_z, the p-value exceeds 0.1, suggesting that the observed data provide no evidence against the presence of variation due to the day's effect at these locations.

We calculated the variances associated with the day and residual effects for the roughness indicators S_a and S_z using both UMVUE and maximum likelihood estimation methods. The results are summarized in Table 5.1. We note that the UMVUE for the variance of the day's effect may not always be non-negative, suggesting that the UMVUE can be unsuitable as an estimator for these data.

The maximum likelihood estimates for the ratio of two standard deviations, denoted as $\widehat{\text{SNR}}$, corresponding to the day's effect and measurement error are obtained across all 14 variables. The results are illustrated in Figure 5.2. The red dashed line in the figure represents the cut-off point for the signal-to-noise ratio, as recommended by Steiner and MacKay (2005).

For both the arithmetic mean height and maximum height indicators, $\widehat{\text{SNR}}$ exhibits spikes at specific locations, such as locations 6 and 10, suggesting higher variation in the day's effect at these locations. In the case of arithmetic mean height data (S_a), the estimated signal-to-noise ratio consistently remains below 2 across all locations. This suggests that measurement error is the dominant cause of variation based on these data. However, for the maximum height data (S_z), the estimated signal-to-noise ratio reaches the cut-off point at one location, indicating that the measurement error is not the dominant cause of variation at that particular location.

5.2.2 Multivariate analysis

For an overall assessment of day-to-day variation, rather than assessing each location separately, we conducted a one-way MANOVA analysis. Each vector of observations comprised 14 variables, corresponding to the roughness indicator at one of the 14 locations. Due to the limitations of the dataset with fewer samples than variables, the sample covariance matrices related to the day's effect and measurement error do not have full ranks, leading to rank-deficient sample covariance matrix estimates.

Table 5.1: UMVUE and Maximum likelihood estimates of the variance components for the day's effect and the measurement error, obtained using a marginal one-way ANOVA model across 14 locations: (a) arithmetic mean height data, (b) maximum height data.

(a) Arithmetic mean height

	UMVUE		Maximum likelihood	
Location	Day	Measurement error	Day	Measurement error
1	-0.3674	1.9618	0	1.5371
2	0.2674	3.9932	0	3.9409
3	0.0259	1.5068	0	1.4271
4	0.0518	1.7086	0	1.6362
5	-0.5351	3.4780	0	2.8181
6	0.6656	1.4951	0.4328	1.4951
7	-0.0238	2.2369	0	2.0687
8	0.1327	2.8369	0	2.7539
9	0.3946	1.8278	0.1939	1.8278
10	0.9749	1.6297	0.6713	1.6297
11	0.3285	1.7853	0.1437	1.7853
12	-0.1507	2.9007	0	2.5868
13	-0.6457	8.1503	0	7.0903
14	1.0928	3.5259	0.6392	3.5259

(b) Maximum height

	UMVUE		Maximum likelihood	
Location	Day	Measurement error	Day	Measurement error
1	-53.4332	420.5338	0	349.7516
2	202.3546	423.6456	133.6407	423.6456
3	-232.1755	825.4680	0	584.6964
4	47.9851	331.5120	16.2873	331.5120
5	113.1867	452.0489	60.4128	452.0489
6	372.0950	69.3914	293.0499	69.3914
7	24.9529	420.6623	0	412.5804
8	441.0145	977.7357	287.6292	977.7357
9	-37.5239	224.4918	0	179.5066
10	153.6675	196.8401	109.8113	196.8401
11	-64.0189	311.9683	0	239.9553
12	-19.6021	342.8833	0	304.3428
13	37.1673	150.7627	19.6830	150.7627
14	112.3476	276.0883	71.4722	276.0883

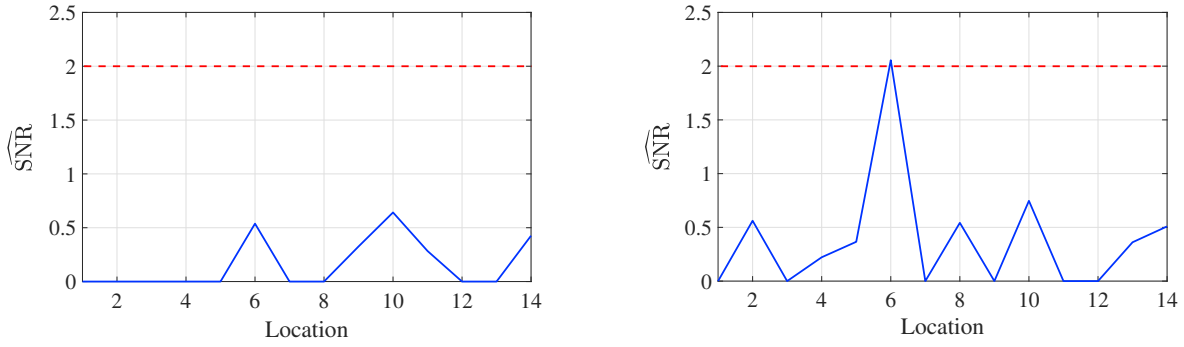

(a) Arithmetic mean height (S_a)

(b) Maximum height (S_z)

Figure 5.2: The maximum likelihood estimates of the ratio of standard deviation for the day's effect and measurement error, referred to as $\widehat{\text{SNR}}$, using a marginal one-way ANOVA model at each of the 14 locations.

For both the arithmetic mean height and maximum height data, we computed two matrices of the sum of squares and products associated with the day's effect and the measurement error. Subsequently, we obtained the UMVUEs of the variance-covariance components. Table 5.2 presents the eigenvalues of these estimates. It is observed that the variance-covariance matrices of the measurement error are singular, and the variance-covariance matrices of the day's effect are indefinite, with only 4 non-negative eigenvalues out of 14.

To address this challenge, we conducted PCA on the original dataset, reducing the dimensionality from 14 variables to 10—matching the degree of freedom of the measurement error. Through this dimension reduction process, we effectively captured 97.5% and 97.8% of the total variation in the dataset corresponding to measurements of S_a and S_z, respectively. After reducing the dimension, we applied a multivariate one-way model and obtained the UMVUE and maximum likelihood estimates of the variance-covariance matrix components for the day's effect and measurement error. The eigenvalues of the estimated variance-covariance matrices are displayed in Table 5.3.

The result of this analysis for each dataset, the arithmetic mean height and maximum height data, is discussed below.

A. Arithmetic mean height data

Concerning the UMVUE for the day's variance-covariance matrix component six eigenvalues are found to be negative out of 10, with some negative quantities exhibiting

Table 5.2: The eigenvalues of the UMVUE estimates of the variance-covariance matrices, using a one-way MANOVA model.

	Arithmetic mean height		Maximum height	
Order	Day	Measurement error	Day	Measurement error
1	8.5053	12.5015	1166.0049	1866.7667
2	3.8365	7.0449	833.2087	1074.6261
3	0.7216	6.5062	339.4760	731.2912
4	0.4530	3.7126	155.6996	581.5624
5	-0.0004	3.3179	-4.6565	438.4744
6	-0.1488	2.0663	-15.2332	272.6237
7	-0.1852	1.6081	-29.3418	194.3011
8	-0.3131	0.9808	-43.2594	137.0455
9	-0.5699	0.7725	-53.9790	90.1361
10	-0.8953	0.5262	-97.6290	37.2049
11	-0.9637	0.0001	-142.6632	0
12	-1.9413	0	-158.1404	0
13	-2.2050	0	-327.3454	0
14	-4.0825	0	-524.1338	0

significant magnitude. As a result, the UMVUE for the day's variance-covariance matrix component is not non-negative definite, after dimension reduction. The maximum likelihood estimate of the variance-covariance matrix component associated with the day's effect has several zero eigenvalues. The first three eigenvalues explain almost 100% of the total variation. This can imply that the variance-covariance matrix of the day's effect is rank deficient.

B. Maximum height data

Similar to the arithmetic mean height case, the UMVUE for the day's variance-covariance matrix component is not non-negative definite here, after dimension reduction, either. In addition, the maximum likelihood estimate of the variance-covariance matrix component associated with the day's effect has several zero eigenvalues, with the first five eigenvalues explaining almost 100% of the total variation.

To assess and compare the day-to-day variability with the measurement error variability, we employ the statistics suggested in Chapter 3. These statistics condense each variance-covariance matrix component into a scalar value. We applied the trace and norm of the

Table 5.3: The eigenvalues of the estimates of the variance-covariance matrix components associated with the day's effect and measurement error, after dimensional reduction.

(a) Arithmetic mean height

	UMVUE		Maximum likelihood	
Order	Day	Measurement error	Day	Measurement error
1	8.4646	12.5008	6.8523	8.3668
2	3.8061	7.0431	3.2678	4.7739
3	0.4625	6.5015	0.3769	4.3809
4	0.0436	3.6885	0.0002	2.9365
5	-0.5335	3.3124	0.0001	2.2217
6	-0.8133	2.0553	0.0001	1.5186
7	-0.9583	1.4364	0	1.2651
8	-1.9392	0.7727	0	0.6406
9	-2.2016	0.5617	0	0.5399
10	-4.0807	0.1035	0	0.1027

(b) Maximum height

	UMVUE		Maximum likelihood	
Order	Day	Measurement error	Day	Measurement error
1	1148.6090	1866.6819	946.8587	1248.9215
2	827. 2275	1072.6129	751.9810	737.8783
3	329.0220	724.1777	275.5912	515.0882
4	96.5489	561.4179	60.9543	492.1334
5	-43.9434	437.2086	0.0227	293.6625
6	-95.4883	262.8319	0.0071	195.4339
7	-141.8639	153.6648	0.0021	143.4157
8	-157.4841	136.1239	0	92.2636
9	-327.0383	55.1857	0	53.4915
10	-524.0330	2.4042	0	2.4018

matrices. Table 5.4 presents the estimated signal-to-noise ratio values. Based on the decision rule for univariate data, for both the arithmetic mean height and maximum height data, the signal-to-noise ratio values are smaller than 2, indicating that the measurement error is the primary contributor to the observed variation.

Table 5.4: The signal-to-noise ratio estimates using the trace and the Frobenius norm of variance-covariance matrix components for arithmetic mean height and maximum height data.

	$\widehat{\text{SNR}}_{\text{tr}}$	$\widehat{\text{SNR}}_{F}$
Arithmetic mean height (S_a)	0.63	0.82
Maximum height (S_z)	0.73	0.86

5.2.3 Functional data analysis

We now apply specialized tools for the analysis of functional data by implementing the regularization method using an RKHS, as discussed in Chapter 4.

Assuming that the sample paths of the day's effect and the measurement error belong to a certain RKHS. In this case, their corresponding covariance functions belong to a tensor product space. We opted for the second-order Sobolev-Hilbert space $\mathcal{W}_2^2$ as the chosen RKHS. For the parametric space, we used $\mathcal{N}_0 = \text{span}\{1, x_1, x_2, x_1x_2, x_1^2, x_2^2\}$. The tuning parameter λ in the regularization problem was determined via a grid search and GCV method, using the GCV function defined in (4.53).

In Table 5.5, we present the 12 largest eigenvalues (in magnitude) associated with the estimates of covariance kernel components for both the day's effect and measurement error. Negative eigenvalues are observed in both the day's effect and measurement error covariance kernels, a phenomenon often attributed to the limitations of small sampling settings. To mitigate the issue of indefiniteness, one potential solution involves projecting the estimates onto the space of positive-definite functions by setting negative eigenvalues equal to zero.

The estimated values of SNR_{tr} and SNR_{L^2} are calculated based on the positive eigenvalues associated with the covariance function estimates of the day's effect and the measurement errors. The results are illustrated in Table 5.6. Following the decision rule for univariate data, both the arithmetic mean height and maximum height data show signal-to-noise ratio values smaller than 2, signifying that the predominant source of the observed variation can be attributed to measurement error.

Table 5.5: The eigenvalues associated with the estimated covariance functions for the day's effect and measurement errors, implementing the regularization approach over the RKHS framework.

	Arithmetic mean height		Maximum height	
Order	Day	Measurement error	Day	Measurement error
1	6.4951	7.0968	876.2953	2157.6042
2	1.3634	5.5049	530.3977	1264.3188
3	0.3105	2.5374	351.9961	914.4360
4	0.1396	1.0253	120.4036	240.6127
5	0.0092	0.0200	4.5002	3.8747
6	0.0000	0.0004	0.1448	0.0370
7	-0.0001	0.0001	0.0022	0.0182
8	-0.0004	0.0000	-0.0062	-0.1825
9	-0.1321	-1.1835	-37.2697	-66.5875
10	-0.2603	-0.8448	-130.3025	-245.3950
11	-1.3892	-1.4899	-389.4536	-696.2877
12	-2.9417	-3.0322	-500.7067	-2016.9273

Table 5.6: The signal-to-noise ratio estimates using the trace and the L^2 norm of covariance functions for arithmetic mean height and maximum height data.

	$\widehat{\text{SNR}}_{\text{tr}}$	$\widehat{\text{SNR}}_{L^2}$
Arithmetic mean height (S_a)	0.72	0.84
Maximum height (S_z)	0.64	0.64

The smooth estimates of the first leading basis functions for both the day's effect and measurement error covariance functions are depicted in Figure 5.3. looking at the curves it can be observed, for both roughness indicators, that the first basis function associated with the day's effect exhibits a smoother pattern with fewer ripples. For a comprehensive view, Figure 5.4 provides the 3D plots of the covariance function estimates for the day's effect and measurement error.

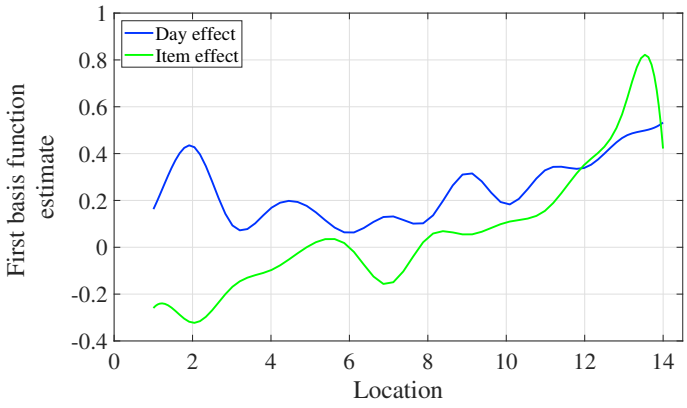

(a)

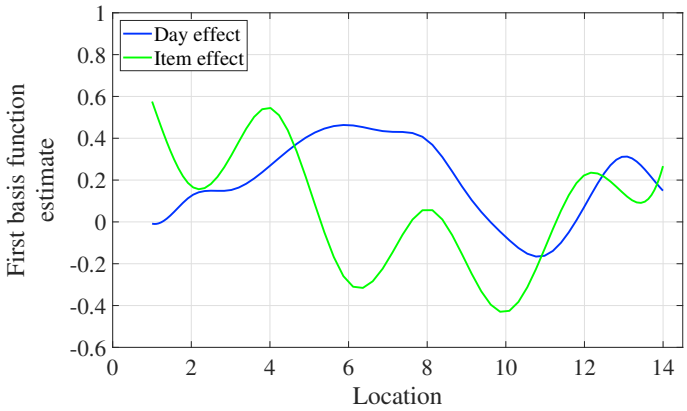

(b)

Figure 5.3: Smooth estimation of the first basis function of day effect and item effect for the arithmetic mean height (top panel) and maximum height (bottom panel) roughness indicators

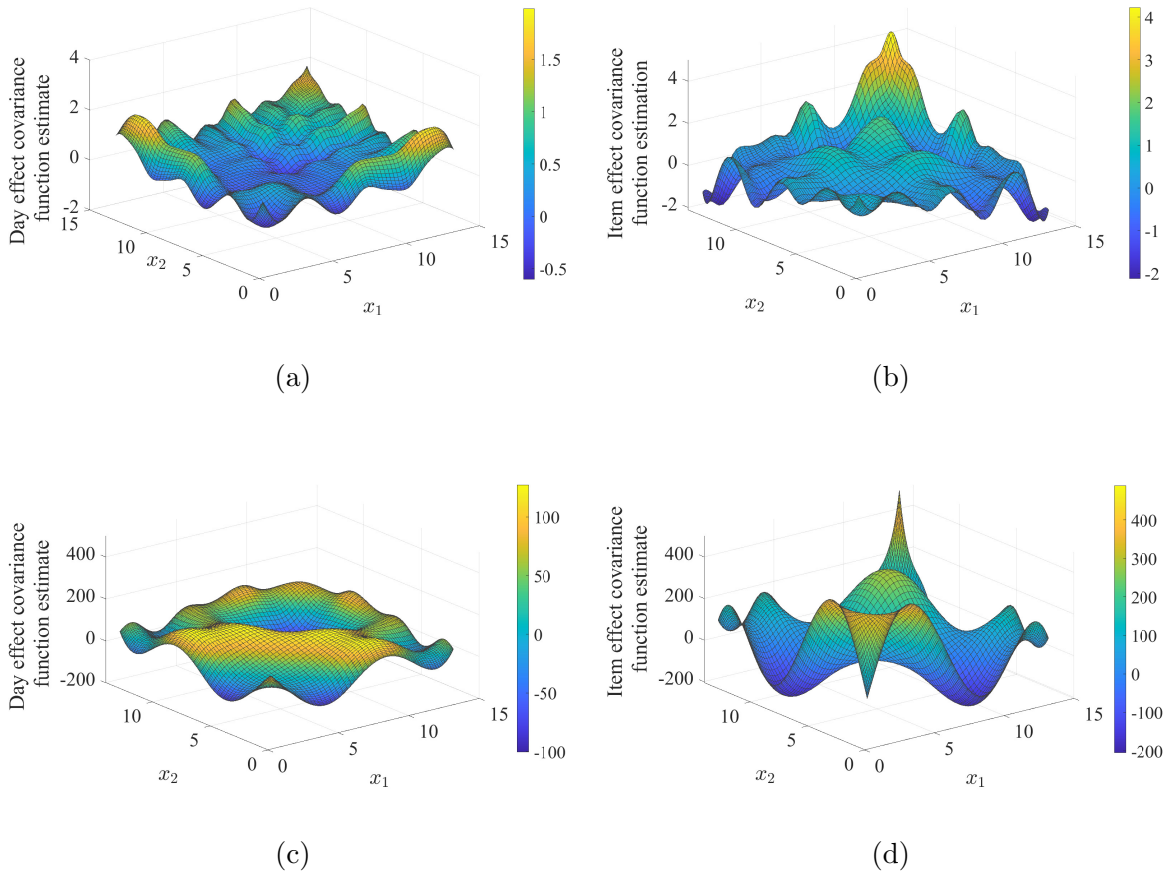

Figure 5.4: Estimates of covariance functions corresponding to the day and item effects for the arithmetic mean height (top panels) and maximum height (bottom panels), using the RKHS smoothing method.

5.3 Comparison of methodologies

In this section, we compare three methodologies employed in this chapter for analyzing the additive manufacturing dataset.

We applied three methodologies to discern the primary source of variation in the measurements of two roughness indicators. The point-wise analysis allowed for an independent examination of variation in the day's effect at each of the 14 locations. While the analysis of arithmetic mean height consistently identified measurement error as the dominant cause of variation across all locations, the examination of maximum height data revealed that at one location, the variation attributable to the day's effect predominated. Consequently, for these data, it may be necessary to employ methodologies that consider overall day-to-day variation.

Both multivariate and functional data analysis approaches enable an overall assessment of the day-to-day effect relative to measurement error. Functional data analysis tools are particularly advantageous when there is prior knowledge of the data's nature, such as the order of collected samples and underlying smoothness. In such cases, functional data analysis offers superior capabilities. However, in the absence of such information, multivariate data analysis tools can be effectively utilized.

5.4 Supplementary material

The dataset used in the case study presented in this chapter is provided in Table 5.7.

Table 5.7: The additive manufacturing case study dataset, including two surface roughness indicators: arithmetic mean height and maximum height, measured in micrometers.

day	location	item 1		item 2		item 3	
		S_a	S_z	S_a	S_z	S_a	S_z
1	1	15.8142	150.9376	16.4418	154.7735	19.5767	185.3556
	2	16.2396	179.6778	18.3226	171.3407	17.9559	190.0342
	3	15.2769	138.7714	17.5159	187.2241	17.4911	215.5314
	4	19.8382	185.9456	18.7139	204.7901	18.4931	187.5317
	5	17.4341	166.5843	17.5417	207.4305	17.6516	217.1608
	6	17.4144	179.1234	15.6851	186.4145	17.8163	207.9204
	7	15.9842	193.4986	17.0782	223.3932	18.4813	184.3721
	8	17.2842	185.9857	16.3717	173.5216	16.4214	183.9491
	9	16.6899	185.0446	16.6050	175.3170	18.2561	186.0849
	10	18.2265	197.5126	15.3234	161.6667	17.5149	188.8636
	11	17.7221	197.8555	19.9222	180.8608	16.8216	178.7585
	12	16.4460	168.0996	19.3555	171.1917	13.7021	149.2174
	13	22.7213	195.3031	15.3238	157.7218	16.5667	174.2890
	14	16.8037	164.4793	19.8869	178.0095	16.3429	200.0500
2	1	18.0337	180.0380	15.8445	146.3601	18.0053	182.0201
	2	16.7270	184.4368	19.6428	183.2617	21.3372	193.2535
	3	16.7348	162.1750	16.1348	191.9976	18.5131	188.9810
	4	17.6263	195.6394	16.8098	157.3294	19.1699	183.1615
	5	22.5559	218.1262	16.4419	217.4865	19.5687	173.8972
	6	19.5192	194.6053	19.2660	197.0146	16.4055	189.5859
	7	18.9229	185.8017	17.2087	152.1666	19.8267	216.0673
	8	19.3084	190.5167	15.8058	174.9040	14.5392	169.2935
	9	20.4839	196.4947	18.0583	158.0377	17.6707	198.9530
	10	16.9187	172.2214	16.3263	171.7709	16.7718	179.6701
	11	19.0916	180.0296	16.9740	171.5532	19.3530	195.1110
	12	18.1106	196.7730	18.1330	176.9972	16.3610	178.0702
	13	19.2155	184.4769	23.6988	191.4654	17.1176	193.7935
	14	21.7119	237.7091	20.0360	206.1837	16.6999	183.6231

day	location	item 1		item 2		item 3	
		S_a	S_z	S_a	S_z	S_a	S_z
3	1	15.9528	189.0304	19.5538	210.5994	18.4232	161.6373
	2	21.0043	255.5313	18.8148	189.9513	17.1109	184.6086
	3	17.5372	220.7395	18.3090	169.2820	19.2929	180.5064
	4	16.8794	180.3613	20.1262	181.1621	18.5829	185.6703
	5	18.2401	184.4683	20.8454	184.2203	17.0007	155.8582
	6	15.5474	162.6579	15.4434	152.1582	16.8525	156.6085
	7	14.8653	166.0205	17.8931	194.7030	16.8552	152.4085
	8	18.3141	203.6321	17.1928	198.9038	21.7974	316.4879
	9	19.4482	177.4798	17.3584	190.8859	18.8804	196.0557
	10	17.1787	176.981	18.3125	176.5729	18.8347	168.7191
	11	19.5680	171.4775	18.6879	186.8132	18.1755	173.0034
	12	19.6343	155.6801	19.0967	200.5407	16.6548	177.6843
	13	17.7350	177.5857	18.0063	199.7107	22.8400	183.3953
	14	19.2537	178.8159	21.7320	173.3913	17.2732	170.1581
4	1	17.2762	161.8631	17.9226	147.6671	16.3791	189.7208
	2	17.9874	166.9865	18.5356	149.3668	13.0690	186.5075
	3	16.0446	186.5664	17.3127	149.9303	18.9040	215.6276
	4	18.5500	170.7229	15.0705	130.7493	17.1407	181.6487
	5	15.7060	150.7718	19.3416	151.0163	18.2732	192.8021
	6	16.9173	156.8372	17.9022	162.9500	15.4346	167.9646
	7	18.9507	177.9755	14.8720	152.7842	16.8112	173.1651
	8	17.4127	166.9821	18.2363	186.5488	16.3774	156.9171
	9	16.7690	175.5213	16.6754	170.7327	16.5278	175.4136
	10	14.1707	137.2782	16.4651	151.0526	16.8182	176.2960
	11	15.3936	150.4212	15.5819	193.6588	18.8871	216.5452
	12	16.0138	169.1214	16.7177	148.8597	15.7553	165.5691
	13	17.3709	184.1335	17.9926	172.4130	15.655	166.0623
	14	16.0679	161.2346	14.5668	179.6443	17.059	188.1869

day	location	item 1		item 2		item 3	
		S_a	S_z	S_a	S_z	S_a	S_z
5	1	15.9997	173.2688	16.8121	148.6221	16.5904	180.9642
	2	16.4902	171.5257	16.1504	152.4072	17.4032	165.5486
	3	19.5245	175.5943	17.0604	147.3706	18.4322	193.2283
	4	17.9370	187.7948	18.8631	167.2399	16.9810	145.8290
	5	19.4714	181.9503	18.3453	169.0899	17.8519	175.5743
	6	15.1143	153.3545	16.8081	156.7802	14.9719	143.2342
	7	18.0412	180.6271	16.0984	187.3097	16.0078	178.8348
	8	18.2084	187.2960	16.7121	181.3355	18.8298	197.3136
	9	19.1414	196.2299	14.8717	153.2942	16.2130	175.8737
	10	20.8908	190.2989	18.4184	211.5840	17.5673	184.6830
	11	17.6168	183.7346	16.6617	164.7389	16.6045	166.7632
	12	17.1072	198.4568	18.8436	176.9580	15.5543	141.4431
	13	18.0304	170.2955	14.5059	153.5340	17.9444	178.3198
	14	16.9599	185.0618	18.4743	186.6141	16.8205	167.6222

References

Ajadi, J. O., Wang, Z. and Zwetsloot, I. M. (2021), 'A review of dispersion control charts for multivariate individual observations', *Quality Engineering* **33**(1), 60–75.

Alt, F. B. and Smith, N. D. (1988), 'Multivariate process control', *Handbook of statistics* **7**, 333–351.

Amemiya, Y. (1985), 'What should be done when an estimated between-group covariance matrix is not nonnegative definite?', *The American Statistician* **39**(2), 112–117.

Amemiya, Y., Anderson, T. W. and Lewis, P. A. (1990), 'Percentage points for a test of rank in multivariate components of variance', *Biometrika* **77**(3), 637–641.

Anderson, B. M., Anderson, T. W. and Olkin, I. (1986), 'Maximum likelihood estimators and likelihood ratio criteria in multivariate components of variance', *The Annals of Statistics* **14**(2), 405–417.

Anderson, T. W. (1984), 'Estimating linear statistical relationships', *The Annals of Statistics* **12**(1), 1–45.

Anderson, T. W. (1989), The asymptotic distribution of characteristic roots and vectors in multivariate components of variance, *in* 'Contributions to probability and statistics', Springer, pp. 177–196.

Anderson, T. W. (2003), *An introduction to multivariate statistical analysis*, 3rd edn, Wiley New York.

Anderson, T. W. and Amemiya, Y. (1991), 'Testing dimensionality in the multivariate analysis of variance', *Statistics & probability letters* **12**(6), 445–463.

Aronszajn, N. (1950), 'Theory of reproducing kernels', *Transactions of the American mathematical society* **68**(3), 337–404.

Automotive Industry Action Group (1995), *Measurement System Analysis (MSA)*, 2nd edn, AIAG, Southfield, MI.

Automotive Industry Action Group (2003), *Measurement System Analysis (MSA)*, 3rd edn, AIAG, Southfield, MI.

Barrentine, L. B. (2003), *Concepts for R&R studies*, Quality Press.

Besse, P. C., Cardot, H. and Ferraty, F. (1997), 'Simultaneous non-parametric regressions of unbalanced longitudinal data', *Computational Statistics & Data Analysis* **24**(3), 255–270.

Bhargava, A. K. and Disch, D. (1982), 'Exact probabilities of obtaining estimated non-positive definite between-group covariance matrices', *Journal of Statistical Computation and Simulation* **15**(1), 27–32.

Borror, C. M., Montgomery, D. C. and Runger, G. C. (1997), 'Confidence intervals for variance components from gauge capability studies', *Quality and Reliability Engineering International* **13**(6), 361–369.

Bosq, D. (2000), *Linear processes in function spaces: theory and applications*, Vol. 149, Springer Science & Business Media.

Browne, R., MacKay, J. and Steiner, S. (2010), 'Leveraged gauge r&r studies', *Technometrics* **52**(3), 294–302.

Browne, R. P., Mackay, R. J. and Steiner, S. H. (2009), 'Improved measurement-system assessment for processes with 100% inspection', *Journal of Quality Technology* **41**(4), 376–388.

Browne, R., Steiner, S. H. and MacKay, R. J. (2010), 'Optimal two-stage reliability studies', *Statistics in medicine* **29**(2), 229–235.

Burdick, R. K. (1994), 'Using confidence intervals to test variance components', *Journal of Quality Technology* **26**(1), 30–38.

Burdick, R. K., Borror, C. M. and Montgomery, D. C. (2003), 'A review of methods for measurement systems capability analysis', *Journal of Quality Technology* **35**(4), 342–354.

Burdick, R. K. and Larsen, G. A. (1997), 'Confidence intervals on measures of variability in R&R studies', *Journal of Quality Technology* **29**(3), 261–273.

Cai, T. T. and Yuan, M. (2011), 'Optimal estimation of the mean function based on discretely sampled functional data: Phase transition', *The annals of statistics* **39**(5), 2330–2355.

Cai, T. and Yuan, M. (2010), 'Nonparametric covariance function estimation for functional and longitudinal data'.

Cardot, H. (2000), 'Nonparametric estimation of smoothed principal components analysis of sampled noisy functions', *Journal of Nonparametric Statistics* **12**(4), 503–538.

Corbeil, R. R. and Searle, S. R. (1976), 'A comparison of variance component estimators', *Biometrics* pp. 779–791.

Culp, S. L., Ryan, K. J., Chen, J. and Hamada, M. S. (2018), 'Analysis of repeatability and reproducibility studies with ordinal measurements', *Technometrics* **60**(4), 545–556.

Danila, O., Steiner, S. H. and MacKay, R. J. (2010), 'Assessment of a binary measurement system in current use', *Journal of Quality Technology* **42**(2), 152–164.

de Almeida, F. A., Leite, R. R., Gomes, G. F., de Freitas Gomes, J. H. and de Paiva, A. P. (2020), 'Multivariate data quality assessment based on rotated factor scores and confidence ellipsoids', *Decision Support Systems* **129**, 113173.

Di, C.-Z., Crainiceanu, C. M., Caffo, B. S. and Punjabi, N. M. (2009), 'Multilevel functional principal component analysis', *The annals of applied statistics* **3**(1), 458.

Djauhari, M. A. (2005), 'Improved monitoring of multivariate process variability', *Journal of Quality Technology* **37**(1), 32–39.

Djauhari, M. A. (2007), 'A measure of multivariate data concentration', *Journal of Applied Probability & Statistics* **2**(2), 139–155.

Djauhari, M. A., Mashuri, M. and Herwindiati, D. E. (2008), 'Multivariate process variability monitoring', *Communications in Statistics-Theory and Methods* **37**(11), 1742–1754.

Donner, A. and Eliasziw, M. (1987), 'Sample size requirements for reliability studies', *Statistics in medicine* **6**, 441–448.

Drouot, A., Zhao, R., Irving, L., Sanderson, D. and Ratchev, S. (2018), 'Measurement assisted assembly for high accuracy aerospace manufacturing', *IFAC-PapersOnLine* **51**(11), 393–398.

Duan, S., Yu, G., Duan, J. and Wang, Y. (2023), 'Sparse positive-definite estimation for large covariance matrices with repeated measurements', *arXiv preprint arXiv:2304.08020* .

Duchon, J. (1977), Splines minimizing rotation-invariant semi-norms in sobolev spaces, *in* 'Constructive Theory of Functions of Several Variables: Proceedings of a Conference Held at Oberwolfach April 25–May 1, 1976', Springer, pp. 85–100.

Ebadi, M., Chenouri, S., Lin, D. K. and H. Steiner, S. (2022), 'Statistical monitoring of the covariance matrix in multivariate processes: a literature review', *Journal of Quality Technology* **54**(3), 269–289.

Ebadi, M., Chenouri, S. and Steiner, S. H. (2023), 'Phase I analysis of high-dimensional processes in the presence of outliers', *Journal of Quality Technology* pp. 1–20.

Esmaeeli, R., Aliniagerdroudbari, H., Hashemi, S. R., Al-Shammari, H., Alhadri, M. and Farhad, S. (2019), Univariate and multivariate gauge repeatability and reproducibility analysis on the high frequency dynamic mechanical analysis (DMA) measurement system, *in* 'Proceedings of the ASME 2019 International Mechanical Engineering Congress and Exposition', Vol. 2B: Advanced Manufacturing, American Society of Mechanical Engineers.

Ferraty, F. and Vieu, P. (2006), *Nonparametric functional data analysis: theory and practice*, Springer Science & Business Media.

Fong, Y., Rue, H. and Wakefield, J. (2010), 'Bayesian inference for generalized linear mixed models', *Biostatistics* **11**(3), 397–412.

González, I. and Sánchez, I. (2010), 'Variable selection for multivariate statistical process control', *Journal of Quality Technology* **42**(3), 242–259.

Graybill, F. A. and Wortham, A. (1956), 'A note on uniformly best unbiased estimators for variance components', *Journal of the American Statistical Association* **51**(274), 266–268.

Gupta, A. K. and Nagar, D. K. (2000), *Matrix variate distributions*, CRC Press.

Hall, P. (2010), Principal component analysis for functional data: Methodology, theory, and discussion, *in* 'The Oxford Handbook of Functional Data Analysis', Oxford University Press, pp. 210–234.

Hall, P., Müller, H.-G. and Wang, J.-L. (2006), 'Properties of principal component methods for functional and longitudinal data analysis', *The annals of statistics* **34**(3), 1493–1517.

Hamada, M. S. (2016), 'A bayesian approach to multivariate measurement system assessment', *Journal of Quality Technology* **48**(3), 246–252.

Hashiguchi, H., Takayama, N. and Takemura, A. (2018), 'Distribution of the ratio of two wishart matrices and cumulative probability evaluation by the holonomic gradient method', *Journal of Multivariate Analysis* **165**, 270–278.

Hastie, T., Tibshirani, R., Friedman, J. H. and Friedman, J. H. (2009), *The elements of statistical learning: data mining, inference, and prediction*, Vol. 2, Springer.

Hayes, J. and Hill, W. (1981), 'Modification of estimates of parameters in the construction of genetic selection indices ('bending')', *Biometrics* pp. 483–493.

Hill, W. and Thompson, R. (1978), 'Probabilities of non-positive definite between-group or genetic covariance matrices', *Biometrics* pp. 429–439.

Horváth, L. and Kokoszka, P. (2012), *Inference for functional data with applications*, Vol. 200, Springer Science & Business Media.

Huwang, L., Yeh, A. B. and Wu, C.-W. (2007), 'Monitoring multivariate process variability for individual observations', *Journal of Quality Technology* **39**(3), 258–278.

ISO GUM (2008), *ISO/IEC GUIDE 98–3: 2008, Guide to the expression of uncertainty in measurement*, International Organisation for Standardisation, Geneva, Switzerland.

James, G. M., Hastie, T. J. and Sugar, C. A. (2000), 'Principal component models for sparse functional data', *Biometrika* **87**(3), 587–602.

Jensen, D. R. (1970), 'The joint distribution of traces of wishart matrices and some applications', *The Annals of Mathematical Statistics* pp. 133–145.

Jin, S., Iquebal, A., Bukkapatnam, S., Gaynor, A. and Ding, Y. (2020), 'A gaussian process model-guided surface polishing process in additive manufacturing', *Journal of Manufacturing Science and Engineering* **142**(1), 011003.

Jin, S., Tuo, R., Tiwari, A., Bukkapatnam, S., Aracne-Ruddle, C., Lighty, A., Hamza, H. and Ding, Y. (2023), 'Hypothesis tests with functional data for surface quality change detection in surface finishing processes', *IISE transactions* **55**(9), 940–956.

Johnstone, I. M. (2009), 'Approximate null distribution of the largest root in multivariate analysis', *The annals of applied statistics* **3**(4), 1616.

Jolliffe, I. T. and Cadima, J. (2016), 'Principal component analysis: a review and recent developments', *Philosophical transactions of the royal society A: Mathematical, Physical and Engineering Sciences* **374**(2065), 20150202.

Khuri, A. I. and Sahai, H. (1985), 'Variance components analysis: a selective literature survey', *International Statistical Review/Revue Internationale de Statistique* pp. 279–300.

Kimeldorf, G. and Wahba, G. (1971), 'Some results on tchebycheffian spline functions', *Journal of mathematical analysis and applications* **33**(1), 82–95.

Klotz, J. H., Milton, R. C. and Zacks, S. (1969), 'Mean square efficiency of estimators of variance components', *Journal of the American Statistical Association* **64**(328), 1383–1402.

Klotz, J. and Putter, J. (1969), 'Maximum likelihood estimation of multivariate covariance components for the balanced one-way layout', *The Annals of Mathematical Statistics* **40**(3), 1100–1105.

Kneip, A. and Gasser, T. (1992), 'Statistical tools to analyze data representing a sample of curves', *The Annals of Statistics* **20**(3), 1266–1305.

Koner, S. and Staicu, A.-M. (2023), 'Second-generation functional data', *Annual review of statistics and its application* **10**, 547–572.

Krzanowski, W. J. and Marriott, F. H. C. (1994), *Multivariate Analysis: Distributions, ordination and inference*, Americas: John Wiley & Sons.

Kubokawa, T. and Tsai, M.-T. (2006), 'Estimation of covariance matrices in fixed and mixed effects linear models', *Journal of multivariate analysis* **97**(10), 2242–2261.

Larsen, G. A. (2002), 'Measurement system analysis: the usual metrics can be noninformative', *Quality Engineering* **15**(2), 293–298.

Lee, K. and Kapadia, C. (1992), 'Mean squared error efficient estimators of the variance components', *Metrika* **39**, 21–26.

Lehmann, E. L. (1999), *Elements of large-sample theory*, Springer.

Li, Y. and Hsing, T. (2010), 'Uniform convergence rates for nonparametric regression and principal component analysis in functional/longitudinal data', *The Annals of Statistics* **38**(6), 3321–3351.

Mader, D. P., Prins, J. and Lampe, R. E. (1999), 'The economic impact of measurement error', *Quality Engineering* **11**(4), 563–574.

Majeske, K. D. (2008), 'Approval criteria for multivariate measurement systems', *Journal of Quality Technology* **40**(2), 140–153.

Majeske, K. D. (2012), 'Approving vision–based measurement systems in the presence of within–part variation', *Quality Engineering* **24**(1), 49–59.

Majeske, K. D. and Andrews, R. W. (2002), 'Evaluating measurement systems and manufacturing processes using three quality measures', *Quality Engineering* **15**(2), 243–251.

Marques, R. A. M., Pereira, R. B. D., Peruchi, R. S., Brandão, L. C., Ferreira, J. R. and Davim, J. P. (2020), 'Multivariate gr&r through factor analysis', *Measurement* **151**, 107107.

Marron, J., Ramsay, J. O., Sangalli, L. M. and Srivastava, A. (2014), 'Statistics of time warpings and phase variations', *Electronic Journal of Statistics* **8**, 1697–1702.

Martínez-Hernández, I. and Genton, M. G. (2020), 'Recent developments in complex and spatially correlated functional data'.

McKendry, C. (2023), *Measurement systems analysis for curve data using functional random effects models*, JMP Discovery Summit Europe Presentations.

Meyer, K. and Kirkpatrick, M. (2010), 'Better estimates of genetic covariance matrices by "bending" using penalized maximum likelihood', *Genetics* **185**(3), 1097.

Montgomery, D. C. (2020), *Introduction to statistical quality control*, 8th edn, John Wiley & Sons.

Montgomery, D. C. and Runger, G. C. (1993a), 'Gauge capability analysis and designed experiments. part I: Basic methods', *Quality Engineering* **6**(1), 115–135.

Montgomery, D. C. and Runger, G. C. (1993b), 'Gauge capability analysis and designed experiments. part II: Experimental design models and variance component estimation', *Quality Engineering* **6**(2), 289–305.

Mostafaiy, B., Faridrohani, M. R. and Chenouri, S. (2019), 'Optimal estimation in functional linear regression for sparse noise-contaminated data', *Canadian Journal of Statistics* **47**(4), 524–559.

Mozaffari, A., Chenouri, S., Toyserkani, E. and Ali, U. (2021), 'Functional boxplots for outlier detection in additive manufacturing', *arXiv preprint arXiv:2110.10867* .

Muirhead, R. J. (1982), *Aspects of multivariate statistical theory*, John Wiley & Sons.

Nadarajah, S. and Kotz, S. (2008), 'Moments of truncated t and f distributions', *Portuguese Economic Journal* **7**, 63–73.

Nie, Y., Yang, Y., Wang, L. and Cao, J. (2022), 'Recovering the underlying trajectory from sparse and irregular longitudinal data', *Canadian Journal of Statistics* **50**(1), 122–141.

Osthus, D., Weaver, B., Casleton, E., Hamada, M. and Steiner, S. (2021), 'On gauge repeatability and reproducibility studies for counts', *Quality Engineering* **33**, 1–14.

Patterson, H. D. and Thompson, R. (1971), 'Recovery of inter-block information when block sizes are unequal', *Biometrika* **58**(3), 545–554.

Peruchi, R., Paiva, A. d., Balestrassi, P., Ferreira, J. and Sawhney, R. (2014), 'Weighted approach for multivariate analysis of variance in measurement system analysis', *Precision Engineering* **38**(3), 651–658.

Peruchi, R. S., Junior, H. M., Fernandes, N. J., Balestrassi, P. P. and Paiva, A. P. (2016), 'Comparisons of multivariate gr&r methods using bootstrap confidence interval', *Acta Scientiarum. Technology* **38**(4), 489–496.

Pham-Gia, T., Thanh, D. N., Phong, D. T. et al. (2015), 'Trace of the wishart matrix and applications', *Open Journal of Statistics* **5**(03).

Pillai, K. S. (1965), 'On the distribution of the largest characteristic root of a matrix in multivariate analysis', *Biometrika* pp. 405–414.

Portnoy, S. (1971), 'Formal bayes estimation with application to a random effects model', *The Annals of Mathematical Statistics* **42**(4), 1379–1402.

Rajagopalan, M. and Broemeling, L. (1983), 'Bayesian inference for the variance components in general mixed linear models', *Communications in Statistics-Theory and Methods* **12**(6), 701–723.

Ramsay, J. O. and Silverman, B. W. (2002), *Applied functional data analysis: methods and case studies*, Springer.

Ramsay, J. O. and Silverman, B. W. (2005), *Functional data analysis*, 2nd edn, Springer.

Rao, C. R. (1983), Likelihood ratio tests for relationships between two covariance matrices, *in* 'Studies in econometrics, time series, and multivariate statistics', Elsevier, pp. 529–543.

Rao, P. S. and Heckler, C. E. (1998), 'Multivariate one-way random effects model', *American Journal of Mathematical and Management Sciences* **18**(1-2), 109–130.

Remadi, S. and Amemiya, Y. (1993), 'Limiting distribution of roots with differential rates of convergence', *Statistics & probability letters* **17**(3), 237–244.

Remadi, S. and Amemiya, Y. (1994), 'Asymptotic properties of the estimators for multivariate components of variance', *Journal of multivariate analysis* **49**(1), 110–131.

Rice, J. A. and Silverman, B. W. (1991), 'Estimating the mean and covariance structure nonparametrically when the data are curves', *Journal of the Royal Statistical Society: Series B (Methodological)* **53**(1), 233–243.

Robinson, D. L. (1987), 'Estimation and use of variance components', *Journal of the Royal Statistical Society Series D: The Statistician* **36**(1), 3–14.

Ruck, A., Gotwalt, C. and Lancaster, L. (2020), *Measurement systems analysis for curve data*, JMP Discovery Summit Americas Presentations.

Sahai, H. (1979), 'A bibliography on variance components', *International Statistical Review/Revue Internationale de Statistique* pp. 177–222.

Scheffé, H. (1959), *The analysis of variance*, John Wiley & Sons.

Schölkopf, B., Herbrich, R. and Smola, A. J. (2001), A generalized representer theorem, *in* 'International conference on computational learning theory', Springer, pp. 416–426.

Searle, S. R., Casella, G. and McCulloch, C. E. (1992), *Variance components*, John Wiley & Sons, Inc.

Shainin, P. D. (1992), Managing spc, a critical quality system element, *in* '46th Annual Quality Congress Proceedings, ASQC', pp. 251–257.

Shalin, G. (2021), Prediction and detection of freezing of gait in parkinson's disease using plantar pressure data, Master's thesis, University of Waterloo.

Shang, H. L. (2014), 'A survey of functional principal component analysis', *AStA Advances in Statistical Analysis* **98**, 121–142.

Shi, L., He, Q., Liu, J. and He, Z. (2016), 'A modified region approach for multivariate measurement system capability analysis', *Quality and Reliability Engineering International* **32**(1), 37–50.

Shi, M. (1993), Multivariate analysis of variance and robust estimation of covariance structures when the data are curves, PhD thesis, The Ohio State University.

Shu, L., Hua, T., Wang, Y., Li, Q., Feng, D. D. and Tao, X. (2010), 'In-shoe plantar pressure measurement and analysis system based on fabric pressure sensing array', *IEEE Transactions on information technology in biomedicine* **14**(3), 767–775.

Smith, R. R., McCrary, S. W. and Callahan, R. N. (2007), 'Gauge repeatability and reproducibility studies and measurement system analysis: A multimethod exploration of the state of practice', *Journal of Industrial Technology* **23**(1).

Srivastava, A., Klassen, E., Joshi, S. H. and Jermyn, I. H. (2010), 'Shape analysis of elastic curves in euclidean spaces', *IEEE Transactions on Pattern Analysis and Machine Intelligence* **33**(7), 1415–1428.

Srivastava, A. and Klassen, E. P. (2016), *Functional and shape data analysis*, Springer.

Srivastava, A., Wu, W., Kurtek, S., Klassen, E. and Marron, J. S. (2011), 'Registration of functional data using Fisher-Rao metric'.

Srivastava, M. and Kubokawa, T. (1999), 'Improved nonnegative estimation of multivariate components of variance', *The Annals of Statistics* **27**(6), 2008–2032.

Srivastava, M. S. (2003), 'Singular wishart and multivariate beta distributions', *The Annals of Statistics* **31**(5), 1537–1560.

Steiner, S. H. and MacKay, R. J. (2005), *Statistical engineering: An algorithm for reducing variation in manufacturing processes*, Vol. 1, Quality Press.

Stevens, N. T., Browne, R., Steiner, S. H. and MacKay, R. J. (2010), 'Augmented measurement system assessment', *Journal of Quality Technology* **42**(4), 388–399.

Stevens, N. T., Steiner, S. H., Browne, R. P. and MacKay, R. J. (2013), 'Gauge r&r studies that incorporate baseline information', *IIE Transactions* **45**(11), 1166–1175.

Sugiura, N. and Nagao, H. (1968), 'Unbiasedness of some test criteria for the equality of one or two covariance matrices', *The Annals of Mathematical Statistics* **39**(5), 1686–1692.

Suriano, S., Wang, H., Shao, C., Hu, S. J. and Sekhar, P. (2015), 'Progressive measurement and monitoring for multi-resolution data in surface manufacturing considering spatial and cross correlations', *Iie Transactions* **47**(10), 1033–1052.

Sweeney, S. (2007), 'Analysis of two-dimensional gage repeatability and reproducibility', *Quality Engineering* **19**(1), 29–37.

Taver, R. (1995), 'Manufacturing solutions for consistent quality and reliability: The 9 step problem solving process', *AMACON, New York* .

Thompson, W. A. (1962), 'The problem of negative estimates of variance components', *The Annals of Mathematical Statistics* pp. 273–289.

Tiao, G. C. and Tan, W. (1965), 'Bayesian analysis of random-effect models in the analysis of variance. i. posterior distribution of variance-components', *Biometrika* **52**(1/2), 37–53.

Tikhonov, A. N. and Arsenin, V. (1977), *Solutions of ill-posed problems*, Winston/Wiley, New York.

Uhlig, H. (1994), 'On singular wishart and singular multivariate beta distributions', *The Annals of Statistics* pp. 395–405.

Van Wieringen, W. N. and De Mast, J. (2008), 'Measurement system analysis for binary data', *Technometrics* **50**(4), 468–478.

Vardeman, S. B. and Jobe, J. M. (2016), *Statistical methods for quality assurance: Basics, measurement, control, capability and improvement*, 2nd edn, Springer, New York.

Venables, W. et al. (1974), 'Null distribution of the largest root statistic', *Journal of the royal Statistical Society, Series C: Applied Statistics, 23, Algorithm AS77* pp. 125–131.

Voelkel, J. G. (2003), 'Gauge R&R analysis for two-dimensional data with circular tolerances', *Journal of quality technology* **35**(2), 153–167.

Wahba, G. (1990), *Spline models for observational data*, SIAM, Philadelphia.

Wang, F.-K. (2013), 'An assessment of gauge repeatability and reproducibility with multiple characteristics', *Journal of Testing and Evaluation* **41**(4), 651–658.

Wang, F.-K. and Yang, C.-W. (2007), 'Applying principal component analysis to a gr&r study', *Journal of the Chinese Institute of Industrial Engineers* **24**(2), 182–189.

Wang, J.-L., Chiou, J.-M. and Müller, H.-G. (2016), 'Functional data analysis', *Annual Review of Statistics and Its Application* **3**, 257–295.

Waterhouse, W. C. (1983), 'Do symmetric problems have symmetric solutions?', *The American Mathematical Monthly* **90**(6), 378–387.

Weaver, B. P., Hamada, M. S., Vardeman, S. B. and Wilson, A. G. (2012), 'A bayesian approach to the analysis of gauge r&r data', *Quality Engineering* **24**(4), 486–500.

Wheeler, D. J. and Lyday, R. W. (1989), *Evaluating the Measurement Process*, 2nd edn, SPC Press, Inc., Knoxville, TN.

Yang, Y., Dong, Z., Meng, Y. and Shao, C. (2021), 'Data-driven intelligent 3d surface measurement in smart manufacturing: review and outlook', *Machines* **9**(1), 13.

Yao, F., Müller, H.-G. and Wang, J.-L. (2005), 'Functional data analysis for sparse longitudinal data', *Journal of the American statistical association* **100**(470), 577–590.

Zhang, J. T. (2013), *Analysis of variance for functional data*, Chapman and Hall/CRC.

Zhang, X. and Wang, J.-L. (2016), 'From sparse to dense functional data and beyond', *The Annals of Statistics* **44**(5), 2281–2321.